Metabolic signaling under nutrient deprivation

Ana Luisa De Sousa Coelho

METABOLIC SIGNALLING DURING NUTRIENT DEPRIVATION

Ana Luísa De Sousa Coelho

2012

UNIVERSITAT DE BARCELONA

Facultat de Farmàcia

Departament de Bioquímica i Biologia Molecular

Programa de Doctorat de Biomedicina

Màster en Biotecnologia Molecular 2006-2007

METABOLIC SIGNALLING DURING NUTRIENT DEPRIVATION

Memòria presentada per Ana Luísa De Sousa Coelho

per optar al títol de doctor de la Universitat de Barcelona

Dr. Pedro F. Marrero
Director

Ana Luísa De Sousa Coelho
La doctoranda

Aquesta tesi ha estat realizada gràcies a la concessió de una "Bolsa de Investigação" de la Fundação para a Ciência e a Tecnologia (FCT), de Portugal (SFRH/BD/41677/2007).

Aos meus Pais e Cristina.

Eu não tenho filosofia: tenho sentidos...
Se falo na Natureza não é porque saiba o que ela é,
Mas porque a amo, e amo-a por isso,
Porque quem ama nunca sabe o que ama
Nem sabe porque ama, nem o que é amar...

Amar é a eterna inocência,
E a única inocência é não pensar...

Alberto Caeiro

Ó mar salgado, quanto do teu sal
São lágrimas de Portugal!
Por te cruzarmos, quantas mães choraram,
Quantos filhos em vão rezaram!
Quantas noivas ficaram por casar
Para que fosses nosso, ó mar!

Valeu a pena? *Tudo vale a pena*
Se a alma não é pequena.
Quem quer passar além do Bojador
Tem que passar além da dor.
Deus ao mar o perigo e o abismo deu,
Mas nele é que espelhou o céu.

Fernando Pessoa

AGRADECIMiENTOS

Ya táááááá!

Bueno, empiezo a escribir la página que más gente va a leer… Los agradecimientos. Durante todos estos años, aunque quizás así más para los últimos, he pensado en esta página (y también en el pica-pica!). Pensaba en este final, que en realidad va en el inicio de este "libro", y pensaba en toda la gente a quien quería agradecer, si me olvidaría de alguien, en como lo haría, y como lo escribiría (y con cuantos errores!), y por qué orden, y en qué idioma!... Tantas cosas he pensado que ahora no sé cómo hacerlo.

Cheguei ao fim de mais uma etapa. Parece que desde sempre fui passando por etapas, a primária, o ciclo, a "Afonso" outra vez, o liceu, a universidade, o doutoramento. E agora, qual é a etapa seguinte?!? Gosto sempre de pensar naquela frase que diz que "a felicidade é o caminho". Gosto de pensar que foi mais uma caminhada... E estou feliz. E por isso quero agradecer à minha Família. Obrigada aos meus Pais por me terem deixado e ajudado a crescer, por terem apoiado as minhas decisões, e terem aceitado ter tantas saudades minhas como eu tive vossas. Pai, obrigada por quereres sempre o melhor para mim, ainda que às vezes tivéssemos as nossas discordâncias. Mãe, obrigada por seres assim e por te pareceres comigo às vezes (!!!), pelos nossos pic-nics, idas à praia, e Argentina! Maninha, obrigada por seres a minha irmã mais velha, por me teres levado contigo onde ias, por me teres "feito" ir para Coimbra, e por teres confiança em mim. E por mais coisas que de certeza ficam por dizer… Obrigada ao meu lindo sobrinho Pedro que me faz sorrir tanto e ter tantas saudades dele. Obrigada João, por fazer parte desta família.

Pero antes de seguir… para que haya llegado hasta esta página tengo que agradecer a mis DOS jefes. Gracias Pedro. Inicialmente por haberme "aceptado" en el grupo, y al largo de todos estos años por toda la ayuda, las listas de objetivos, la motivación cuando esta se iba… Gracias Diego. Por todas las ideas y las propuestas de esos experimentos tan sencillitos… De verdad, gracias a los dos por haber estado, gracias por haberme hecho crecer en este mundo de la ciencia, y gracias por confiar en mí.

ST team, team approach!!! GRACIAS! En serio, os tengo que agradecer tanto por lo importante que habéis sido en todo este camino. Ya me imagináis escribiendo esto, …o no!? Con las lagrimillas cayendo por las mejillas, limpiando los mocos en la manga… Gracias por haberme ayudado a integrarme en el grupo y por todo lo que me habeis enseñado. Por las cenas, los karaokes, los amigos invisibles! Cris Mayo, gracias por haberme iniciado en mi proyecto. Nuria, gracias por los consejos de post-doc. Xisca, gracias por haberme ayudado a crecer, no creas que solo me has hecho llorar, me has enseñado mucho. María del Mar, gracias por todo. Has sido siempre un ejemplo para mí. Joana, que sepas que nunca has sido mi saco de boxeo, aunque te haya tocado llevar con algunas de mis "malas caras" y respuestas secas. Te agradezco por la paciencia, las discusiones científicas y los miles de consejos. Mis compañeras rookies!!! Anna, gracias por haberme acompañado de tan cerca y por toda la ayuda en el laboratorio. Gracias por esas bravas en el "pequeñito" los viernes que salíamos tarde. Gracias por tener esa antena y ser tan sorda como yo a la vez! Marionaaaaa! Gracias por querer ayudar siempre, y lo hiciste conmigo desde mis primeros pasos temblorosos en el ST. Gracias por ser tan compañera y Amiga. Elena, gracias por haber venido. (Ahora me rio, mira que frase…) Gracias por tu tranquilidad, por los consejos

químicos (y otros!) y por tu presencia Amiga. Gracias por apoyarme y acompañarme tan de cerca en esta última fase de la tesis. Gracias a mis dos "alumnos", Gaby y Carlos, que me permitisteis enseñaros como he sabido. Gracias también a Joan Carles, Joan y Carme, y a todo el ST del Parc, por todos los martes, discusiones, anticuerpos, protocolos y sugerencias. Gracias Albertinho, ahora eres tu El Futuro! Obrigada Joana e Xana, vocês também são O Futuro.

Gracias a todo el departamento. Gracias a las secretarias por su trabajo indispensable. Gracias Brugués por toda la papelada que te ido dando y pidiendo, que siempre lo has sabido resolver, con una sonrisa y tranquilidad. Gracias también a cada uno de los grupos por haberme ayudado y dejado entrar en su laboratorio en cualquier momento, por una estufa giratoria, por un baño con agitación, por los glucómetros, pidiendo ayuda en un protocolo que no me sale, o simplemente para pedir un boli prestado o para compartir una autoclave. Gracias a los que hemos compartido tardes muy largas y fines de semana!

Gracias a mi Dani catalán, un reminiscente de mi época de Erasmus, un Amigo. Gracias por haber seguido en mi vida todos estos años. Gracias a mi otro Dani, el de Zaragozzzaaaaaa! Gracias por todos los momentos que hemos pasado juntos, me enorgullece ser la primera persona que conociste ese año que vinimos para Barcelona. Gracias a Jordi compi, por haberme apoyado en los momentos que parecían difíciles, y por NYC. Gracias a Joan, mi gordo. Gracias a Karel, mi loco.

Prima Ana Lúcia, um obrigada por termos embarcado nesta viagem juntas em 2006, nessa tarde que apanhamos o autocarro para Lisboa com a lagriminha a cair, mas a rir de nervosinhas, tal como quando andamos de avião pela primeira vez em 1993. Obrigada por esse primeiro ano juntas, pelas rodagens de figurantes, pelas rosas de S. Jordi ao fim da noite, por seres minha prima e Amiga.

Obrigada aos meus Amigos "Cromos" da faculdade. "Carla e Ana Lu". Obrigada Carla, por me teres acompanhado durante tantos anos e por me acolheres na tua família. Obrigada Nuno, por seres tão meu Amigo e detalhista, por arranjares sempre um tempinho para nos vermos. Obrigada Manique, foste a minha cara amiga e de salvação na nevada de Londres… Também não me esqueço da tua meia-cara queimada na Figueira… Obrigada Ana Raquel, pela tua maneira de ver as coisas sempre mais simples do que me pareciam.

Obrigada Rita. Pelas noites que dormimos tarde porque ainda havia mais qualquer coisa para dizer. Por Coimbra e por tudo o resto que temos vindo a construir. "Já percebo porque é que vocês são tão amigas…" descreve tudo. Obrigada Tino. Por seres meu Amigo, por teres paciência comigo, por me sorrires, por me fazeres rir, por me abraçares, e por Agosto (de ti).

E obrigada a todos os que fazem parte da minha vida, aos meu tios e tias, primos e primas (obrigada Daniela), e avó. Obrigada à Joana, Inês e Iris. Obrigada PAtineiteirS, Sylvia e Priscila, tenho saudades nossas!

Y no se sabe bien porqué pero se queda para último… Gracias Francisco. Gracias por haber entrado en mi vida y hacerme tan feliz. Amo-te.

Ana Lu

INDEX

ANNEX

PRESENTATION AND AIM OF THE STUDY

During his life, an individual is subjected to diverse nutritional changes. The ability to sense nutrient availability and regulate energy homeostasis is an ancient and fundamental process. Nonetheless, cells integrate information regarding not only nutrient availability, but also growth factor and hormonal receptor activation, stress, and internal energy through an elaborate array of signalling pathways. The molecular basis of gene regulation by these is an important field of research for studying the regulation of physiological functions. Among all tissues, the liver plays an indispensable role, integrating the nutrient intake and the delivery of carbohydrates and lipids to peripheral tissues.

Due to the importance of the lipid homeostasis and previous work from our group, the regulation of fatty acid oxidation and ketogenesis gene expression in liver had a central role in this study. Still, it must be remarked that as a result of the course of the incoming findings, it was given a special emphasis in two kinds of nutrient deprivation: fasting and amino acid deficiency; and to FGF21, a circulating hepatokine that affects carbohydrate and lipid metabolism.

Specifically, the aims of this work were to study:

- The role of SIRT1 in the regulation of fatty acid oxidation and ketogenesis in response to nutritional changes.
- The role of SIRT1 in the regulation of FGF21 by HMGCS2.
- The regulation of FGF21 under amino acid deprivation.
- The metabolic signalling under leucine-deficiency in response to fasting.
- The role of FGF21 in the amino acid deprivation phenotype.

The presented work is initially centered in the regulation of fatty acid oxidation and ketogenesis by the homolog of the yeast silencing information regulator 2 (SIRT1), which has been implicated in several aspects of food limitation and caloric restriction in mammals. The dependence of SIRT1 enzymatic activity on NAD^+ suggests that SIRT1 could serve as a metabolic sensor and couple the energy status of the cell. The role of this deacetylase enzyme in several situations such as the lactancy/weaning transition, caloric restriction, and fasting, is explored. Then, the role of SIRT1 in the HMGCS2 regulation of FGF21 expression is also examined. These last results are integrated in the published article "Human HMGCS2 regulates fatty acid oxidation and FGF21 expression in HepG2 cells".

Afterward, the work is more focalized in the amino acid starvation. At first, the published article "Activating transcription factor 4-dependent induction of FGF21 during amino acid deprivation" is presented. Herein, FGF21 is shown to be induced under amino acid starvation conditions both in a hepatic cell line and in mouse liver, and also it is identified and characterized as an ATF4-target gene. Secondly, because FGF21 is known to be highly induced upon fasting, the effects of accumulating both nutritional stress conditions, i.e. amino acid deficient feeding and fasting, are investigated. And lastly, the recently submitted manuscript "FGF21 mediates the lipid metabolism response to amino acid starvation" illustrates that important metabolic changes that occur under amino acid deprivation are FGF21-dependent.

INTRODUCTION

1. NUTRITIONAL CHANGES CHARACTERISTIC OF MAMMALS

Every cell regulates gene expression in response to changes in the external environment. In unicellular organisms, specific mechanisms gradually developed to allow the cells to metabolize fuels according to their availability in the external milieu. Multicellular organisms need to ensure appropriate provision of substrates to tissues without having direct access to the nutrient source.

Mammals have the ability to adapt their own metabolic demand to survive in a variable environment. There are several external stimuli to which they must be able to respond. Among these are thermal fluctuations, rhythmic changes imposed by alternation of day and night, the need to adapt to discontinuous intake of food, periods of malnutrition, etc. Most of the adaptations to the environment are controlled not only by hormonal or neuronal signals, but also by major (glucose, fatty acids, and amino acids) or minor (iron, vitamin, etc.) dietary constituents, which may regulate gene expression in a hormone-independent manner (Pégorier et al, 2004).

The liver plays a central role in this response. Hepatocytes are regularly exposed to both dietary and systemic signals, respectively from the portal blood flow and the arterial blood supply, which coordinate gene expression and maintain homeostasis (Jump and Clarke, 1999; Langhans, 2003).

1.1. LACTANCY/WEANING

In most of the mammals, birth and weaning are two periods of nutritional transition. Whereas the fetus oxidizes mainly glucose, lactate and amino acids, the newborn is fed with milk: a high fat and low carbohydrate diet. At weaning, milk is replaced progressively by the adult diet which contains less fat and more carbohydrate.

Birth leads to a sudden decrease in glucose availability. During suckling, the newborn adapts itself to the new nutritional environment by increasing its capacity to produce glucose *de novo* (gluconeogenesis) to achieve its high glucose needs. Due to the massive appearance of lipids in blood, coming from milk, oxidation of fatty acids is enhanced in the

liver and at the peripheral level, allowing using this fuel for energy metabolism. Ketone bodies are synthetized from fatty acids in the liver, and lipogenesis is decreased in the liver and in white adipose tissue (WAT) (Girard et al., 1992).

At weaning, these adaptations are turned around. The transition from a high-fat diet to a high-carbohydrate diet goes along with a progressive decrease in the ketogenic capacity of the liver. Metabolic target genes involved in gluconeogenesis and fat oxidation start to decline. The lipogenic rate in the liver and WAT, as well as the storage of triglycerides (TG), is increased. The nutritional and hormonal factors involved in these metabolic adaptations are numerous, but insulin and glucagon are thought to play a major role (Ferré et al., 1986; Girard et al., 1985).

1.2. OVERNIGHT FASTING AND STARVATION

The overnight (o/n) fasting is a physiological situation. However, during this period several important changes take place. The metabolic changes include glycogen mobilization, fat mobilization, gluconeogenesis, fatty acid oxidation and ketogenesis. There are also changes in the hormone levels as insulin, glucagon, adipokines and glucocorticoids. And in the levels of regulatory proteins as peroxisome proliferator-activated receptor (PPAR)γ, PPARγ coactivator-1α (PGC1α), forkhead protein FOXO and SIRT1, among others.

Physiological adaptations to periods of starvation are aimed to preserve glucose for the brain. During a short-term food limitation (i.e. o/n fasting in humans), the low level of glucose in blood leads to a decreased secretion of insulin and an increased secretion of glucagon. This firstly induces glycogenolysis and gluconeogenesis in the liver, and the mobilization of TG from WAT. Liver glycogen stores are mobilized via glucagon and the activation of liver phosphorylase enzymes. Hepatic glycogen is broken down to glucose-6-phosphate, which is converted to glucose and released into the blood stream. Additionally, gluconeogenic precursors, such as lactate and alanine, may be delivered from muscle to the liver to synthesize glucose (Storlien et al., 2004).

Maintenance of energy and nutrient homeostasis during food deprivation is accomplished through an increase in mitochondrial fatty acid oxidation in peripheral tissues

(Gerhart-Hines et al., 2007). Prolonged starvation leads to the production of ketone bodies by the liver, which are released in the blood and used as an energy source for the brain. Glucocorticoids from the adrenal glands help to induce gluconeogenesis, reduce glucose utilization by the muscle, and increase lypolysis and protein breakdown (Bordone and Guarente, 2005). Energy expenditure during starvation is reduced and protein oxidation diminishes. In normal circumstances lean body mass is relatively constant, but there is a continuous turnover of protein (synthesis and breakdown to amino acids) as tissues are continually renewed and replaced.

As referred above, fat breakdown is essential in starvation to provide the caloric needs for metabolism. Lipids are stored in adipose tissue in the form of triacylglycerol (TAG). During starvation, TAG is broken down into free fatty acids (FFA), which are released into the circulation and supply other tissues such as skeletal muscle, heart, liver, and kidney with energy (Zechner et al., 2005). Glycerol is also released from the breakdown of TAG and is converted to glucose by the liver.

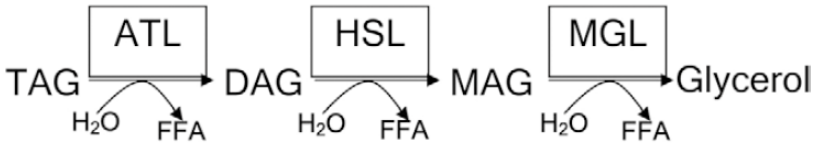

FIGURE I-1. **Metabolism of TAG in adipose tissue.** Adipose triacylglycerol lipase (ATL or ATGL) functions in the initial hydrolysis of TAG into diacylglycerol (DAG) and FFA. The second step is the breakdown of DAG into monoacylglycerol (MAG) mediated by hormone-sensitive lipase (HSL). MAG is then catabolyzed into FFA and glycerol by the enzyme monoacylglycerol lipase (MGL). Finn and Dice, 2006.

In starvation, macroautophagy provides a nutrient source for energy generation, promoting survival. Autophagy is a process of self-cannibalization, where cells capture their own cytoplasm and organelles and consume them in lysosomes. It is a mechanism that protects cells from cell death by multiple mechanisms, which include maintenance of bioenergetic homeostasis, recycling of misfolded and aggregate-prone proteins, and removal of uncoupled or permeabilized mitochondria (Kroemer et al., 2010). Common nutrient,

growth factor, hormone, and stress signals regulate autophagy. High concentrations of AMP (that activate AMPK), the fasting hormone glucagon, and also adrenergic receptor activation, are able to inhibit mTORC1 and trigger autophagy in the liver (Rabinowitz and White, 2010). After depletion of glycogen stores, autophagy in liver and heart (but not in brain) generates fatty acids and amino acids, which are catabolized to yield energy. In the liver, this energy drives gluconeogenesis and ketogenesis. As starvation continues, degradation of adipose tissue and muscle play an increasing role in supplying substrates to the liver, which exports glucose and ketone bodies to feed the brain.

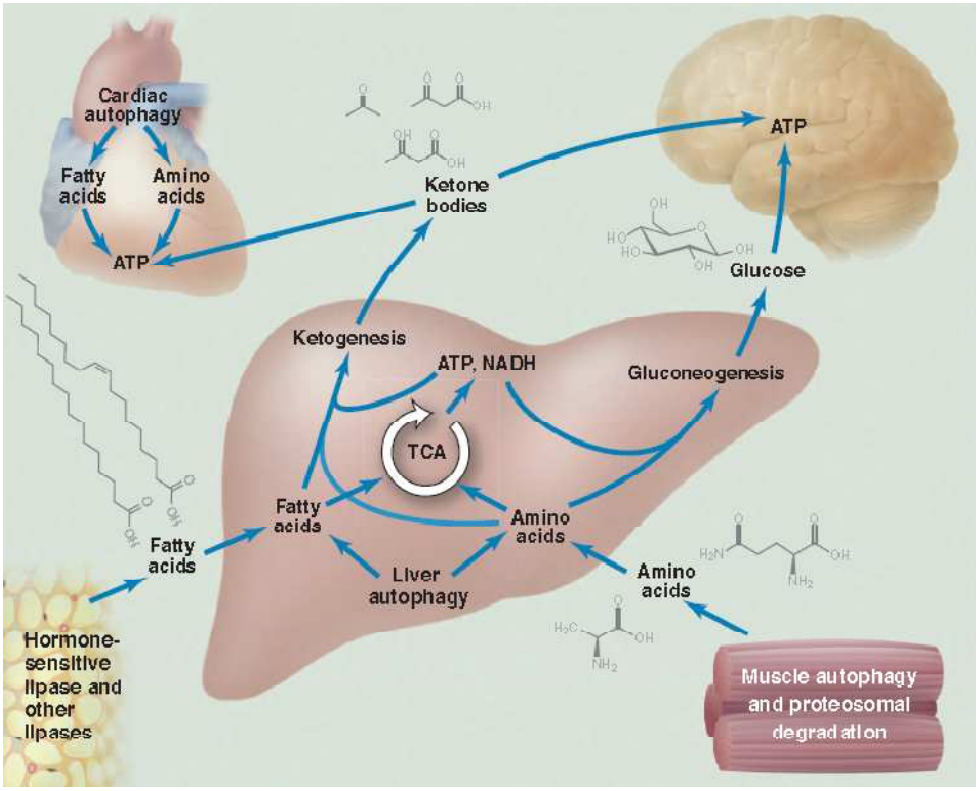

FIGURE I-2. Metabolic pathways activated during starvation. Rabinowitz and White, 2010.

Interestingly, all cells have internal nutrient stores for use during starvation. As mentioned, glycogen and lipid droplets are apparently designed for this purpose. Additionally, ribosomes may provide a store of amino acids for proteome remodeling when nutrient conditions are unfavorable. Autophagy has a key role in providing access to such nutrient stores.

1.3. CALORIC RESTRICTION

Caloric restriction (CR) refers to a dietary regime that is low in calories without malnutrition. In mammals, a characteristic set of physiological changes takes place during long-term CR, which may overlap the rapid physiological adaptations to short-term food limitation (i.e. o/n fasting). One such change is the use of dietary fat or fat mobilized from WAT for energy. Another is a large reduction in blood insulin levels accompanied by an increase in insulin sensitivity, i.e. the ability of insulin to promote glucose utilization (Weindruch and Walford, 1988). In addition, gluconeogenesis is activated in the liver. These changes keep glucose available for the brain, and are closely associated with the longevity elicited by CR.

Increasing evidence implicates mammalian sirtuins as regulators of CR-induced physiological responses, which includes lipid metabolism, glucose homeostasis, stress responses and insulin secretion (Schwer and Verdin, 2008). The mammalian Sir2 ortholog SIRT1 seems to mediate in part the physiological effects produced by CR (Guarente and Picard, 2005).

Although numerous theories have been proposed to explain how CR works, the most favored theory is that it activates a biological defense response that evolved to help organisms survive adversity (Masoro et al., 2000).

1.4. AMINO ACID DEPRIVATION

In eukaryotic cells, amino acids are required as an energy supply, as building blocks for protein synthesis, and also as signaling molecules that activate the serine/threonive kinase Target of Rapamycin (TOR). Importantly, TOR participates in the regulation of energy metabolism and protein synthesis (Kim and Guan, 2011).

In mammals, plasma amino acid concentrations may be affected by dietary or pathological conditions, such as protein undernutrition, imbalanced diet and various forms of stress as trauma or sepsis. Responses to fasting in higher eukaryotes are initiated in part by hormonal changes in response to decreasing levels not only of glucose, but also of amino

acids in the blood. Conversely, during starvation, the breakdown of protein is due largely to the reduction of the insulin/glucagon ratio. In the early stages of fasting gluconeogenic amino acids may come from rapidly turning-over tissue pools, such as the lining of the gastrointestinal tract. However, in the long term, skeletal muscle is the major supply of gluconeogenic precursors, as it is the largest protein mass in the body.

Multicellular organisms are unable to synthesize all amino acids, meaning that there are nine amino acids (valine, isoleucine, leucine, lysine, methionine, phenylalanine, threonine, histidine and tryptophan) that cannot be synthesized *de novo*, and have to be supplied by the food. Additionally, there is no important dispensable amino acid store. So, if necessary, an organism has to hydrolyze muscle protein to produce free amino acids. Because they have to regulate amino acid homeostasis accurately, mammals have evolved a wide range of adaptive mechanisms to detect and respond to fluctuations in dietary nutrients. Macrophagy in the liver is inhibited by insulin and amino acids, and stimulated by the fasting-hormone glucagon (Mizushima et al., 2004). The proper regulation of autophagy is essential to maintain cellular homeostasis.

The size of the cellular pool of each amino acid is the result of a balance between input and removal. The metabolic outlets for amino acids are protein synthesis and amino acid degradation, whereas the inputs are *de novo* synthesis (for non-essential amino acids), protein breakdown and dietary supply.

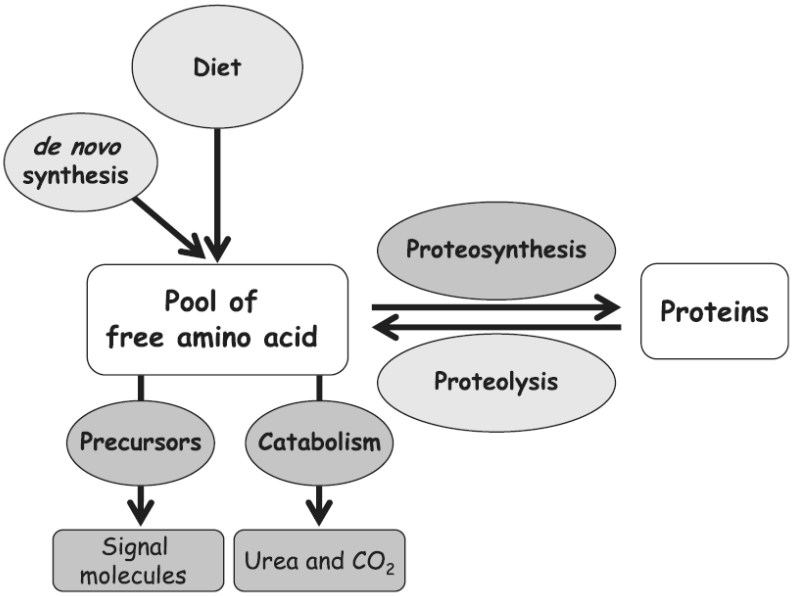

FIGURE I-3. Biochemical systems involved in the homeostasis of proteins and amino acids. Adapted from Chaveroux et al., 2010.

Animal studies have shown that rodents have several strategies for regulating the ingestion of indispensable (i.e. essential) amino acids, including an aversive behavior toward food deficient in essential amino acids (Hao et al., 2005; Maurin et al., 2005). In fact, a decline in the blood level for the deficient amino acid is correlated with a decrease in feeding (Koehnle et al., 2004), and studies have identified the anterior pyriform cortex region of the brain as the location where protein quality is detected.

In order to adapt to amino acid availability, mammals have to adjust several physiological functions. The response to amino acid deprivation in mammals is characterized by both repression of protein synthesis and upregulation of amino acid biosynthesis and transporters (Anthony et al., 2004; Averous et al., 2003; Kilberg et al., 2005). So, mammalian cells have to regulate expression of specific genes involved in transport, intermediary metabolism, oxidative stress and energy metabolism. In cultured cell lines, innumerable amino acid responsive genes have been identified (Shan et al., 2010).

One of the signal transduction pathways that is triggered in response to protein or amino acid starvation is referred to as the GCN2/eIF2α/ATF4 or the amino acid response (AAR) signal transduction pathways (Bruhat et al., 2009). GCN2 is thought to play a dual role in mammals by upregulating the synthesis of nonessential amino acids and regulating a complex array of adaptation to face the loss of essential amino acids (Anthony et al., 2004; Berlanga et al., 1999; Maurin et al., 2005; Sood et al., 2000; Zhang et al., 2002).

Recently, it was shown that GCN2 is required for inhibiting fatty acid synthesis and mobilizing lipid stores that occurs in response to leucine deprivation in mice (Guo and Cavener, 2007). These results provided new evidence that dietary amino acid availability may alter metabolic pathways beyond protein homeostasis.

2. MOLECULAR MECHANISMS REGULATING THE ADAPTATION OF METABOLIC PATHWAYS DURING NUTRITIONAL CHANGES

2.1. CREB/TORC2 SIGNAL TRANSDUCTION PATHWAY

Under low nutrient conditions, glucose supply to metabolically active tissue, such as the brain and red blood cells, is maintained via hepatic glucose production, a process termed gluconeogenesis, resulting from the transcriptional activation of gluconeogenic genes. For instance, in response to fasting, secretion of both pancreatic hormone glucagon and adrenal hormone glucocorticoid are induced to enhance hepatic glucose production (Pilkins et al., 1988). Activation of cAMP-dependent transcriptional program is mainly mediated by CREB/TORC2-dependent transcriptional machinery (Herzig et al., 2001).

The cAMP response is dependent on phosphorylation of the cAMP response element binding (CREB) protein and recruitment of the coactivators Cbp/p300 to promoters of gluconeogenic genes. However, the CREB coactivator TORC2 which acts upstream of PGC1α, is probably the main mediator of the fasting response (Koo et al., 2005).

Consistent with the finding that the gluconeogenic response is self-limiting and declines upon prolonged exposure to cAMP (Sasaki et al., 1984), it was described that TORC2 activity is tightly regulated during fasting by SIK1. This inhibitory kinase forms part of an auto-regulatory loop that attenuates the gluconeogenic programme by phosphorylating TORC2 and thus promoting its export to the cytoplasm. TORC2 activity is additionally modulated at the cellular level by AMPK (Koo et al., 2005).

The involvement of several transcription factors and coactivators in the nutritional and hormonal control of gluconeogenesis, either interacting with CREB, or binding to closely spaced cis-acting elements in regulatory regions of gluconeogenic genes, has been suggested (Matsumoto and Accili, 2006). Among them there are Foxa2, C/EBPα and HNF4α, although it remains unclear how the nutritional and hormonal status affects their activity.

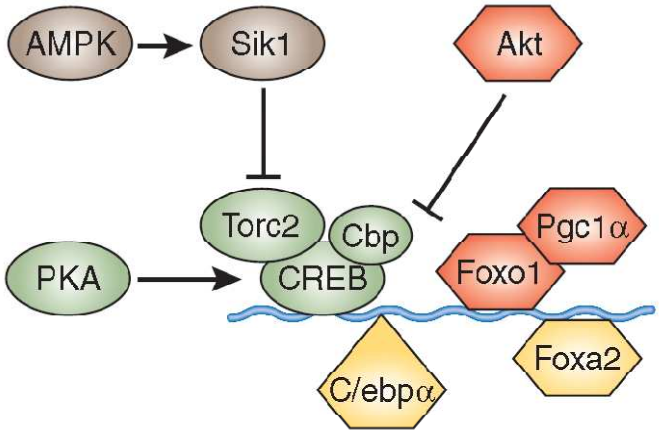

FIGURE I-4. Pathways of gluconeogenesis. The transcription factors and coactivators which were suggested to be involved are shown above the DNA double strand (in blue). Matsumoto and Accili, 2006.

Under feeding conditions, insulin is released and silences hepatic PGC1α expression and transcriptional activity, via the Akt-mediated phosphorylation and nuclear export of the forkhead family activator FOXO1, inhibiting the gluconeogenic pathway (Brunet et al., 1999; Li et al., 2007; Puigserver et al., 2003). Additionally, there is some evidence for Akt-dependent inactivation of Cbp, which may participate in turning off the cAMP response (Zhou et al., 2004). It was recently shown that CaMKII activity is increased by cAMP and glucagon and also in response to fasting *in vivo*. It was demonstrated that this calcium-sensing enzyme plays an essential role in the regulation of both glycogenolysis and gluconeogenesis, by affecting FoxO1 nuclear localization (Ozcan et al., 2012).

The cytosolic isoform of phosphoneolpyruvate carboxykinase (PEPCK-C) and glucose-6-phosphatase (G6Pase) are two rate-limiting enzymes for gluconeogenesis, transcriptionally regulated by glucagon and insulin (Sutherland et al., 1996). PEPCK-C, also known as PCK1, is also a key enzyme in glyceroneogenesis in the liver, white and brown adipose tissues and skeletal muscle (Franckhauser et al., 2002). Transcription of the gene for PEPCK-C is acutely regulated by hormones, diet and number of small effector molecules (Chakravarty et al., 2005). G6Pase catalyses the terminal step of gluconeogenesis and glycogenolysis, the hydrolysis of inorganic phosphate from glucose-6-phosphate (Van Schaftingen and Gerin, 2002).

Peroxisome proliferator activated receptor (PPAR)-gamma coactivator 1α (PGC1α) is an important factor in the regulation of metabolism. In the liver, PGC1α is upregulated during fasting and in diabetes, and it stimulates the expression of the G6Pase and PEPCK genes (Yoon et al., 2001). PGC1α contributes to the transcriptional activation of genes involved in adaptive thermogenesis, mitochondrial biogenesis, respiration, gluconeogenesis, fatty acid oxidation and ketogenesis (Finck et al., 2006; Lin et al., 2005).

2.2. FATTY ACID SIGNAL TRANSDUCTION PATHWAY

2.2.1. FATTY ACID OXIDATION

Hepatic fatty acid oxidation (FAO) is essential for example during fasting to guarantee an adequate supply of substrates that can be metabolized by other tissues. As a result of changes in the hormonal status, lipolysis of stored triglycerides (TG) in adipose tissue is robustly activated. The fatty acids (FA) released are delivered to the liver, where they are either re-esterified and secreted, or oxidized in the mitochondria (Kersten et al., 1999).

These long-chain fatty acids (LCFA) which have been released can be taken up from blood into cells passively, or via transporter proteins. Upon cellular uptake, LCFA that have accumulated in hepatocytes, are activated to acyl-CoA by cytosolic acyl-CoA synthase (ACS). The so-called carnitine shuttle or CPT system, which provides the net transport of LC acyl-CoA across the mitochondrial membranes, is composed by three proteins, carnitine palmitoyltransferase 1 (CPT1) on the outer membrane, carnitine acyl-carnitine translocase (CACT) and carnitine palmitoyltransferase 2 (CPT2) on the inner mitochondrial membrane (McGarry and Brown, 1997). In the liver, CPT1A is the primary isoform expressed, and catalyses the rate-limiting step in the entry of cytosolic LC-CoA into the mitochondria, where β-oxidation takes place, by a variety of enzymatic reactions that ultimately leads to the production of acetyl-CoA.

FFA entry into the mitochondria is a highly regulated process. During the fed state, high levels of malonyl-CoA not only inhibit β-oxidation of fatty acids by directly inhibiting CPT1, but also stimulate lipogenesis (Foster, 2004).

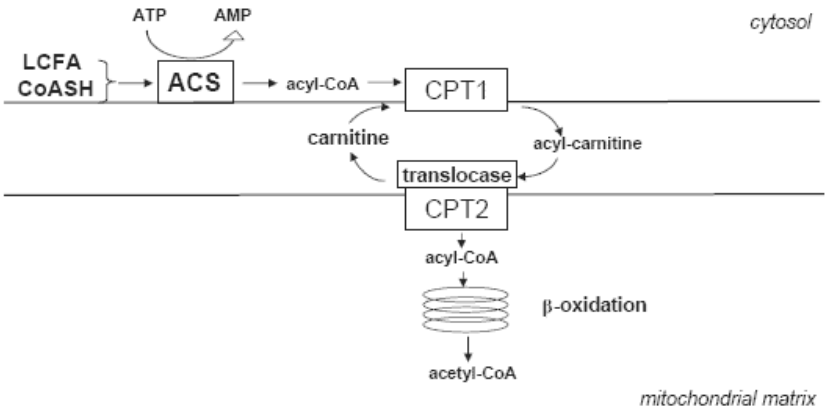

FIGURE I-5. Scheme of the transport of LCFA through the mitochondrial membrane. ACS, acyl-CoA synthetase; CoASH, free Coenzyme A; CPT1 and CPT2, carnitine palmitoyltransferase; LCFA, long chain fatty acid. Adapted from Sahlin et al., 2008.

2.2.2. KETOGENESIS

Ketogenesis is a tightly regulated metabolic pathway carried out in the liver and crucial to the supply of lipid-derived energy to the brain under normal conditions, and to peripheral tissues during starvation, sustained exercise and in diseases such as diabetes (McGarry and Foster, 1980). During a long period of starvation, the liver needs to maintain the Krebs cycle for intrahepatic ATP production and gluconeogenesis for supplying glucose to extrahepatic tissues. Because these two processes require the same intermediates, having oxaloacetate as rate-limiting, both begin to slow down. As a result, acetyl-CoA accumulates in the mitochondria (Lopes-Cardozo et al., 1975). So, through a series of condensation reactions, ketone bodies (acetoacetate, β-hydroxyutyrate and acetone) are produced in the liver from acetyl-CoA derived from the oxidation of fatty acids (Laffel, 1999), and to a lesser extent, from ketogenic amino acids. Ketone body production implies the reduction of acetoacetate to β-hydroxybutyrate with the concomitant generation of NAD^+.

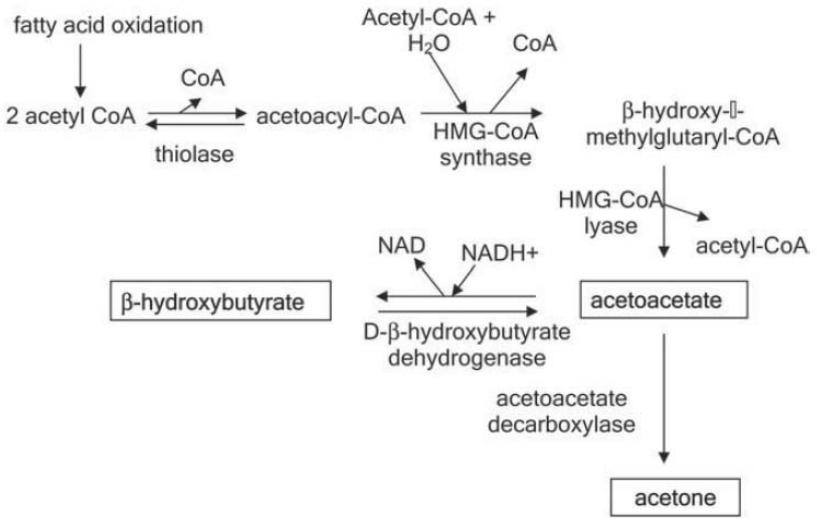

FIGURE I-6. Formation of ketone bodies within mitochondria by condensation of acetyl-CoA. The metabolic conversions of acetoacetate, β-hydroybutyrate, and acetone are also shown. Finn and Dice, 2006.

Mitochondrial 3-hydroxy-3-methylglutaryl-CoA synthase (HMG-CoA synthase or HMGCS2) is the first and rate-limiting enzyme in this pathway and it is regulated at both the transcriptional and post-transcriptional levels by mechanisms that can increase both the amount and the activity of the enzyme (Hegardt, 1998; Kostiuk et al., 2010; Quant, 1994; Shimazu et al., 2010). Specifically, results from our group revealed that the *Hmgcs2* gene contains a peroxisome proliferator response element (PPRE) in its promoter region and is under the transcriptional regulation of the peroxisome proliferator activated receptor α (PPARα) (Ortiz et al., 1999; Rodriguez et al., 1994). Fasting, cAMP, and fatty acids increase its transcriptional rate, while refeeding and insulin repress it. Results from our group have also shown that FKHRL1/FoxO3a, a member of the forkhead in rhabdosarcoma (FKHR) subclass of the Fox family of transcription factors, contributes to the regulation of HMGCS2 gene expression by insulin (Nadal et al., 2002).

2.2.3. PPARα

The peroxisome proliferator-activated receptor alpha (PPARα) is a ligand-activated transcription factor that belongs to the nuclear hormone receptor superfamily (Mangelsdorf et al., 1995). PPARα binds to characteristic PPAR response elements (PPRE), a direct repeat

of two hexanucleotides spaced by one nucleotide, as heterodimers with the retinoid X receptor (RXR) in target genes. In response to nutritional, hormonal and environmental stimuli, PPARα plays a central role in the control of lipid metabolism, including lipid transport, mitochondrial fatty acid β-oxidation and ketogenesis (Mandard et al., 2004), being crucial in the adaptive response to fasting. Its activation in liver was also shown to promote gluconeogenesis (Bernal-Mizrachi et al., 2003). In addition to upregulating gene expression, PPARα is also capable of negative modulation.

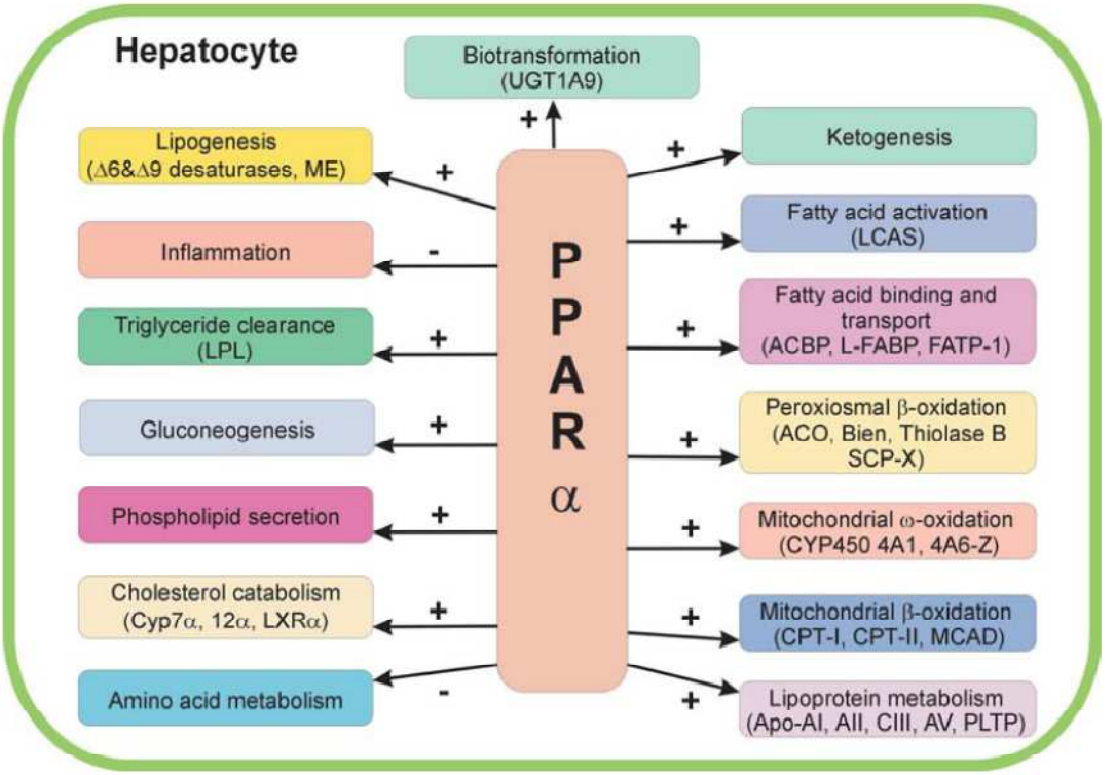

FIGURE I-7. Diverse functions of PPARα in the hepatocyte. Mandard et al., 2004.

PPARα is enriched in tissues with high oxidative energy demands that depend on mitochondrial FAO as a primary energy source, such as heart and liver. PPARα is also expressed at high levels in brown adipose tissue (BAT), a specialized tissue in which mitochondrial FAO provides the reducing equivalents necessary for the generation of heat via the uncoupling of oxidative phosphorylation (Kliewer et al., 1994).

Numerous genes involved in hepatic fatty acid oxidation were shown to be induced by PPARα. Results from our group have been relevant for the identification and

characterization of functional PPREs in key-regulatory genes. Additionally to the HMGCS2 gene, both muscle and liver CPT1 human isotypes, CPT1B and CPT1A, respectively, were identified as direct positive PPARα-regulated genes through a functional PPRE present in their promoter and first intron, respectively (Mascaró et al., 1998; Napal et al., 2005); a partially conserved PPRE was found within the CPT2 gene promoter that confers responsiveness to PPARα ligands (Barrero et al., 2003).

Initially, endogenous ligand-activation of PPARα was believed to occur primarily during fasting as large amounts of FFA released from WAT entered the blood plasma (Kersten et al., 1999; Kliewer et al., 2001). Also, clear evidence indicates that dietary FAs are able to lead to a potent activation of PPARα (Patsouris et al., 2006; Ren et al., 1997). Nevertheless, recent data suggests that PPARα in liver cannot be ligand-activated by plasma FFAs, while it can be activated by fatty acids synthesized *de novo* (Chakravarthy et al., 2005). It is proposed that fat absorbed from the diet or synthesized *de novo* via fatty acid synthase (FAS) in the liver constitutes "new" fat, capable of activating PPARα to ensure normal glucose and lipid homeostasis; whereas the fat that is derived from peripheral mobilization of adipose stores constitutes a different hepatic compartment ("old" fat) that does not seem to activate PPARα as effectively as new fat, leading to fatty liver. Additionally, because in contrast to *de novo* synthesized fat, dietary fat was shown to be inadequate for the maintenance of cholesterol homeostasis, it was also suggested the existence of different PPARα pools (Chakravarthy et al., 2005). Later, a model for the generation of an endogenous PPARα ligand in liver was proposed, where the binding of a phosphatidylcholine species (specifically 16:0/18:1-GPC) to PPARα in the nucleus, activates the transcription machinery turning on PPARα-dependent genes and affecting hepatic lipid metabolism (Chakravarthy et al., 2009).

However, if plasma FFAs, from an active lipolysis in WAT, do not activate hepatic PPARα during fasting, it is likely that PGC1α (or other coactivators) may contribute to the induction of classical PPARα target genes during fasting, via increasing PPARα-dependent binding of PGC1α to gene promoters (Rhee et al., 2003; Vega et al., 2000; Yoon et al., 2001).

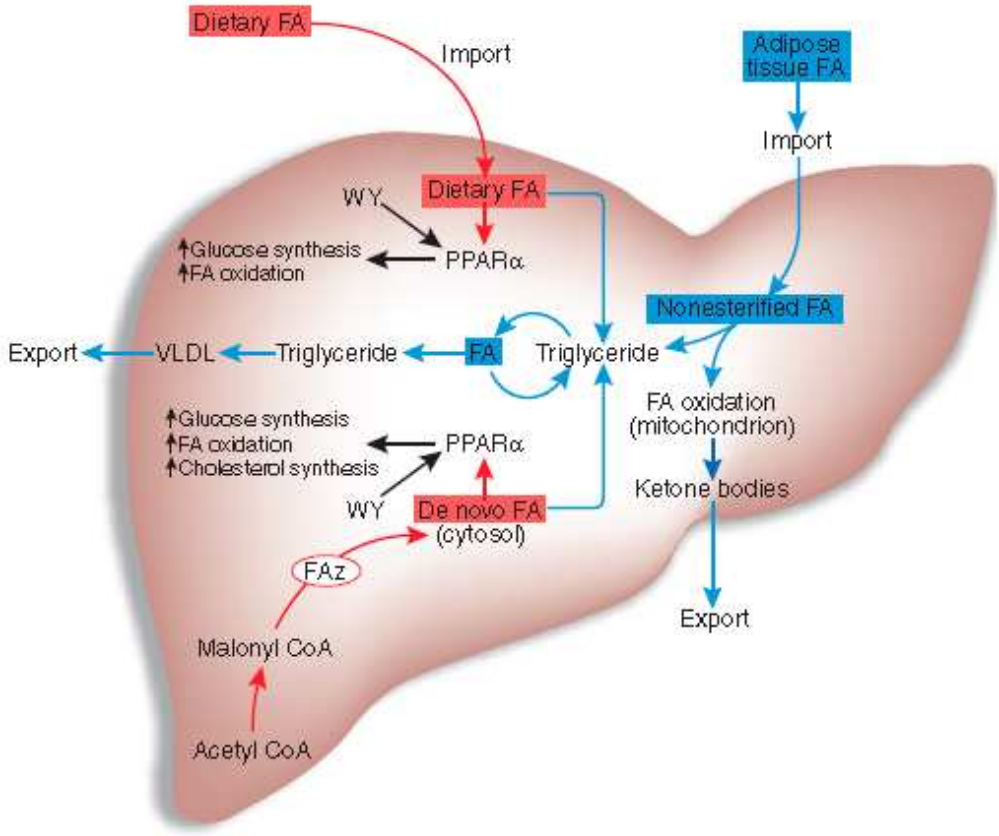

FIGURE I-8. **Fatty acid metabolism in hepatocytes, involving "new" fat (in red) and "old" fat (in blue).** Gibbons, 2005.

2.3. AMINO ACID RESPONSE (AAR) SIGNAL TRANSDUCTION PATHWAY

In the earliest steps leading to the initiation of translation in protein synthesis, amino acids are acylated to tRNA by their cognate amino-acyl tRNA synthetase enzymes. Clearly, a continuous supply of all amino acids must be available for protein synthesis to proceed. Although non-essential amino acids are continuously available, if levels of an essential (i.e. indispensable) amino acid decrease enough, its tRNA will deacylated (i.e. uncharged).

The initial step in the AAR pathway is the activation by uncharged tRNAs of the GCN2 kinase, which then phosphorylates the α subunit of translation initiation factor eIF2 (eIF2α) on serine 51 (Kimball and Jefferson, 2004; Wek et al., 2006). Phospho-eIF2α binds eIF2B in a non-functional complex and leads to a decrease in the translation of most mRNAs by

inhibiting the delivery of the initiator Met-tRNAi to the initiation complex. Hence, phospho-eIF2α suppresses general protein synthesis, but promotes a paradoxical increase in translation of a selected number of mRNAs, including that coding for the activating transcription factor 4 (ATF4), through a mechanism based on ribosome scanning and reinitiation efficiency, involving upstream open reading frames (ORFs) (Vattem and Wek, 2004). Once induced, ATF4 directly or indirectly induces transcription of a subset of specific target genes (Harding et al., 2003; Kilberg et al., 2009). In unstressed or normal growth conditions, there are low levels of translation of the ATF4 coding region, and ATF4 protein is also selectively degraded by the proteosome (Rzymski et al., 2009).

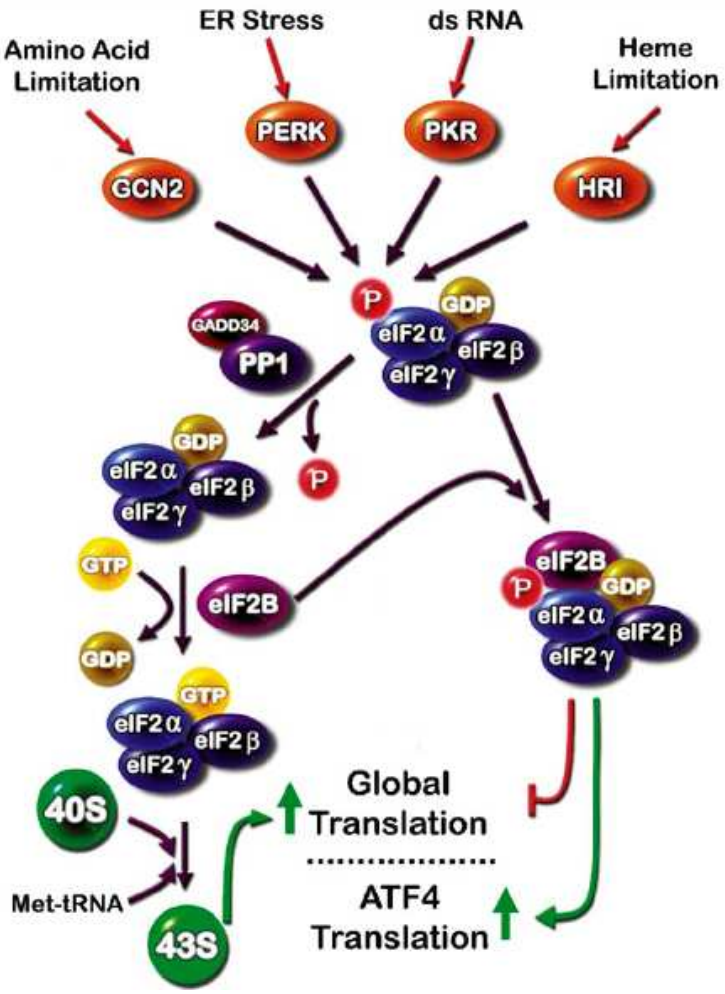

FIGURE I-9. The amino acid response (AAR) pathway. Adapted from Kilberg et al., 2009.

ATF4 is expressed in response to a variety of stress conditions by enhanced translation from preexisting mRNA (Vattem et al., 2004). GCN2 is only one of the four known eIF2α kinases, which collectively respond to a wide array of cellular stress. Other members include the protein kinase-like endoplasmic reticulum (ER)-resident kinase (PERK), the heme-regulated kinase (heme-controlled inhibitor, HRI) and the interferon-inducible, double-stranded RNA-activated protein kinase (PKR). Indeed, ER stress (Harding et al., 2000), the presence of dsDNA (Zhang et al., 2001), and heme deficiency (Zhan et al., 2002) each lead to eIF2α phosphorylation that, in turn, promotes increased ATF4 translation.

ATF4 triggers increased transcription by binding to CCAAT-enhancer binding protein-activating transcription factor (C/EBP-ATF) response elements (CARE), so named because they are composed of a half-site for the C/EBP family and a half-site for the ATF family of transcription factors, also called amino acid response elements (AARE) (Fawcett et al., 1999). Among the known ATF4-activated genes are the transcription factors C/EBPβ (Thiaville et al., 2008), ATF3 (Pan et al., 2007) and C/EBP homology protein (CHOP) (Chérasse et al., 2007), which then act as ATF4 counter regulatory signals. In fact, most of the information available concerning the regulation of gene transcription by amino acid availability in mammals has been obtained first by studying the expression of the CHOP and ASNS genes (Barbosa-Tessmann et al., 2000; Bruhat et al., 1997; Zhong et al., 2003). ATF4 has several interacting partners. Interestingly, its binding site, as well as it diverse functions, are frequently determined by its heterodimerization partners (Ameri and Harris, 2008).

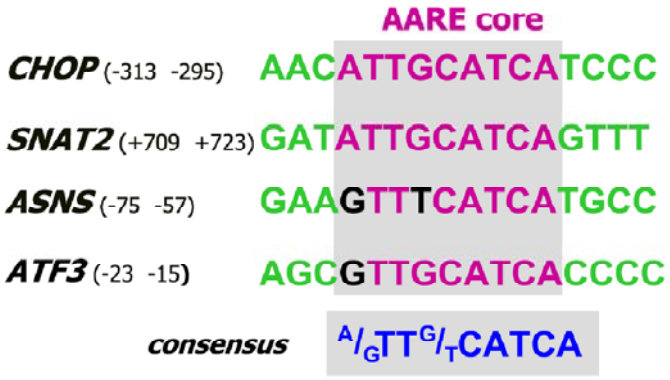

FIGURE I-10. Genomic C/EBP-ATF composite sites of ATF4-responsive genes. Chaveroux et al., 2010.

3. INTEGRATIVE MOLECULAR MECHANISMS REGULATING METABOLISM

3.1. SIRT1

SIRT1 is one of the seven mammalian orthologs (sirtuins SIRT1-7) of the yeast protein silent information regulator 2 (Sir2), a conserved NAD^+-dependent protein deacetylase, that regulates life span extension and gene silencing in yeast (Imai et al, 2000). Sirtuins are also referred to as class III histone deacetylases (HDACS). Nicotinamide adenine dinucleotide (NAD^+) is a critical cofactor for sirtuin enzymatic activity. The deacetylase catalytic domain is highly conserved within all members of mammalian sirtuins that have been described so far, which is composed of two distinct motifs that bind NAD^+ and the acetyl-lysine substrate, respectively, and is located within exons 3 through 8 (Brachmann et al., 1995; Voelter-Mahlknecht and Mahlknecht, 2006).

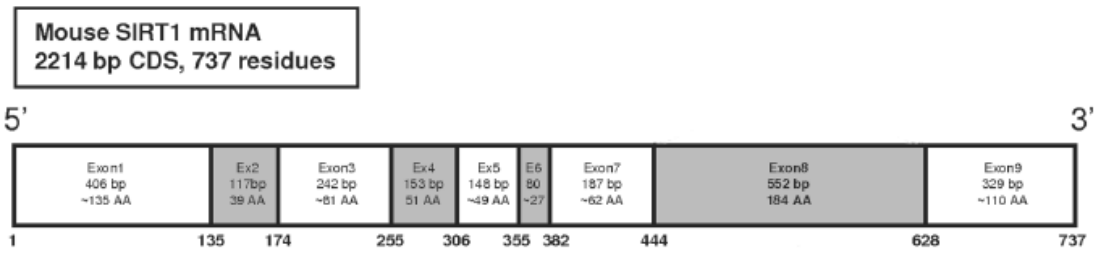

FIGURE I-11. Scheme of mouse SIRT-FL coding mRNA sequence (737 residues; based on NM_019812.2, GI: 227430307). Adapted from Lynch et al., 2010.

SIRT1 exerts its functions through deacetylation of target proteins, such as histones, transcription factors, and coregulators (Feige and Johan, 2008). SIRT1 catalyzes a reaction that couples lysine deacetylation to NAD^+ hydrolysis (Tanny et al., 2001). During this reaction, NAD^+ is hydrolyzed to nicotinamide (NAM) and O-acetyl-ADP ribose (Borra et al., 2002; Tanner et al., 2000). SIRT1 uses NAD^+ as a co-substrate to cleave the acetyl groups from target proteins. NAM is then a competitive inhibitor in the reverse reaction.

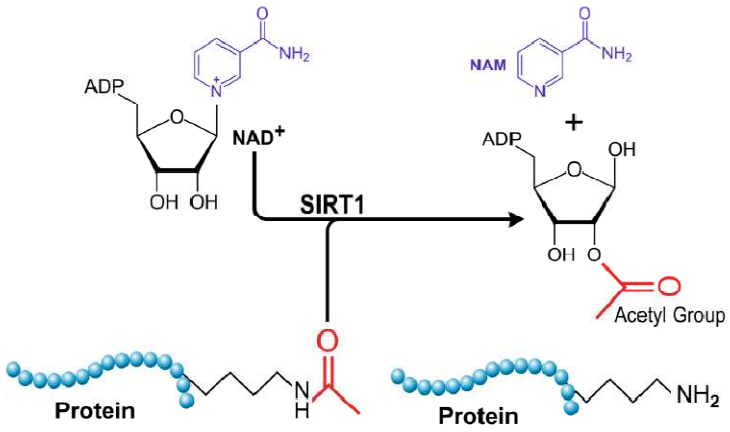

FIGURE I-12. SIRT1 deacetylation reaction. Schug and Li, 2011.

SIRT1 has emerged as a key regulator of energy metabolism. Indeed, SIRT1 modulates gene expression in metabolically active tissues, such as skeletal muscle (Gerhart-Hines et al., 2007), liver (Rodgers et al., 2005) and WAT (Picard et al., 2004) in response to lack of nutrients. SIRT1 has been found to be activated by both caloric restriction and starvation in higher eukaryotes (Cohen et al., 2004) and to trigger lipolysis and loss of fat (Picard et al., 2004), and to control glucose homeostasis (Rodgers et al., 2005). Nevertheless, SIRT1 has also been shown to control several other processes, as cell differentiation, circadian cycle, mitochondrial function, stress responses, gene silencing, senescence and cellular survival (Blander and Guarente, 2004). It has been proposed that activation of sirtuins may counteract the pathogenetic mechanisms underlying many age-related diseases (Chalkiadaki and Guarente, 2012).

Consistently, SIRT1 biological effects are mediated by its ability to deacetylate and regulate multiple substrates, including PGC1α (Rodgers et al., 2005), p53 (Luo et al., 2001), forkhead transcription factors (Brunet et al., 2004), NF-κB (Yeung et al., 2004), MyoD (Fulco et al., 2005), UCP2 (Bordone et al., 2006), and histone proteins that form the nucleosome (Imai et al., 2000; Landry et al., 2000), among others.

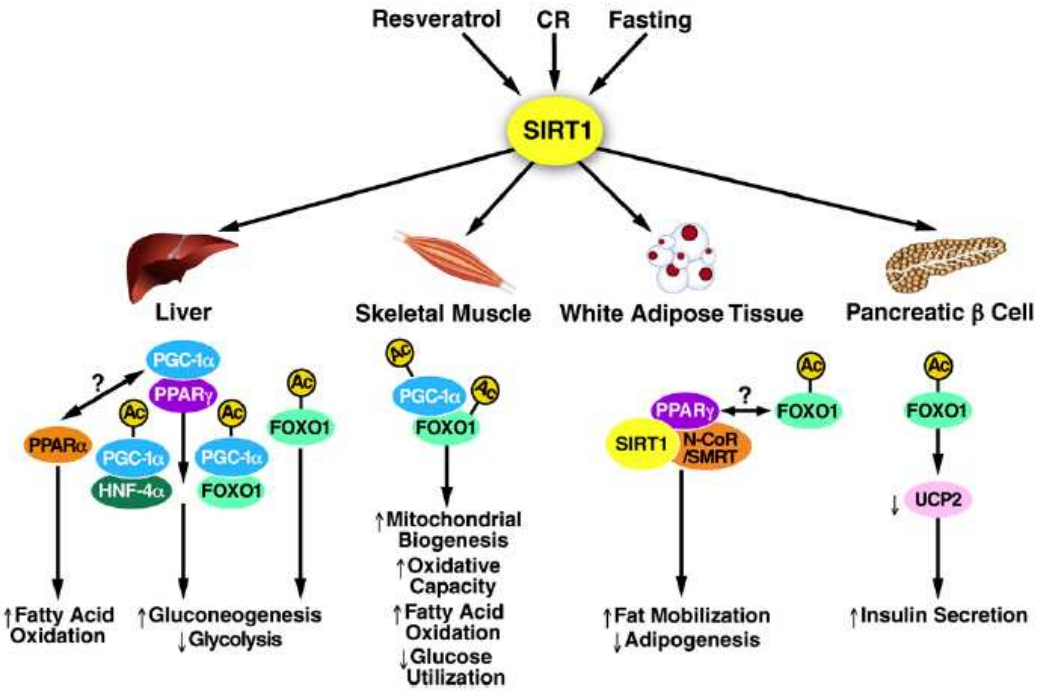

FIGURE I-13. **Roles of SIRT1 in mammalian metabolism**. Adapted from Schwer and Verdin, 2008.

Resveratrol (RVT), a polyphenol found in red wine, was described to have the ability to mimic caloric restriction, and it was suggested that it worked by direct activation of SIRT1 (Howitz et al., 2003). However, a series of studies provided some evidence that RVT was activating SIRT1 indirectly through AMPK (Cantó et al., 2010; Um et al., 2010). Recently, it was shown that RVT directly inactivates phosphodiesterase enzymes (PDEs), leading to an increase in cAMP levels and to a signalling cascade that activates SIRT1 indirectly, in a mechanism involving Epac1 (a cAMP affector protein), Ca^{2+}, AMPK and NAD^{+} (Park et al., 2012).

SIRT1 initiates the formation of the autophagy machinery by regulating the autophagosome (Lee et al., 2008). Because SIRT1-null mice normally die perinatally, there is a possibility that one of the causes is the failure to activate the autophagic process that occurs during the period immediately after birth, to support the immediate energy demands of neonates (Cheng et al., 2003; Kuma et al., 2004). Surviving SIRT1 knockout mice display severe developmental abnormalities including exencephaly (type of cephalic disorder wherein the brain is located outside the skull), sterility and heart/retinal defects (Ghosh et

al., 2008; McBurney et al., 2003; Wang et al., 2008). As a whole, these observations provide direct evidence that endogenous SIRT1 protein plays critical and specific roles during development. Therefore, tissue-specific approaches have been employed to overcome the lethality and to study SIRT1 function in adult animals: mice carrying a liver specific disruption of SIRT1 have been developed (Chen et al., 2008; Wang et al., 2010).

The SIRT1 catalytic activity dependence on NAD^+ provides a crucial link between cellular metabolic status and gene regulation (Zhang et al., 2010). Intriguingly, it was recently proposed that protein acetylation may govern how cells choose glycolytic versus oxidative metabolism as a function of the energy available, therefore helping to determine the storage or utilization of carbon energy (Guarente, 2011). For instance, diets rich in carbohydrate energy drive glycolysis, convert NAD^+ to NADH, inactivate sirtuins, and increase acetylation and activity of glycolytic enzymes. The high degree of protein acetylation in the cytosolic/nuclear pool during energy excess could then be seen as another mechanism, along with fat synthesis, of storing carbon energy. Conversely, diets poor in energy would limit glycolysis, activate SIRT1, and trigger protein deacetylation in the cytosolic/nuclear pool. Under these conditions acetate generated by SIRT1 deacetylation of many proteins would be a substrate for acetyl-CoA synthetase (ACS) to generate acetyl-CoA, that along with the oxidation of fatty acids, this would drive the TCA cycle and oxidative phosphorylation to yield ATP and CO^2. Due to its NAD^+-dependence and deacetylase activity, SIRT1 is probably the central metabolic sensor and mediator of these processes.

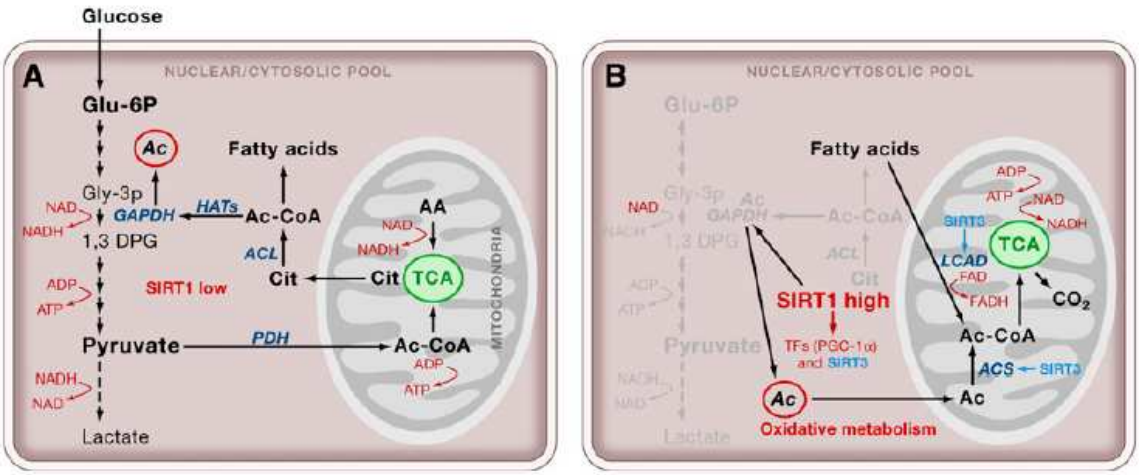

FIGURE I-14. SIRT1 as the link between acetylation and metabolism. Guarente, 2011.

3.2. FGF21

FGF21 is a member of a family of atypical fibroblast growth factors (FGFs), which include FGF19 (FGF15 in mice) and FGF23, which lack the conventional FGF heparin-binding domain (Goetz et al., 2007; Itoh et al., 2008). As a consequence, these FGFs can diffuse away from their tissues of origin and function in an endocrine fashion as hormones. FGF21 signals through cell-surface receptors composed of classic FGF receptors (FGFR) complexed with β-klotho. β-Klotho and FGFR1-4 are abundantly expressed in liver, adipose tissues, and pancreas (Kurosu et al., 2007).

Fasting remarkably increases hepatic FGF21 expression, which is known to be downstream of the nuclear receptor PPARα, which itself plays a significant role in lipid oxidation. Indeed, FGF21 is physiologically induced under conditions that activate PPARα including consumption of a ketogenic diet (KD) or fibrate treatment (Inagaki et al., 2007; Badman et al., 2007). Because FGF21 is a fasting-induced hormone that has pronounced effects on carbohydrate and fatty acid metabolism in liver, it has been proposed that FGF21 could act subsequent to glucagon during nutritional deprivation to obtain and coordinate diverse aspects of the adaptive starvation response (Potthoff et al., 2009).

In liver, FGF21 induces gluconeogenesis, fatty acid oxidation, and ketogenesis, a metabolic profile characteristic of fasting (Badman et al., 2007; Inagaki et al., 2007). FGF21 administration rapidly induces hepatic expression of PGC1α (Potthoff et al., 2009). In WAT, FGF21 stimulates glucose uptake and stimulates lipolysis (Coskun et al., 2008; Inagaki et al., 2007). However, there is still some discrepancy between results from different groups, which have observed that FGF21 suppressed lipolysis (Arner et al., 2008) in spite of increasing it. The basis for these divergences is not clear.

So, it seems that this hepatic hormone potently regulate peripheral glucose tolerance and hepatic lipid metabolism (Badman et al., 2007; Kharitonenkov et al., 2005). Other effects include sensitizing the mice to the hibernation-like state of torpor (Inagaki et al., 2007) and blunting the growth hormone (GH)-signaling pathway (Inagaki et al., 2008). FGF21 have also been shown to have the ability to protect against diet-induced obesity, improve insulin sensitivity, and reduced plasma and hepatic triglyceride concentrations in diabetic rodents and monkeys (Chavez et al., 2009; Kharitonenkov et al, 2007; Xu et al., 2009). Interestingly,

while little is known about how FGF21 regulates transcription, one of these studies has shown that the decrease in hepatic triglyceride levels was associated with a decrease in lipogenic gene expression, due to a reduction of the transcription factor SREBP1c (Badman et al., 2009; Xu et al., 2009). FGF21 also stimulates ERK1/2 phosphorylation and modulates gene expression in liver, BAT and WAT (Fisher et al., 2010).

Recently, it was shown that the full insulin sensitizing effects of the thiazolidinedione drug (TZD) rosiglitazone, a potent PPARγ agonist, require FGF21 (Dutchak et al., 2012). FGF21 stimulated PPARγ at least in part by preventing its post-translational sumoylation and inactivation. Also in WAT, FGF21 was described to promote the browning of white fat in response to cold or adrenergic stimulation (Fisher et al., 2012). So, it is suggestive to think that in WAT, FGF21 may act in an autocrine/paracrine fashion, much like canonical FGFs.

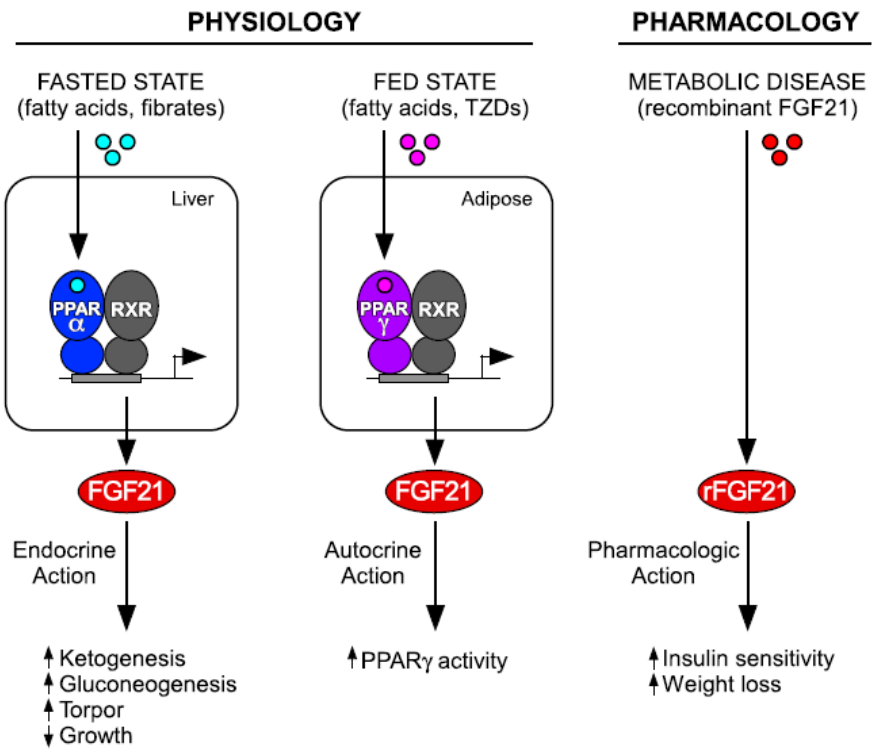

FIGURE I-15. **Endocrine, autocrine, and pharmacological actions of FGF21**. Pottoff et al., 2012.

Several studies have been performed in the last years to further elucidate the regulation of FGF21, especially in liver. As an example, hepatic FGF21 was found to be regulated by thyroid hormone (Adams et al., 2010) and it was demonstrated that RORα

regulates both the expression and secretion of FGF21 (Wang et al., 2010). Additionally, it has been proposed a negative feedback loop, where GH directly stimulates FGF21 gene transcription in the liver, at least in part, through STAT5 (Yu et al., 2012). Still, one group has suggested that FGF21 expression is regulated by the carbohydrate response element binding protein (ChREBP) and by glucose (Iizuka et al., 2009). Consistently, it has been propounded that human FGF21 is increased with nutritional crisis, including both starvation and overfeeding (Uebanso et al., 2011). In WAT, it has been described that FGF21 gene is a direct target of PPARγ (Wang et al., 2008).

Of interest, although FGF21 has become particularly promising because its potential therapeutic uses, it was shown that pharmacological doses of FGF21 induced severe bone loss, by favoring bone marrow mesenchymal cells into adipocytes, instead of osteoclasts in mice, by potentiating the activity of PPARγ (Wei et al., 2012). So, despite the rapid progress that has been made in understanding how FGF21 is regulated and FGF21's multiple actions, there is certainly much more to be learned about the physiology of this hormone.

PUBLICATIONS

AND UNPUBLISHED RESULTS

1. ROLE OF SIRT1 IN THE REGULATION OF FATTY ACID OXIDATION AND KETOGENESIS IN RESPONSE TO NUTRITIONAL CHANGES

1.1. CHARACTERIZATION OF THE SIRT1-LIVER SPECIFIC KNOCKOUT (LKO) MICE

SIRT1-liver specific KO mice express a mutant SIRT1 protein that lacks part of its catalytic domain. The exon 4 of the Sirt1 gene has been deleted by a Cre-loxP-mediated approach using an albumin-Cre transgene to generate liver-specific SIRT1 mutant mice ($SIRT1^{Exon4/Exon4}$,Alb-Cre; SIRT1-LKO hereafter) (Chen et al., 2008; Cheng et al., 2003).

We have first confirmed the liver specific SIRT1-knockout, as SIRT1-LKO liver showed the loss of the SIRT1 protein and the appearance of a slightly smaller protein missing exon 4 (SIRT1-ΔExon4) (Figure R-1A). The appearance of the conditionally deleted SIRT1 exon 4 in liver was concomitant with a relative increase in the global acetylation levels of the liver protein total extract (Figure R-1B), suggesting that SIRT1 mediated their deacetylation and confirming the importance of the missing 51 amino acids of the conserved SIRT1 catalytic domain in its deacetylase activity.

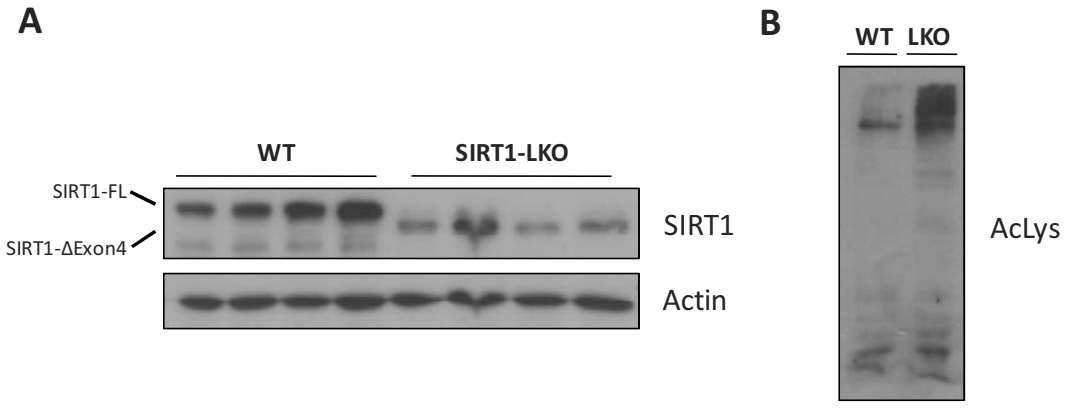

FIGURE R-1. Comparison of liver samples of wild type (WT) and SIRT1-LKO mice. (A) SIRT1 is specifically knocked out in the liver of SIRT1-LKO mice. A representative Western blot with an antibody against SIRT1 is shown. Actin was used as a loading control. (B) Hyperacetylation of proteins is observed in the liver of SIRT1-LKO mice. Proteins extracted from livers of WT and SIRT1-LKO mice were analyzed by Western blotting analysis with an antibody specific for acetylated lysine (AcLys).

1.2. REGULATION OF FATTY ACID OXIDATION AND KETOGENESIS IN THE LIVER OF SIRT1-LKO MICE ON A CALORIC RESTRICTED DIET

Because we were interested in the role of SIRT1 in the regulation of fatty acid oxidation (FAO) and ketogenesis gene expression, we have analyzed the mRNA levels of CPT1a, CPT2 and HMGCS2, and PEPCK as a control, in the liver of WT and SIRT1-LKO mice subjected to a 40% calorie restricted diet for up to 3 months (Chen et al., 2008).

There were no significant changes at the mRNA level, except for CPT1a in response to caloric restriction, between WT and SIRT1-LKO mice subject for this dietary manipulation (Figure R-2).

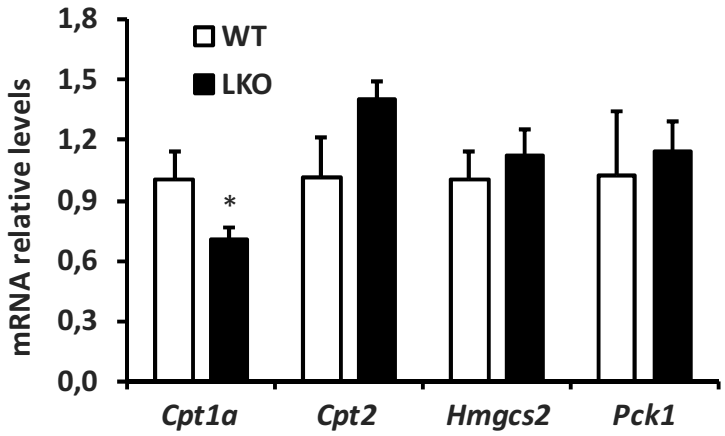

FIGURE R-2. **Fatty acid oxidation and ketogenesis key-genes respond normally to caloric resctriction, both in WT and SIRT1-LKO mice.** *Cpt1a*, *Cpt2*, *Hmgcs2* and *Pck1* mRNA levels were analyzed by real time PCR in the liver of mice subjected to caloric restriction. Results are means ± SEM each group (n=4 mice) *p<0.05 relative to WT.

1.3. ROLE OF SIRT1 IN THE REGULATION OF FATTY ACID OXIDATION AND KETOGENESIS IN THE METABOLIC ADAPTATIONS TO THE CHANGE OF NUTRITION IN EARLY AGES

SIRT1 has been shown to control hepatic glyconeogenic/glycolytic pathways in response to nutrients (Rodgers et al., 2005). So, we have hypothesized that SIRT1 could have a role in the metabolic adaptation to the changes of nutrient at weaning, when milk is replaced by the adult diet which contains less fat and more carbohydrate.

To test this hypothesis, two groups of litter pups were used. The first group was sacrificed during suckling at day 17 (D17). The second group was separated from its progenitor (weaning) at day 21 and sacrificed the following day (D22). Liver specific SIRT1-knockout was assessed by three different strategies: 1) by screening for Cre recombinase expression by PCR analysis from tail genomic DNA (Figure R-3A); 2) by checking differential migration of the PCR product amplified with primers flanking the missing exon 4 of cDNA obtained from liver (Figure R-3B); 3) by SIRT1 immunoblotting of liver total protein extracts (Figure R-3C).

The albumin promoter, which is active in both hepatoblasts and hepatocytes, have been described to have a 20-fold increase in transcriptional activity from E9.5 to E12.5 (embryonic day 9.5 and 12.5, respectively). Then, the level of albumin continues to increase as the liver develops (Cascio and Zaret, 1991). Although we have confirmed that Cre recombinase under control of the albumin promoter was expressed (Figure R-3A), complete deletion of SIRT1 exon 4 was not achieved at days neither 17 nor 22 after birth. In the corresponding Cre expressing mice there were 2 bands in the flanking exon 4 PCR analysis (Figure R-3B), and 2 bands in the Western blot (Figure R-3C). This indicates the presence of both SIRT1-full length (SIRT1-FL) and SIRT1-ΔExon4 mRNA and protein in the liver of Cre-expressing mice.

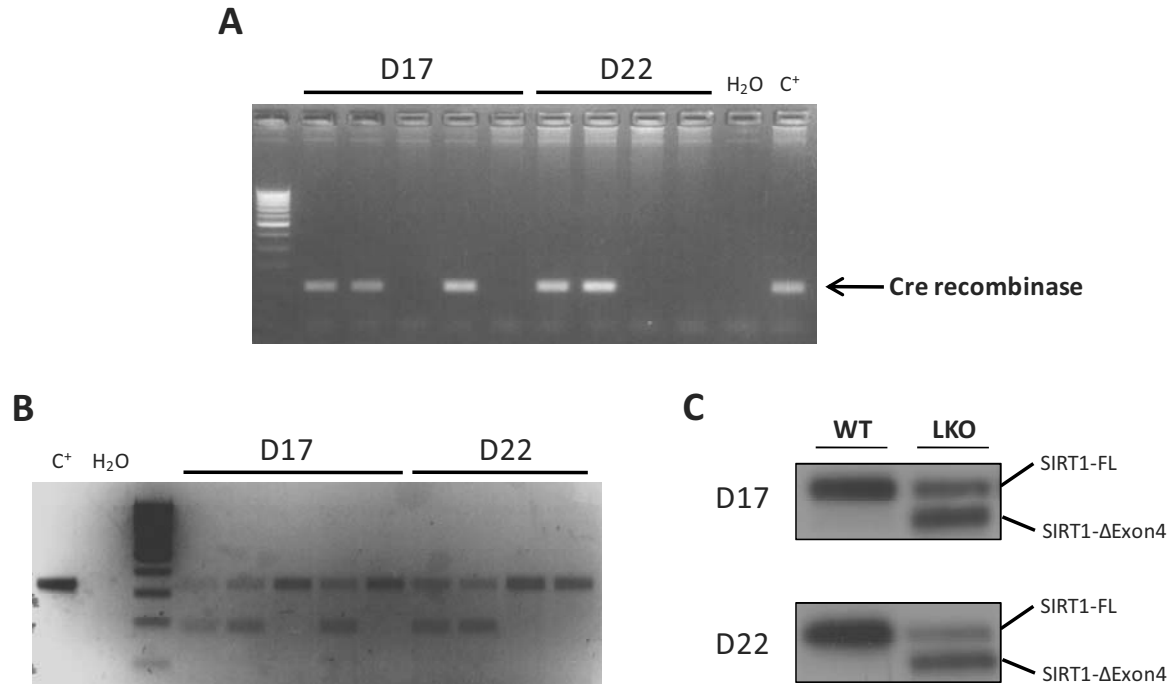

FIGURE R-3. Genotyping and analysis of the exon 4 deletion in the liver of SIRT1-LKO mice. (A) PCR analysis of the Cre recombinase in tail genomic DNA. (B) PCR analysis of the exon 4 in cDNA obtained from liver of WT and SIRT1-LKO mice. (C) Western blot with an antibody against SIRT1 of protein liver samples. D17 and D22 refer to postnatal days 17 and 22, respectively.

Even without having a 100% knockout there was a decrease in the levels of SIRT1-WT protein. So, liver mRNA levels were still analyzed. Neither fatty acid oxidation (*Cpt1a*), ketogenesis (*Hmgcs2*), nor gluconeogenic (*Pck1*) liver pathways were significantly affected by the liver-specific knockdown of SIRT1, in both suckling and post-weaning conditions (Figures R-4A, R-4B and R-4C). As expected, mRNA level of *Fas* was induced in liver after weaning, in agreement with an increase of the lipogenic rate in the liver, although there were no changes between genotypes (Figure R-4D).

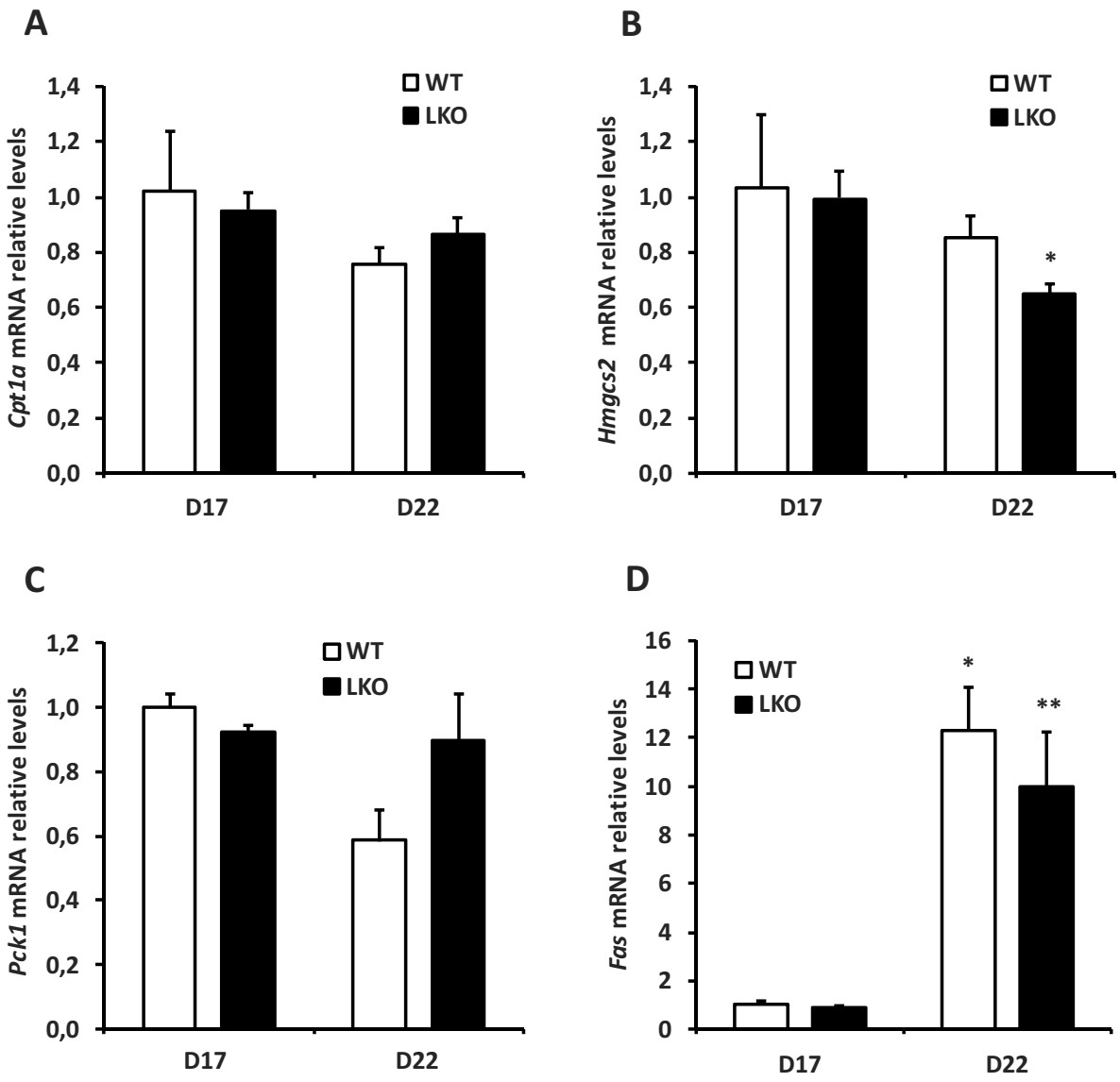

FIGURE R-4. Fatty acid oxidation and ketogenesis genes are normally expressed in both WT and SIRT1-LKO mice in early ages. mRNA expression of *Cpt1a*, *Hmgcs2*, *Pck1* and *Fas* in liver was determined using real time PCR. Results are means ± SEM each group (n=2-7 mice) *p<0.05 **p<0.01 relative to D17 correspondent genotype.

1.4. ROLE OF SIRT1 IN METABOLIC DISEASES

Sirtuins were initially found to slow aging in lower organisms and more recently shown to mediate many effects of calorie restriction on metabolism and longevity in mammals (Wood et al., 2004; Lavu et al., 2008). If SIRT1 is involved in the response to aging, old SIRT1-LKO mice might be more susceptible to age-associated metabolic diseases as obesity, type 2 diabetes, hypertension, etc.

To investigate systemic insulin sensitivity, we first weight and performed a glucose tolerance test (GTT) in 7 months-old mice. There were no differences in weight (Figure R-5A) neither in glucose tolerance between WT and SIRT1-LKO mice (Figure R-5B). However, although not statistically different, 20min after the injection, SIRT1-LKO mice showed higher glucose levels on glucose challenge than WT mice, but no further differences in the following time-response were detected.

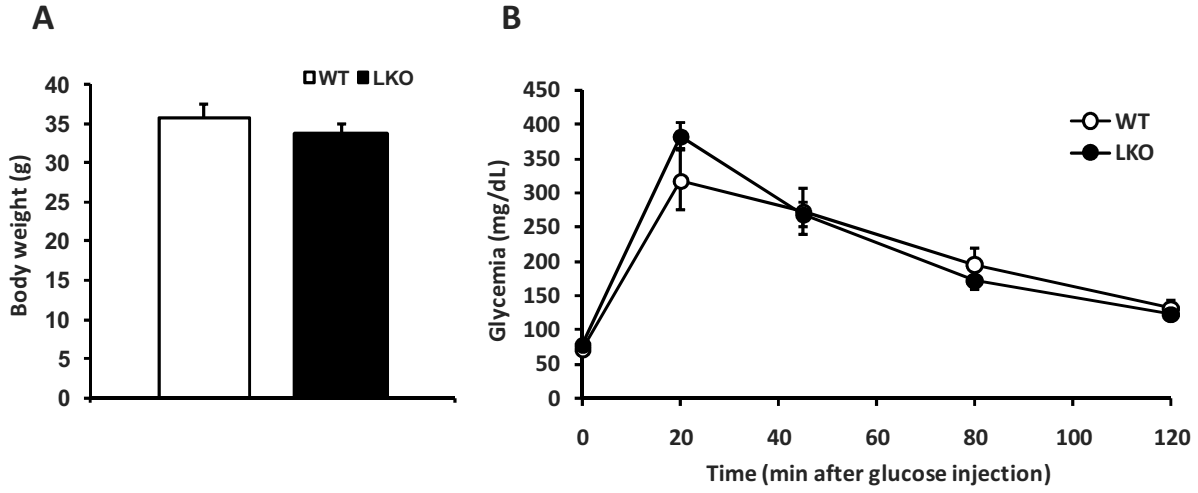

FIGURE R-5. Metabolic parameters of SIRT1-LKO aged mice show no differences in the normal aging tendency to obesity or development of glucose tolerance. 28-weeks old WT and SIRT1-LKO were weighted (A) and a glucose tolerance test (GTT) was performed (B). Results are means ± SEM each group (n=4-8 mice).

1.5. SIRT1-DEPENDENT REGULATION OF FATTY ACID OXIDATION AND KETOGENESIS BY PPARα IN HEPG2 CELLS

It was recently demonstrated that acute down-regulation of SIRT1 in mouse liver using adenoviral delivery showed increased expression of lipogenic genes, and decreased expression of genes involved in fatty acid β-oxidation (Rodgers and Puigserver, 2007). Interestingly, most of the effects of SIRT1 were only apparent in the fasted state.

We decided to use a cell system to better understand the effect of SIRT1 in the PPARα regulation of the FAO and ketogenesis key-enzymes. To have a hepatic environment a human hepatoma cell line was used. HepG2 cells were infected with adenovirus expressing human PPARα (AdPPARα) and mouse SIRT1 (AdSIRT1), and treated for 16h with 30μM WY14643, a specific PPARα ligand. Protein adenoviral-overexpression was confirmed by Western blot with specific antibodies (Figure R-6A). PPARα induced the expression of its known target genes CPT1A, HMGCS2 and FGF21, and also of PEPCK. SIRT1 overexpression by itself had almost no effect, although it increased PPARα induction of the above referred genes (Figure R-6B). The endogenous CPT1A and HMGCS2 protein levels were also induced upon PPARα and SIRT1 overexpression (Figure R-6A).

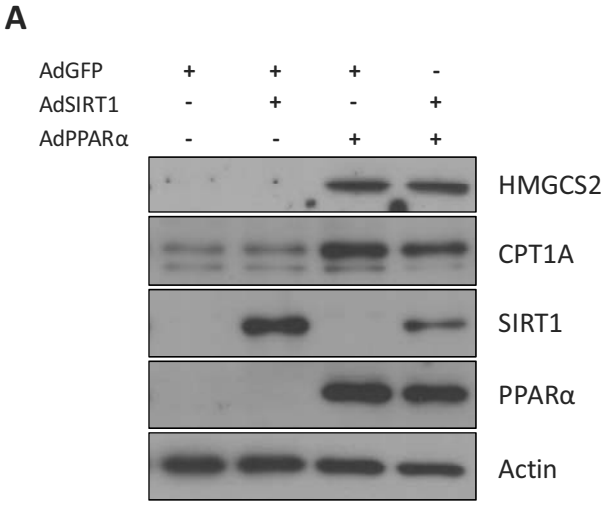

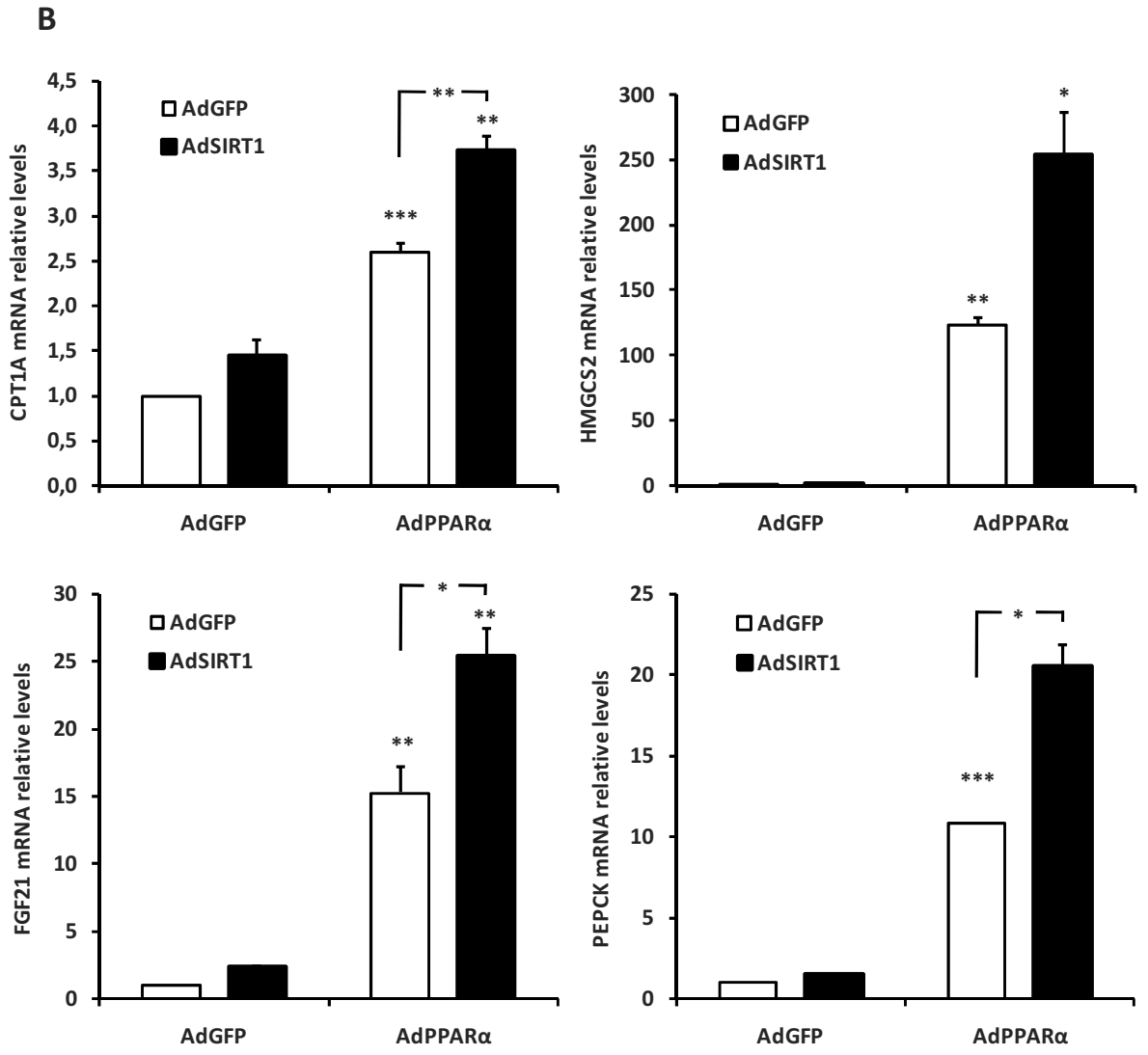

FIGURE R-6. PPARα target genes are further induced when SIRT1 is overexpressed. (A) Protein levels of overexpressed SIRT1 and PPARα, and endogenous levels of CPT1A and HMGCS2 were determined by Western blot. AdGFP was used to normalize the MOIs of the adenoviruses used. (B) mRNA expression of CPT1A, HMGCS2, FGF21 and PEPCK was determined in HepG2 cells using real time PCR. Results are means ± SEM for at least two independent experiments *p<0.05, **p<0.01, ***p<0.001.

To go further, we have interfered SIRT1 in HepG2 cells overexpressing PPARα, through a specific siRNA. SIRT1 downregulation was confirmed by Western blot (Figure R-7A). PPARα-induced expression of PEPCK and FGF21 was statistically SIRT1-dependent, as it was impaired in cells depleted form SIRT1 (siSIRT1) but not in siCtl, an unspecific siRNA used as control (Figure R-7B). Although not statistically significant, this same pattern of inhibition of the PPARα activation was also clearly observed for HMGCS2.

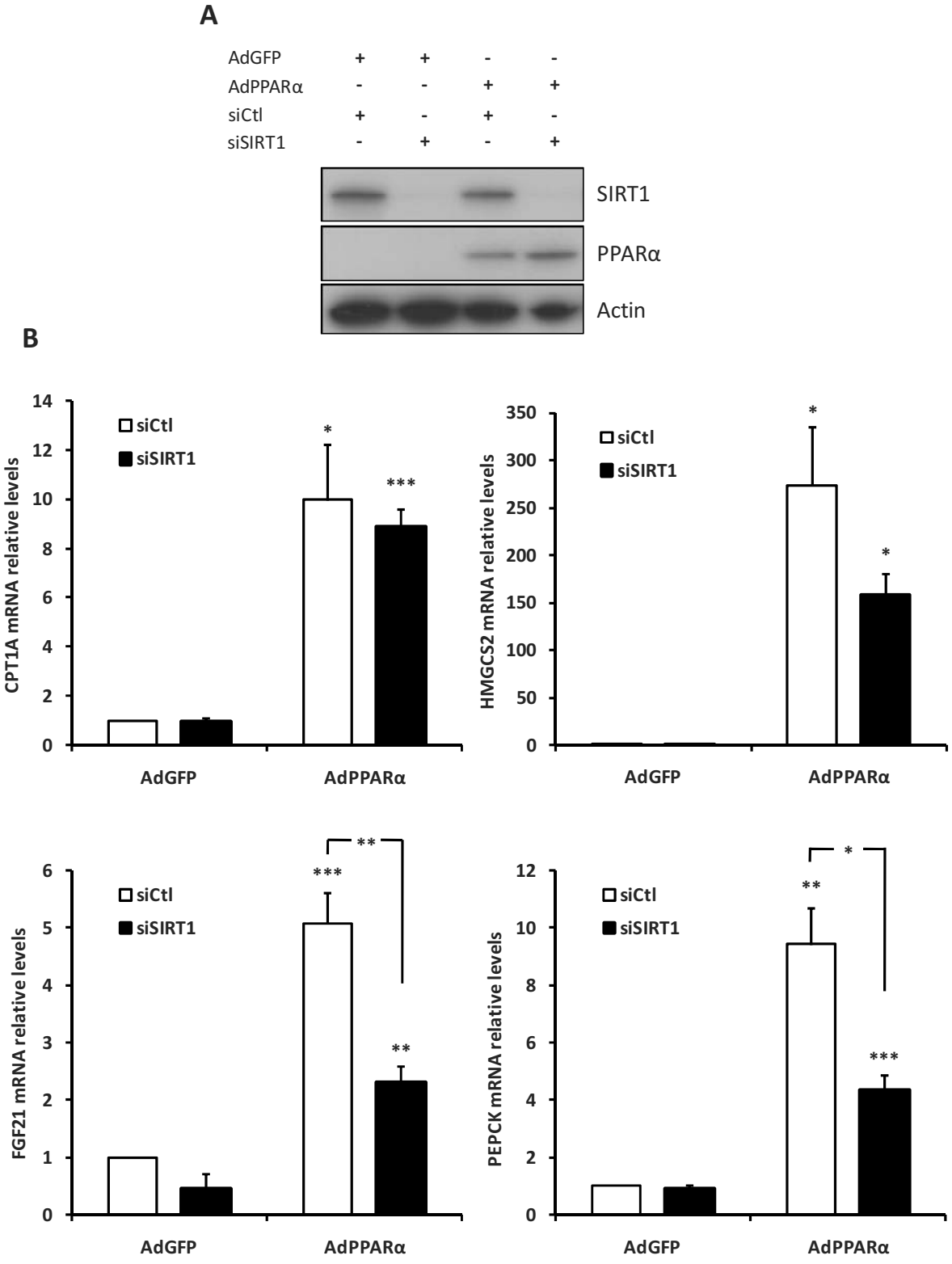

FIGURE R-7. PPARα induction of its target genes is impaired in HepG2 cells depleted from SIRT1. (A) Protein levels of endogenous SIRT1 downregulation and PPARα overexpression were determined by Western blot. (B) mRNA expression of CPT1A, HMGCS2, FGF21 and PEPCK was determined in HepG2 cells using real time PCR. Results are means ± SEM for at least two independent experiments *p<0.05, **p<0.01, ***p<0.001.

1.6. ROLE OF SIRT1 IN THE METABOLIC ADAPTATIONS TO FASTING

Fatty acid oxidation and ketogenesis are induced in fasting conditions and its key-enzymes are PPARα target genes. Based on our results in the cellular system, we hypothesized that SIRT1 deficiency would affect the fasting response of these pathways, as also of gluconeogenesis. To do so, 16 weeks-old WT and SIRT1-LKO mice were divided in two groups and sacrificed *ad libitum* (AL) or after a 15h fasting (15h Fast.).

Glycemia levels were measured and liver mRNA levels were assessed by quantitative real time PCR. We found that the expression of *Pck1*, the gene that encodes for PEPCK, was moderately but significantly induced in the liver of SIRT1-LKO mice after 15h fasting (Figure R-8B), consistent with also an increase in fasting glucose levels (Figure R-8A), possibly indicating an increased gluconeogenesis. Next, we examined the hepatic mRNA expression levels of two other cAMP-inducible genes involved in the response to fasting. Surprisingly, the mRNA levels of *G6pase*, another key-enzyme of gluconeogenesis, and of *Ppargc1α* (PGC1α), a known coactivator of the gluconeogenic program, remained unchanged (Figure R-8C and R-8D).

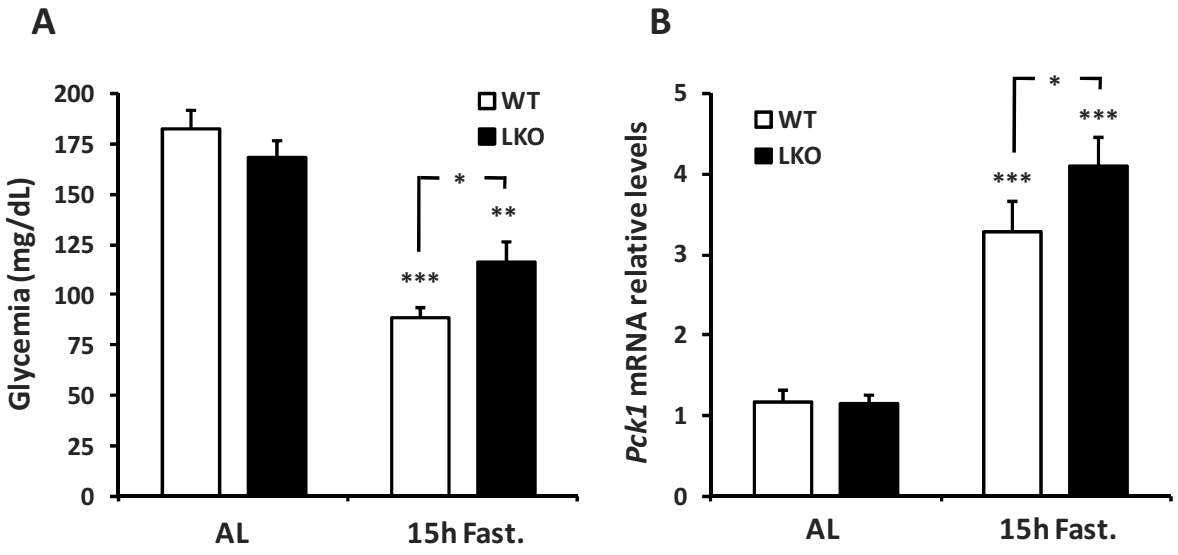

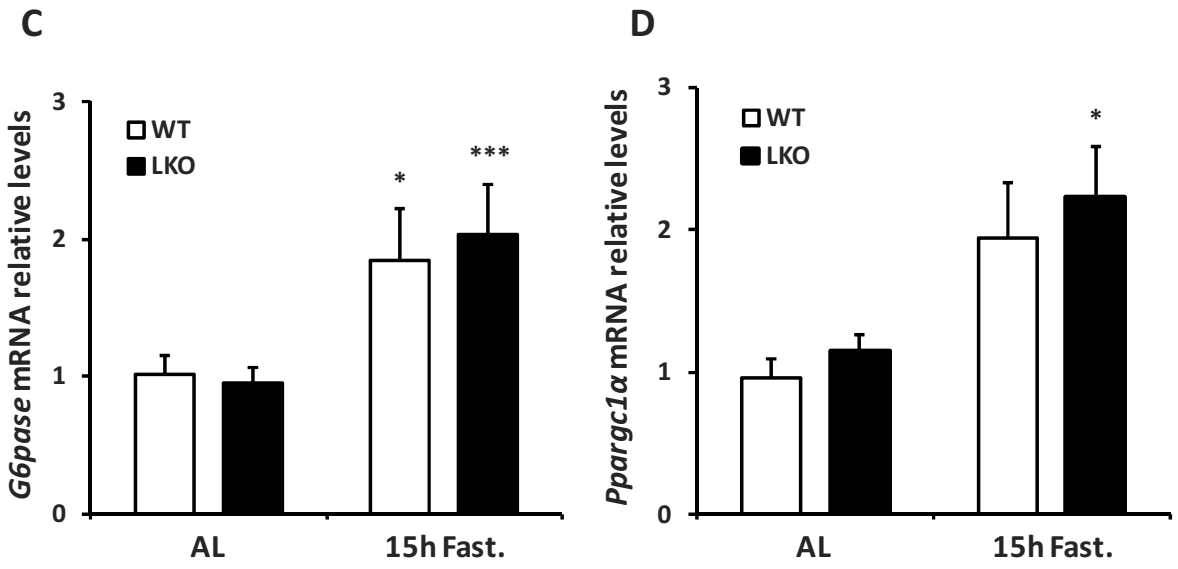

FIGURE R-8. Gluconeogenesis is slightly upregulated in SIRT1-LKO mice after overnight fasting. (A) Glucose levels were determined in blood. mRNA expression of *Pck1* (B), *G6pase* (C) and *Ppargc1α* (D) in liver was determined using real time PCR. Results are means ± SEM each group (n=5-10 mice) *p<0.05, **p<0.01, ***p<0.001 relative to *ad libitum* (AL) correspondent genotype.

2. ROLE OF SIRT1 IN THE REGULATION OF FGF21 BY HMGCS2

2.1. ARTICLE 1: **HUMAN HMGCS2 REGULATES FATTY ACID OXIDATION AND FGF21 EXPRESSION IN HEPG2 CELLS**

Journal of Biological Chemistry 286(23):20423-30, 2011.

Vilà-Brau A, De Sousa-Coelho AL, Mayordomo C, Haro D, Marrero PF.

Department of Biochemistry and Molecular Biology, School of Pharmacy and the Institute of Biomedicine of the University of Barcelona (IBUB), E-08028 Barcelona.

SUMMARY IN SPANISH (RESUMEN EN CASTELLANO):

HMGCS2 (hidroximetilglutaril CoA sintasa 2), el gen que regula la producción de cuerpos cetónicos, apenas se expresa en líneas celulares cultivadas. En este estudio, hemos restaurado la expresión y la actividad de HMGCS2 en las células HepG2. Hemos demostrado que la enzima *wild type* puede inducir a la β-oxidación de los ácidos grasos y la cetogénesis, mientras que un mutante catalíticamente inactivo (C166A) no genera ningún de estos procesos. La expresión de PPARα en estas células también induce la β-oxidación de ácidos grasos y la expresión de HMGCS2 endógena. Curiosamente, la inducción mediada por PPARα fue abolida cuando la expresión de HMGCS2 fue disminuida a través de RNAi. Estos resultados indican que la expresión HMGCS2 es suficiente y necesaria para el control de la oxidación de los ácidos grasos en estas células. Al analizar el patrón de expresión de varios genes diana de PPARα en la línea celular HepG2 "cetogénica", hemos detectado que la expresión de FGF21 fue específicamente inducida por la actividad HMGCS2, o por la inclusión de la forma oxidada de cuerpos cetónicos (acetoacetato) en el medio de cultivo. Este efecto fue anulado por el RNAi específico de SIRT1, por lo que proponemos un mecanismo dependiente de SIRT1 de la inducción de FGF21 por acetoacetato. Estos datos sugieren un nuevo mecanismo de *feedforward* por el cual HMGCS2 podría regular las respuestas adaptativas metabólicas durante el ayuno. Este mecanismo podría ser fisiológicamente relevante, ya que la inducción de FGF21 en el ayuno era dependiente de la actividad de SIRT1 *in vivo*.

THE JOURNAL OF BIOLOGICAL CHEMISTRY VOL. 286, NO. 23, pp. 20423–20430, June 10, 2011

Human HMGCS2 Regulates Mitochondrial Fatty Acid Oxidation and *FGF21* Expression in HepG2 Cell Line*

Received for publication, March 11, 2011, and in revised form, April 13, 2011 Published, JBC Papers in Press, April 18, 2011, DOI 10.1074/jbc.M111.235044

Anna Vilà-Brau[1], **Ana Luísa De Sousa-Coelho**[2,3], **Cristina Mayordomo**[3], **Diego Haro, and Pedro F. Marrero**[4]

From the Department of Biochemistry and Molecular Biology, School of Pharmacy and the Institute of Biomedicine of the University of Barcelona, E-08028 Barcelona, Spain

HMGCS2 **(hydroxymethylglutaryl CoA synthase 2), the gene that regulates ketone body production, is barely expressed in cultured cell lines. In this study, we restored HMGCS2 expression and activity in HepG2 cells, thus showing that the wild type enzyme can induce fatty acid β-oxidation (FAO) and ketogenesis, whereas a catalytically inactive mutant C166A did not generate either process. Peroxisome proliferator-activated receptor (PPAR) α expression also induces fatty acid β-oxidation and endogenous *HMGCS2* expression. Interestingly, PPARα-mediated induction was abolished when *HMGCS2* expression was down-regulated by RNAi. These results indicate that *HMGCS2* expression is both sufficient and necessary to the control of fatty acid oxidation in these cells. Next, we examined the expression pattern of several PPARα target genes in this now "ketogenic" HepG2 cell line. *FGF21* (fibroblast growth factor 21) expression was specifically induced by HMGCS2 activity or by the inclusion of the oxidized form of ketone bodies (acetoacetate) in the culture medium. This effect was blunted by SirT1 (sirtuin 1) RNAi, so we propose a SirT1-dependent mechanism for FGF21 induction by acetoacetate. These data suggest a novel feed-forward mechanism by which HMGCS2 could regulate adaptive metabolic responses during fasting. This mechanism could be physiologically relevant, because fasting-mediated induction of liver *FGF21* was dependent on SirT1 activity *in vivo*.**

The liver plays a central role in the adaptive response to fasting. The plasma hormone profile in this situation, low insulin and high glucagon, induces the release of large amounts of fatty acids from the adipose tissue to be used by peripheral tissues to spare glucose consumption. Therefore, the liver of a starved animal actively oxidizes fatty acid, which provides the energy necessary to sustain gluconeogenesis. It also supplies the acetyl-CoA needed for active ketone body synthesis, which replaces glucose as the energy substrate for the brain and other tissues (1).

Two enzymes determine the metabolic fate of fatty acids in the liver of starved animals: carnitine palmitoyltransferase-1 (CPT1) A (EC 2.3.1.21) and hydroxymethylglutaryl CoA synthase 2 (HMGCS2) (EC 4.1.3.5). *CPT1A* encodes a malonyl-CoA-sensitive protein that regulates mitochondrial long chain fatty acid oxidation (1), whereas *HMGCS2* encodes a mitochondrial protein that controls the 3-hydroxy-3-methylglutaryl-CoA (HMG-CoA)[5] cycle, by which acetoacetate, β-hydroxybutyrate, and NAD^+ are generated (2). The expression of both genes is regulated by peroxisome proliferator-activated receptor α (PPARα) (3–6), a fatty acid-activated nuclear receptor that regulates metabolic changes in the liver associated with starvation (7). Another gene directly regulated by PPARα in liver is *FGF21* (fibroblast growth factor 21), a signaling molecule induced in the ketotic state (8, 9).

Consistently, during starvation, PPARα null mice show severe hypoglycemia and hypoketonemia (7). The hypoglycemia is due to a reduced capacity for hepatic gluconeogenesis secondary to a 70% lower rate of fatty acid oxidation (10). However, the decrease in fatty acid oxidation is not due to inappropriate expression of hepatic *CPT1A*, which is similar in both genotypes, but to impaired *HMGCS2* expression in the PPARα null mouse liver (10).

It has been proposed that HMGCS2 interacts with PPARα and acts as a co-activator to up-regulate transcription from the PPRE of its own gene (11, 12). The HMGCS2-PPARα interaction is enhanced by HMGCS2 palmitoylation (12), underlying a putative mechanism by which PPARα is activated by one of its target gene products when fatty acids are available. However, this is a specific mechanism for HMGCS2, because other PPARα target genes are not co-activated by HMGCS2 expression (11).

In addition to this network of genes regulated by PPARα activation, another enzyme may contribute to the metabolic adaptation to fasting: SirT1 (sirtuin 1). This NAD^+-dependent protein deacetylase is a general regulator of energy homeostasis in response to nutrient availability (13). Hepatic deletion of *SIRT1* alters PPARα signaling, especially the induction of FGF21 mRNA by PPARα ligands (14).

A common feature in hepatoma cell lines is the low capacity for long chain fatty acid oxidation and ketone body production, which correlates with low expression of *HMGCS2* (15). Over-

* This work was supported by Grants BFU2007-67322/BMC (to P. F. M.) and SAF2010-15217 (to D. H.) from the Spanish Ministerio de Educación y Ciencia and RCMNC03/08 (to D. H.) and also by funding from the Catalan government (Ajut de Suport als Grups de Recerca de Catalunya Grants 2005SGR00857 and 2009SGR163).

[1] Supported by Scholarship from Catalan government (Ajut al Personal Investigador, FI 2007–2011).

[2] Supported by the Fundação para a Ciência e a Tecnologia through the Portuguese government.

[3] Both authors contributed equally to this work.

[4] To whom correspondence should be addressed: Departamento de Bioquímica y Biología Molecular, Facultad de Farmacia, Universidad de Barcelona, Joan XXIII s/n, E-08028 Barcelona, Spain. Tel.: 34-934034500; Fax: 34-934024520; E-mail: pedromarrero@ub.edu.

[5] The abbreviations used are: HMG-CoA, 3-hydroxy-3-methylglutaryl-CoA; 3-HB, 3-hydroxybutyrate; AcAc, acetoacetate.

expression of PPARα in HepG2 cell can restore the expression of this and other genes, and it induces fatty acid β-oxidation (6). Therefore, we examined whether PPARα-mediated expression of *HMGCS2* acts as co-activator of this process.

In this paper we show that, in HepG2 cells, wild type human *HMGCS2* expression induces both fatty acid oxidation and ketogenesis. Using shRNAs, we also show that *HMGCS2* expression is necessary for PPARα-mediated induction of fatty acid oxidation. In addition, we show that *HMGCS2* expression stimulates *FGF21* expression. We also report that *FGF21* is induced by starvation by a mechanism involving SirT1 activity. Finally, we show that these events are dependent on HMGCS2 activity, because a catalytic dead mutant (C166A) failed to induce either fatty acid β-oxidation or *FGF21* expression, whereas acetoacetate (an oxidized form of ketone bodies) can stimulate FGF21 mRNA induction by a SirT1-dependent mechanism. We propose a feed-forward model in which ketogenesis activates a SirT1-mediated response and long chain fatty acid oxidation.

EXPERIMENTAL PROCEDURES

Plasmids—pcDNA3-HMGCS2-wt was cloned by EcoRI digestion of human HMGCS2 cDNA (16) and ligated into pcDNA3. pcDNA3-HMGCS2-C166A mutant plasmid was generated from pcDNA3-HMGCS2-wt by site-directed mutagenesis using QIAquick mutagenesis kit (Qiagen) with the following oligonucleotides: forward, 5′-gataccaccaatgccgcctacggtggtactgcctcc-3′, and reverse, 5′-ggaggcagtaccaccgtaggcggcattggtggtatc-3′, following the manufacturer's instructions. For GST pulldowns, pGEX-4T-human PPARα (17) was used.

Animal Experiments—SirT1 liver-specific knock-out (SirT1-LKO) mice were a gift from Dr. L. Guarente (18). SirT1-LKO mice were generated by crossing a mice with a SirT1 allele containing a floxed exon 4 (19) with Cre-expressing mice driven by the liver-specific albumin promoter on the C57BL/6 background. All of the mice were housed in cages on a 12 h light:12 h dark cycle at controlled temperature (25 ± 1 °C).

Four-month-old SirT1 LKO mice and their age-matched littermate Lox controls ($Cre^{-/-}$, $SirT1^{flox/flox}$) were either fed *ad libitum* a standard laboratory chow diet or subjected to a 15-h overnight fast. All of the animals were sacrificed at Zeitgeber time 3 (*i.e.* 3 h after the onset of the 12-h light span). The livers were extracted and immediately snap frozen in liquid nitrogen and stored at −80 °C until analysis. Blood was collected by cardiac puncture and kept on ice until centrifugation (1500 × *g*, 15 min at 4 °C). The serum obtained was either used immediately for assays or stored at −80 °C until analysis. All of the experimental protocols with mice were performed with approval of the animal ethics committee of the University of Barcelona (Barcelona, Spain).

Cell Culture—The human hepatocellular carcinoma cells HepG2 were cultured at 37 °C in a humidified atmosphere containing 5% CO_2 in Eagle's minimum essential medium supplemented with 100 units/ml penicillin G, 100 μg/ml streptomycin, and heat-inactivated 10% fetal bovine serum. HEK293 cell line was cultured in DMEM supplemented with antibiotics and 10% fetal bovine serum. All of the cell culture products were obtained from Invitrogen. Acetoacetate and 3-hydroxybutyrate were obtained from Sigma-Aldrich.

Adenoviruses Generation—Recombinant adenoviruses were constructed as described previously (20). Briefly, cDNAs from WT and mutant forms of HMGCS2 were obtained from pcDNA3-HMGCS2-wt and pcDNA3-HMGCS2-C166A, respectively, by KpnI and XhoI digestion and cloned into pAdTrack-CMV shuttle vector. The resultant plasmid was linearized by digesting with PmeI and co-transformed into *Escherichia coli* BJ5183 cells with pAdEasy-1 plasmid, which contains the adenoviral backbone. This *E. coli* strains allows homologous recombination between both plasmids, giving rise to recombinant adenoviruses. When their identity had been confirmed by restriction endonuclease analyses, these viruses were transfected into the adenovirus packaging cell line HEK293. Recombinant adenoviruses were amplified in these cells, purified by CsCl gradient and titrated using the Adeno-X rapid titer kit (BD Biosciences). As a negative control, we generated adenoviruses expressing only GFP. The parent plasmids were a gift from B. Vogelstein (The John Hopkins Oncology Center).

Adenoviral Infection—In general, HepG2 cells were seeded 24 h before infection. The cells were infected with minimum essential medium supplemented with 10% FBS at a multiplicity of infection of 40 for 48 h.

HepG2 shRNA Stable Cell Lines—Several retroviral-based plasmids containing a shRNA to human *HMGCS2* were purchased from Origene (Rockville, MD). Scrambled shRNA was used as a negative control. The sequence of the human HMGCS2-specific 29-mer shRNA with highest efficacy reported here was CGTCTGTTGACTCCAGTGAAGCGCATTCT. Stable clones were generated using a Phoenix™ retroviral expression system (Orbigen, San Diego, CA). Briefly, Phoenix cells were seeded at 3 × 10^6 cells/100-mm plate and transfected with 10 μg of shRNA plasmids using Lipofectamine LTX (Invitrogen) according to the manufacturer's recommendations 18 h later. 48 h after transfection, retrovirus in the supernatant were harvested and filtered with a 0.45-μm low binding protein filter and added to HepG2 cells with 4 μg/ml Polybrene (Sigma Aldrich). HepG2 cells were placed under selection with 1.0 μg/ml puromycin (Sigma-Aldrich) until clones were formed. The clones were recovered with glass cylinders (Sigma-Aldrich) and split when they reached confluence. Successful knockdown of specific gene products was confirmed by Western blot.

siRNA Transfection—HepG2 cells were seeded 24 h before transfection at a density of 4 × 10^5 cells/well in 6-well plates. Specific siGENOME SMARTpool against human HMGCS2 (M-010179-01) and SIRT1 (T2004-01) were purchased from Thermo Scientific Dharmacon. siGENOME nontargeting siRNA 1 (D-001210-01-05) was used as a control. A concentration of 10 nM was transfected with Dharmafect 4 (Thermo Scientific Dharmacon) according to the manufacturer's instructions. The cells were harvested 72 h post-transfection, and successful knockdown was assessed Western blot analysis.

Mitochondria Isolation—To assay HMGCS2 activity, mitochondria were obtained from 48-h infected HepG2 cells with indicated adenoviruses. The cells were harvested in cold PBS

and centrifuged (500 × *g* for 10 min). The pellet obtained was resuspended in 0.4 ml of homogenization buffer (150 mM KCl, 5 mM Tris-HCl, pH 7.2) and lysed by 10 cycles with each of the pestles of a mechanical Douncer homogenizer. The supernatant of a first centrifugation (250 × *g* for 10 min) was submitted to a second centrifugation (16,000 × *g* for 30 min). The resulting pellet was resuspended in three volumes of resuspension buffer (0.4 mM DTT, 1.5% Triton X-100, 100 mM Tris-HCl, pH 8) and desalted through a Bio-Spin chromatography columns (Bio-Rad). Mitochondrial protein was quantified following Bradford and stored at −80 °C.

Enzymatic Activity Assay—HMGCS activity determination was carried out as described previously (21). HMGCS activity was measured as the incorporation of [1-^{14}C]acetyl-CoA into HMG-CoA at 30 °C in 10 min. The reaction was initiated by adding mitochondrial protein preparation to a reaction mixture (100 mM Tris-HCl, 1 mM EDTA, 20 μM acetoacetyl-CoA, 200 μM [^{14}C]acetyl-CoA 12,000 cpm/nmol (ITISA Biomedica)) in a final volume of 200 μl. After 10 min, the enzymatic reaction was stopped by adding 300 μl of 6 N hydrochloric acid and was incubated for 2 h at 100 °C. Radiolabeled HMG-CoA was recovered from the vials, diluted in Ecolite scintillation liquid (ICN) and counted in an automatic analyzer. HMGCS activity is expressed as nmol of produced HMG-CoA per minute.

Palmitate Oxidation—Palmitate oxidation was performed in MW24 plates as described previously (22). Briefly, the cells were incubated with 0.5 ml/well of forced medium (glucose and pyruvate-deprived DMEM containing 0.5 mM palmitate, 0.1 mM fatty acid-free BSA, 3 mM glucose, and 0.2 mM carnitine) for 16 h before the assay. Then the cells were incubated for 2 h in forced medium with radiolabeled palmitate at a final concentration of 0.5 mM (2.8 μCi/μmol [1-^{14}C]palmitate; Amersham Biosciences). The reaction was stopped with 0.7 mM perchloric acid, and radiolabeled released $^{14}CO_2$ was recovered for 1 h in Whatman paper soaked with 25 μl of β-phenylethylamine (Sigma-Aldrich). Then the trapped $^{14}CO_2$ in the Whatman paper was quantified in a scintillation analyzer. To measure the acid-soluble products, we followed the assay as described previously (23). Briefly, the cells were scrapped, neutralized with 0.5 N KOH, and incubated at 60 °C for 30 min. The medium was then acidified by the addition of 150 mM sodium acetate and 0.3 N H_2SO_4. The cells were centrifuged at 1,000 × *g* for 7 min and extracted with 1:1 chloroform/methanol. The aqueous phase was counted in a scintillation analyzer (acid-soluble product). Total palmitate oxidation was calculated as the sum of CO_2 trapped plus acid-soluble products recovered.

Ketone Body Determination—The concentration of total ketone bodies in the medium of infected HepG2 cells was determined using Autokit Total Ketone Bodies (Wako, Germany), according to the manufacturer's instructions. When the sample (medium from HepG2) is mixed with R1 (20 mM phosphate buffer, pH 7, 4.27 mM thio-NAD^+) and R2 (0.2 M Good's buffer, pH 9.0, 3200 IU/ml 3-hydroxybutyrate dehydrogenase, and 2.65 mM NADH), AcAc, and 3-HB present in the medium are converted to 3-HB and AcAc, respectively, in the presence of 3-hydroxybutyrate dehydrogenase, NADH, and thio-NAD. Then the 3-HB and AcAc produced in the enzymatic reactions are reverted to AcAc and 3-HB, again. During these cyclic reactions, NAD^+ and thio-NADH are produced. The concentration of total ketone bodies in each sample is determined by measuring the rate of thio-NADH production. Thio-NADH is measured spectrophotometrically at 405 nm using a calibration curve previously performed by plotting the absorbance corresponding to 3-HB standards of known concentrations.

Western Blot Analysis—Whole protein cell extracts were obtained from infected HepG2 cells or liver of mice. Briefly, the cells were homogenized in Nonidet P-40 lysis buffer (150 mM NaCl, 50 mM Tris-HCl, 1% Nonidet P-40) supplemented with a mixture of protease inhibitors (Sigma Aldrich) and 0.1 mM phenylmethylsulfonyl fluoride (Sigma Aldrich). Proteins from mouse liver were obtained by homogenization in radioimmune precipitation assay buffer (1% Triton X-100, 150 mM NaCl, 5 mM EDTA, 10 mM Tris, pH 7.0) containing protease inhibitor mixture (Sigma Aldrich). Protein extracts were subjected to centrifugation at 16,000 × *g* for 15 min. The supernatant (whole protein cell extract) was quantified following Bradford and stored at −80 °C. Whole protein cell extracts were loaded in a 8% SDS-PAGE gel and then transferred to Immobilon-P membranes (Millipore, Bedford, MA) and probed with different antibodies. The antibodies used were: human HMGCS2 polyclonal antibody obtained as described previously (24) or mHMGCS from Santa Cruz Biotechnologies (1:500, catalog number sc-33828); SIRT1 antibody from Upstate Biotechnologies (1:1000, catalog number 07-131) or from Santa Cruz Biotechnologies (1:500, catalog number sc-15404); PPARα antibody from Santa Cruz Biotechnologies (1:1000, catalog number sc-1985); RXRα antibody from Santa Cruz Biotechnologies (1:500, catalog number: sc-553); actin antibody from Sigma-Aldrich (1:1000, catalog number A2066); and tubulin antibody from Calbiochem (1:1000, catalog number: CP06). Detection was carried out using an ECL kit Chemiluminiscence detection kit for HRP (Biological Industries).

Immunocytochemistry—HepG2 were seeded onto coverslips (6 × 10^5 cell/p60) 24 h before infection. HepG2 cells were infected with adenovirus, as indicated in the figure legends, and after 48 h of infection they were fixed with 4% paraformaldehyde. Antibody staining on fixed cells was done using a standard protocol. The cells were permeabilized using 0.1% Triton X-100 (Sigma Aldrich). The primary antibodies used were goat anti-PPARα (1:1000, Santa Cruz Biotechnologies, sc-1985) and rabbit anti-HMGCS2 (1:100, Santa Cruz Biotechnologies, sc-33828). Secondary antibodies were obtained from Invitrogen: Alexa Fluor® 488 donkey anti-goat IgG (H+L) *2 mg/ml (1:1000), Alexa Fluor® 647 chicken anti-rabbit (H+L) *2 mg/ml (1:500). DAPI (6.25 μg/ml; Sigma) was used to label DNA. Fluorochrome-labeled samples were analyzed and captured using a Leica SP2 confocal microscope. Final artwork was processed using ImageJ software.

Pulldown Assay—GST and GST-PPARα fusion proteins were produced in *E. coli* and purified on glutathione-Sepharose beads (Amersham Biosciences), as described previously (17). The amount and integrity of GST was checked by SDS-PAGE and Coomassie Blue staining. 250 μg of whole cell protein extracts from HepG2-infected cells were incubated in the presence of equivalent amounts of immobilized GST or GST-PPARα (12.5 μg) in 1 ml of binding buffer NETN (20 mM Tris,

pH 8, 100 mM NaCl, 1 mM EDTA, 0.5% Nonidet P-40), supplemented with 0.5% nonfat milk, protease inhibitor mixture (Sigma), and 1 mM DTT for 4 h at 4 °C with agitation. The samples were then centrifuged for 1 min at 500 × *g*, and the resin was washed twice in NETN at room temperature. After that the samples were boiled, mixed with 2× Laemmli buffer and resolved by SDS-PAGE in a 8% polyacrylamide gel. Bound proteins were detected by immunoblot using anti-HMGCS2 (24) or RXRα antibody from Santa Cruz Biotechnologies (1:500, catalog number sc-553).

Real Time RNA Analysis—Total RNA was extracted from cells or liver by Tri-Reagent (Ambion) and was further treated with DNase I (Ambion). For real time PCR analysis, cDNA was synthesized from total RNA by murine leukemia virus reverse transcriptase (Invitrogen) with random hexamers (Roche Diagnostics). cDNA was subjected to PCR real time analysis using TaqMan universal PCR master mix (Invitrogen catalog number 11743) and the specific gene expression primer pair TaqMan probes from Applied Biosystems (for HepG2, human gene probes were used: FGF21, Hs00173927_m1; CPT1A, Hs00157079_m1; HMGCS2, Hs00985427_m1; cytosolic phosphoenolpyruvate carboxykinase 1, Hs00159918_m1; CPT2, Hs00988962_m1; and PPARα, Hs00231882_m1; for mice experiments, mouse probes were used: HMGCS2, Mm00550050_m1; FGF21, Mm00840165_g1; CPT1A, Mm00550438_m1; and SIRT1, Mm00490758_m1). Relative mRNA abundance was obtained by normalizing to 18 S levels (Applied Biosystems).

Measurement of Serum FGF21—Mouse FGF21 ELISA kit was obtained from Millipore (catalog number EZRMFGF21-26K) for the quantification of FGF21 in mice serum. The assay was conducted according to the manufacturer's protocol. Briefly, a calibration curve was constructed by plotting the difference of absorbance values at 450 and 590 nm *versus* the FGF21 concentrations of the calibrators, and concentrations of unknown samples (performed in duplicate) were determined by using this calibration curve.

Statistical Analysis—The data are expressed as the means ± standard deviation. The significance of differences was determined using SPSS statistical software (SPSS Worldwide Headquarters, Chicago, IL). $p < 0.05$ was considered statistically significant.

RESULTS

Human HMGCS2 Expression Induces Fatty Acid Oxidation and Ketogenesis in HepG2 Cell Line—Wild type or a mutant form of HMGCS2 enzymes and human PPARα were expressed in HepG2 cell line by using adenoviral vector systems. The HMGCS2 C166A mutant was predicted as a dead enzyme because an equivalent cysteine residue 129 has been characterized as the catalytic site in the homologous HMGCS1, the cytosolic enzyme involved in cholesterol synthesis (25, 26). Fig. 1 shows recombinant expression of human HMGCS2 in terms of activity (Fig. 1*A*) and protein (Fig. 1*C*, *bottom panels*) levels. The HMGCS2 enzymatic activity (approximately 0.5 milliunit/mg) that was achieved from adenoviruses-mediated expression was similar to that observed in liver mitochondria from feed mouse (data not shown and Ref. 27). Fig. 1*A* also shows that the

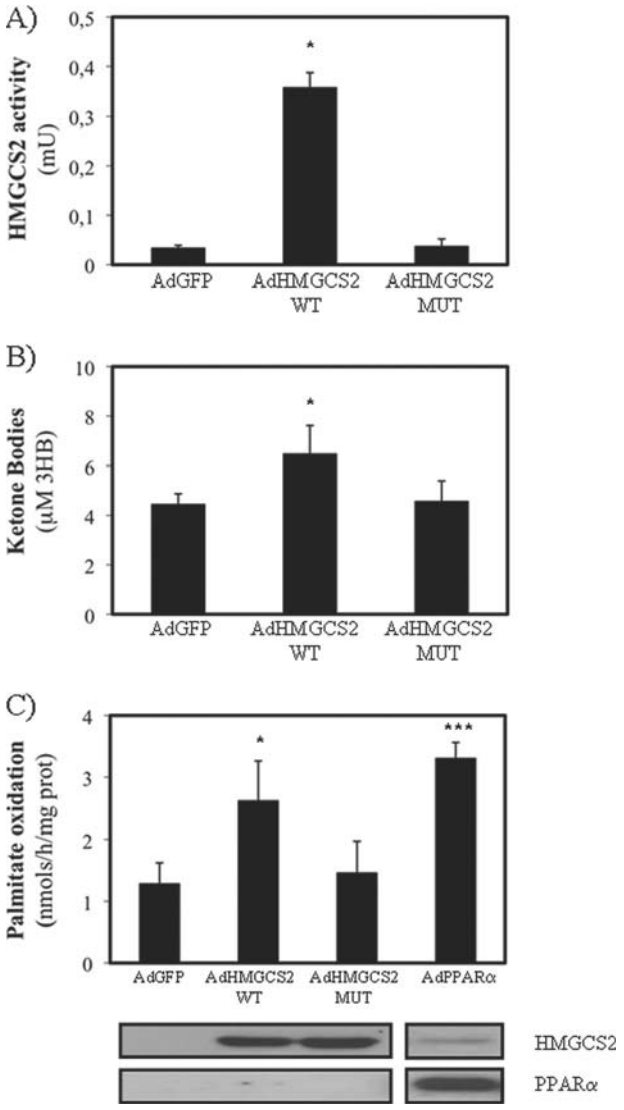

FIGURE 1. **Effect of wild type or mutant HMGCS2 expression on activity, ketogenesis, and fatty acid β-oxidation.** HepG2 cells were infected with adenovirus control (*AdGFP*) or expressing wild type (*AdHMGCS2 WT*) or C166A mutant (*AdHMGCS2 MUT*) human HMGCS2 for 48 h. *A*, enzymatic activity was measured in dialyzed mitochondria preparation. *B*, total ketone bodies were determined in the medium. *C*, total [^{14}C]palmitate oxidation was measured in HepG2 cells infected with adenoviruses expressing human HMGCS2 variants or human PPARα (*AdPPARα*). The average of three independent experiments is shown. The *bottom panel* shows a representative Western blot of recombinant PPARα and recombinant (*left*) or endogenous (*right*) HMGCS2. 10 μg of whole cell extract were loaded to show recombinant HMGCS2 expression, and 70 μg were loaded to show endogenous HMGCS2. *, $p < 0.05$, ***, $p < 0.001$.

C166A mutant (AdHMGCS2 MUT) expresses an inactive HMGCS2 enzyme. Fig. 1*B* shows that expression of HMGCS2 was sufficient to induce ketone body production by the HepG2 cells, and as expected, the expression of the dead enzyme lacks this ability. Interestingly, Fig. 1*C* shows that recombinant expression of human HMGCS2 was also sufficient to induce fatty acid oxidation. Fig. 1*C* also shows that the induction of β-oxidation mediated by HMGCS2 expression is similar to the induction mediated by PPARα expression that, as expected (6), also induces HMGCS2 protein levels (Fig. 1*C*, *bottom panels*) and HMGCS2, CPT1a, and FGF21 mRNA levels (Table 1). These data suggest that expression of HMGCS2 in HepG2 cell

TABLE 1

mRNA induction of different PPARα target genes

HepG2 cells were infected with adenovirus expressing human PPARα or human wild type or C166A mutant of HMGCS2. The mRNA levels were determined by real time PCR. The data represent the fold of induction of the specific mRNA after adenovirus infection of at least three independent experiments. PCK1, cytosolic phosphoenolpyruvate carboxykinase; ND, not determined.

	AdPPARα	AdHMGCS2 WT	AdHMGCS2 MUT
HMGCS2	45.0 ± 15.7[a]	ND	ND
CPT1A	2.74 ± 0.9[b]	1.27 ± 0.7	0.86 ± 0.2
CPT2	7.35 ± 5.1	ND	ND
PCK1	5.95 ± 3.3[b]	ND	ND
FGF21	15.4 ± 5.8[b]	3.3 ± 1.03[b]	1.0 ± 0.3
PPARα	ND	1.41 ± 0.2	1.61 ± 0.3

[a] $p < 0.001$.
[b] $p < 0.05$.

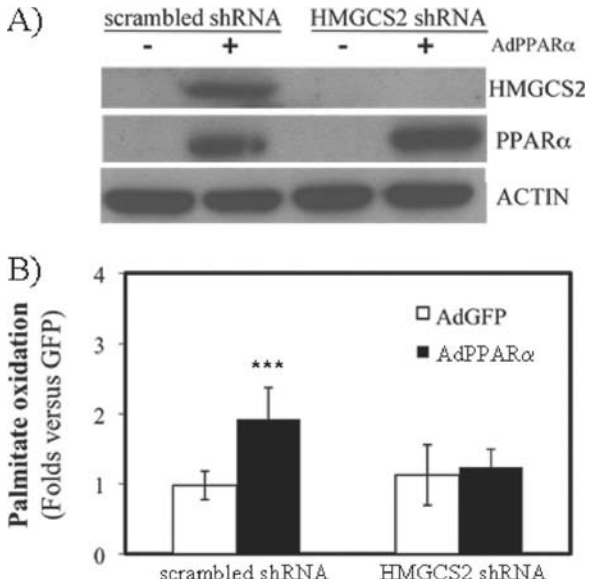

FIGURE 2. **Effect of HMGCS2 expression on PPARα-mediated induction of fatty acid β-oxidation.** HepG2 stable cell lines expressing a shRNA control (scrambled shRNA) or a shRNA specific for HMGCS2 were infected with human PPARα expressing adenovirus (*AdPPARα*). *A*, representative Western blot analysis of recombinant PPARα, endogenous HMGCS2, and actins as loading control. 70 μg of whole cell extract were loaded. *B*, total [^{14}C]palmitate oxidation was measured in HepG2 cells expressing (scrambled shRNA) or not expressing (HMGCS2 shRNA) HMGCS2. The results are expressed in PPARα fold induction *versus* GFP infection. The average of three independent experiments is shown. ***, $p < 0.001$.

line is sufficient to restore the HMG-CoA cycle (28) and that activation of ketogenesis from acetyl-CoA in turn activates fatty acid β-oxidation.

Human HMGCS2 Expression Is Necessary for PPARα-mediated Induction of Fatty Acid Oxidation—PPARα expression in HepG2 cells induces both HMGCS2 and mitochondrial fatty acid oxidation (6). Therefore, we hypothesized that active ketogenesis could be necessary for PPARα-mediated induction of fatty acid β-oxidation. Fig. 2*A* shows that a specific shRNA abrogated HMGCS2 induction mediated by PPARα. Fig. 2*B* shows that β-oxidation induction mediated by PPARα was blunted by down-regulation of HMGCS2 expression. These data suggest that PPARα induces fatty acid oxidation but importantly that the expression of the ketogenic key enzyme HMGCS2 is needed for the induction.

HMGCS2 Regulates FGF21 Expression in HepG2 Cell Line—The effect of HMGCS2 on PPARα-mediated stimulation of fatty acid oxidation could be mediated by direct HMGCS2 co-

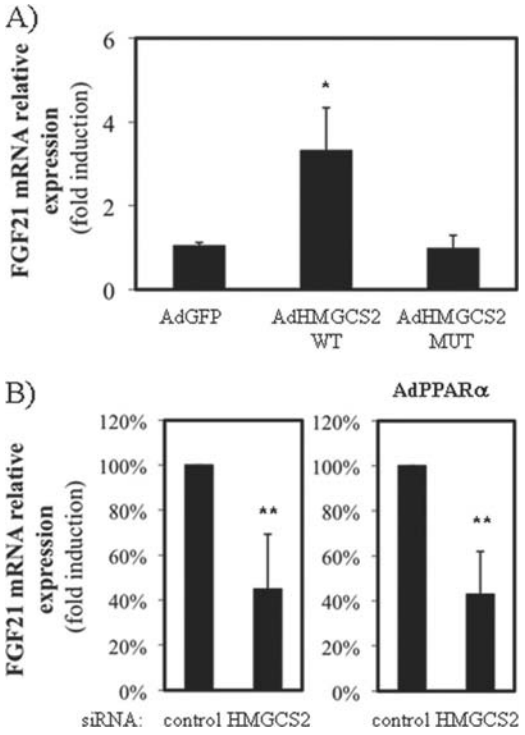

FIGURE 3. **HMGCS2 regulates FGF21 expression in HepG2 cell line.** *A*, FGF21 mRNA levels of cells infected with adenoviruses expressing GFP (*AdGFP*), wild type (*AdHMGCS2 WT*), or C166A dead mutant (*AdHMGCS2 MUT*) human HMGCS2. *B*, FGF21 mRNA levels of HepG2 transfected with siRNA control siRNA (nontargeting) or specific siRNA against HMGCS2 and infected with adenoviruses expressing GFP (*left panel*) or human PPARα (*AdPPARα*; *right*) is shown. The results are expressed as the percentages of induction by PPARα in the presence of HMGCS2 (100%) or in the absence of HMCGC2. The average of five independent experiments is shown. *, $p < 0.05$, **, $p < 0.01$.

activation (11, 12) or a metabolic effect driven by stimulation of fatty acid degradation (Fig. 2). Therefore, we analyzed the effect of HMGCS2 expression on PPARα target genes. Fig. 3*A* shows that overexpression of HMGCS2 induced FGF21 expression and that catalytic activity of the enzyme was needed for this mRNA induction. Fig. 3*B* shows that knockdown of HMGCS2 down-regulated FGF21 mRNA levels in the absence (Fig. 3*B*, *right panel*) or presence (Fig. 3*B*, *left panel*) of PPARα. This effect was specific for FGF21, because the mRNA levels of other PPARα target genes were not affected by HMGCS2 expression (Table 1).

To follow the activator effect of HMGCS2, we performed luciferase promoter assays in which no co-activation by HMGCS2 was observed on PPARα mediated-induction of CPT1a or HMGCS2 promoters (data not shown). These data are consistent with the lack of nuclear co-localization of recombinant PPARα and endogenous HMGCS2 shown by immunohistochemistry analysis in HepG2 cells (Fig. 4*A*). In addition, pulldown experiments showed that no interaction of HMGCS2 overexpressed in HepG2 with the GST-PPARα purified protein that can interact with its RXRα partner (Fig. 4*B*). These results indicate that the effect on FGF21 expression observed in HepG2 cells was not related to co-activation of PPARα by HMGCS2.

FGF21 Is a SirT1 Target Gene during Fed-to-Fast Transition—An alternative metabolic hypothesis for HMGCS2 stimulation of FGF21 is that the effect of HMGCS2 on ketogenesis and

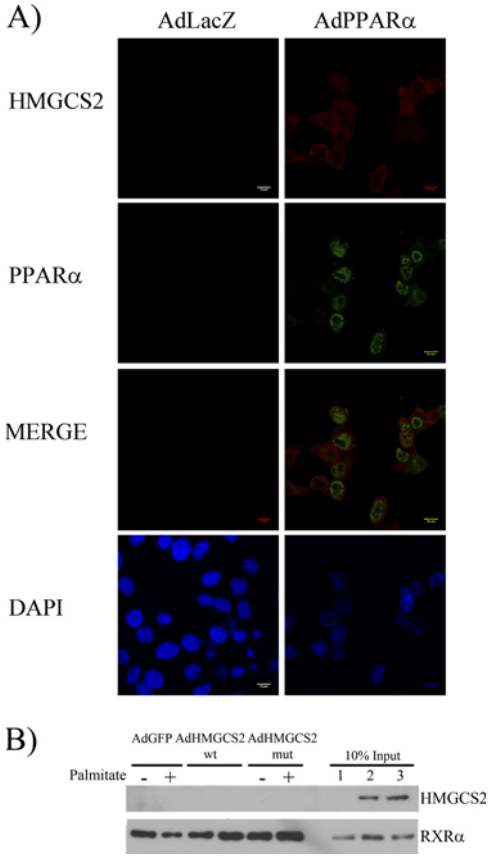

FIGURE 4. **Recombinant PPARα does not co-localize nor interact with endogenous HMGCS2.** *A*, immunohistochemical analysis of recombinant PPARα and endogenous HMMGCS2 expression in HepG2 cell. Cells infected with adenovirus control (*AdLacZ*) or adenovirus encoding human PPARα (A*dPPARα*)) were fixed and stained with DAPI and incubated with anti-PPARα or anti-HMGCS2 antibody followed by Alexa Fluor 488 or Alexa Fluor 647, respectively, and viewed with a confocal microscope. *B*, pulldown experiment of recombinant GST-PPARα. HepG2 cells were infected with adenoviruses expressing GFP (*AdGFP*), wild type (*AdHMGCS2 WT*), or C166A dead mutant (*AdHMGCS2 MUT*) human HMGCS2 were treated (+) or not (−) with palmitate 0.5 mm for 16 h. Whole protein cell extracts of the infected HepG2 cells were incubated with GST-PPARα generated in *E. coli*. GST recombinant protein was captured by glutathione-Sepharose beads, and the recovered beads were immunoblotted with anti-HMGCS2 and RXRα antibodies. Inputs show endogenous RXRα and recombinant HMGCS2 variants in whole protein cell extracts.

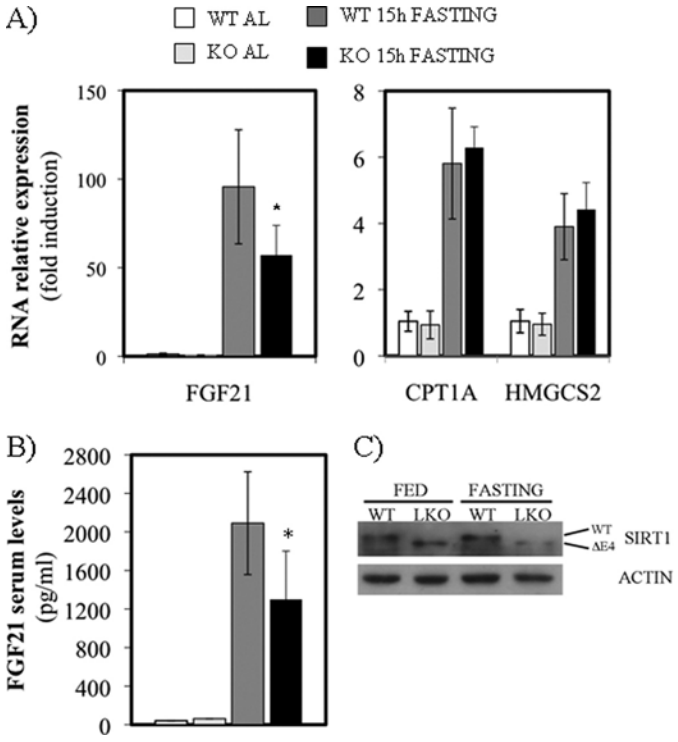

FIGURE 5. **FGF21 is a SIRT1 target gene during fed-to-fast transition.** *A*, quantitative RT-PCR analysis of FGF21 (*left panel*) and HMGCS2 and CPT1A (*right panel*) gene expression in liver from mice fed *ad libitum* (*AL*) or fasted for 15 h normalized to 18 S expression. *B*, ELISA measurement of FGF21 in serum. *C*, Western blot of liver extracts from mice WT and LKO between 5 and 10 animals/group were used. *Open bars* represent WT mice fed *ad libitum*, *pale gray bars* represent SIRT1 LKO fed *ad libitum*, *dark gray bars* represent 15-h fasted WT mice, and *closed bars* represent 15-h fasted SIRT1 LKO. *, $p < 0.05$.

FGF21 expression could be correlated throughout the NAD^+ intracellular levels because: (i) ketone body production implies the reduction of acetoacetate to β-hydroxybutyrate with the concomitant generation of NAD^+ (2) and (ii) the effect of PPARα ligands on FGF21 expression are dependent on SirT1 activity (14). Therefore, we hypothesize that HMGCS2 could affect FGF21 expression via a mechanism relaying on ketogenesis stimulation of SirT1 activity. To confirm this hypothesis, we studied the mRNA expression FGF21 in wild type or SirT1 liver knock-out mice during the fed-to-starved transition. Fig. 5*A* shows that FGF21 induction mediated by starvation was dependent on SirT1. Fig. 5*A* also shows a specific effect for FGF21, because the starvation-associated induction of other PPARα target genes, like CPT1A and HMGCS2, was not affected (*black bars* compared with *dark gray bars*). Fig. 5*B* shows that the circulating levels of FGF21 protein were impaired in starved SirT1 LKO, indicative of the physiological relevance of SIRT1 dependence. Fig. 5*C* shows that SirT1 is specifically knocked out in the livers of SirT1 LKO mice (18).

Acetoacetate Modulates FGF21 mRNA Expression by a SirT1-dependent Mechanism—Next, to pursue the hypothesis about NAD^+ levels, we treated HepG2 cells with the oxidizing (acetoacetate) or reducing (β-hydroxybutyrate) partners of ketone bodies. Fig. 6*A* shows that acetoacetate induced FGF21 expression in a dose-dependent manner, whereas β-hydroxybutyrate did so to a lesser extent. Fig. 6*B* (*left panel*) shows that acetoacetate mediated induction of FGF21 expression was dependent on SirT1 expression. Fig. 6*B* (*right panel*) shows that acetoacetate did not affect endogenous SirT1 levels and that the siRNA treatment was efficient. These results suggest that the products of ketogenesis can stimulate gene expression through the SirT1 activity and therefore that HMGCS2 could control metabolic processes other than ketogenesis in this cell line.

DISCUSSION

Fatty acid β-oxidation and ketogenesis are induced during fasting or lactation (1) and also in pathological situations such as diabetes (reviewed in Ref. 29). PPARα mediates the induction of genes responsible for controlling both processes. The *HMGCS2* gene controls ketogenesis (2) and is a PPARα target (4–6). Studies with the homologous *HMGCS1* (19, 20) (an isotype that catalyzes the same reaction in the cytosol, where it controls the mevalonate pathway) suggested that cysteine 166 is part of the active site of the mitochondrial HMGCS2 enzyme.

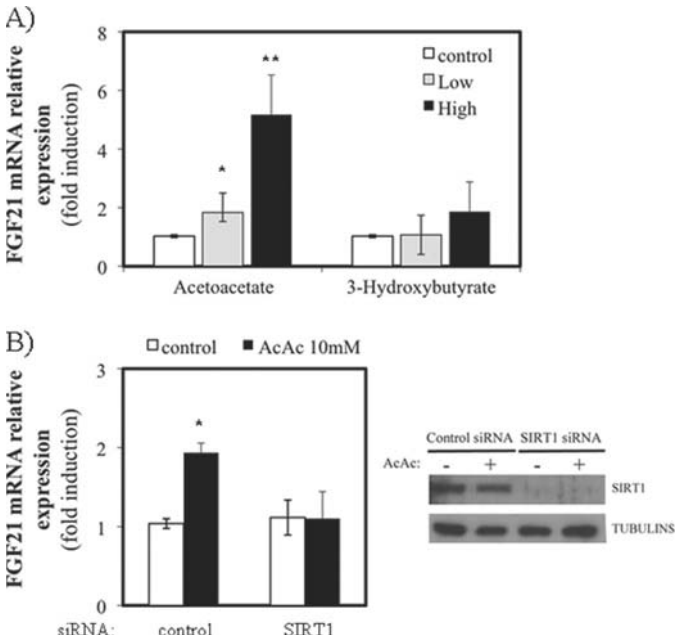

FIGURE 6. **FGF21 is induced by acetoacetate in HepG2 cell line.** *A*, HepG2 cells were treated with acetoacetate 1 (low) or 10 mM (high) or with 3-hydroxybutyrate 2 (low) or 20 mM (high) for 5 h in regular growth medium. Relative expression of FGF21 mRNA was assessed by real time PCR. The average of three independent experiments is shown. *B*, *left panel*, levels of mRNA of FGF21 in cells transfected with a siRNA control or siRNA specific for SIRT1 in the absence (*open bars*) or 10 mM acetoacetate (*closed bars*). *Right panel*, the levels of SIRT1 protein cells transfected with a control siRNA or specific SIRT1 siRNA, in the absence (−) or the presence (+) of 10 mM acetoacetate. The average of three independent experiments is shown. *, $p < 0.05$, **, $p < 0.01$.

Therefore, in this paper, we generated two adenoviruses expressing wild type and a catalytically inactive mutant (C166A; Fig. 1*A*) of the human HMGCS2. When HMGCS2 activity was expressed, HepG2 cells become ketogenic (Fig. 2*B*). Interestingly, we also observed that these cells had a greater capacity to oxidize long chain fatty acids. The β-oxidation induction was similar to that seen in PPARα-infected cells (Fig. 1*C*). These results suggest that expression of the gene not only controls ketogenesis but can also control the β-oxidation pathway in certain circumstances.

Recombinant PPARα expression in HepG2 cells induces β-oxidation of fatty acids and the expression of genes such as *FGF21*, *HMGCS2*, and *CPT1A* (Ref. 6 and Table 1). It has been proposed that HMGCS2 is a co-activator of PPARα (11) through a mechanism involving the HMGCS2 palmitoylation of Cys-166 (12). In fact, we found that expression of HMGCS2 was involved in the induction of fatty acid oxidation mediated by PPARα (Fig. 2). However, our data do not support the role of HMGCS2 as a PPARα co-activator. We did not observe an interaction between PPARα and HMGCS2 nor a nuclear co-localization of both proteins (Fig. 4). In addition, no effect of co-activation was observed at the level of reporter gene even for HMGCS2, which was proposed (12) as the target of PPARα co-activation (data not shown). Therefore, we have sought an alternative hypothesis to explain the role of HMGCS2 in controlling fatty acid oxidation.

Liver synthesizes acetoacetate through the 3-hydroxy-3-methylglutaryl-CoA (HMG-CoA) cycle, which is driven by the three mitochondrial located enzymes acetoacetyl-CoA thiolase (EC 2.3.1.9), hydroxymethylglutaryl-CoA synthase (HMGCS2; EC 4.1.3.5), and hydroxymethylglutaryl-CoA lyase (EC 4.1.3.4) and produces 1 mol of acetoacetate, 1 mol of acetyl-CoA, and 2 mol of free CoA from three molecules of acetyl-CoA (2). Acetoacetate is further reduced to β-hydroxybutyrate through mitochondrial β-hydroxybutyrate dehydrogenase (EC 1.1.1.30), driven by high levels of NADH in hepatic mitochondria. Interestingly, in humans (30) and other mammals (31), a cytosolic isotype of β-hydroxybutyrate dehydrogenase has been characterized, suggesting a reversible conversion between acetoacetate and β-hydroxybutyrate depending on the $[NAD^+]/[NADH]$ ratio. In addition, diet manipulation, like caloric restriction, affects the $[NAD^+]/[NADH]$ ratio in liver and muscle (18). In this study we hypothesized that *HMGCS2*, widely expressed in human tissues (16), could modulate $[NAD^+]/[NADH]$ ratio by feed-forward ketogenesis. HMGCS2 activity specifically induces FGF21 mRNA levels in HepG2 cells (Fig. 3*A*), whereas other PPARα target genes remained unaffected (Table 1). Also, knockdown of HMGCS2 clearly affected FGF21 expression and its induction by PPARα (Fig. 3*B*). FGF21 has been shown to be highly sensitive to SirT1 activity on ligand-dependent PPARα transactivation (14), and our data clearly indicate that fasting-induced expression of FGF21 was blunted in SirT1 liver-specific knock-out, whereas other PPARα target genes were unaffected in this experimental condition (Fig. 5). This result indicates that FGF21, in terms of mRNA levels or the circulating protein, is highly sensitive to SirT1 activity during fasting.

To explain our data, we propose that under certain circumstances HMGCS2 activity, through acetoacetate generation, could modulate the cytosolic $[NAD^+]/[NADH]$ ratio and therefore SirT1 activity. Consistent with this hypothesis, we observed that the addition of acetoacetate, but not β-hydroxybutyrate, to the HepG2 cell medium induces *FGF21* expression in a mechanism dependent on SirT1 (Fig. 6). Therefore, HMGCS2 seems to have a specific effect on gene expression, which does not depend on PPARα co-activation. However, our results do not fully explain why HMGCS2 expression is necessary for the induction of β-oxidation mediated by PPARα. It is possible that changes in the mitochondrial $[NAD^+]/[NADH]$ ratio are also partly responsible for this phenomenon. However, it is also possible that removal of acetyl-CoA, as acetoacetate, accelerates the catabolic process and that both FGF21 mRNA expression and β-oxidation are stimulated by HMGCS2 through independent mechanisms.

Proliferating cells do not express HMGCS2 activity (10, 15). The human gene is a target of c-*Myc*, and its expression is characteristic of differentiated cells of the colon (24). The role of oxidative metabolism in cell transformation has recently been highlighted (reviewed in Ref. 32). In fact, it has been found that p53 up-regulates fatty acid oxidation induced by glucose starvation (33), and it is proposed that this effect would be part of its role as a tumor suppressor gene because active β-oxidation would protect the cell from Warburg effect (reviewed in Ref. 34). We have not observed a clear effect of HMGCS2 gene expression on cell proliferation, a target gene of p53 (data not shown). However, we have shown how *HMGCS2* expression produces metabolic effects capable of inducing the expression

of genes such as *FGF21* and altering the oxidative flux of long chain fatty acids.

In conclusion, our results suggest that *HMGCS2* expression affects the PPARα-mediated response. However, we propose an alternative mechanism to the previously proposed co-activation of PPARα (11, 12). Our mechanism would be related to changes in the metabolites of the cell induced by the acceleration of ketogenesis, although these changes could be related to factors other than SirT1 activity.

Acknowledgments—We are truly grateful to Dr. Leonard Guarente and Dr. Hung-Chun Chang (Department of Biology, MA Institute of Technology) for liver-specific SirT1 KO mice.

REFERENCES

1. McGarry, J. D., and Foster, D. W. (1980) *Annu. Rev. Biochem.* **49,** 395–420
2. Hegardt, F. G. (1999) *Biochem. J.* **338,** 569–582
3. Napal, L., Marrero, P. F., and Haro, D. (2005) *J. Mol. Biol.* **354,** 751–759
4. Rodríguez, J. C., Gil-Gómez, G., Hegardt, F. G., and Haro, D. (1994) *J. Biol. Chem.* **269,** 18767–18772
5. Ortiz, J. A., Mallolas, J., Nicot, C., Bofarull, J., Rodríguez, J. C., Hegardt, F. G., Haro, D., and Marrero, P. F. (1999) *Biochem. J.* **337,** 329–335
6. Hsu, M. H., Savas, U., Griffin, K. J., and Johnson, E. F. (2001) *J. Biol. Chem.* **276,** 27950–27958
7. Kersten, S., Seydoux, J., Peters, J. M., Gonzalez, F. J., Desvergne, B., and Wahli, W. (1999) *J. Clin. Invest.* **103,** 1489–1498
8. Inagaki, T., Dutchak, P., Zhao, G., Ding, X., Gautron, L., Parameswara, V., Li, Y., Goetz, R., Mohammadi, M., Esser, V., Elmquist, J. K., Gerard, R. D., Burgess, S. C., Hammer, R. E., Mangelsdorf, D. J., and Kliewer, S. A. (2007) *Cell Metab.* **5,** 415–425
9. Badman, M. K., Pissios, P., Kennedy, A. R., Koukos, G., Flier, J. S., and Maratos-Flier, E. (2007) *Cell Metab.* **5,** 426–437
10. Le May, C., Pineau, T., Bigot, K., Kohl, C., Girard, J., and Pégorier, J. P. (2000) *FEBS Lett.* **475,** 163–166
11. Meertens, L. M., Miyata, K. S., Cechetto, J. D., Rachubinski, R. A., and Capone, J. P. (1998) *EMBO J.* **17,** 6972–6978
12. Kostiuk, M. A., Keller, B. O., and Berthiaume, L. G. (2010) *FASEB J.* **24,** 1914–1924
13. Nemoto, S., Fergusson, M. M., and Finkel, T. (2004) *Science* **306,** 2105–2108
14. Purushotham, A., Schug, T. T., Xu, Q., Surapureddi, S., Guo, X., and Li, X. (2009) *Cell Metab.* **9,** 327–338
15. Prip-Buus, C., Bouthillier-Voisin, A. C., Kohl, C., Demaugre, F., Girard, J., and Pegorier, J. P. (1992) *Eur. J. Biochem.* **209,** 291–298
16. Mascaró, C., Buesa, C., Ortiz, J. A., Haro, D., and Hegardt, F. G. (1995) *Arch. Biochem. Biophys.* **317,** 385–390
17. Barrero, M. J., Camarero, N., Marrero, P. F., and Haro, D. (2003) *Biochem. J.* **369,** 721–729
18. Chen, D., Bruno, J., Easlon, E., Lin, S. J., Cheng, H. L., Alt, F. W., and Guarente, L. (2008) *Genes Dev.* **22,** 1753–1757
19. Cheng, H. L., Mostoslavsky, R., Saito, S., Manis, J. P., Gu, Y., Patel, P., Bronson, R., Appella, E., Alt, F. W., and Chua, K. F. (2003) *Proc. Natl. Acad. Sci. U.S.A.* **100,** 10794–10799
20. He, T. C., Zhou, S., da Costa, L. T., Yu, J., Kinzler, K. W., and Vogelstein, B. (1998) *Proc. Natl. Acad. Sci. U.S.A.* **95,** 2509–2514
21. Clinkenbeard, K. D., Reed, W. D., Mooney, R. A., and Lane, M. D. (1975) *J. Biol. Chem.* **250,** 3108–3116
22. García-Martínez, C., Marotta, M., Moore-Carrasco, R., Guitart, M., Camps, M., Busquets, S., Montell, E., and Gómez-Foix, A. M. (2005) *Am. J. Physiol. Cell Physiol* **288,** C1264–C1272
23. Zhou, W., Han, W. F., Landree, L. E., Thupari, J. N., Pinn, M. L., Bililign, T., Kim, E. K., Vadlamudi, A., Medghalchi, S. M., El Meskini, R., Ronnett, G. V., Townsend, C. A., and Kuhajda, F. P. (2007) *Cancer Res.* **67,** 2964–2971
24. Camarero, N., Mascaró, C., Mayordomo, C., Vilardell, F., Haro, D., and Marrero, P. F. (2006) *Mol. Cancer Res.* **4,** 645–653
25. Misra, I., Narasimhan, C., and Miziorko, H. M. (1993) *J. Biol. Chem.* **268,** 12129–12135
26. Rokosz, L. L., Boulton, D. A., Butkiewicz, E. A., Sanyal, G., Cueto, M. A., Lachance, P. A., and Hermes, J. D. (1994) *Arch. Biochem. Biophys.* **312,** 1–13
27. Valera, A., Pelegrin, M., Asins, G., Fillat, C., Sabater, J., Pujol, A., Hegardt, F. G., and Bosch, F. (1994) *J. Biol. Chem.* **269,** 6267–6270
28. Quant, P. A. (1994) in *Essays in Biochemistry* (Tipton, K. F., ed) pp. 13–24, Portland Press, London
29. Eledrisi, M. S., Alshanti, M. S., Shah, M. F., Brolosy, B., and Jaha, N. (2006) *Am. J. Med. Sci.* **331,** 243–251
30. Guo, K., Lukacik, P., Papagrigoriou, E., Meier, M., Lee, W. H., Adamski, J., and Oppermann, U. (2006) *J. Biol. Chem.* **281,** 10291–10297
31. Koundakjian, P. P., and Snoswell, A. M. (1970) *Biochem. J.* **119,** 49–57
32. DeBerardinis, R. J., Lum, J. J., Hatzivassiliou, G., and Thompson, C. B. (2008) *Cell Metab.* **7,** 11–20
33. Ide, T., Brown-Endres, L., Chu, K., Ongusaha, P. P., Ohtsuka, T., El-Deiry, W. S., Aaronson, S. A., and Lee, S. W. (2009) *Mol. Cell.* **36,** 379–392
34. Levine, A. J., and Puzio-Kuter, A. M. (2010) *Science* **330,** 1340–1344

3. REGULATION OF FGF21 UNDER AMINO ACID DEPRIVATION

3.1. ARTICLE 2: **ACTIVATING TRANSCRIPTION FACTOR 4-DEPENDENT INDUCTION OF FGF21 DURING AMINO ACID DEPRIVATION**

Biochemal Journal 443(1):165-71, 2012.

De Sousa-Coelho AL, Marrero PF, Haro D.

Department of Biochemistry and Molecular Biology, School of Pharmacy and the Institute of Biomedicine of the University of Barcelona (IBUB), E-08028 Barcelona

SUMMARY IN SPANISH (RESUMEN EN CASTELLANO):

La privación de nutrientes o el ayuno se correlacionan frecuentemente con la limitación de aminoácidos. La privación de aminoácidos inicia una cascada de transducción de señal que empieza con la activación de la fosforilación de eIF2 por la quinasa GCN2, la reducción global de la síntesis de proteínas y el aumento de la traducción de ATF4. Este factor de transcripción modula un amplio espectro de genes implicados en la adaptación al estrés nutricional. La hormona FGF21 se induce durante el ayuno en el hígado y su expresión induce a un estado metabólico que es capaz de mimetizar un estado de ayuno a largo plazo. FGF21 es crítico para la inducción de la oxidación de los ácidos grasos en el hígado, la cetogénesis y la gluconeogénesis, procesos metabólicos que son esenciales para la respuesta metabólica de adaptación al ayuno. En el presente estudio, hemos demostrado que FGF21 se induce en respuesta a la privación de aminoácidos, tanto en el hígado de ratón como en las células humanas de cultivo HepG2. Hemos identificado a FGF21 como un gen diana de ATF4 y hemos localizado dos secuencias conservadas de unión a ATF4, en la región reguladora 5' del gen humano FGF21, que son responsables por la activación transcripcional dependiente de ATF4 de este gen. Estos resultados suman la inducción del gen FGF21 en el programa de la transcripción iniciada por los niveles crecientes de ATF4 y ofrece un nuevo mecanismo para la inducción de la expresión del gen FGF21 en la privación de nutrientes.

BJ www.biochemj.org

BJ Metabolism

Biochem. J. (2012) **443**, 165–171 (Printed in Great Britain) doi:10.1042/BJ20111748

Activating transcription factor 4-dependent induction of FGF21 during amino acid deprivation

Ana Luísa DE SOUSA-COELHO, Pedro F. MARRERO and Diego HARO[1]

Department of Biochemistry and Molecular Biology, School of Pharmacy and the Institute of Biomedicine of the University of Barcelona (IBUB), Av. Joan XXIII s/n, E-08028 Barcelona, Spain

Nutrient deprivation or starvation frequently correlates with amino acid limitation. Amino acid starvation initiates a signal transduction cascade starting with the activation of the kinase GCN2 (general control non-derepressible 2) phosphorylation of eIF2 (eukaryotic initiation factor 2), global protein synthesis reduction and increased ATF4 (activating transcription factor 4). ATF4 modulates a wide spectrum of genes involved in the adaptation to dietary stress. The hormone FGF21 (fibroblast growth factor 21) is induced during fasting in liver and its expression induces a metabolic state that mimics long-term fasting. Thus FGF21 is critical for the induction of hepatic fat oxidation, ketogenesis and gluconeogenesis, metabolic processes which are essential for the adaptive metabolic response to starvation. In the present study, we have shown that FGF21 is induced by amino acid deprivation in both mouse liver and cultured HepG2 cells. We have identified the human *FGF21* gene as a target gene for ATF4 and we have localized two conserved ATF4-binding sequences in the 5′ regulatory region of the human *FGF21* gene, which are responsible for the ATF4-dependent transcriptional activation of this gene. These results add *FGF21* gene induction to the transcriptional programme initiated by increased levels of ATF4 and offer a new mechanism for the induction of the *FGF21* gene expression under nutrient deprivation.

Key words: activating transcription factor 4 (ATF4), amino acid deprivation, fibroblast growth factor 21 (FGF21), liver, metabolism, nutrient deprivation.

INTRODUCTION

Mammals have developed a wide range of mechanisms to detect and respond to episodes of malnutrition and starvation. Nutrient deprivation or starvation frequently correlates with amino acid limitation. Amino acid starvation initiates a signal transduction cascade starting with the activation of the GCN2 (general control non-derepressible 2) kinase, phosphorylation of eIF2 (eukaryotic initiation factor 2), and increased synthesis of ATF4 (activating transcription factor 4) [1].

Dietary amino acid availability alters metabolic pathways beyond protein homoeostasis since there is a link between dietary amino acids and lipid metabolism. A GCN2-dependent inhibition of fatty acid synthase activity and expression of lipogenic genes in liver, and increased mobilization of lipid stores, occur in response to leucine deprivation in mice [2]. In addition, increased expression of β-oxidation genes and decreased expression of lipogenic genes and activity of fatty acid synthase in WAT (white adipose tissue), and increased expression of UCP1(uncoupling protein 1) in BAT (brown adipose tissue), has been observed [3,4]. GCN2 triggers the amino acid-response signal transduction pathway when GCN2 kinase activity is activated by its binding to any uncharged tRNA molecule [5,6]. Although global protein synthesis is reduced, the translation of a group of mRNA species is increased as a part of this response. Among these is ATF4 [7,8], a transcription factor that binds to CARE [C/EBP (CCAAT/enhancer-binding protein)/ATF-response element; also named AARE (amino acid-response element)] and modulates a wide spectrum of genes involved in the adaptation to dietary stress [9]. Food deprivation reduces free intracellular amino acid, and increases eIF2α phosphorylation and *ATF4* mRNA levels in skeletal muscle [10].

FGF (fibroblast growth factor) 21 is a member of the FGF family, predominantly produced by the liver, but also by other tissues such as WAT, BAT, skeletal muscle and pancreatic β-cells [11–14]. FGF21 expression in liver is under tight control by PPAR (peroxisome-proliferator-activated receptor) α [15–18], it is induced in the liver during fasting and its expression induces a metabolic state that mimics long-term fasting. Thus FGF21 is critical for the induction of hepatic fat oxidation, ketogenesis and gluconeogenesis, which are metabolic processes critical for the adaptive metabolic response to starvation [19].

In the present study, we have shown that the hormone FGF21 is induced by amino acid deprivation both in mice liver and cultured HepG2 cells. We have identified the human *FGF21* gene as a target gene for ATF4 and we have localized two evolutionary conserved ATF4-binding sequence in the 5′ regulatory region of the human *FGF21* gene. These sequences are responsible for the ATF4-dependent transcriptional activation of this gene. These results add *FGF21* gene induction to the transcriptional programme initiated by increased levels of ATF4 and offer a new mechanism for the induction of the *FGF21* gene expression under nutrient deprivation.

EXPERIMENTAL

Animals and diets

Eight-week-old male C57BL/6J mice were fed on either a control diet (nutritionally complete diet) or a (−)leu diet (diet devoid

Abbreviations used: AARE, amino acid-response element; AMPK, AMP-activated protein kinase; ATF4, activating transcription factor 4; BAT, brown adipose tissue; C/EBP, CCAAT/enhancer-binding protein; CARE, C/EBP/ATF-response element; ChIP, chromatin immunoprecipitation; eIF2, eukaryotic initiation factor 2; EMSA, electrophoretic mobility-shift assay; FGF, fibroblast growth factor; GCN2, general control non-derepressible 2; HisOH, histidinol; HMGCS2, 3-hydroxy-3-methylglutaryl-CoA synthase 2; hnRNA, heterogeneous nuclear RNA; MEM, minimal essential medium; PPAR, peroxisome-proliferator-activated receptor; PGC-1α, PPARγ co-activator-1α; siRNA, small interfering RNA; SREBP1c, sterol-regulatory-element-binding protein 1c; UCP1, uncoupling protein 1; WAT, white adipose tissue.

[1] To whom correspondence should be addressed (email dharo@ub.edu).

of the essential amino acid leucine) for 7 days. Food intake and body weight were recorded daily. Sample collections and quantification of FGF21 in serum were carried out as described in [20]. Both diets were obtained from Research Diets. All of the experimental protocols with mice were performed with approval of the animal ethics committee of the University of Barcelona (Barcelona, Spain).

Cell culture and treatment conditions

HepG2 cells were cultured in fresh MEM (minimal essential medium) and 10 % (v/v) fetal bovine serum for 16 h before initiating all treatments. Wy14643 and HisOH (histidinol) were purchased from Sigma–Aldrich. MG132 was obtained from Calbiochem. Cells were transfected as described previously [20]. Adenovirus expressing PPARα was a gift from F. Villarroya (University of Barcelona).

RNA isolation and relative quantitative RT (reverse transcription)–PCR

Levels of *HMGCS2* (3-hydroxy-3-methylglutaryl-CoA synthase 2) and *FGF21* mRNA were determined as described previously [20]. cDNA was synthesized from 1 μg of total RNA by MMLV (Moloney murine leukaemia virus) reverse transcriptase (Invitrogen) with random hexamers (Roche Diagnostics) according to the manufacturer's instructions. TaqMan Gene Expression Master Mix and TaqMan Gene Expression Assays (Invitrogen/Applied Biosystems) were used for the PCR step. Amplification and detection were performed using the StepOnePlus Real-Time PCR System. Each mRNA from a single sample was measured in duplicate. For HepG2 cells, human gene probes were used: *FGF21*, Hs00173927_m1; *HMGCS2*, Hs00985427_m1. For mice experiments, a mouse probe (*Fgf21*, Mm00840165_g1) was used. Relative mRNA abundance was obtained by normalizing to 18S levels (Applied Biosystems). To measure the transcriptional activity from the human *FGF21* gene, oligonucleotides derived from *FGF21* intron 2 and exon 3 were used to measure the short-lived unspliced transcript (hnRNA, heterogeneous nuclear RNA) [21]. Real-time quantitative PCR was performed by using a SYBR Green I-containing PCR mixture (Applied Biosystems), following the manufacturer's recommendations. Sequences of primers were 5′-CCTGGATCCTGGGTCTTACA-3′ in intron 2 and 5′-CGGTGTGGGGACTTGTTC-3′ in exon 3.

Plasmid constructions

The *FGF21* promoter (nucleotides $-768/+115$)–luciferase plasmid was generated in the pGL3-basic plasmid (Promega). 5′ Deletions were generated by PCR from human genomic DNA. The mutations were made by site-directed mutagenesis [QIAquick mutagenesis kit (Qiagen)] by replacing the sequences of the AARE1 and AARE2 core for CAGATGGAC. Human ATF4 expression vector (pRK-ATF4) [22] was from Addgene (plasmid 26114).

Western blot analysis

Western blot assays for HepG2 and liver cell extracts were carried out using antibodies against ATF4 (sc-200, Santa Cruz Biotechnology) and actin (A2066, Sigma).

ChIP (chromatin immunoprecipitation) analysis

Cross-linked chromatin from HepG2 cells was sonicated using a Bioruptor® Next Gen (Diagenode). Real-time quantitative PCR was performed by using a SYBR Green I-containing mixture with specific primers to amplify the human *FGF21* AARE1 and AARE2, and exon 1 as a negative control. Relative occupancy of the immunoprecipitated factor at a locus was calculated using the formula $2(C_T^{IgG} - C_T^{ATF4})$, where C_T^{IgG} and C_T^{ATF4} are mean threshold cycles of PCR from negative-control ChIP (non-immune IgG) and target ChIP (anti-ATF4 antibody) respectively. The sequence of the primers used were F1, 5′-AGCCAACCTGTCTTCCCTCT-3′, and R1, 5′-ATGCTCAGACCCTGGACATC-3′, for AARE1; F2, 5′-GCTTGAGACCCCAGATCCTT-3′, and R2, 5′-CATTTGGCAGGAGCTACAGA-3′, for AARE2; and 5′-GGACTGTGGGTTTCTGTGCT-3′ and 5′-ATCTCCAGGTGGGCTTCTGT-3′ for the unrelated control in exon 1.

In vitro transcription and translation

pcDNA3 empty vector, ATF4 and C/EBPβ were transcribed and translated by using commercially available kits according to the manufacturer's instructions (Promega).

Labelling probe with digoxigenin

Each oligonucleotide (0.5 nmol) was annealed by heating at 65 °C for 10 min and slowly cooled to room temperature (22 °C) in a buffer of 10 mM Tris/HCl (pH 8), 1 mM EDTA and 150 mM NaCl. The double-stranded oligonucleotide was then labelled using the reagents provided in the DIG Gel Shift Kit, 2nd Generation (Roche).

EMSA (electrophoretic mobility-shift assay)

An aliquot of 2 μl of each factor synthesized *in vitro* was pre-incubated on ice for 10 min in 25 mM Hepes (pH 7.9), 60 mM KCl, 5 % glycerol, 0.75 mM dithiothreitol, 0.1 mM EDTA, 2.5 mM $MgCl_2$, 1 μg of polylysine and 1 μg of poly(dI-dC) · (dI-dC). The total amount of protein was kept constant in each reaction through the addition of pcDNA3 empty vector. When indicated, a 50-fold excess of unlabelled AARE1 or AARE2, or mutAARE1 or mutAARE2, was added to the reaction mixture. Next, 40 fmol of digoxigenin-labelled probe was added and the incubation was continued for 15 min at room temperature. The final volume for all the reactions was 20 μl. Samples were electrophoresed at 4 °C on a 6 % polyacrylamide gel in 0.5 % TBE buffer [45 mM Tris, 45 mM boric acid and 1 mM EDTA (pH 8.0)], and the DNA was transferred on to a positively charged nylon membrane. The DNA was then cross-linked to the membrane using a UV Stratalinker® (Stratagene). Immunological detection was performed following the manufacturer's instructions, and exposing the membrane to an imaging device. The EMSA oligonucleotides used were as follows. AARE1 (wild-type): forward, 5′-TGAAAGAAACACCAGGATTGCATCAGGGAGGAGGAGGCTG-3′, and reverse, 5′-CAGCCTCCTCCTCCCTGATGCAATCCTGGTGTTTCTTTCA-3′; mutAARE1: forward, 5′-TGAAAGAAACACCAGGcagatggacGGGAGGAGGAGGCTG-3′, and reverse, 5′-CAGCCTCCTCCTCCCgtccatctgCCTGGTGTTTCTTTCA-3′; AARE2 (wild-type): forward, 5′-ATTGAAAGGACCCCAGGTTACATCATCCATTCAGGCTGC-3′, and reverse, 5′-GCAGCCTGAATGGATGATGTAACCTGGGGTCCTTTCAAT-3′, mutAARE2: forward, 5′-ATTGAAAGGACCCCAGcagatggacTCCATTCAGGCTG-3′, and reverse, 5′-GCAGCCTGAATGGAgtccatctgCTGGGGTCCTTTCAAT-3′. Mutagenic residues are in lower-case type.

siRNA (small interfering RNA) transfection

The human *ATF4* siRNA (L-005125-00), siControl non-targeting siRNA (D-001210-01) and DharmaFECT 4 transfection reagent

were purchased from Dharmacon. Transfection was performed according to the manufacturer's instructions. After HisOH treatment, total RNA and nuclear protein extracts were isolated and analysed by real-time PCR and immunoblotting respectively.

Measurement of serum FGF21

A mouse FGF21 ELISA kit was obtained from Millipore for the quantification of FGF21 in mouse serum. The assay was conducted according to the manufacturer's protocol. Briefly, a calibration curve was constructed by plotting the difference of absorbance values at 450 and 590 nm against the FGF21 concentrations of the calibrators, and concentrations of unknown samples (performed in duplicate) were determined using this calibration curve.

Data analysis/statistics

All results are expressed as means ± S.E.M. Significant differences were assessed using a two-tailed Student's t test. $P < 0.05$ was considered statistically significant.

RESULTS

FGF21 expression is induced by the 26S proteasome inhibitor MG132

Considering the central role of PPARα in metabolic homoeostasis, we investigated how the turnover of PPARα affected the expression of its target genes. We checked the mRNA levels of *FGF21* and *HMGCS2*, two prototypical PPARα target genes [15–18,23], in HepG2 cells infected with adenovirus expressing PPARα and exposed to DMSO or to the 26S proteasome inhibitor MG132. As expected, MG132 treatment blocked the PPARα-dependent expression of *HMGCS2* (Figure 1A), indicating that the transcriptional activity of PPARα is increased by protein degradation [24]. Contrary to what we had predicted, the expression of *FGF21* was strongly increased by the MG132 treatment in a time-dependent manner (Figure 1B). The opposite effects of MG132 treatment on the expression of *HMGCS2* and *FGF21* genes points to a different mechanism controlling the expression of the *FGF21* gene in response to the inhibition of the proteasome activity.

Amino acid starvation induces FGF21 expression

We hypothesized that proteasome inhibition in HepG2 cells could decrease the pool of free amino acids. This hypothesis prompted us to test whether *FGF21* expression is induced during amino acid starvation. For this purpose, we treated HepG2 cells with HisOH, a potent and reversible inhibitor of protein synthesis that acts by decreasing the activation of histidine, mimicking amino acid starvation [25]. Using real-time PCR, we measured the *FGF21* mRNA levels in HisOH-treated HepG2 cells, and observed that amino acid deprivation produced a time-dependent induction of *FGF21* mRNA (Figure 2A). To test whether this induction was due to an increase in *FGF21* gene transcription, we measured the *FGF21* primary transcript (hnRNA) levels; HisOH treatment clearly induced *FGF21* hnRNA levels in a time-dependent manner, and this induction was maximal after 4 h of treatment (Figure 2B).

FGF21 is an ATF4 target gene

Proteasome inhibition leads to an increase in eIF2α phosphorylation, a significant reduction in protein synthesis and a concomitant induction of *ATF4* expression [26]. To test whether the HisOH-induced increase in *FGF21* expression was due to ATF4, we first analysed the effect of HisOH treatment on ATF4 protein levels in HepG2 cells. The analysis of total HepG2 protein extracts by Western blotting showed that HisOH induced an increase in the ATF4 protein levels soon after 2 h of treatment (Figure 2C). Next, we analysed the sequence of the 5′-flanking region of the human *FGF21* gene, looking for putative ATF4-binding sites. We found two putative AAREs starting at positions −152 and −610 upstream of the transcription start site. These sites matched the consensus for the CAREs and are conserved among several mammalian species (Figure 3A). In order to test whether *FGF21* gene transcription was induced by ATF4, we made several constructs with the luciferase gene as a reporter (Figure 3B) and transfected HepG2 cells with those constructs and an expression vector for human ATF4. The expression of ATF4 induced the wild-type reporter in a concentration-dependent manner (Figure 3C). This induction was totally obliterated either when the AARE1 was mutated (mut1) or when both elements were deleted (delta2). Induction was diminished when AARE2 was mutated (mut2) (Figure 3D). These results identify both AARE sequences as ATF4-responsive elements in the *FGF21* human gene.

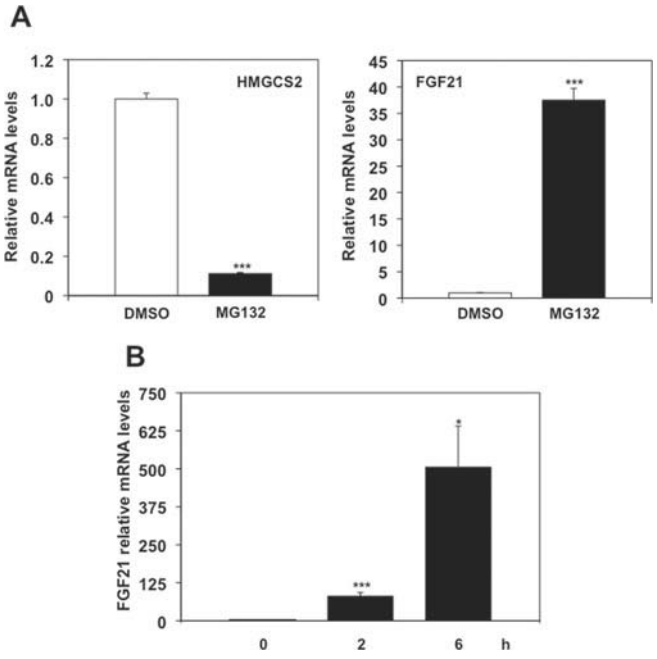

Figure 1 MG132 induces *FGF21* expression

HepG2 cells were infected with adenovirus expressing PPARα for 48 h. As indicated, cells were pre-treated for 1 h with DMSO or 40 μM MG132, and then with 50 μM Wy14643 for a further 5 h. (**A**) The relative mRNA levels of *HMGCS2* or *FGF21* were determined using TaqMan real-time PCR. (**B**) HepG2 cells were incubated with vehicle or MG132 for the time indicated. Relative mRNA expression of *FGF21* was determined. Results are means ± S.E.M. for three independent experiments. $^*P < 0.05$, $^{***}P < 0.001$.

ATF4 binds to both AAREs in *FGF21*

To analyse further the functionality of this sequence, we confirmed the *in vivo* binding by ChIP experiments. As shown in Figure 4(B), the chromatin binding of ATF4 was greatly increased in both ATF4-responsive sequences in HisOH-treated cells. In order to test the ability of ATF4 to bind to both AAREs, we performed EMSA using digoxigenin-labelled oligonucleotides containing the ATF4 composite sites (AAREs) of the human *FGF21* gene (Figure 4C). *In vitro* translated ATF4 and C/EBPβ

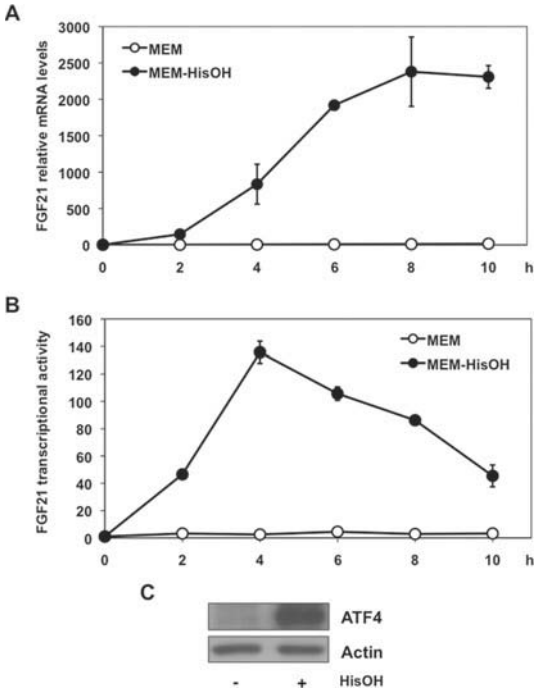

Figure 2 HisOH induces *FGF21* transcription

HepG2 cells were incubated in control medium (MEM) or in HisOH-containing medium (MEM-HisOH), and total RNA was extracted at the time indicated. (**A**) The steady-state mRNA level was determined using TaqMan real-time PCR. (**B**) The *FGF21* pre-mRNA was determined by real-time PCR using specific primers spanning the intron 2–exon 3 junction. The immature RNA levels were plotted as transcriptional activity of *FGF21*. Results are means ± S.E.M. for three independent experiments. (**C**) Protein levels of ATF4 were determined by Western blot analysis. A representative Western blot of endogenous ATF4 is shown where actin is used as a loading control.

were incubated with labelled probes containing the wild-type AARE1 (lanes 1–7) and AARE2 (lanes 8–14) sequences. The specificity of this interaction was demonstrated by competition experiments with a 50-fold molar excess of unlabelled wild-type (lanes 5 and 12) or mutant (lanes 6 and 13) probes. The presence of ATF4 in the complex was confirmed by a supershift experiment with an anti-ATF4 antibody (lanes 7 and 14).

ATF4 mediates the amino-acid-starvation-induced increase in FGF21 expression

To test whether the induction of *FGF21* produced by amino acid starvation was mediated by ATF4, we treated HepG2 cells with HisOH while simultaneously depleting ATF4 by transfecting an ATF4-targeting siRNA. The analysis by real-time PCR showed that the *FGF21* mRNA levels after 4 h of HisOH treatment were significantly lower when ATF4 was depleted compared with the control siRNA-treated cells (Figure 5). We have also investigated the effect of other stress stimuli on the expression of FGF21. As expected, treatment of HepG2 cells with tunicamycin increased the ATF4 protein levels and consequently *FGF21* mRNA levels; this increase was significantly diminished by the siRNA-mediated interference of ATF4 (results not shown).

Leucine deprivation increases *FGF21* mRNA levels in mouse liver

To analyse the effect of amino acid deprivation on FGF21 expression *in vivo*, we fed mice on a (−)leu diet or a control

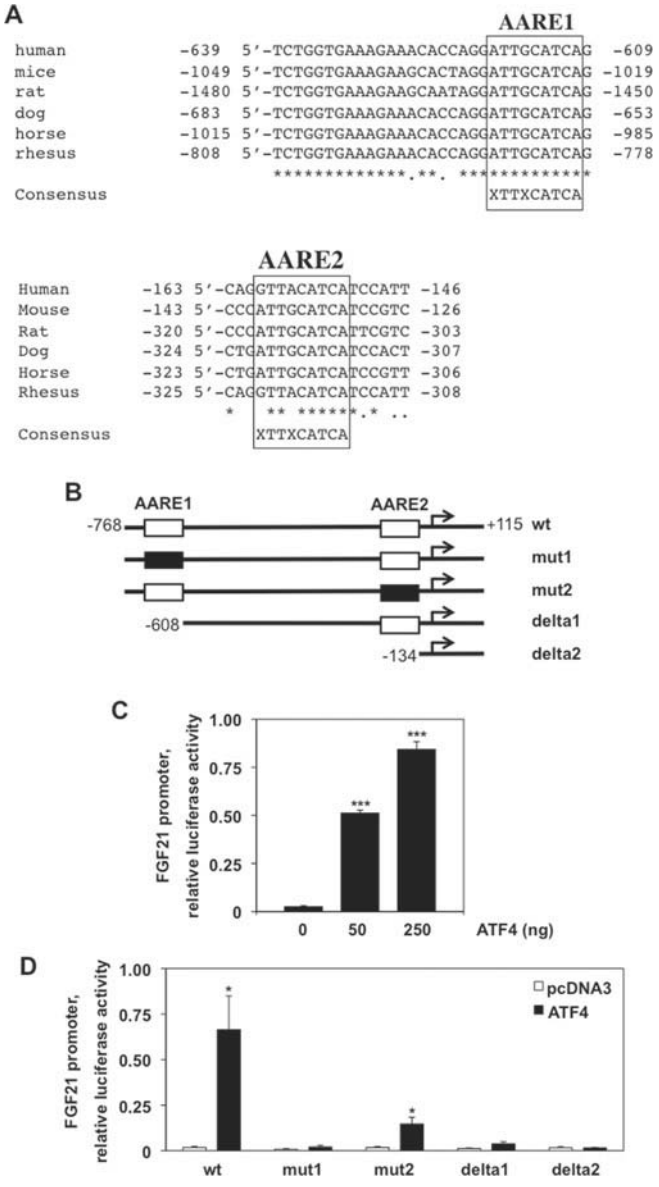

Figure 3 *FGF21* is an ATF4 target gene

(**A**) Alignment of *FGF21* promoter sequence of different mammals, in which the two conserved AAREs are boxed. The asterisks indicate the sequence identity, and the consensus sequence for both elements is shown at the bottom. (**B**) Scheme of the human *FGF21* promoter/luciferase reporter constructs. (**C**) Luciferase activity of the human *FGF21* promoter reporter construct co-transfected with different amounts of an expression plasmid for human ATF4. (**D**) Promoter activation for each construct in the presence (closed bars) or in the absence (open bars) of ATF4 co-transfection. Results are means ± S.E.M. for three independent experiments with two plates each. $^{*}P < 0.05$, $^{***}P < 0.001$. wt, wild-type.

diet for 7 days. The analysis by real-time PCR showed that the *Fgf21* mRNA levels were greatly increased in liver from mice fed on a leucine-deprived diet compared with the control-fed animals (Figure 6A). The circulating FGF21 levels quantified by ELISA were also, consequently, increased in the serum of leucine-deprived animals, paralleling hepatic gene expression (Figure 6B). The circulating levels that were reached, approximately 3.5 ng/μl, where even higher than those observed during starvation [15,20]. As expected, ATF4 protein levels were induced in liver under leucine deprivation (Figure 6C).

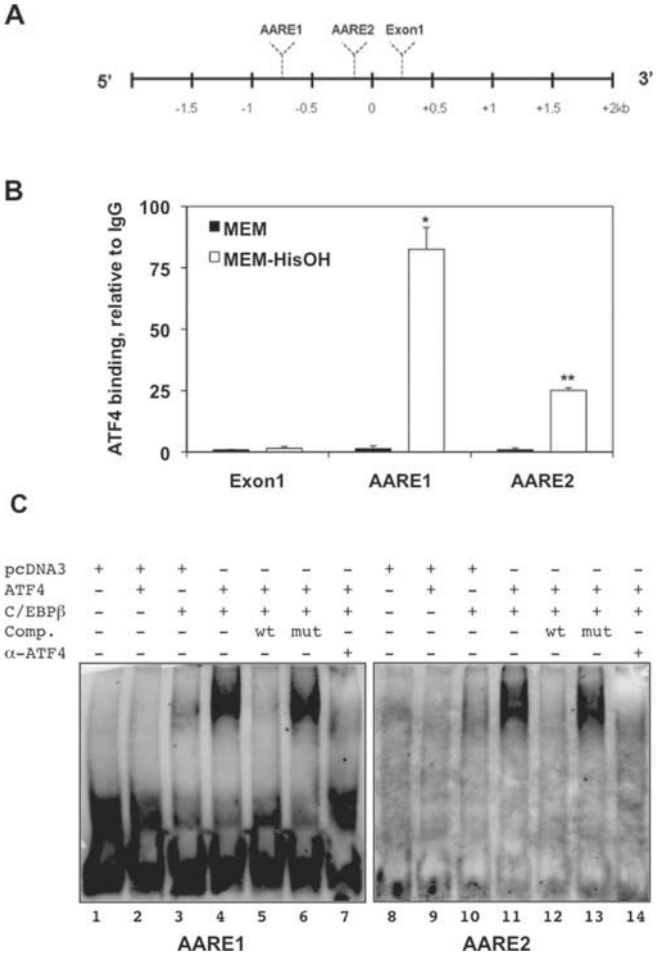

Figure 4 ATF4 binds to the *FGF21* gene

(**A**) Scheme of the human *FGF21* gene indicating the different amplicons produced for the ChIP analysis. (**B**) HepG2 cells were incubated in MEM (control) or treated with 2 mM HisOH (MEM-HisOH) for 4 h. A ChIP assay was performed. The ATF4 enrichment on AARE1 and AARE2 of the human promoter upon treatment is shown. Results are means ± S.E.M. for two independent experiments. $*P < 0.05$, $**P < 0.01$. (**C**) EMSAs were performed. *In vitro* translated ATF4 and C/EBPβ were incubated with labelled probes containing the wild-type AARE1 (lanes 1–7) and AARE2 (lanes 8–14) sequences. Competition experiments were performed with a 50-fold molar excess of unlabelled AARE1 or AARE2 (wt, lane 5 and 12), or mutAARE1 or mutAARE2 (mut, lane 6 and 13). The presence of ATF4 in the complex was confirmed by a supershift experiment with an anti-ATF4 antibody (lanes 7 and 14).

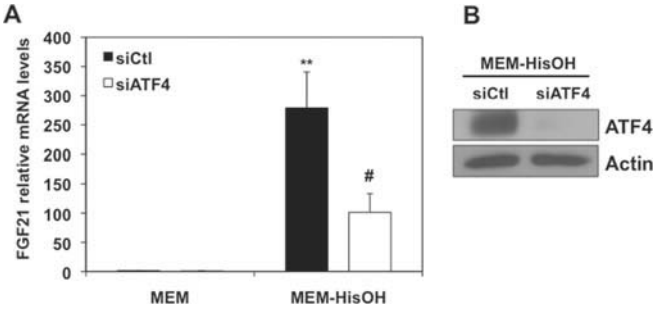

Figure 5 Effect of siRNA-mediated ATF4 knockdown on endogenous *FGF21* expression

HepG2 cells were transfected with either control siRNA or ATF4 siRNA. At 48 h post-transfection, cells were incubated in MEM, or MEM containing 2 mM HisOH for 4 h. (**A**) Relative mRNA expression of *FGF21* was determined using real-time PCR. Results are means ± S.E.M. for four independent experiments. $**P < 0.01$ for the effects of HisOH treatment relative to the control, $\#P < 0.05$ for siATF4 compared with control siRNA in HisOH-treated cells. (**B**) Protein levels of ATF4 were determined by Western blot analysis of nuclear extracts to check the knockdown efficiency.

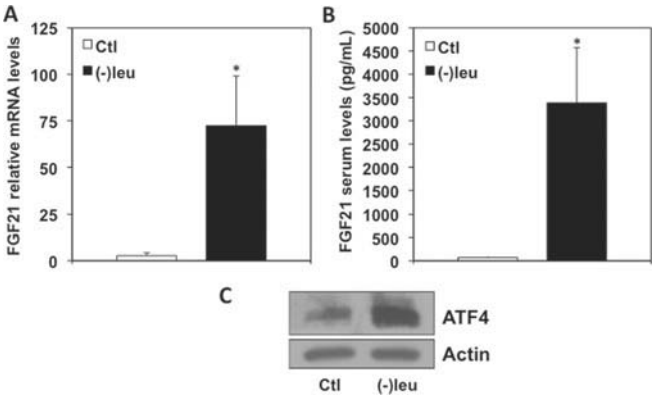

Figure 6 Leucine deprivation induces FGF21 serum levels and mRNA expression in liver

Mice were fed on either a control diet or a leucine-deficient diet for 7 days. (**A**) mRNA expression of *Fgf21* was determined using real-time PCR. (**B**) ELISA measurement of FGF21 in serum. Results are means ± S.E.M. for each group ($n = 5$–6 mice). $*P < 0.05$ for the effects of (−)leu diet compared with control diet. (**C**) Protein levels of ATF4 were determined by Western blot analysis in liver nuclear extracts. A representative Western blot of endogenous ATF4 is shown where actin is used as a loading control. Ctl, control diet.

DISCUSSION

FGF21 is a member of the endocrine FGF subfamily produced by the liver, but also by other tissues such as WAT, BAT, skeletal muscle and pancreas, which plays a role in the adaptation to metabolic states that require increased fatty acid oxidation. The expression of FGF21 is controlled by several transcriptional activators such as PPARα in the liver [15–18], and PPARγ in the adipose tissue [27–29], and it is negatively regulated by PGC-1α (PPARγ co-activator-1α). The PGC-1α-mediated reduction of FGF21 expression is dependent on Rev-Erbα and the synthesis of haem, a ligand of Rev-Erbα [30]. In the present study, we have shown that FGF21 is induced by amino acid deprivation in both mouse liver and cultured HepG2 cells. Furthermore, the results of the present study identify the human *FGF21* gene as a target gene for ATF4, and we have localized two evolutionarily conserved functional ATF4-binding sequences in the 5′ regulatory region of the human *FGF21* gene that are responsible for the ATF4-dependent transcriptional activation of this gene. Our results show that, in accordance with results published previously [31,32], ATF4 binds *in vitro* to both sites as a heterodimer with C/EBPβ. Comparison of *FGF21* mRNA and pre-mRNA levels suggests that both transcription and mRNA stabilization contribute to the ATF4-mediated induction of *FGF21* expression, as has been described previously for ATF3, a known ATF4-activated gene [33,34]. The decline in *FGF21* transcription after 4 h of amino acid deprivation could be caused by the increased expression of ATF3 and other ATF4-activated genes, such as C/EBPβ and CHOP (C/EBP-homologous protein), that act as counter-regulatory signals and lead to a self-limiting cycle of ATF4-dependent transcription [35,36]. The ATF4-dependent induction of *FGF21* shown in the present study suggests a new explanation of the effect of ATF4 on the regulation of obesity, glucose homoeostasis and energy expenditure [37]. Amino acid and other nutrient depletion, through the activation of several kinases, induce eIF2α phosphorylation, selective translation of some stress-responsive transcripts, including that of ATF4, and

certain autophagy genes [38]. We have investigated the effect on FGF21 expression of other stress stimuli that, like nutrient stress, are also able to induce autophagy. Our results show that FGF21 expression is also induced by ER (endoplasmic reticulum) stress. As expected, treatment of HepG2 cells with tunicamycin increased ATF4 protein levels and, consequently, *FGF21* mRNA levels.

A dietary amino acid imbalance alters metabolism beyond protein homoeostasis. The results of the present study suggest that FGF21 could be a link between amino acid imbalance and the metabolic cell response to nutrient deprivation. For example, a protein-free diet resulted in a decrease in serum cholesterol levels and decreased expression of genes involved in cholesterol biosynthesis in rat liver [39]. Nevertheless, the cholesterol levels and the expression of cholesterol synthesis genes were unchanged in the liver of mice deprived of leucine [2]. However, it has been described that expression of lipogenic genes, including *SREBP1c* (sterol-regulatory-element-binding protein 1c) and *FASN* (fatty acid synthase), and the activity of fatty acid synthase in the liver are repressed, and that lipid stores in adipose tissue are mobilized in mice upon leucine deprivation. It has recently been shown that the expression of FGF21 repressed the transcription of *SREBP1c* and decreased the amount of mature SREBP1c in HepG2 cells [40]. All of these results and those of present study suggest that FGF21 would mediate the reduction in lipogenesis observed under leucine deprivation.

The effect on the expression of lipogenic genes and activity of fatty acid synthase has also been described in WAT, where leucine deprivation, in addition, increases energy expenditure, lipolysis and expression of β-oxidation genes and increases the expression of UCP1 in BAT [3]. These effects could be mediated by the induction of FGF21, a hepatic hormone whose action is necessary for the appropriate metabolism of lipids when fatty acids are the major fuel source. Mice maintained on a leucine-deficient diet for 7 days showed a dramatic reduction in abdominal fat mass [2] caused by increased fat mobilization and suppressed fatty acid synthesis in WAT as well as increased energy expenditure [3]. Our data demonstrate that the increased hepatic production of FGF21 under this nutritional deprivation may contribute to this effect.

It has been proposed recently that leucine deprivation improves whole-body insulin sensitivity and insulin signalling in liver by sequentially activating GCN2 and decreasing mTOR (mammalian target of rapamycin)/S6K1 (S6 kinase 1) signalling [41]. Furthermore, activation of AMPK (AMP-activated protein kinase), under these circumstances, also contributes to increased insulin sensitivity [41]. The activation of GCN2 under amino acid starvation would lead to an increase in the expression of ATF4 which, as we have shown in the present study, will produce an increase in the expression and circulating levels of FGF21, which plays a crucial role in mediating the adaptive response of the liver to nutritional deprivation [42], contributing to the regulation of fatty acid oxidation, ketogenesis, TCA (tricarboxylic acid) cycle flux and carbohydrate metabolism. In addition, FGF21 regulates energy expenditure in adipocytes through activation of AMPK and SIRT1 (sirtuin 1) activities [43]. These effects may thus improve insulin sensitivity. Our results suggest that FGF21 mediates the induction of AMPK observed under leucine deprivation, although further work is needed to prove this point.

In conclusion, our results expand our current knowledge of how FGF21 expression is regulated in liver, adding *FGF21* gene induction to the transcriptional programme initiated by increased levels of ATF4 and offering a new mechanism for the induction of the *FGF21* gene expression in response to nutrient availability.

AUTHOR CONTRIBUTION

Ana Luísa De Sousa-Coelho planned the experiments, undertook the experimentation, analysed the experimental data and wrote the paper; Pedro Marrero and Diego Haro designed the research, analysed the experimental data and wrote the paper.

ACKNOWLEDGEMENT

We thank Dr Yihong Ye (Laboratory of Molecular Biology, National Institutes of Health, Bethesda, MD, U.S.A.) for the pRK-ATF4 plasmid.

FUNDING

This work was supported by the Ministerio de Educación y Ciencia [grant numbers SAF2010-15217 (to D.H.) and BFU2007-67322/BMC (to P.F.M.)]; and the Ajut de Suport als Grups de Recerca de Catalunya [grant number 2009 SGR163]. A.L.D.S.C. was supported by the Fundação para a Ciência e a Tecnologia (FCT) from the Portuguese Government.

REFERENCES

1 Kilberg, M. S., Shan, J. and Su, N. (2009) ATF4-dependent transcription mediates signaling of amino acid limitation. Trends Endocrinol. Metab. **20**, 436–443
2 Guo, F. and Cavener, D. R. (2007) The GCN2 eIF2α kinase regulates fatty-acid homeostasis in the liver during deprivation of an essential amino acid. Cell Metab. **5**, 103–114
3 Cheng, Y., Meng, Q., Wang, C., Li, H., Huang, Z., Chen, S., Xiao, F. and Guo, F. (2010) Leucine deprivation decreases fat mass by stimulation of lipolysis in white adipose tissue and upregulation of uncoupling protein 1 (UCP1) in brown adipose tissue. Diabetes **59**, 17–25
4 Cheng, Y., Zhang, Q., Meng, Q., Xia, T., Huang, Z., Wang, C., Liu, B., Chen, S., Xiao, F., Du, Y. and Guo, F. (2011) Leucine deprivation stimulates fat loss via increasing CRH expression in the hypothalamus and activating the sympathetic nervous system. Mol. Endocrinol. **25**, 1624–1635
5 Hao, S., Sharp, J. W., Ross-Inta, C. M., McDaniel, B. J., Anthony, T. G., Wek, R. C., Cavener, D. R., McGrath, B. C., Rudell, J. B., Koehnle, T. J. and Gietzen, D. W. (2005) Uncharged tRNA and sensing of amino acid deficiency in mammalian piriform cortex. Science **307**, 1776–1778
6 Maurin, A. C., Jousse, C., Averous, J., Parry, L., Bruhat, A., Cherasse, Y., Zeng, H., Zhang, Y., Harding, H. P., Ron, D. and Fafournoux, P. (2005) The GCN2 kinase biases feeding behavior to maintain amino acid homeostasis in omnivores. Cell Metab. **1**, 273–277
7 Vattem, K. M. and Wek, R. C. (2004) Reinitiation involving upstream ORFs regulates *ATF4* mRNA translation in mammalian cells. Proc. Natl. Acad. Sci. U.S.A. **101**, 11269–11274
8 Lu, P. D., Harding, H. P. and Ron, D. (2004) Translation reinitiation at alternative open reading frames regulates gene expression in an integrated stress response. J. Cell Biol. **167**, 27–33
9 Ameri, K. and Harris, A. L. (2008) Activating transcription factor 4. Int. J. Biochem. Cell Biol. **40**, 14–21
10 Ebert, S. M., Monteys, A. M., Fox, D. K., Bongers, K. S., Shields, B. E., Malmberg, S. E., Davidson, B. L., Suneja, M. and Adams, C. M. (2010) The transcription factor ATF4 promotes skeletal myofiber atrophy during fasting. Mol. Endocrinol. **24**, 790–799
11 Nishimura, T., Nakatake, Y., Konishi, M. and Itoh, N. (2000) Identification of a novel FGF, FGF-21, preferentially expressed in the liver. Biochim. Biophys. Acta **1492**, 203–206
12 Johnson, C. L., Weston, J. Y., Chadi, S. A., Fazio, E. N., Huff, M. W., Kharitonenkov, A., Köester, A. and Pin, C. L. (2009) Fibroblast growth factor 21 reduces the severity of cerulein-induced pancreatitis in mice. Gastroenterology **137**, 1795–1804
13 Izumiya, Y., Bina, H. A., Ouchi, N., Akasaki, Y., Kharitonenkov, A. and Walsh, K. (2008) FGF21 is an Akt-regulated myokine. FEBS Lett. **582**, 3805–3810
14 Hondares, E., Iglesias, R., Giralt, A., Gonzalez, F. J., Giralt, M., Mampel, T. and Villarroya, F. (2011) Thermogenic activation induces FGF21 expression and release in brown adipose tissue. J. Biol. Chem. **286**, 12983–12990
15 Badman, M. K., Pissios, P., Kennedy, A. R., Koukos, G., Flier, J. S. and Maratos-Flier, E. (2007) Hepatic fibroblast growth factor 21 is regulated by PPARα and is a key mediator of hepatic lipid metabolism in ketotic states. Cell Metab. **5**, 426–437
16 Inagaki, T., Dutchak, P., Zhao, G., Ding, X., Gautron, L., Parameswara, V., Li, Y., Goetz, R., Mohammadi, M., Esser, V. et al. (2007) Endocrine regulation of the fasting response by PPARα-mediated induction of fibroblast growth factor 21. Cell Metab. **5**, 415–425
17 Gälman, C., Lundåsen, T., Kharitonenkov, A., Bina, H. A., Eriksson, M., Hafström, I., Dahlin, M., Amark, P., Angelin, B. and Rudling, M. (2008) The circulating metabolic regulator FGF21 is induced by prolonged fasting and PPARα activation in man. Cell Metab. **8**, 169–174

18 Lundåsen, T., Hunt, M. C., Nilsson, L. M., Sanyal, S., Angelin, B., Alexson, S. E. and Rudling, M. (2007) PPARα is a key regulator of hepatic FGF21. Biochem. Biophys. Res. Commun. **360**, 437–440
19 Reitman, M. L. (2007) FGF21: a missing link in the biology of fasting. Cell Metab. **5**, 405–407
20 Vilà-Brau, A., De Sousa-Coelho, A. L., Mayordomo, C., Haro, D. and Marrero, P. F. (2011) Human HMGCS2 regulates mitochondrial fatty acid oxidation and FGF21 expression in HepG2 cell line. J. Biol. Chem. **286**, 20423–20430
21 Lipson, K. E. and Baserga, R. (1989) Transcriptional activity of the human thymidine kinase gene determined by a method using the polymerase chain reaction and an intron-specific probe. Proc. Natl. Acad. Sci. U.S.A. **86**, 9774–9777
22 Wang, Q., Mora-Jensen, H., Weniger, M. A., Perez-Galan, P., Wolford, C., Hai, T., Ron, D., Chen, W., Trenkle, W., Wiestner, A. and Ye, Y. (2009) ERAD inhibitors integrate ER stress with an epigenetic mechanism to activate BH3-only protein NOXA in cancer cells. Proc. Natl. Acad. Sci. U.S.A. **106**, 2200–2205
23 Rodríguez, J. C., Gil-Gómez, G., Hegardt, F. G. and Haro, D. (1994) Peroxisome proliferator-activated receptor mediates induction of the mitochondrial 3-hydroxy-3-methylglutaryl-CoA synthase gene by fatty acids. J. Biol. Chem. **269**, 18767–18772
24 Blanquart, C., Mansouri, R., Fruchart, J. C., Staels, B. and Glineur, C. (2004) Different ways to regulate the PPARα stability. Biochem. Biophys. Res. Commun. **319**, 663–670
25 Hansen, B. S., Vaughan, M. H. and Wang, L. (1972) Reversible inhibition by histidinol of protein synthesis in human cells at the activation of histidine. J. Biol. Chem. **247**, 3854–3857
26 Jiang, H. Y. and Wek, R. C. (2005) Phosphorylation of the α-subunit of the eukaryotic initiation factor-2 (eIF2α) reduces protein synthesis and enhances apoptosis in response to proteasome inhibition. J. Biol. Chem. **280**, 14189–14202
27 Muise, E. S., Azzolina, B., Kuo, D. W., El-Sherbeini, M., Tan, Y., Yuan, X., Mu, J., Thompson, J. R., Berger, J. P. and Wong, K. K. (2008) Adipose fibroblast growth factor 21 is up-regulated by peroxisome proliferator-activated receptor γ and altered metabolic states. Mol. Pharmacol. **74**, 403–412
28 Moyers, J. S., Shiyanova, T. L., Mehrbod, F., Dunbar, J. D., Noblitt, T. W., Otto, K. A., Reifel-Miller, A. and Kharitonenkov, A. (2007) Molecular determinants of FGF-21 activity-synergy and cross-talk with PPARγ signaling. J. Cell. Physiol. **210**, 1–6
29 Wang, H., Qiang, L. and Farmer, S. R. (2008) Identification of a domain within peroxisome proliferator-activated receptor γ regulating expression of a group of genes containing fibroblast growth factor 21 that are selectively repressed by SIRT1 in adipocytes. Mol. Cell. Biol. **28**, 188–200
30 Estall, J. L., Ruas, J. L., Choi, C. S., Laznik, D., Badman, M., Maratos-Flier, E., Shulman, G. I. and Spiegelman, B. M. (2009) PGC-1α negatively regulates hepatic FGF21 expression by modulating the heme/Rev-Erbα axis. Proc. Natl. Acad. Sci. U.S.A. **106**, 22510–22515
31 Siu, F., Bain, P. J., LeBlanc-Chaffin, R., Chen, H. and Kilberg, M. S. (2002) ATF4 is a mediator of the nutrient-sensing response pathway that activates the human asparagine synthetase gene. J. Biol. Chem. **277**, 24120–24127
32 Lopez, A. B., Wang, C., Huang, C. C., Yaman, I., Li, Y., Chakravarty, K., Johnson, P. F., Chiang, C. M., Snider, M. D., Wek, R. C. and Hatzoglou, M. (2007) A feedback transcriptional mechanism controls the level of the arginine/lysine transporter cat-1 during amino acid starvation. Biochem. J. **402**, 163–173
33 Pan, Y. X., Chen, H., Thiaville, M. M. and Kilberg, M. S. (2007) Activation of the *ATF3* gene through a co-ordinated amino acid-sensing response programme that controls transcriptional regulation of responsive genes following amino acid limitation. Biochem. J. **401**, 299–307
34 Pan, Y. X., Chen, H. and Kilberg, M. S. (2005) Interaction of RNA-binding proteins HuR and AUF1 with the human *ATF3* mRNA 3′-untranslated region regulates its amino acid limitation-induced stabilization. J. Biol. Chem. **280**, 34609–34616
35 Chen, H., Pan, Y. X., Dudenhausen, E. E. and Kilberg, M. S. (2004) Amino acid deprivation induces the transcription rate of the human asparagine synthetase gene through a timed program of expression and promoter binding of nutrient-responsive basic region/leucine zipper transcription factors as well as localized histone acetylation. J. Biol. Chem. **279**, 50829–50839
36 Su, N. and Kilberg, M. S. (2008) C/EBP homology protein (CHOP) interacts with activating transcription factor 4 (ATF4) and negatively regulates the stress-dependent induction of the asparagine synthetase gene. J. Biol. Chem. **283**, 35106–35117
37 Seo, J., Fortuno, E. S., Suh, J. M., Stenesen, D., Tang, W., Parks, E. J., Adams, C. M., Townes, T. and Graff, J. M. (2009) Atf4 regulates obesity, glucose homeostasis, and energy expenditure. Diabetes **58**, 2565–2573
38 Kroemer, G., Mariño, G. and Levine, B. (2010) Autophagy and the integrated stress response. Mol. Cell **40**, 280–293
39 Endo, Y., Fu, Z., Abe, K., Arai, S. and Kato, H. (2002) Dietary protein quantity and quality affect rat hepatic gene expression. J. Nutr. **132**, 3632–3637
40 Zhang, Y., Lei, T., Huang, J. F., Wang, S. B., Zhou, L. L., Yang, Z. Q. and Chen, X. D. (2011) The link between fibroblast growth factor 21 and sterol regulatory element binding protein 1c during lipogenesis in hepatocytes. Mol. Cell. Endocrinol. **342**, 41–47
41 Xiao, F., Huang, Z., Li, H., Yu, J., Wang, C., Chen, S., Meng, Q., Cheng, Y., Gao, X., Li, J. et al. (2011) Leucine deprivation increases hepatic insulin sensitivity via GCN2/mTOR/S6K1 and AMPK pathways. Diabetes **60**, 746–756
42 Domouzoglou, E. M. and Maratos-Flier, E. (2011) Fibroblast growth factor 21 is a metabolic regulator that plays a role in the adaptation to ketosis. Am. J. Clin. Nutr. **93**, 901S–905S
43 Chau, M. D., Gao, J., Yang, Q., Wu, Z. and Gromada, J. (2010) Fibroblast growth factor 21 regulates energy metabolism by activating the AMPK–SIRT1–PGC-1α pathway. Proc. Natl. Acad. Sci. U.S.A. **107**, 12553–12558

Received 3 October 2011/10 January 2012; accepted 11 January 2012
Published as BJ Immediate Publication 11 January 2012, doi:10.1042/BJ20111748

3.2. ANNEX TO ARTICLE 2

3.2.1. SPECIFICITY OF THE FGF21 REGULATION BY AMINO ACID STARVATION IN HEPG2 CELLS TREATED WITH HISOH

Egr1 (Early growth response 1) was found to be the most upregulated gene in a microarray performed in HepG2 cells treated with histidinol (HisOH) (Shan et al., 2010). Following the same procedure of the referenced work, HepG2 cells were treated with 5mM HisOH for 4 hours before harvest. We have analyzed Egr1 expression as a positive control, which showed a 100-fold induction compared to non-treated cells (Figure R-9A). CPT1A and HMGCS2 were not affected by HisOH treatment (Figure R-9B, inside box), while FGF21 levels were increased around 120 times compared to control (Figure R-9B). This result indicates that genes that regulate fatty acid oxidation and ketogenesis are not affected by amino acid starvation mimicked by HisOH in a hepatoma cell line. Although FGF21, CPT1A and HMGCS2 are all PPARα target genes that are induced by a global nutrient deprivation as fasting, here we show that FGF21 is specifically induced upon amino acid deprivation.

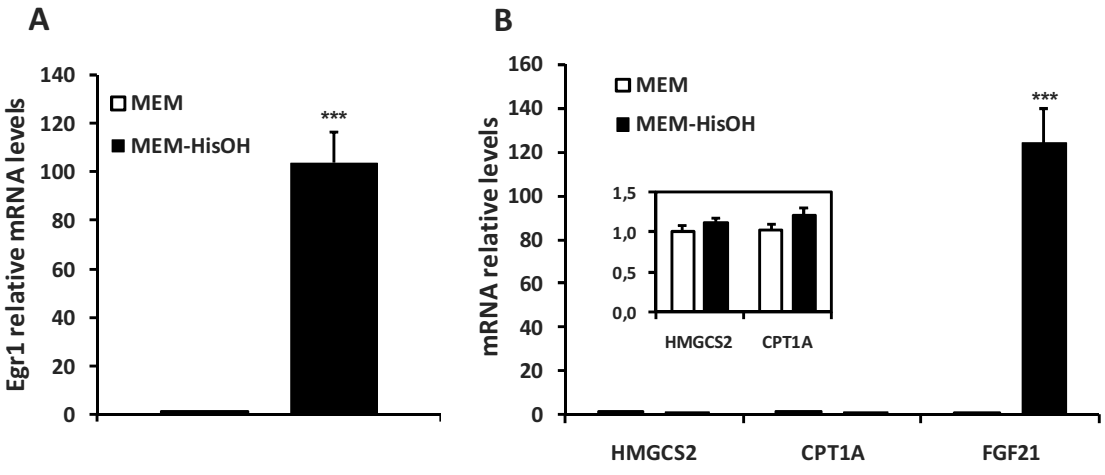

FIGURE R-9. HisOH treatment specifically induces FGF21 mRNA levels in HepG2 cells. HepG2 cells were treated with 5mM HisOH for 4 hours and Egr1 (A), CPT1A, HMGCS2 and FGF21 (B) mRNA levels were analyzed. Results are means ± SEM (n=2) ***p<0.001 relative to MEM control (open bars).

3.2.2. ATF4-DEPENDENT INDUCTION OF FGF21 EXPRESSION IN RESPONSE TO PROTEOSOME INHIBITION AND ENDOPLASMATIC RETICULUM (ER) STRESS

Because we had seen that MG132 treatment induced FGF21 mRNA levels in HepG2 cells in a dose-dependent manner (Figure 1B, ARTICLE 2), we wanted to check if, as described (Jian et al., 2005), MG132 treatment induced ATF4 expression. HepG2 cells were treated with 10µM MG132 for 6 hours and nuclear extracts were obtained. Effectively, ATF4 protein levels were hugely increased compared to non-treated cells (Figure R-10A). It is known that increases in ATF4 translation can be achieved by several stress conditions. To address the role of ER stress in the activation of FGF21, HepG2 cells were treated with 5mg/µL tunicamycin (Tun., a potent inducer of ER stress) for 24h. As expected, ATF4 protein levels were increased (Figure R-10A).

To check whether tunicamycin treatment was also increasing FGF21 mRNA levels and whether this effect was ATF4-dependent, HepG2 cells were transfected with a specific ATF4-siRNA or a control-siRNA (unspecific), and treated or not with tunicamycin. FGF21 was highly induced upon tunicamycin treatment, and this increase was significantly downregulated when cells were depleted from ATF4 (Figure R-10B). These results confirm that both inhibition of the proteasome degradation by MG132 and induction of ER stress by tunicamycin in HepG2 cells, are stress conditions that increase ATF4 protein levels and increase FGF21 mRNA levels, in an ATF4-dependent manner.

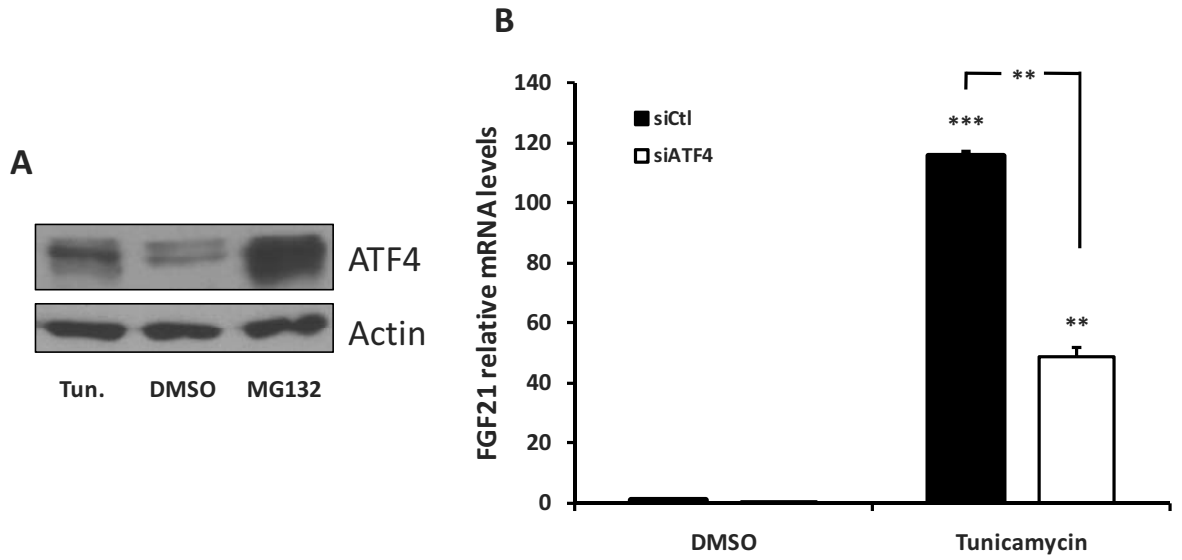

FIGURE R-10. Tunicamycin induction of FGF21 in HepG2 cells is ATF4-dependent. HepG2 cells were treated with 10µM MG132 for 6h, 5mg/µL tunicamycin (Tun.) for 24h, or DMSO (vehicle). (A) An immunoblot against ATF4 was performed in nuclear cell extracts. Actin was used as loading control. A representative Western blot is shown. (B) FGF21 mRNA levels were examined in HepG2 cells treated or not with tunicamycin, in cells transfected with an unspecif (siCtl) or ATF4-specific siRNA (siATF4). Results are means ± SEM (n=2) **p<0.01, ***p<0.001 relative to DMSO.

3.2.3. TRANSCRIPTIONAL ACTIVATION OF FGF21 IN RESPONSE TO AMINO ACID STARVATION AND ER STRESS, IN HEPG2 CELLS

By measuring the FGF21 primary transcript (hnRNA) levels, we have seen that HisOH induced FGF21 transcription (Figure 2B, ARTICLE 2). To go further, we have assayed the construct of the human FGF21 promoter region containing both AAREs (Figure R-11A) cloned in the luciferase reporter plasmid, by measuring luciferase activity. As predicted, FGF21 promoter activity was increased in a time-dependent manner by HisOH treatment (Figure R-11B), as well as after 24h treatment with tunicamycin (Tun.) (Figure R-11C).

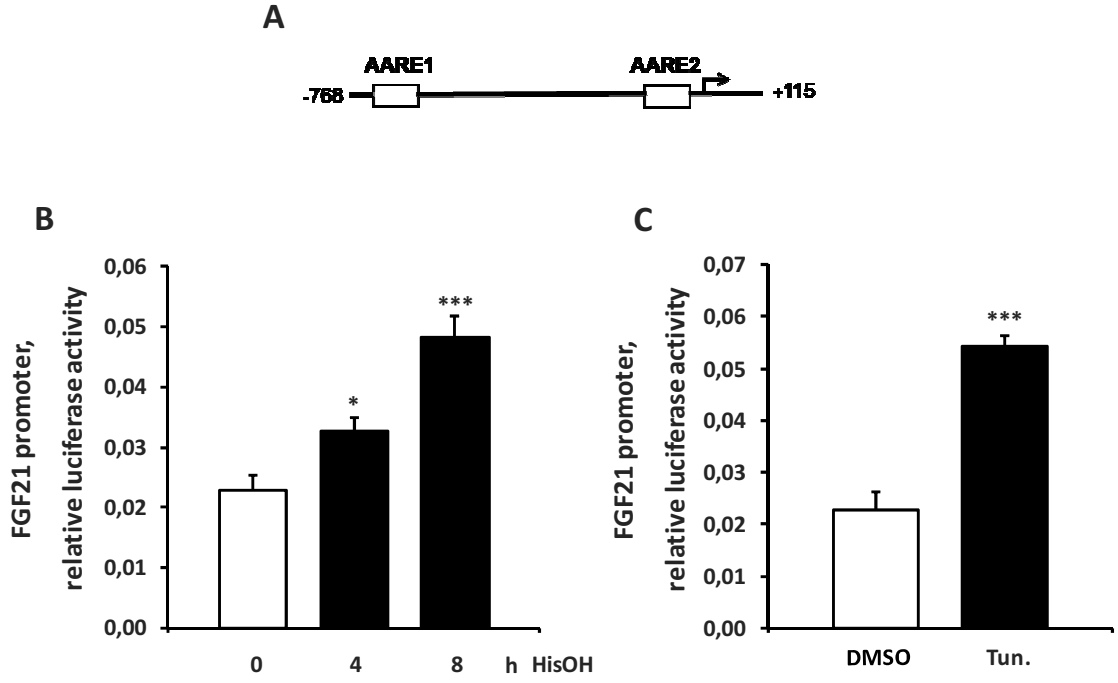

FIGURE R-11. Both HisOH and tunicamycin treatments induce FGF21 promoter activity. (A) Scheme of the human FGF21 promoter reporter construct used. Luciferase activity measured after HisOH (B) or tunicamycin (Tun.) (C) treatments. Results are means ± SEM (n=4) *p<0.05, *** p<0.001 relative to control (open bars).

3.2.4. ATF3 REPRESSION OF THE ATF4 ACTION ON THE FGF21 TRANSCRIPTIONAL ACTIVITY

A self-limiting cycle of ATF4 action has been demonstrated for several AARE-containing genes (Pan et al., 2007). A model for the asparagine synthethase (ASNS) gene was described, in which ATF4 activation of C/EBPβ and ATF3 expression leads to a self-limiting regulation of ATF4-dependent transcription (Kilberg et al., 2009). FGF21 gene expression showed to have this same behaviour upon amino starvation, mimicked by HisOH treatment (Figure 2B, ARTICLE 2). Next, we have co-transfected along with the human FGF21 promoter (Figure R-11A), both ATF4 and ATF3 expression vectors. ATF4-induction of the FGF21 promoter activity was decreased by ATF3 in a dose-dependent manner (Figure R-12).

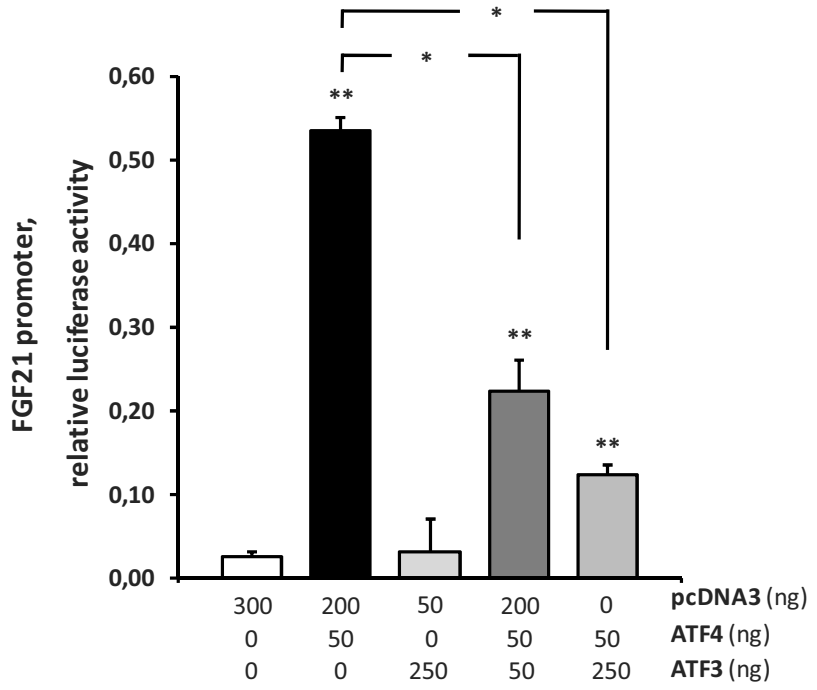

FIGURE R-12. ATF3 blocks ATF4-induction of the human FGF21 promoter. HepG2 cells were co-transfected with the indicated amounts of plasmids. pcDNA3-empty vector was used to normalize the transfected DNA amount. Results are means ± SEM (n=2) **p<0.01 relative to empty vector (open bar), *p<0.05 relative to ATF4 (close dark bar).

3.2.5. ATF4 BINDING TO BOTH AMINO ACID RESPONSE ELEMENTS (AARE) IN THE HUMAN FGF21 PROMOTER

To corroborate our published results, that ATF4 was able to occupy both newly identified AAREs in the human FGF21 promoter (Figure 4, ARTICLE 2), additional work was performed. To the ChIP analysis, the chromatin was sheared to obtain fragments between 100 and 1000 bp (Figure R-13A). Because AARE1 and AARE2 are only separated by less than 500 bp, three different PCR primers sets were defined to detect the specific occupancy of ATF4 for each AARE (Figure R-13C). As observed, enrichment in ATF4 binding is observed when each AARE region is individually amplified, while it is not, when amplifying the complete region containing both response elements (Figure R-13B).

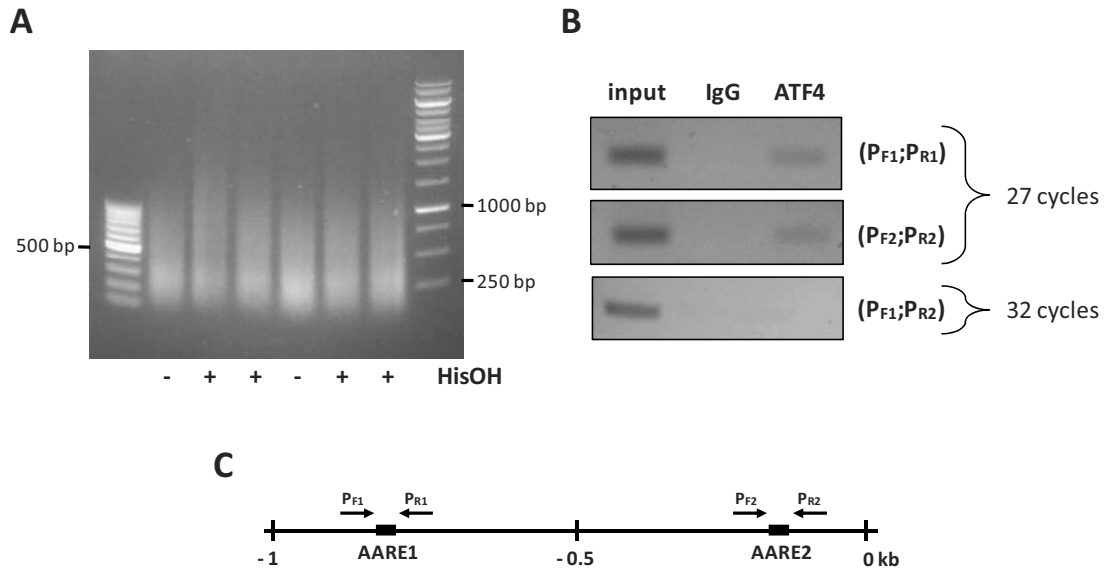

FIGURE R-13. ATF4 is able to bind both AAREs individually in the human FGF21 promoter. (A) Sheared chromatin of HepG2 cells after HisOH treatment. (B) PCR analysis of the chromatin immunoprecipited with IgG or specific ATF4 antibody. (C) Scheme of the PCR primers sets used.

These last results allowed us completing the FGF21 regulation under amino acid starvation in HepG2 cells. We have seen that other mechanisms that induce selective ATF4 translation, as ER stress, are also able to activate the transcription of FGF21. We have also finished establishing that FGF21 behaviour under amino acid deprivation is similar to other well studied genes related to amino acid metabolism, as the asparagine synthethase (ASNS).

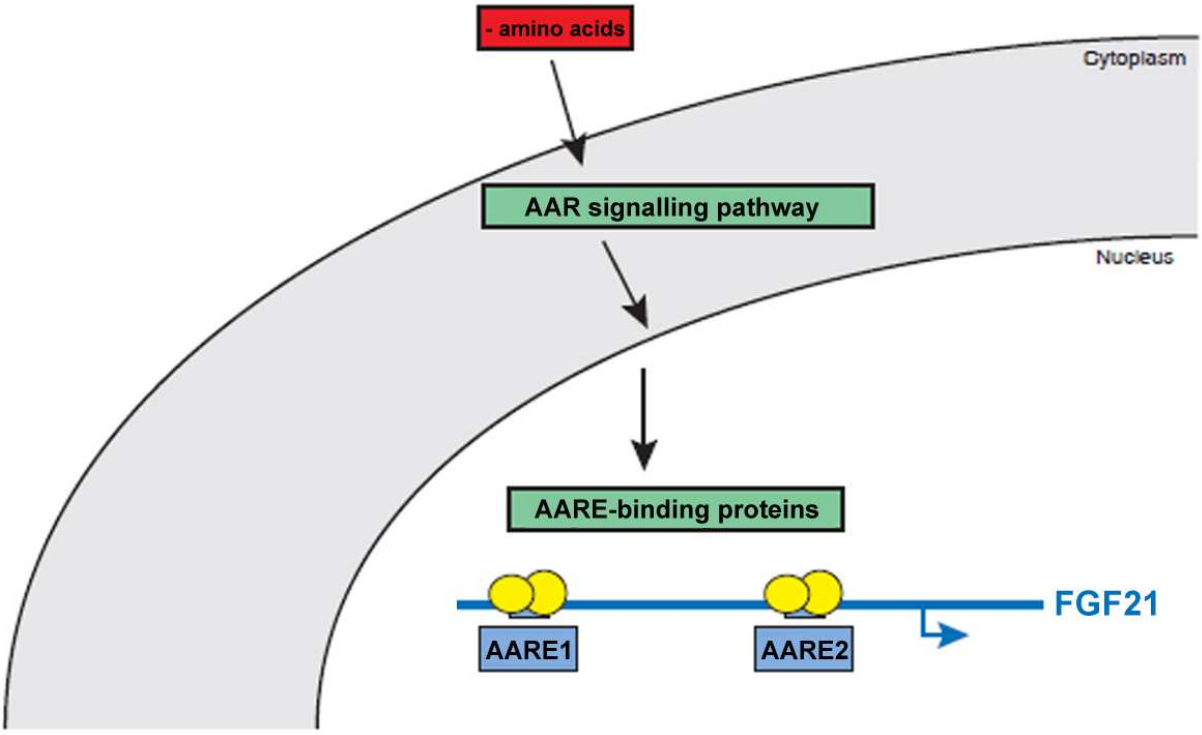

FIGURE R-14. Scheme for the ATF4 transcriptional activation of the human FGF21 gene by amino acid deprivation.

4. METABOLIC SIGNALLING UNDER LEUCINE DEPRIVATION IN RESPONSE TO FASTING

4.1. LEUCINE-DEFICIENT DIET EFFECTS IN THE TYPICAL CHANGES IN THE METABOLITE LEVELS IN RESPONSE TO FASTING

We have shown that FGF21 was induced during amino acid deprivation (ARTICLE 2). FGF21 is also strongly induced in liver in response to fasting or ketogenic diet (Badman et al., 2007; Inagaki et al., 2007; Lundasen et al., 2007). So, we were interested to know whether FGF21 induction by a leucine-deficient [(-)leu] diet would affect, or be affected by, the adaptive fasting response. To do so we have fed mice for 7 days within a control diet (nutrionally complete diet), and then we have randomly separated mice in two groups, where one was kept with control diet (Ctl diet) and the other was given a (-)leu diet for another 7 days. Weights and food intake were recorded daily. At day 14, mice were randomly separated in a total of 4 groups, where 2 groups (one from each diet) were fasted overnight. *Ad libitum* and fasted mice were sacrificed around 11:00 am (Figure R-15).

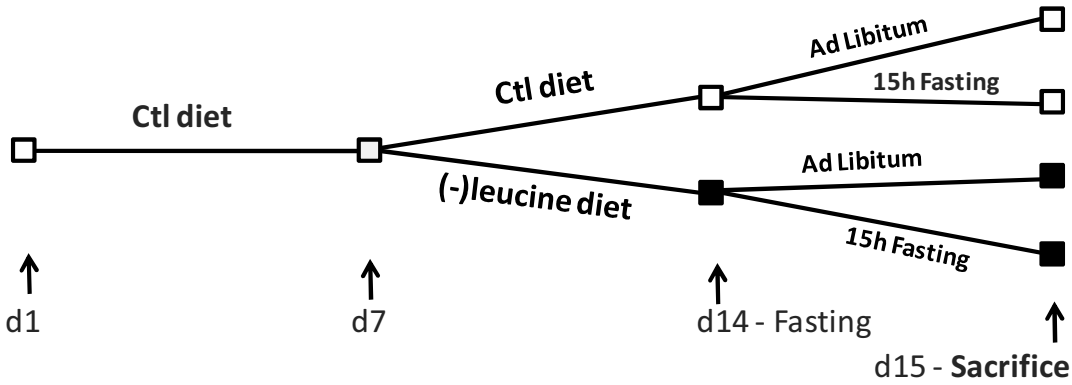

FIGURE R-15. Design of the study. A scheme of the experimental procedure is presented. At day 7 (d7) one of the former groups was given (-)leu diet. At day 14 (d14), one group from each diet was subjected to overnight fasting. Open marks (▫) correspond to Ctl diet and closed marks (▪) to leucine-deficient diet.

In agreement with published work (Guo and Cavener, 2007), we have observed that mice fed with a (-)leu diet ate significantly less (Figure R-16A) and lose weight (Figure R-16B), compared to control (Ctl).

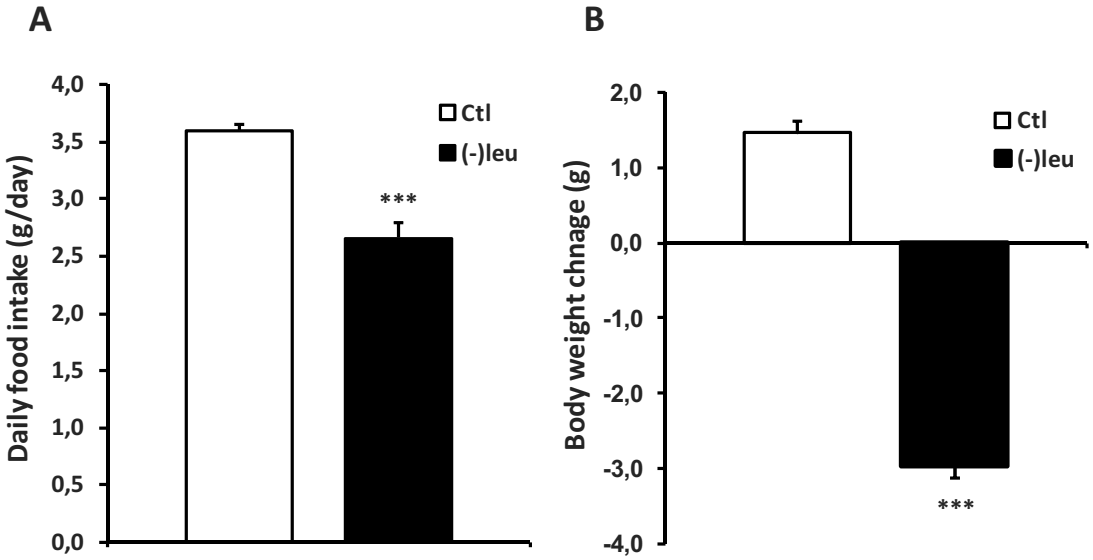

FIGURE R-16. Phenotypical differences between mice on control (Ctl) and leucine-deficient diet. (A) Daily food intake. (B) Body weight change. Results are means ± SEM each group (n=4-6 mice) ***p<0.001 relative to control diet.

Fasting is characterized by lower glycemia, and higher free fatty acids (FFAs or NEFAs) and ketone bodies levels in blood. We have observed that *ad libitum* FFAs were decreased in mice fed a (-)leu diet. However, there were no further differences in the fasting increased FFAs serum levels between Ctl and (-)leu diets (Figure R-17A). Moreover, there were no differences in the glycemia (Figure R-17B) nor in ketone bodies levels (Figure R-17C), between Ctl and (-)leu groups, as measured by β-hydroxybutyrate serum levels, in fasted mice. Nevertheless, there was an intriguing increase in the β-hydroxybutyrate levels in the *ad libitum* group of mice fed the (-)leu diet, compared to Ctl (Figure R-17C).

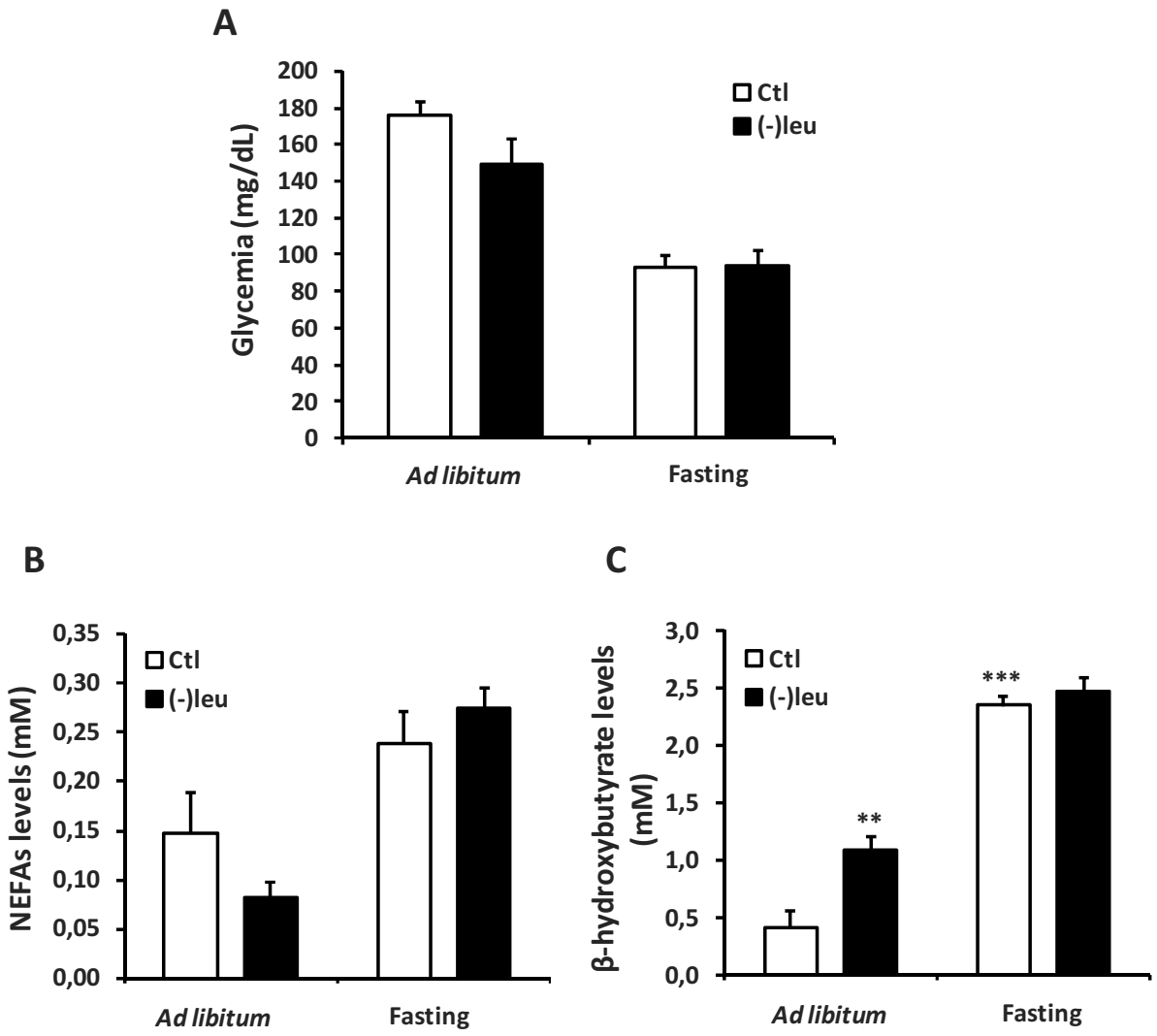

FIGURE R-17. **Mice fed either control or leucine-deficient diet respond normally to an overnight fasting.** Glycemia levels (A), serum non-esterified fatty acids (NEFAs) (B) and β-hydroxybutyrate (C) levels were measured. Results are means ± SEM each group (n=4-6 mice) **p<0.01 ***p<0.001 relative to *ad libitum* control diet.

4.2. LEUCINE DEPRIVATION EFFECTS IN THE EXPRESSION OF β-OXIDATION GENES IN LIVER, AFTER AN OVERNIGHT FASTING.

The expression of β-oxidation and fatty-acid transport genes in the livers of mice fed a (-)leu diet for 7 days compared with control diet have been already examined (Guo and Cavener, 2007). As described, no changes between groups were observed in the fed state in the expression of *Cpt1α*, *Hmgcs2*, *Pck1* and *Ppargc1α* (Figure R-18). However, after a fasting

period, β-oxidation, ketogenesis and gluconeogenesis key-genes were further up-regulated in the (-)leu diet group compared to control. The highest induction was seen in the *Ppargc1α* (PGC1α) gene, a known coactivator on these processes (Figure R-18).

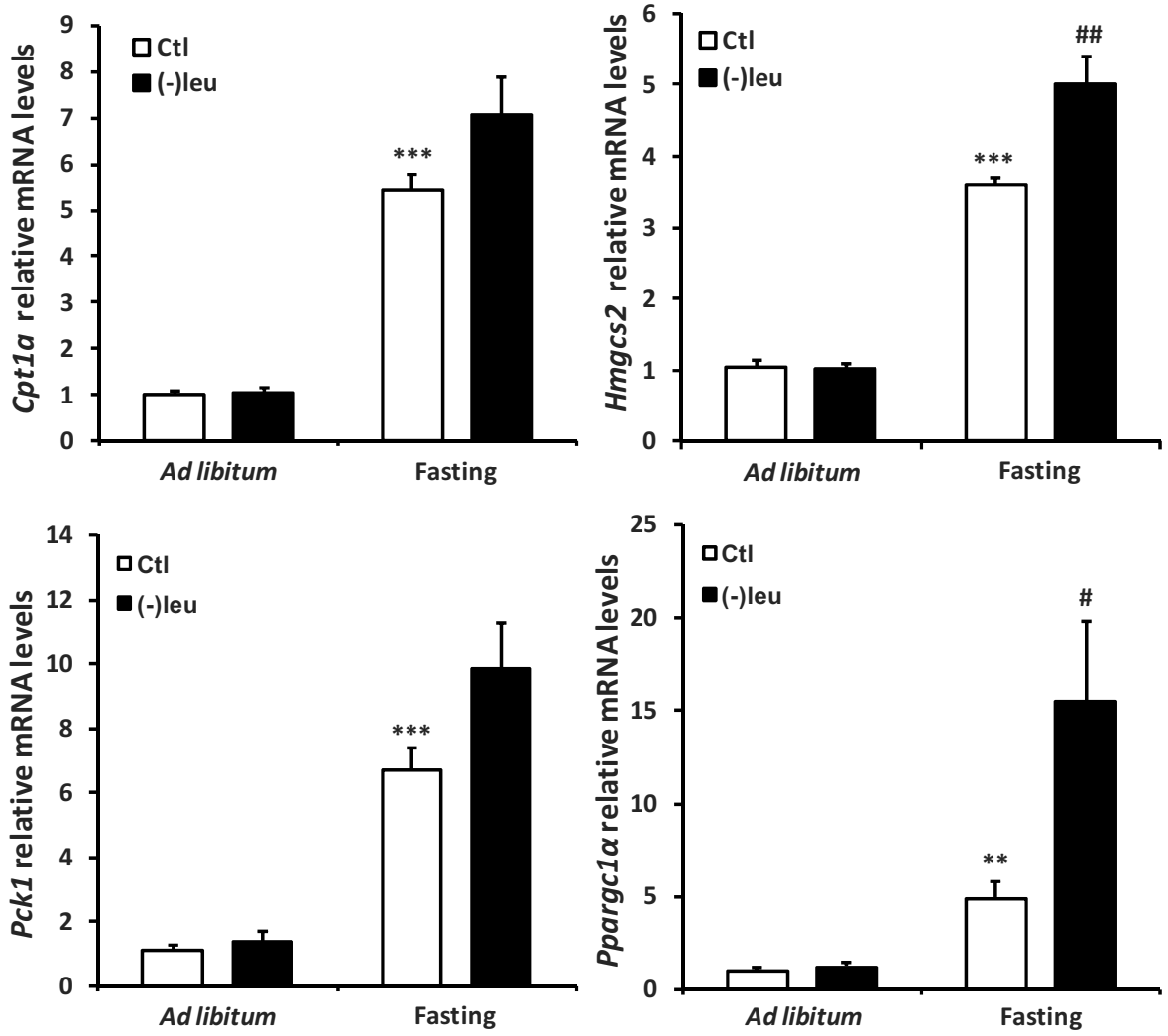

FIGURE R-18. Fasting-induced genes are upregulated under a leucine-deficient diet. mRNA expression of *Cpt1a*, *Hmgcs2*, *Pck1* and *Ppargc1α* in liver was determined using real time PCR. Results are means ± SEM each group (n=5-6 mice) **p<0.01, ***p<0.001 relative to *ad libitum* control diet; #p<0.05, ##p<0.01 relative to fasting control diet.

4.3. DIFFERENTIAL FGF21 ACTIVATION UNDER LEUCINE DEPRIVATION AFTER FASTING, COMPARED TO *AD LIBITUM*

We have shown that FGF21 was induced by amino acid deprivation in mouse liver (Figure 6, ARTICLE 2). Surprisingly, while in the fed state FGF21 showed a very high induction under leucine deprivation, increased fasted FGF21 levels hardly triplicate its expression in (-)leu diet compared to control (Figure R-19A). It means that although there was still an increase, there was no accumulative induction by both fasting and amino acid deprivation signalling. As expected, circulating FGF21 levels paralleled these changes in liver expression (Figure R-19B and R-19C).

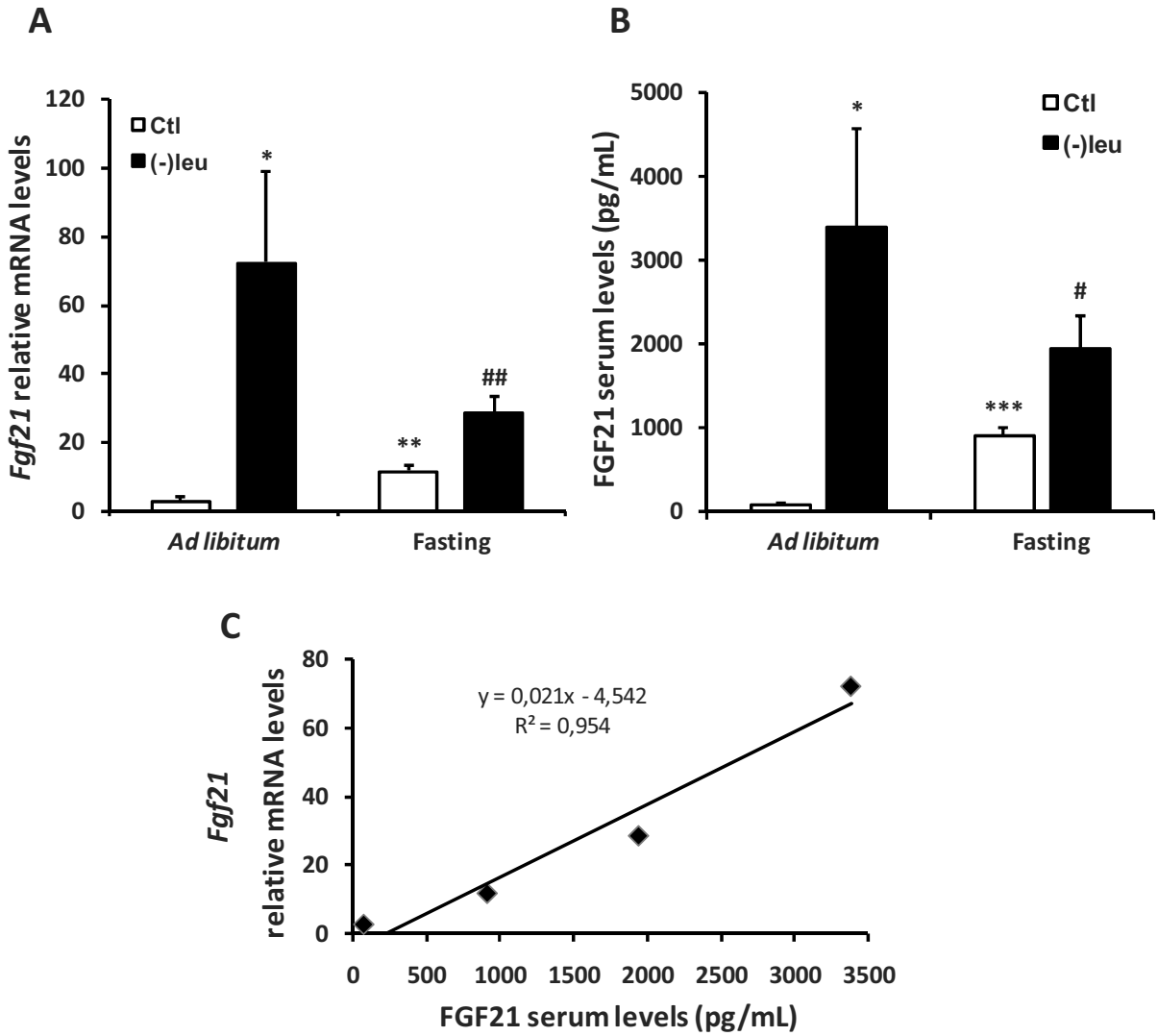

FIGURE R-19. FGF21 expression under a leucine-deficient diet is differentially induced in the fed or in the fasted state. (A) mRNA expression of *Fgf21* in liver was determined using real time PCR. (B) Serum FGF21 was measured by ELISA. (C) A positive correlation between the hepatic mRNA induction and serum FGF21 levels is shown. Results are means ± SEM each group (n=5-6 mice) *p<0.5, **p<0.01, ***p<0.001 relative to *ad libitum* control diet; #p<0.05, ##p<0.01 relative to fasting control diet.

5. ROLE OF FGF21 IN THE AMINO ACID DEPRIVATION PHENOTYPE

5.1. SUBMITTED MANUSCRIPT: **FGF21 MEDIATES THE LIPID METABOLISM RESPONSE TO AMINO ACID STARVATION**

De Sousa-Coelho AL [1, 3], Hondares E [2, 3], Villarroya F [2, 3],

Marrero PF [1, 3], Haro D [1, 3]

[1] Department of Biochemistry and Molecular Biology, School of Pharmacy, University of Barcelona

[2] Department of Biochemistry and Molecular Biology, School of Biology, University of Barcelona and CIBER Fisiopatología de la Obesidad y Nutrición

[3] Institute of Biomedicine of the University of Barcelona (IBUB)

SUMMARY IN SPANISH (RESUMEN EN CASTELLANO):

La expresión de genes lipogénicos en el hígado está reprimida en ratones privados de leucina en la dieta. La reducción de la expresión de PPARγ y SREBP1c dependiente de GCN2, media este efecto. La hormona FGF21, que se induce en el hígado durante el ayuno y es fundamental para la respuesta de adaptación metabólica a la inanición, también se induce como parte del programa transcripción iniciado por el aumento de los niveles de ATF4 debido a la privación de aminoácidos, como hemos demostrado recientemente. En este trabajo se presentan resultados que demuestran que FGF21 es el vínculo entre el desequilibrio de aminoácidos y la respuesta metabólica celular a la privación de nutrientes.

Hemos encontrado que los ratones *knockout* de FGF21 (FGF21-KO) mostraron una pérdida de peso significativamente atenuada bajo la privación leucina, y que la deficiencia de FGF21 evita los cambios en el hígado, tejido adiposo blanco (WAT) y tejido adiposo marrón (BAT) en ratones privados de leucina. Después de la privación leucina, se encontró que en los ratones FGF21-KO, la represión de la expresión de los genes lipogénicos en el hígado y en el

WAT, y el aumento de la fosforilación de la HSL en el WAT, estaban parcialmente bloqueados. La deficiencia en FGF21 también ha bloqueado el aumento del mRNA la *Ucp1* y *Dio2* en el BAT, en la privación leucina.

Nuestros resultados demuestran el importante papel de FGF21 en la regulación del metabolismo de los lípidos durante la privación de aminoácidos. Debido a que la hormona FGF21 es un regulador importante del gasto energético y del metabolismo, con efectos antiobesidad y antidiabéticos, nuestro trabajo añade la manipulación de la dieta como una posibilidad para controlar la expresión de este candidato prometedor para el tratamiento de la resistencia a la insulina, la obesidad y el síndrome metabólico.

FGF21 mediates the lipid metabolism response to amino acid starvation

Ana Luísa De Sousa-Coelho[a,c], Elayne Hondares[b,c], Francesc Villarroya[b,c], Pedro F. Marrero[a,c], Diego Haro[a,c]

[a] Departament de Bioquímica i Biologia Molecular, Facultat de Farmacia, Universitat de Barcelona, Av Joan XXIII s/n, 08028 Barcelona, Spain

[b] Departament de Bioquímica i Biologia Molecular, Facultat de Biologia, Universitat de Barcelona and CIBER Fisiopatología de la Obesidad y Nutrición, Av Diagonal 643, 08028 Barcelona, Spain

[c] Institut de Biomedicina de la Universitat de Barcelona (IBUB)

Corresponding author: Diego Haro, E-mail: dharo@ub.edu; Tel: (+34) 934034500; Fax: (+34) 934024520.

Running head: Role of FGF21 during leucine deprivation

Keywords: metabolism, white adipose tissue, brown adipose tissue, liver, FGF21, leucine deprivation.

ABSTRACT

Lipogenic gene expression in liver is repressed in mice upon leucine deprivation. The hormone FGF21, which is critical to the adaptive metabolic response to starvation, is also induced under amino acid deprivation. Upon leucine deprivation, we found that FGF21-deficient mice showed unrepressed expression of lipogenic genes in liver and white adipose tissue, and decreased phosphorylation of HSL in white adipose tissue. The increased expression of *Ucp1* in brown adipose tissue under these circumstances is also impaired in FGF21-deficient mice. Our results demonstrate the important role of FGF21 in the regulation of lipid metabolism during amino acid starvation.

INTRODUCTION

Mammals have developed a wide range of mechanisms to detect and respond to episodes of malnutrition and starvation. Nutrient deprivation or starvation frequently correlates with amino acid limitation. Amino acid starvation initiates a signal transduction cascade, starting with the activation of the general control non-derepressible 2 (GCN2) kinase, phosphorylation of eukaryotic initiation factor 2 (eIF2), and increased synthesis of activating transcription factor (ATF) 4 (Kilberg et al. 2009).

GCN2 triggers the amino acid response signal transduction pathway when GCN kinase activity is activated by its binding to any uncharged tRNA molecule (Hao et al. 2005; Maurin et al. 2005). Although global protein synthesis is reduced, the translation of a group of mRNA species is increased as part of this response. These species include ATF4 (Lu et al. 2004; Vattem and Wek 2004), a transcription factor that binds to CARE (C/EBP-ATF response elements that are also called amino acid response elements [AARE]) and modulates a wide spectrum of genes involved in adaptation to dietary stress (Ameri and Harris 2008). Food deprivation reduces free intracellular amino acid and increases eIF2α phosphorylation and *Atf4* mRNA levels in skeletal muscle (Ebert et al. 2010).

Fibroblast growth factor (FGF) 21 is a member of the FGF family with endocrine properties. It is predominantly produced by liver, but also by other tissues such as white and brown adipose tissue, skeletal muscle, and pancreas (Nishimura et al. 2000; Izumiya et al. 2008; Johnson et al. 2009; Hondares et al. 2011). FGF21 expression in liver is under tight control by peroxisome proliferator-activated receptor (PPAR) α (Badman et al. 2007; Inagaki et al. 2007; Lundåsen et al. 2007; Gälman et al. 2008). It is induced in the liver during fasting and its expression induces a metabolic state that mimics long-term fasting. Thus, FGF21 is critical for the induction of hepatic fat oxidation, ketogenesis and gluconeogenesis, which are metabolic processes critical for the adaptive metabolic response to starvation (Reitman 2007). We have recently found that *Fgf21* is a target gene for ATF4. Consequently, FGF21 is induced by amino acid deprivation both in mice liver and HepG2 cultured cells as part of the transcriptional program initiated by increased levels of ATF4 (De Sousa-Coelho et al. 2012).

A dietary amino acid imbalance alters metabolic pathways beyond protein homeostasis, since there is a link between dietary amino acids and lipid metabolism. GCN2-dependent inhibition of fatty acid synthase (FAS) activity, expression of lipogenic genes in liver and

increased mobilization of lipid stores occur in response to leucine deprivation in mice (Guo and Cavener 2007). In addition, the following have been observed: increased expression of β-oxidation genes, decreased expression of lipogenic genes, activation of fatty acid synthase in white adipose tissue (WAT), and increased expression of uncoupling protein 1 (*Ucp1*) in brown adipose tissue (BAT) (Cheng et al. 2010; Cheng et al. 2011).

The coincidence between the metabolic response to essential amino acid deprivation and to FGF21, the induction of *Fgf21* under amino acid deprivation (De Sousa-Coelho et al. 2012), and the repression of the transcription and maturation of sterol regulatory element binding protein (SREBP) 1c induced by FGF21 in HepG2 cells (Zhang et al. 2011) led us to consider that FGF21 could be an important mediator between amino acid deprivation and lipid metabolism in liver and white and brown adipose tissue.

To investigate this hypothesis, we examined the response of FGF21-deficient mice to deprivation of the essential amino acid leucine. As expected, we found a huge increase in FGF21 expression in liver of wild type animals, along with a repression of lipogenic genes after 7 days of leucine deprivation. In this condition, FGF21-deficient mice developed liver steatosis caused by unrepressed expression of lipogenic genes. In WAT, the expression of lipogenic genes was also repressed and the phosphorylation of hormone-sensitive lipase (HSL) was increased under leucine deprivation. The absence of leucine also induced an increase in the expression of *Ucp1* and type 2 deiodinase (*Dio2*) in BAT. We found that all these effects in white and brown adipose tissue were also impaired in FGF21-deficient mice. Here, we show the involvement of FGF21 in the regulation of lipid metabolism during amino acid starvation, thus reinforcing its important role in coordinating energy homeostasis under a variety of nutritional conditions.

RESULTS AND DISCUSSION

FGF21 gene expression is induced by leucine deprivation specifically in liver but not in brown or white adipose tissue. According to our previously reported results (De Sousa-Coelho et al. 2012), mice maintained on a leucine-deficient ([-]leu) diet show a dramatic increase in FGF21 circulating levels (Figure 1A). To check the origin of this circulating FGF21 we analyzed *Fgf21* gene expression in several tissues. Consistent with the liver as the main site of FGF21 production and release into the blood, *Fgf21* mRNA levels in liver paralleled those in serum, whereas mRNA levels were unchanged in BAT and, unexpectedly, significantly decreased in epididymal (e) WAT in wild type mice maintained on a (-)leu diet (Figure 1B). As expected, *Fgf21* mRNA levels were undetectable in any analyzed tissue in the FGF21-KO mice.

FGF21 deficiency significantly attenuates weight loss under leucine deprivation. When fed a leucine-deprived diet, mice undergo rapid weight loss (Cheng et al. 2010). The goal of the present study is to investigate whether this phenomenon is FGF21-dependent. For this purpose, wild type and FGF21-KO mice were fed a control or leucine-deficient diet for 7 days. We found that weight loss was partially blunted in FGF21-KO mice (Figures 2A and 2B), while the reduction in food intake caused by leucine deprivation (~30%) was unchanged between genotypes (Figure 2C). The observation that white adipocytes from FGF21 transgenic mice are substantially smaller than those from wild type mice (Kharitonenkov et al. 2005; Inagaki et al. 2007), and that leucine deprivation decreased adipocyte volume (Cheng et al. 2010), led us to examine whether this effect was FGF21-dependent. A histological analysis of eWAT showed that leucine deprivation resulted in a reduction in adipocyte volume compared with mice fed a control diet. By contrast, the adipocyte volume was only slightly reduced in (-)leu FGF21-KO mice and remained unchanged in FGF21-KO mice on the control diet (Figure 2D). We note that other groups reported increased (Hotta et al. 2009) or decreased (Dutchak et al. 2012) adipocyte size in FGF21-KO mice on regular diets. We have no explanation for these discrepancies, beyond potential minor differences in the composition of the diet.

Increased phosphorylation of HSL under leucine deprivation is FGF21-dependent. It has been previously described that leucine deprivation increases lipolysis in WAT (Cheng

et al. 2010). It has also been suggested that FGF21 stimulates lipolysis in WAT during normal feeding, but inhibits it during fasting (Hotta et al. 2009). Therefore, to examine the role of FGF21 in lipolysis, we evaluated the mRNA levels of adipose triglyceride lipase (*Atgl*) and *Hsl* and the levels of phosphorylated HSL. These are the first and second enzymes, respectively, that regulate lipolysis (Greenberg et al. 2001; Schoenborn et al. 2006), in WAT. We did not find any statistically significant changes in *Atgl* or *Hsl* mRNA levels upon leucine deprivation (Figure 3A). Consistent with changes in body weight, a lack of FGF21 significantly decreased levels of phosphorylated (P)-HSL in WAT (Figure 3B), which suggests that lipolysis was impaired.

FGF21 deficiency prevents changes in liver, WAT and BAT in leucine-deprived mice. A link between FGF21 and SREBP1c during lipogenesis in hepatocyte in culture has recently been proposed (Zhang et al. 2011). As lipogenic genes are downregulated in liver of mice deprived of leucine (Guo and Cavener 2007), we speculated that FGF21 may regulate their expression. To investigate this possibility, we examined levels of *Fas*, *Srebp1c* and acetyl-CoA carboxylase (*Acc*) 1 mRNA in liver of wild type and FGF21-KO mice maintained either on the control or (-)leu diet. As expected, the lipogenic gene expression program was decreased on the (-)leu diet. However, this reduction was diminished in mice lacking FGF21 (Figure 4A), even though the amino acid starvation response program was correctly initiated in these animals, as shown by the increased levels of ATF4 protein (Figure 4B) and the increase in mRNA levels of asparagine synthetase (*Asns*), a prototypical ATF4 target gene (Figure 4C). The induction of *Asns* gene expression, for which the gene product catalyzes the glutamine and ATP-dependent conversion of aspartic acid to asparagine, suggests that FGF21 is not involved in the control of amino acid metabolism under amino acid starvation.

The expression pattern of the lipid synthesis genes is not reflected by liver triglyceride levels, but is indicated by hematoxylin and eosin staining. This shows a decreased amount of clear regions that may reflect lipid accumulation under leucine deprivation in wild type animals that does not occur in the FGF21-KO mice (Figure 4D).

As expected, gene expression analysis in eWAT revealed that the mRNA levels of the lipogenic genes *Fas*, *Srebpc* and *Acc1* were lower in mice maintained on the (-)leu diet. These changes were blunted in the FGF21-KO mice, particularly for *Fas* (Figure 4E).

The endocrine effect of FGF21 on adipose tissue under leucine deprivation that we observed here is different from the recently described autocrine effect on this tissue in a fed state, in which FGF21 induces lipogenesis through the regulation of PPARγ activity (Dutchak et al. 2012). The decreased FGF21 expression in adipose tissue under leucine deprivation also contrasts with its induction after one day of fasting (Muise et al. 2008). FGF21 administration to diet-induced obese mice leads to a dramatic decrease in the WAT *Fgf21* transcript. However, controversially, it induces an increase in the expression of adipogenic genes (Coskun et al. 2008). It seems, therefore, that the response to increased levels of FGF21 depends on its origin and other factors, which may reflect the metabolic state and the energy requirements of the organism.

Thermogenesis in BAT is mediated by the upregulation of UCP1 (Matthias et al. 2000). It has been proposed that the induction of FGF21 production by the liver mediates direct activation of brown fat thermogenesis during the fetal-to-neonatal transition (Hondares et al. 2010). FGF21 also regulates PGC1α and browning of white adipose tissues in adaptive thermogenesis (Fisher et al. 2012). Consistent with previous results (Cheng et al. 2010), leucine deprivation increased levels of *Ucp1* and *Dio2* mRNAs in wild type mice BAT. These changes were blocked in FGF21-KO (Figure 4F). Because UCP1 expression is related to energy expenditure, the absence of induction of *Ucp1* in FGF21-KO under leucine deprivation may contribute to the decrease in weight loss observed under these circumstances. mRNA levels of *Pgc1α*, which regulates the expression of UCP1 (Handschin and Spiegelman 2006), were also increased. However, they did not differ between WT and FGF21 KO mice under either control or (-)leu diet conditions.

In summary we found that FGF21 plays an essential role in mediating the changes in lipid metabolism observed upon leucine deprivation (Figure 5). We have shown that FGF21-deficient mice under these circumstances showed unrepressed lipogenesis in liver and white adipose tissue, decreased phosphorylation of HSL in white adipose tissue indicating impaired lipolysis, and impaired induction of *Ucp1* expression in brown adipose. Thus, our results demonstrate that FGF21 plays an important role in the regulation of lipid metabolism during amino acid starvation.

MATERIALS AND METHODS

Animals and diets. Male C57BL/6J wild type (WT) and *FGF21*-null mice (B6N; 129 S5-Fgf21^{tm1Lex}/Mmucd, obtained from the Mutant Mouse Regional Resource Center), were housed in a temperature-controlled room (22+-1ºC) on a 12:12 h light/dark cycle and were provided free access to commercial rodent chow and tap water prior to the experiments. Control (nutritionally complete amino acid) and (-)leu (leucine-deficient) diets were obtained from Research Diets, Inc. (New Brunswick, NJ). All diets were isocaloric and compositionally the same in terms of carbohydrate and lipid components. At the beginning of the feeding experiment, twelve- to fifteen-week old male mice were first acclimated to the control diet for 7 days, and then randomly assigned to either the control diet group, with continued free access to the nutritionally complete diet, or the (-)leu diet group, with free access to the diet devoid of the essential amino acid leucine for 7 days. Food intake and body weight were recorded at least every two days. Animals were anesthetized by isoflurane inhalation, and blood was collected from heart for the assay described below. After sacrifice, tissues were isolated and immediately snap frozen and stored at -80ºC for future analysis. The Animal Ethics Committee of the University of Barcelona approved these experiments.

Serum measurements. Serum was obtained by centrifugation of clotted blood and stored at -80ºC. A mouse FGF21 enzyme-linked immunosorbent assay (ELISA) kit was obtained from Millipore for the quantification of FGF21 in mice serum. The assay was conducted according to the manufacturer's protocol. Briefly, a calibration curve was constructed by plotting the difference in absorbance values at 450 and 590 nm versus the FGF21 concentrations of the calibrators, and concentrations of unknown samples (performed in duplicate) were determined using this calibration curve (Vilà-Brau et al. 2011).

RNA isolation and relative quantitative RT-PCR. Total RNA was extracted from the frozen tissues (liver, eWAT and BAT) using TRI reagent solution (Ambion) followed by DNase I treatment (Ambion) to eliminate genomic DNA contamination. To measure the relative mRNA levels, quantitative RT-PCR was performed using TaqMan reagents. cDNA was synthesized from one microgram of total RNA by MLV reverse transcriptase (Invitrogen) with random hexamers (Roche Diagnostics), according to the manufacturer's instructions. TaqMan Gene Expression Master Mix and TaqMan Gene Expression Assays (Invitrogen/Applied Biosystems) were used for the PCR step. Amplification and detection

were performed using the Step-One Plus Real-Time PCR System. Each mRNA from a single sample was measured in duplicate, using 18S ribosomal RNA as an internal control. Results were obtained by the comparative threshold cycle (Ct) method and expressed as fold of the experimental control.

Protein extracts preparation. To obtain liver nuclear extracts, frozen liver was triturated within a mortar in liquid nitrogen and immediately homogenized with a Dounce homogenizer in 1 mL of HB buffer (15mM Tris-HCl [pH 8], 15mM NaCl, 60mM KCl, 0.5mM EDTA), and centrifuged at 800 x g for 5 min. The resulting pellet was resuspended in 100µL of HB buffer supplemented with 0.05% Triton X-100 (Sigma), and centrifuged for 10min at 1.000 x g. Nuclear pellets were washed with 1 mL of HB buffer supplemented with 0.05% Triton X-100 and 1 mL of HB buffer. Nuclei were incubated at 4ºC for 30min in 50µL of HB buffer containing 360 mM KCl and centrifuged for 5min at 10,000 x g. The supernatant corresponding to the nuclear extract was collected, frozen, and stored at -80℃. To obtain WAT total extracts, eWAT was homogenized in RIPA buffer and centrifuged at 12,000 x g for 15min at 4ºC. The supernatant was collected and frozen at -80ºC until analysis. Protein concentration was assayed using Bio-Rad reagent. All of the buffers were supplemented with a mixture of protease inhibitors (Sigma Aldrich), 0.1mM phenylmethylsulfonyl fluoride (PMSF), and a phosphatase inhibitor cocktail (IPC3, Sigma Aldrich).

Immunoblotting. Total and nuclear proteins were resolved by SDS-polyacrylamide gel electrophoresis and transferred onto a Hybond-P PVDF membrane (Millipore). Membranes were blocked for 1h at room temperature. The blots were then incubated with primary antibody in blocking solution overnight at 4ºC. Antibodies were diluted according to the manufacturer's instructions. The blots were washed three times and incubated with horseradish peroxidase-conjugated secondary antibody in blocking buffer for 2h at room temperature. After three washes, the blots were developed using the EZ-ECL Chemiluminescence Detection Kit for HRP (Biological Industries).

Antibodies. Anti-HSL (41075) and anti-phospho HSL (41265) were purchased from Cell Signaling Technology, anti-ATF4 (sc-200) from Santa Cruz Biotechnology, Inc. (Santa Cruz, CA), and anti-actin (A2066) from Sigma.

Histological examinations. For the histological analysis, tissues (liver and epididymal WAT) were fixed in 10% formalin (Sigma Aldrich) and embedded in paraffin. Then, 4-µm-thick sections were cut and stained with hematoxylin and eosin (H&E). Images were

acquired using a Leica CTR 4000 microscope. Quantitative data were obtained using the IMAT program developed in the Science and Technology Center of the University of Barcelona. The selection of the test objects has been performed according to color and choosing the same limits for binarization for all images.

Data analysis/statistics. All data are expressed as means ± SEM. Significant differences were assessed by a two-tailed student's t-test. $p<0.05$ was considered statistically significant.

ACKNOWLEDGMENTS

We thank Daniela Alfarrobinha for graphical assistance. This work was supported by the "Ministerio de Educación y Ciencia" [SAF2010-15217 to D.H.]; and the "Ajut de Suport als Grups de Recerca de Catalunya" [2009 SGR163]. ALDSC was supported by "Fundação para a Ciência e a Tecnologia (FCT)" from Portuguese Government.

REFERENCES

Ameri K, Harris AL. 2008. Activating transcription factor 4. *Int J Biochem Cell Biol* **40**: 14-21.

Badman MK, Pissios P, Kennedy AR, Koukos G, Flier JS, Maratos-Flier E. 2007. Hepatic fibroblast growth factor 21 is regulated by PPARalpha and is a key mediator of hepatic lipid metabolism in ketotic states. *Cell Metab* **5**: 426-437.

Cheng Y, Meng Q, Wang C, Li H, Huang Z, Chen S, Xiao F, Guo F. 2010. Leucine deprivation decreases fat mass by stimulation of lipolysis in white adipose tissue and upregulation of uncoupling protein 1 (UCP1) in brown adipose tissue. *Diabetes* **59**: 17-25.

Cheng Y, Zhang Q, Meng Q, Xia T, Huang Z, Wang C, Liu B, Chen S, Xiao F, Du Y et al. 2011. Leucine Deprivation Stimulates Fat Loss via Increasing CRH Expression in The Hypothalamus and Activating The Sympathetic Nervous System. *Mol Endocrinol* **25**:1624-1635.

Coskun T, Bina HA, Schneider MA, Dunbar JD, Hu CC, Chen Y, Moller DE, Kharitonenkov A. 2008. Fibroblast growth factor 21 corrects obesity in mice. *Endocrinology* **149**: 6018-6027.

De Sousa-Coelho AL, Marrero PF, Haro D. 2012. Activating transcription factor 4-dependent induction of FGF21 during amino acid deprivation. *Biochem J* **443**:165-171.

Dutchak PA, Katafuchi T, Bookout AL, Choi JH, Yu RT, Mangelsdorf DJ, Kliewer SA. 2012. Fibroblast Growth Factor-21 Regulates PPARγ Activity and the Antidiabetic Actions of Thiazolidinediones. *Cell* **148**: 556-567.

Ebert SM, Monteys AM, Fox DK, Bongers KS, Shields BE, Malmberg SE, Davidson BL, Suneja M, Adams CM. 2010. The transcription factor ATF4 promotes skeletal myofiber atrophy during fasting. *Molecular endocrinology* **24**: 790-799.

Fisher FM, Kleiner S, Douris N, Fox EC, Mepani RJ, Verdeguer F, Wu J, Kharitonenkov A, Flier JS, Maratos-Flier E et al. 2012. FGF21 regulates PGC-1α and browning of white adipose tissues in adaptive thermogenesis. *Genes Dev* **26**: 271-281.

Greenberg AS, Shen WJ, Muliro K, Patel S, Souza SC, Roth RA, Kraemer FB. 2001. Stimulation of lipolysis and hormone-sensitive lipase via the extracellular signal-regulated kinase pathway. *J Biol Chem* **276**: 45456-45461.

Guo F, Cavener DR. 2007. The GCN2 eIF2alpha kinase regulates fatty-acid homeostasis in the liver during deprivation of an essential amino acid. *Cell Metab* **5**: 103-114.

Gälman C, Lundåsen T, Kharitonenkov A, Bina HA, Eriksson M, Hafström I, Dahlin M, Amark P, Angelin B, Rudling M. 2008. The circulating metabolic regulator FGF21 is induced by prolonged fasting and PPARalpha activation in man. *Cell Metab* **8**: 169-174.

Handschin C, Spiegelman BM. 2006. Peroxisome proliferator-activated receptor gamma coactivator 1 coactivators, energy homeostasis, and metabolism. *Endocr Rev* **27**: 728-735.

Hao S, Sharp JW, Ross-Inta CM, McDaniel BJ, Anthony TG, Wek RC, Cavener DR, McGrath BC, Rudell JB, Koehnle TJ et al. 2005. Uncharged tRNA and sensing of amino acid deficiency in mammalian piriform cortex. *Science* **307**: 1776-1778.

Hondares E, Iglesias R, Giralt A, Gonzalez FJ, Giralt M, Mampel T, Villarroya F. 2011. Thermogenic activation induces FGF21 expression and release in brown adipose tissue. *J Biol Chem* **286**: 12983-12990.

Hondares E, Rosell M, Gonzalez FJ, Giralt M, Iglesias R, Villarroya F. 2010. Hepatic FGF21 expression is induced at birth via PPARalpha in response to milk intake and contributes to thermogenic activation of neonatal brown fat. *Cell Metab* **11**: 206-212.

Hotta Y, Nakamura H, Konishi M, Murata Y, Takagi H, Matsumura S, Inoue K, Fushiki T, Itoh N. 2009. Fibroblast growth factor 21 regulates lipolysis in white adipose tissue but is not required for ketogenesis and triglyceride clearance in liver. *Endocrinology* **150**: 4625-4633.

Inagaki T, Dutchak P, Zhao G, Ding X, Gautron L, Parameswara V, Li Y, Goetz R, Mohammadi M, Esser V et al. 2007. Endocrine regulation of the fasting response by PPARalpha-mediated induction of fibroblast growth factor 21. *Cell Metab* **5**: 415-425.

Izumiya Y, Bina HA, Ouchi N, Akasaki Y, Kharitonenkov A, Walsh K. 2008. FGF21 is an Akt-regulated myokine. *FEBS Lett* **582**: 3805-3810.

Johnson CL, Weston JY, Chadi SA, Fazio EN, Huff MW, Kharitonenkov A, Köester A, Pin CL. 2009. Fibroblast growth factor 21 reduces the severity of cerulein-induced pancreatitis in mice. *Gastroenterology* **137**: 1795-1804.

Kharitonenkov A, Shiyanova TL, Koester A, Ford AM, Micanovic R, Galbreath EJ, Sandusky GE, Hammond LJ, Moyers JS, Owens RA et al. 2005. FGF-21 as a novel metabolic regulator. *J Clin Invest* **115**: 1627-1635.

Kilberg MS, Shan J, Su N. 2009. ATF4-dependent transcription mediates signaling of amino acid limitation. *Trends in endocrinology and metabolism: TEM* **20**: 436-443.

Lu PD, Harding HP, Ron D. 2004. Translation reinitiation at alternative open reading frames regulates gene expression in an integrated stress response. *J Cell Biol* **167**: 27-33.

Lundåsen T, Hunt MC, Nilsson LM, Sanyal S, Angelin B, Alexson SE, Rudling M. 2007. PPARalpha is a key regulator of hepatic FGF21. *Biochem Biophys Res Commun* **360**: 437-440.

Matthias A, Ohlson KB, Fredriksson JM, Jacobsson A, Nedergaard J, Cannon B. 2000. Thermogenic responses in brown fat cells are fully UCP1-dependent. UCP2 or UCP3 do not substitute for UCP1 in adrenergically or fatty scid-induced thermogenesis. *J Biol Chem* **275**: 25073-25081.

Maurin AC, Jousse C, Averous J, Parry L, Bruhat A, Cherasse Y, Zeng H, Zhang Y, Harding HP, Ron D et al. 2005. The GCN2 kinase biases feeding behavior to maintain amino acid homeostasis in omnivores. *Cell Metab* **1**: 273-277.

Muise ES, Azzolina B, Kuo DW, El-Sherbeini M, Tan Y, Yuan X, Mu J, Thompson JR, Berger JP, Wong KK. 2008. Adipose fibroblast growth factor 21 is up-regulated by peroxisome proliferator-activated receptor gamma and altered metabolic states. *Mol Pharmacol* **74**: 403-412.

Nishimura T, Nakatake Y, Konishi M, Itoh N. 2000. Identification of a novel FGF, FGF-21, preferentially expressed in the liver. *Biochim Biophys Acta* **1492**: 203-206.

Reitman ML. 2007. FGF21: a missing link in the biology of fasting. *Cell Metab* **5**: 405-407.

Schoenborn V, Heid IM, Vollmert C, Lingenhel A, Adams TD, Hopkins PN, Illig T, Zimmermann R, Zechner R, Hunt SC et al. 2006. The ATGL gene is associated with free fatty acids, triglycerides, and type 2 diabetes. *Diabetes* **55**: 1270-1275.

Vattem KM, Wek RC. 2004. Reinitiation involving upstream ORFs regulates ATF4 mRNA translation in mammalian cells. *Proc Natl Acad Sci U S A* **101**: 11269-11274.

Vilà-Brau A, De Sousa-Coelho AL, Mayordomo C, Haro D, Marrero PF. 2011. Human HMGCS2 Regulates Mitochondrial Fatty Acid Oxidation and FGF21 Expression in HepG2 Cell Line. *J Biol Chem* **286**: 20423-20430.

Zhang Y, Lei T, Huang JF, Wang SB, Zhou LL, Yang ZQ, Chen XD. 2011. The link between fibroblast growth factor 21 and sterol regulatory element binding protein 1c during lipogenesis in hepatocytes. *Mol Cell Endocrinol* **343**: 41-47.

FIGURE LEGENDS

Figure 1. FGF21 is differently regulated by leucine deprivation in liver and adipose tissues. (A) FGF21 protein concentrations in serum were measured by ELISA. (B) *Fgf21* mRNA in BAT, eWAT and liver was measured by qRT-PCR. Error bars represent the mean ± standard error of the mean (SEM) *a*, p<0.05 versus Ctl WT; *b*, p<0.05 versus Ctl FGF21-KO; *c*, p<0.05 versus (-)leu WT (n=6/group).

Figure 2. FGF21 is required for leucine-deficient diet effects on body weight and adipocyte size, without affecting food consumption. (A) Body weight of mice fed with Ctl or (-)leu diet. The weight on the first day was considered 100% for each mouse. (B) Body weight change after 7 days of feeding the Ctl or (-)leu diet. (C) Daily food intake. (D) Representative hematoxylin and eosin-stained eWAT sections from WT and FGF21-KO mice (×20 magnification). Scale bar, 50 μM. Adipocyte size (right panel) was measured as described in Experimental Procedures, using at least three different randomly chosen fields of eWAT sections from each mouse. Error bars represent the mean ± standard error of the mean (SEM). *a*, p<0.05 versus Ctl WT; *b*, p<0.05 versus Ctl FGF21-KO; *c*, p<0.05 versus (-)leu WT (n=6/group).

Figure 3. Lack of FGF21 prevents the increase in P-HSL in WAT in leucine-deprived mice. (A) *Atgl* and *Hsl* mRNA levels were measured by qRT-PCR. (B) Phosphorylated and total HSL protein levels were measured in WT and FGF21-KO eWAT homogenates by Western blot analysis. The bottom panel shows quantification by densitometry of phosphorylated HSL normalized to total HSL, using Image J software. Error bars represent the mean ± standard error of the mean (SEM). *a*, p<0.05 versus Ctl WT; *b*, p<0.05 versus Ctl FGF21-KO; *c*, p<0.05 versus (-)leu WT (n=6/group).

Figure 4. FGF21-KO liver and adipose tissues have altered gene expression and lipid accumulation in response to leucine deprivation. *Fas*, *Srebp1c* and *Acc1* gene expression in mice liver was measured by qRT-PCR in mice liver (A) and eWAT (E). Nuclear ATF4 protein levels (B) and *Asns* and *Atf4* mRNA levels (C) were measured in FGF21-KO mice liver by Western blot analysis and qRT-PCR, respectively. Actin was used as a loading control. A representative blot is shown. (D) Histological appearance and

hepatic lipid accumulation of H&E liver staining of WT and FGF21-KO mice maintained either on a Ctl or a (-)leu diet. Representative H&E-stained hepatocytes are shown (×20 magnification). Scale bar, 50 μM. Lipid accumulation (right panel) was measured as described in Experimental Procedures, using at least three different randomly chosen fields of liver sections from each mouse. (F) Thermogenic gene expression was measured by qRT-PCR in BAT. Error bars represent the mean ± standard error of the mean (SEM). *a*, $p<0.05$ versus Ctl WT; *b*, $p<0.05$ versus Ctl FGF21-KO; *c*, $p<0.05$ versus (-)leu WT (n=6/group).

Figure 5. Working model of the FGF21 regulatory pathway under leucine deprivation.

FIGURES

De Sousa-Coelho_Fig1

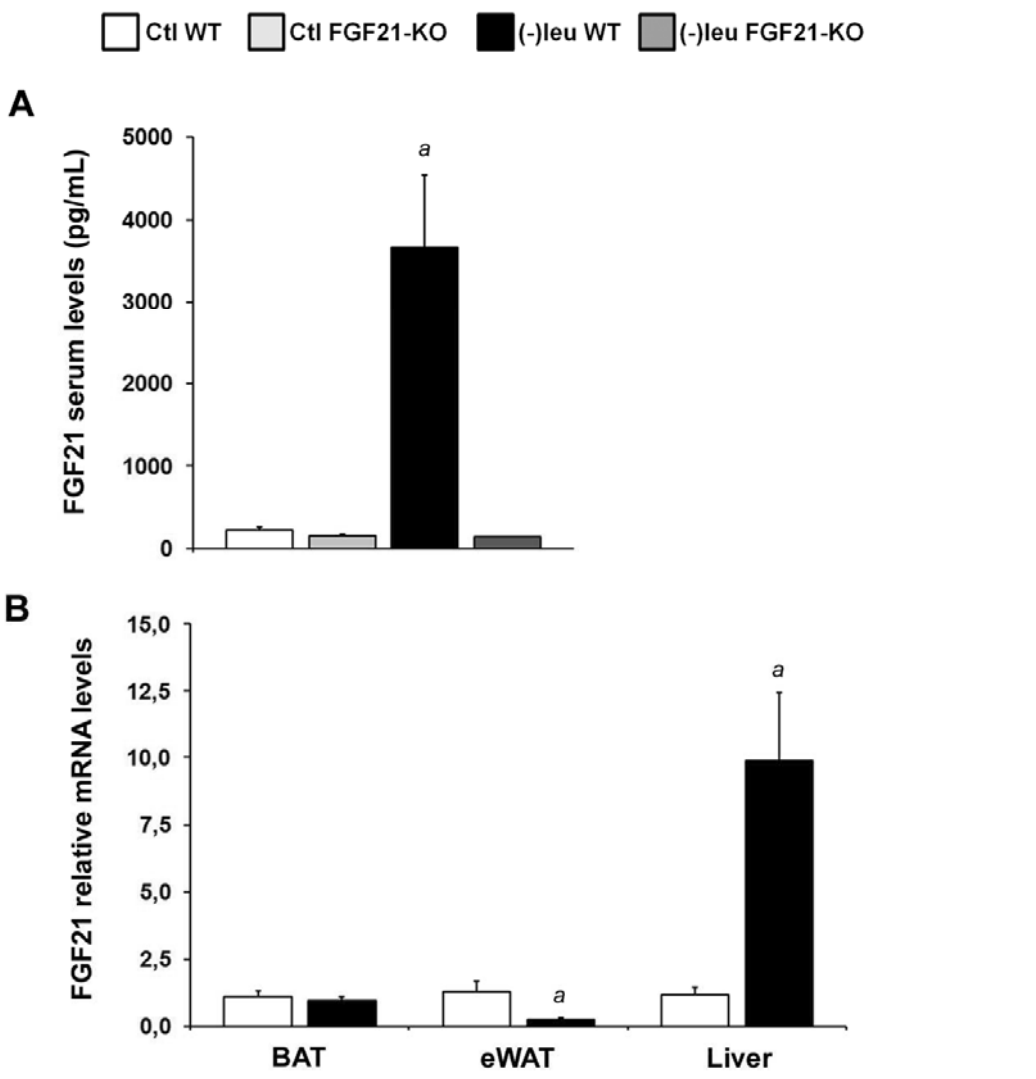

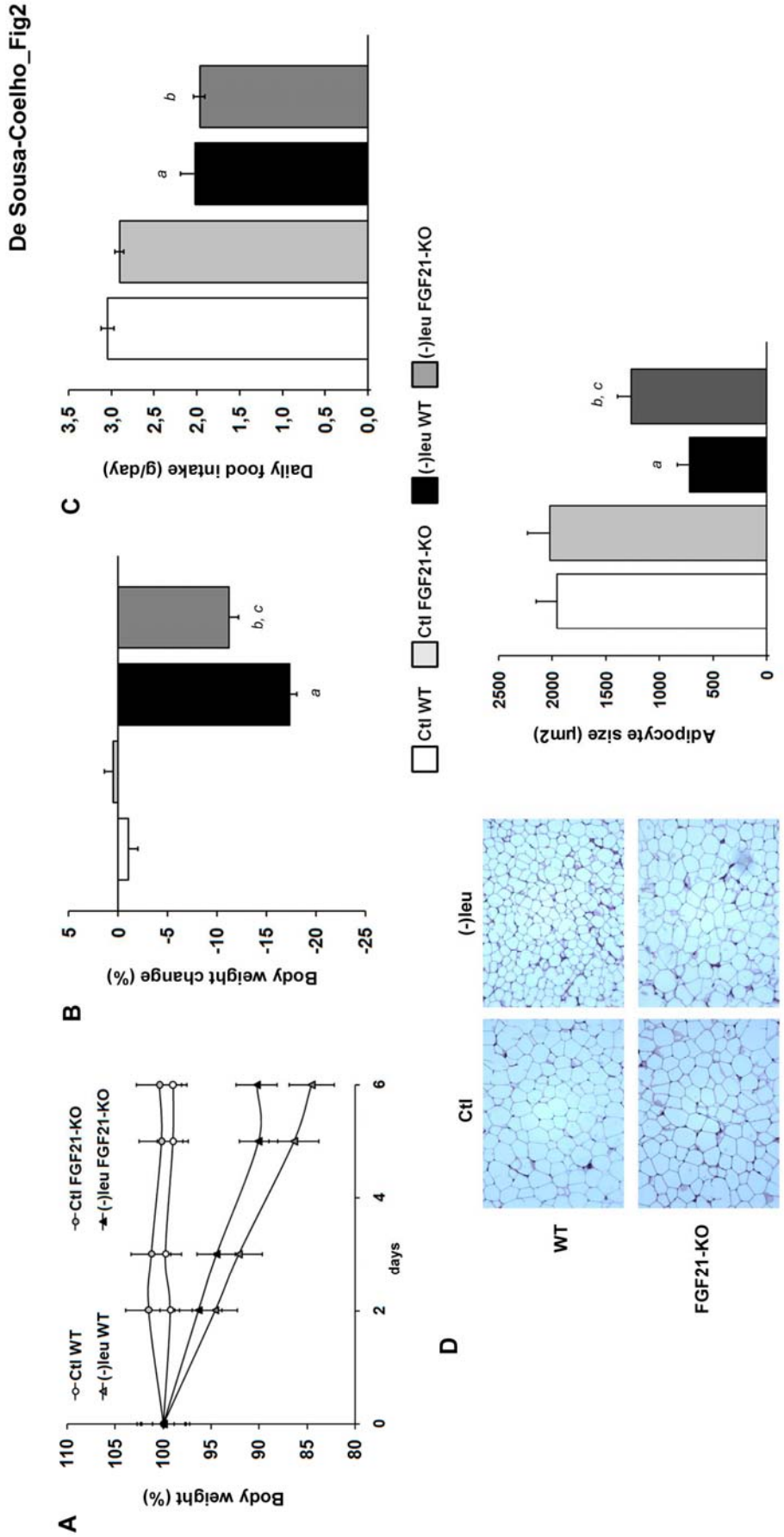
De Sousa-Coelho_Fig2
A
Body weight (%)
Ctl WT
(-)leu WT
Ctl FGF21-KO
(-)leu FGF21-KO
days
B
Body weight change (%)
a
b, c
C
Daily food intake (g/day)
a
b
D
Ctl
(-)leu
WT
FGF21-KO
Ctl WT
Ctl FGF21-KO
(-)leu WT
(-)leu FGF21-KO
Adipocyte size (µm2)
a
b, c

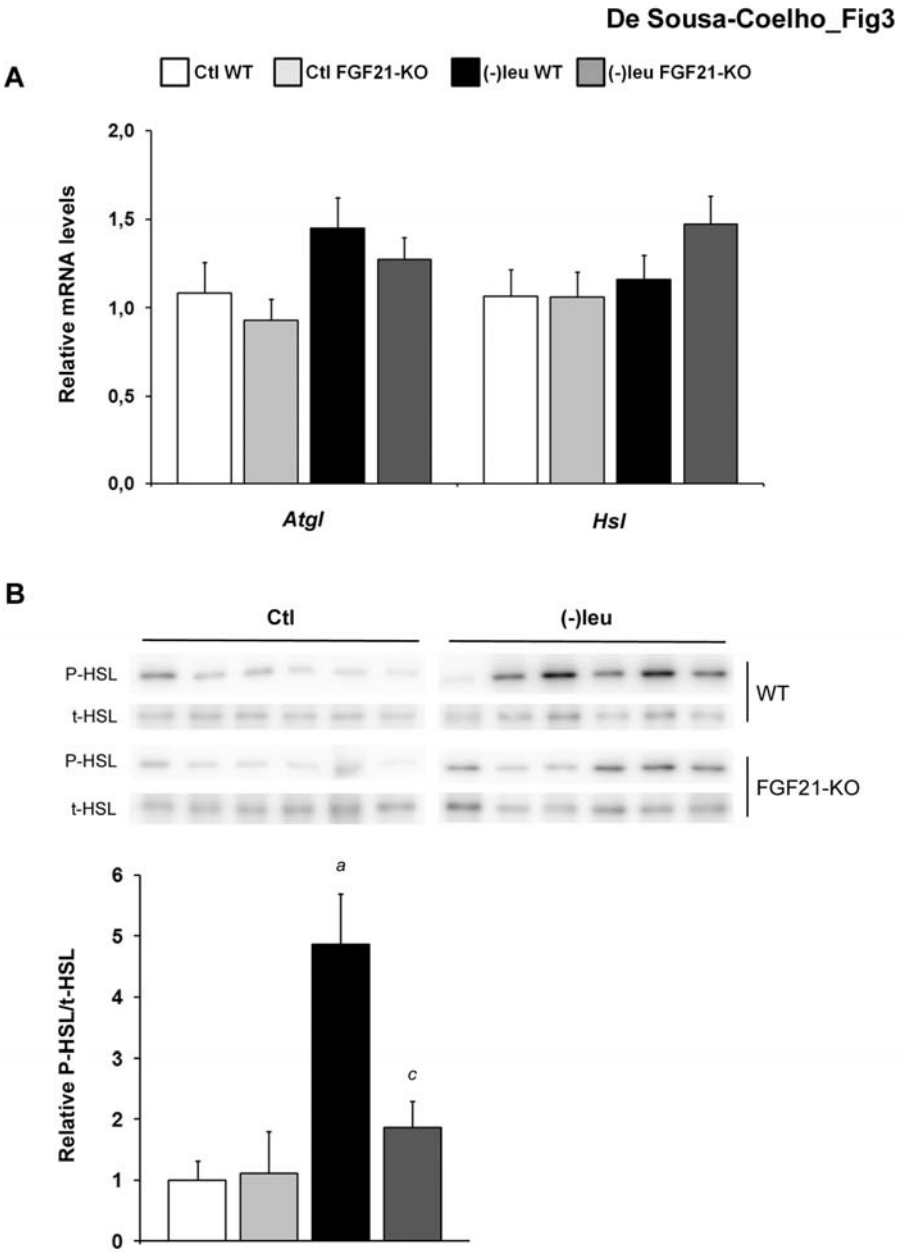
De Sousa-Coelho_Fig3
A
Ctl WT
Ctl FGF21-KO
(-)leu WT
(-)leu FGF21-KO
Relative mRNA levels
2,0
1,5
1,0
0,5
0,0
Atgl
Hsl
B
Ctl
(-)leu
P-HSL
t-HSL
P-HSL
t-HSL
WT
FGF21-KO
Relative P-HSL/t-HSL
6
5
4
3
2
1
0
a
c

De Sousa-Coelho_Fig4

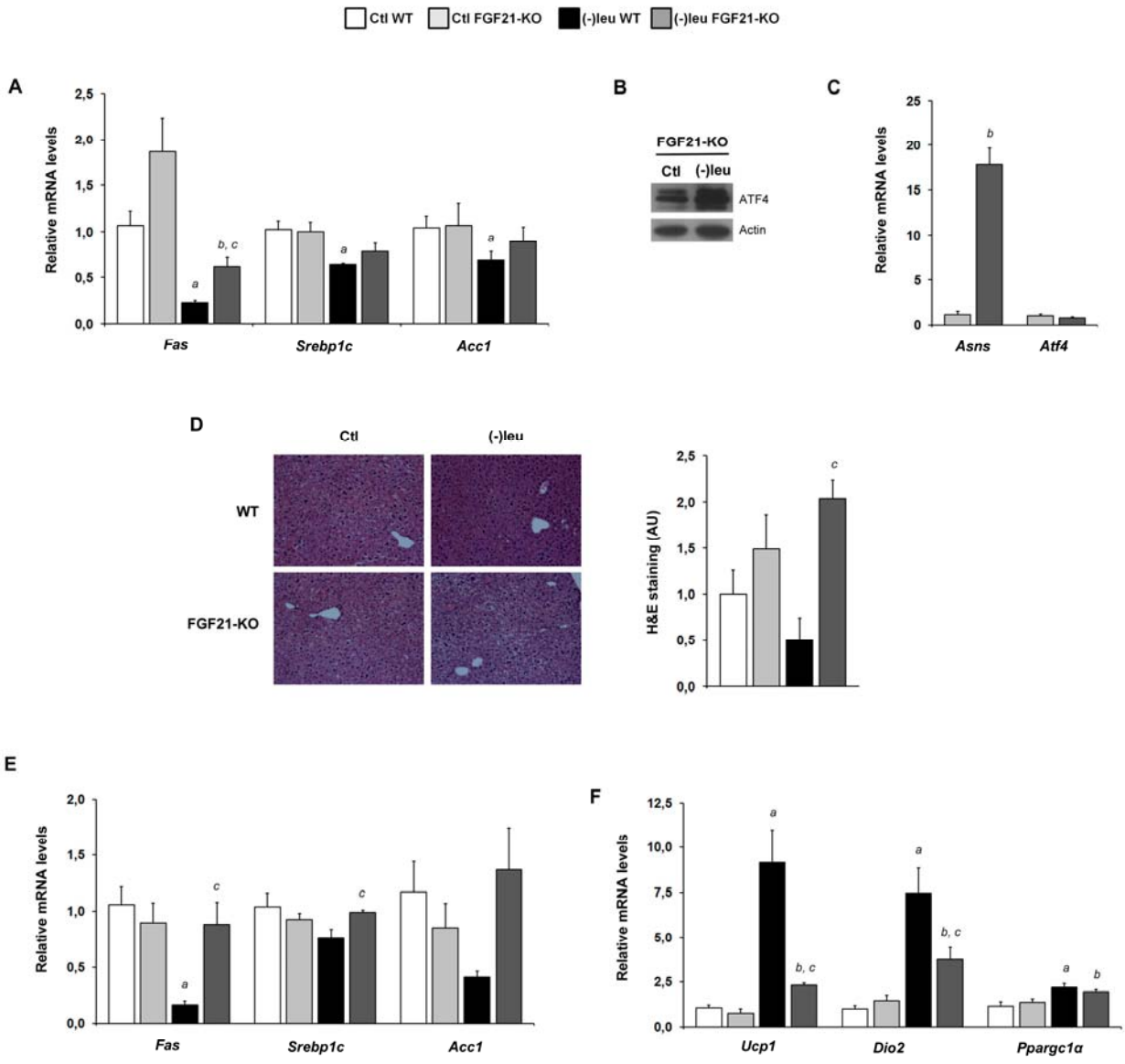

De Sousa-Coelho_Fig5

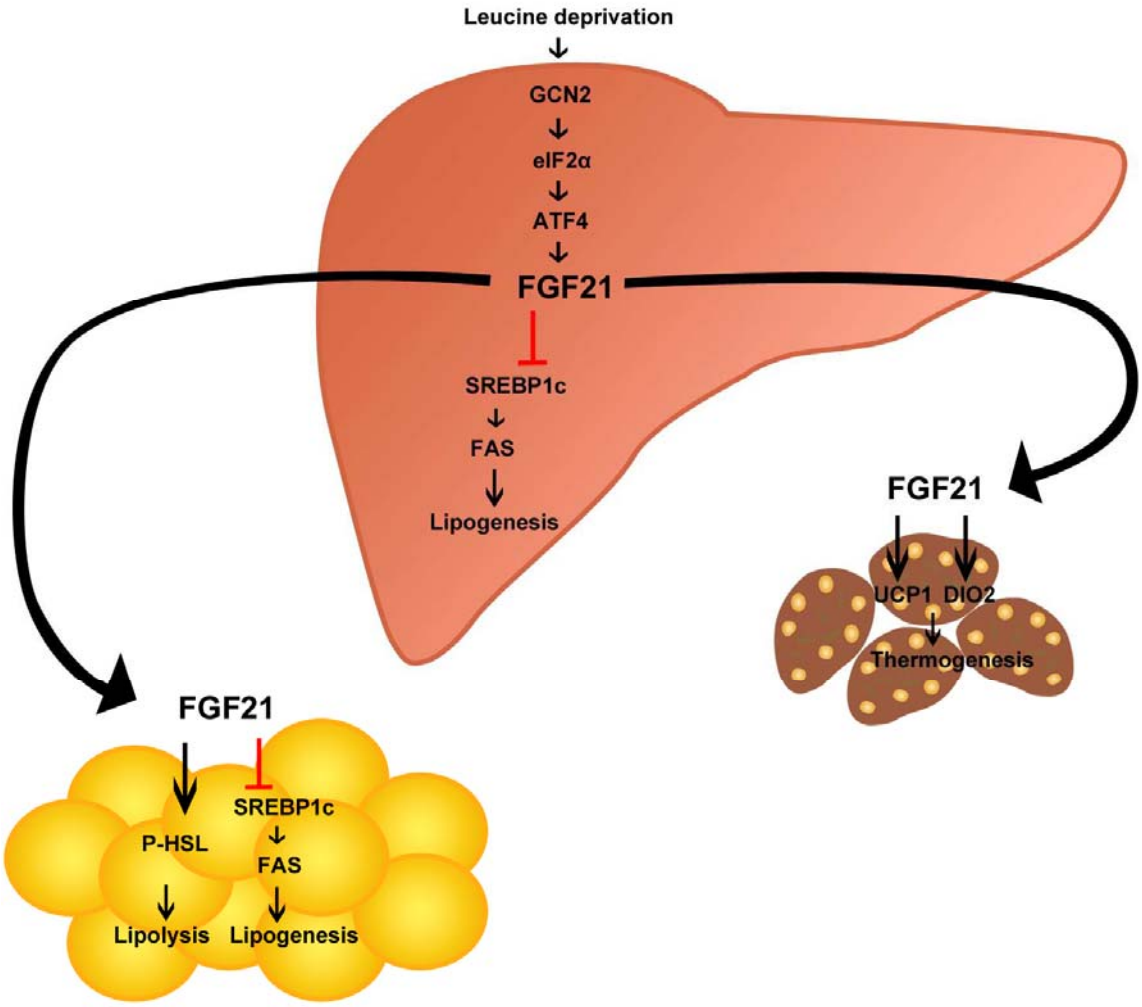

OVERALL SUMMARY

OF THE RESULTS AND DISCUSSION

1. ROLE OF SIRT1 IN THE REGULATION OF FATTY ACID OXIDATION AND KETOGENESIS

SIRT1 liver-specific knockout mice (SIRT1-LKO hereafter) lacks a portion of the reported deacetylase catalytic domain (SIRT1-Δexon4) (Min et al., 2001; Milne et al., 2007) and is therefore predicted to exhibit significantly altered deacetylase activity. Our first analysis confirmed the appearance of the deleted SIRT1 exon4 in the SIRT1-LKO mice liver extracts, which was concomitant with a relative increase in the global protein lysine acetylation in liver (Figure R-1). This observation suggests that SIRT1 mediated their deacetylation, and confirms the importance of the missing 51 amino acids of the conserved SIRT1 catalytic domain in its deacetylase activity.

It has been demonstrated that many SIRT1 activators recapitulate many of the molecular events downstream of caloric restriction (CR) in vivo, such as enhancing mitochondrial biogenesis and improving metabolic signaling pathways (Howitz et al., 2003; Smith et al., 2009). However, our preliminary results suggest that SIRT1 does not control fatty acid oxidation, ketogenesis, or gluconeogenesis, in a low calorie diet (Figure R-2). We have found that fatty acid oxidation and ketogenesis, exemplified by *Cpt1*, *Cpt2* and *Hmgcs2* gene expression was not affected in SIRT1-LKO mice under CR. Additionally, we have observed that as the control littermates, SIRT1-LKO was capable of up-regulating the gluconeogenic gene *Pck1* in response to CR, as previously described (Chen et al., 2008). The interpretation of the fact that *Cpt1a* levels were statistically decreased in SIRT1-LKO mice was kept in standby while following this work.

From following results we have demonstrated that these same metabolic pathways (fatty acid oxidation, ketogenesis, and gluconeogenesis) were unaffected by the absence of SIRT1 exon 4 in liver, during the lactancy/weaning transition, when the activity of its key-regulatory enzymes are known to start to decline (Figure R-4). Interestingly, the expected

decrease in the gluconeogenic gene expression at weaning seemed to be somehow impaired in the liver of SIRT1-LKO mice, although these changes were not statistically significant. From these preliminary results we have now some evidence that SIRT1 may be involved in a pathway necessary to the physiological fall of PEPCK expression.

Because ageing is associated with increased insulin resistance and obesity (Ferrannini et al., 1997), and accumulating evidence indicates that sirtuins can be beneficial in the prevention of metabolic and age-related diseases (Chalkiadaki and Guarente, 2012), we found relevant to measure the glucose and insulin sensitivity in aged-mice, in order to test whether SIRT1 catalytic activity was crucial to the ageing tendency to diabetes.

Both the glucose tolerance test (GTT) and body weights remained unaltered between genotypes in 28-weeks (7-months) old mice (Figure R-5). Ageing is accompanied by changes in the levels and distribution of fat. While it is true that these mice were gradually gaining weight and evidently ageing, it was probably too pretentious to consider these mice old enough to test the effects of SIRT1 on aging-related metabolic diseases. For example, other studies have considered mice with 4-6 months of age as young mice, and with 1.5-2 years, as old mice (Ortega-Molina et al., 2012).

Recently, in a study performed with mice with deleted exons 5 and 6 of SIRT1 in the liver (SIRT1$^{Exon5\text{-}6/Exon5\text{-}6}$,Alb-Cre) (Wang et al., 2011), it was shown that at 2 months of age the whole-body insulin sensitivity was normal in these SIRT1-LKO mice, although at 6 months of age, around 30% of the mutants tested displayed insulin resistance. Finally, they have shown that at 14 months of age, all SIRT1 mutant animals tested displayed insulin resistance, indicating that indeed SIRT1 mutant mice are prone to gradually develop insulin resistance while getting older.

Nervertheless, the results of several studies have not generated a clear picture of the role of SIRT1 in the development of insulin resistance. For instance, while it has been reported that a mediated siRNA reduction of SIRT1 expression in β cell lines leads to an increase in the expression of uncoupling protein 2 (UCP2) and a reduction in insulin

secretion (Bordone et al., 2006), SIRT1 has been identified as having a protective role in skeletal muscle by preventing insulin resistance in this tissue (Fulco and Sartorelli, 2008).

To gain insight the role of SIRT1 in the regulation of fatty acid oxidation and ketogenesis, we have overexpressed SIRT1 through an adenovirus in HepG2 cells. When the mRNA levels of the key enzymes of these processes were analyzed we have seen no differences between cells overexpressing GFP (adenovirus control, AdGFP) or SIRT1 (AdSIRT1). PPARα is known to be a common and very important transcription factor in their regulation (Hsu et al., 2001). We have confirmed that genes involved in these pathways were activated when PPARα was overexpressed (AdPPARα) in HepG2 cells. Very interestingly, when both proteins (SIRT1 and PPARα) were overexpressed, the expression levels of CPT1A, HMGCS2, FGF21, and also of PEPCK, were further induced (Figure R-6). This result was suggesting that if SIRT1 was regulating these genes, it was certainly through PPARα signalling. To support these results, the contrary strategy was used. While not affecting the basal expression, we have observed that the PPARα induction was partially lost in the SIRT1-knockdown cells (Figure R-7). According to these results it was tempting to conceive that SIRT1 was indeed controlling these pathways, although indirectly and in a PPARα-dependent fashion.

Hepatic PPARα plays a crucial role in the adaptive response to fasting (Kersten et al., 1999). To corroborate our last results *in vivo*, SIRT1-LKO mice were subjected to overnight fasting (~16 h).

As anticipated, our results showed that glycemia levels mice were decreased in WT mice upon fasting. However, SIRT1-LKO mice had statistically significant higher fasting glucose levels in blood, compared to WT. As expected, *Pck1* mRNA levels, the rate-limiting enzyme of gluconeogenesis, were increased in fasting. According to the unpredicted increase in glycemia, its expression was further increased in the SIRT1-LKO mice liver (Figures R-8A and R-8B).

PEPCK and G6Pase are widely used as markers for gluconeogenesis. As this result was suggesting an increase in the gluconeogenic rate, the *G6pase* and also the *Ppargc1α* mRNA levels were measured. None of these genes were differently upregulated in the SIRT1-LKO mice liver upon fasting, compared to WT (Figures R-8C and R-8D).

There are conflicting reports in the literature about the effect of SIRT1 activation on the transcription of the gene for PEPCK. On the one hand, studies have shown that activation of SIRT1 stimulates PEPCK gene transcription, thus stimulating hepatic glucose output via deacetylation of PGC1α (Rodgers et al., 2005; Rodgers and Puigserver, 2007). In agreement, others have reported a decrease in PEPCK mRNA in the livers of diabetic rats in which SIRT1 mRNA had been reduced (Erion et al., 2009).

On the other hand, it was reported that overexpression of SIRT1 did not result in hyperglycemia in transgenic mice, which instead were protected from insulin-resistant diabetes (Banks et al., 2008). In addition, it has been reported that mild whole-body overexpression of SIRT1 improves insulin sensitivity and glucose homeostasis of mice when fed high-fat diet (HFD), indicating that at least in high calorie conditions, SIRT1 may block hepatic gluconeogenesis (Pfluger et al., 2008). Others have reported that the activation of SIRT1 by resveratrol or IsoNAM markedly repressed transcription of the gene for PEPCK in HepG2 cells (Yang et al., 2009).

It was also shown that disrupting SIRT1 activity resulted in an increase in glucose output (Liu et al., 2008). The latter described that SIRT1 inhibits gluconeogenesis through disruption of TORC2 (CRTC2) signalling. They have shown that during prolonged fasting (>18h in mice), SIRT1 deacetylates TORC2 and promotes its ubiquitin-dependent degradation. Moreover, their results indicated that in response to fasting, TORC2 and FOXO1 regulate gluconeogenic gene expression sequentially, as during this period, SIRT1 activates gluconeogenesis through deacetylating FOXO1, which seems to be critical in maintaining the glucose homeostasis.

This last report probably brought out the explanation to our results (Figure R-8). In the absence of SIRT1 deacetylase activity, PEPCK would be continuously activated by acetylated TORC2 upon fasting, which would be reflected in increased glycemia levels in SIRT1-LKO mice.

Still, it remains to explain how siRNA-mediated SIRT1 deficiency impaired the PEPCK induction by PPARα in HepG2 cells (Figure R-7), which seems to be a contradictory result to what we have found in mice. It is reasonable to think that some of the SIRT1 effects can be mediated by a non-catalytic mechanism, as it has been already proposed in neurons (Pfister et al., 2008), where the neuroprotective effect of SIRT1 was not reduced by treatments with pharmacological inhibitors of SIRT1 deacetylase activity. Nonetheless, other explanation can be that SIRT1 acts differently depending on which molecular mechanism is activated. Interestingly, it was suggested that PEPCK, a PPARγ target gene in the adipose tissue, is not a PPARα target gene in the liver *in vivo* (Kersten et la., 1999), although its promoter contains an intermediate-affinity PPAR response element (Juge-Aubry et al., 1997).

There are thus a series of studies, and our own results, that come to opposite conclusions regarding the effect of SIRT1 on hepatic gluconeogenesis in the liver. It seems therefore that activation of SIRT1 can either inhibit or enhance hepatic glucose production through deacetylating or interacting with different proteins. The underlying molecular mechanism may be more complex *in vivo*, where interactions between many different cell types and circulating factors determine metabolism. So, the involvement of SIRT1 in glucose homeostasis is still controversial and requires further investigation.

2. ROLE OF SIRT1 IN THE HMGCS2 REGULATION OF FGF21 EXPRESSION

ARTICLE 1: **HUMAN HMGCS2 REGULATES FATTY ACID OXIDATION AND FGF21 EXPRESSION IN HEPG2 CELLS**

During the course of this work, SIRT1-mediated deacetylation of PGC-1α has been reported to play a critical role in the regulation of hepatic fatty acid oxidation (Rodgers and Puigserver, 2007). Moreover, more recently, hepatic deletion of SIRT1 was shown to have impaired PPARα signalling, whereas overexpression of SIRT1 activated PPARα. The increase in the expression of PPARα gene targets under these conditions was also observed, specifically for FGF21 (Purushotham et al., 2009). Their results were in agreement with our own in HepG2, regarding FGF21 regulation (Figures R-6 and R-7).

Concomitantly, parallel work from our laboratory demonstrated that human HMGCS2 overexpression in HepG2 cells was capable to induce both fatty acid oxidation and ketogenesis (Figure 1, ARTICLE 1). We have also determined that HMGCS2 expression was necessary for PPARα-mediated induction of fatty acid oxidation (Figure 2, ARTICLE 1), and very interesting, that HMGCS2 overexpression stimulated FGF21 expression (Figure 3, ARTICLE 1).

Our hypothesis was that HMGCS2 stimulation of FGF21 was correlated with the SIRT1 activity throughout the increased NAD^+ intracellular levels provided by the increased levels of ketone bodies, by the reduction of acetoacetate to β-hydroxybutyrate.

To test it, we have analyzed the *Fgf21* mRNA levels in the liver of WT and SIRT1-LKO mice fasted overnight. The remarkable increase of hepatic FGF21 expression that was observed in WT was impaired in the liver of SIRT1-LKO mice. To support this result, FGF21 circulatory levels were also measured in serum. The very same pattern was observed, confirming the dependence of the SIRT1 intact catalytic activity to correctly induce FGF21 expression and secretion during fasting. We have also measured the expression of other PPARα target genes such as *Cpt1a* and the *Hmgcs2* itself. As predicted, its mRNA levels were

induced upon fasting. However, there were no changes between phenotypes (Figure 5, ARTICLE 1).

We were somehow surprised with this last result because it has already been described that CPT1a is a target gene of SIRT1 (Rodgers and Puigserver, 2007), and also by our own results in HepG2 cells (Figure R-6B). In the former article they show that acute hepatic downregulation of SIRT1 severely abrogates the fasting induction of fatty acid oxidation genes. One of the explanations for the discrepancies of both results may be the divergences between knockdown and knockout hepatocytes, and it may indicate that adaptative mechanisms can compensate for chronic, but not for acute, SIRT1 ablation.

Collectively, our results were indicating that FGF21 expression is highly and specifically sensitive to SIRT1 activity during fasting, while the other two studied PPARα-target genes are not, probably due to unknown compensatory mechanisms activated to alleviate the chronic absence of intact SIRT1 catalytic activity in the liver, or to a mechanism independent of PPARα activation.

To sustain the hypothesis about NAD^+ levels, HepG2 were depleted from SIRT1 trough a specific siRNA, and treated with acetoacetate (AcAc). Previous results from our group indicated that the oxidized form of ketone bodies induced FGF21 expression in a dose-dependent manner, whereas β-hydroxybutyrate did so to a minor extent. We have confirmed that FGF21 induction mediated by acetoacetate was dependent on the SIRT1 expression (Figure 6, ARTICLE 1).

From our results it seemed that through acetoacetate generation, HMGCS2 activity could modulate the cytosolic $[NAD^+]/[NADH]$ ratio and therefore SIRT1 activity. So, the model we propose is a feed-forward model in which ketogenesis activates a SIRT1-mediated response and long chain fatty acid oxidation. Reinforcing this model, it has been recently suggested that under these conditions (i.e. fasting) the acetate generated by SIRT1 deacetylation of its target proteins would be a substrate for acetyl-CoA synthetase (ACS) to generate acetyl-CoA (Guarente, 2011). Because SIRT1 cleaves NAD^+ to nicotinamide and O-acetyl ADP-ribose each reaction cycle, it is plausible to add our model to one of the ways for NAD^+ to be regenerated.

3. REGULATION OF FGF21 UNDER AMINO ACID DEPRIVATION

ARTICLE 2: **ACTIVATING TRANSCRIPTION FACTOR 4-DEPENDENT INDUCTION OF FGF21 DURING AMINO ACID DEPRIVATION**

Following up our working project, we were very interested in studying the role of PPARα in the regulation of metabolic homeostasis. To investigate how the turnover of PPARα affected the expression of its target genes, PPARα-overexpressing HepG2 cells were exposed either to DMSO (vehicle) or to the 26S proteasome inhibitor MG132, and to WY14643, a PPARα-specific synthetic ligand.

As expected, MG132-treatment blocked the PPARα-dependent expression of HMGCS2, a prototypical PPARα target gene (Rodríguez et al., 1994), confirming that the transcriptional activity of PPARα is increased by its rapid turnover and consequent protein degradation (Figure 1A, ARTICLE 2). It had been demonstrated that the interaction of PPARα with its heterodimerization partner RXRα leads to an increase in the turnover of the protein; while in contrast, interaction with the corepressor N-CoR, which inhibits its transcriptional activity, leads to a stabilization of the protein (Blanquart et al, 2004). Preliminary results from our laboratory go along with this effect, as we have seen that treating cells with its specific ligand decreases PPARα stability whilst increasing its transcriptional activity on its target genes.

Contrary to what we had predicted, the expression of FGF21, also a PPARα target gene (Badman et al., 2007), was strongly increased by the MG132 treatment (Figure 1A, ARTICLE 2). As foreseen, detached from PPARα overexpression and activation, FGF21 was induced by MG132 treatment in a time-dependent manner in HepG2 cells (Figure 1B, ARTICLE 2). So, our results were indicating that this activation was not associated to PPARα.

Protein ubiquitination and subsequent degradation by the proteasome are known to be important mechanisms regulating cell cycle, growth and differentiation, and apoptosis. The main metabolic systems responsible for the maintenance of whole-body protein and amino acid homeostasis include protein synthesis and degradation, amino acid oxidation, amino acid intake and *de novo* synthesis (Waterlow and Jackson, 1981). Given this, we

hypothesized that proteasome inhibition in HepG2 could be decreasing the pool of free amino acids and activating the amino acid response (AAR) signal transduction pathway, driving us to test whether FGF21 expression is induced during amino acid starvation.

To test this hypothesis, we treated HepG2 cells with histidinol (HisOH), a potent and reversible inhibitor of protein synthesis (Hansen et al, 1972). HisOH blocks charching of histidine onto the corresponding tRNA, thus mimicking histidine deprivation and activating the AAR cascade. Several reports have shown that HisOH treatment mirrors histidine-deficient medium with regard to the AAR signal pathway induction (Hutson and Kilberg, 1994; Thiaville et al., 2008; Shan et al., 2010). Indeed, we have found that FGF21 was highly induced; meanwhile the CPT1A and HMGCS2 expression levels were not affected by HisOH treatment (Figure R-9B). This result reinforces the specificity of the FGF21 regulation by amino starvation. Curiously, our results also showed that the Early growth response 1 (Egr1) gene, which had been found to be the most upregulated gene after HisOH treatment in HepG2 cells (Shan et al., 2010), presented the same level of activation than FGF21 (Figure R-9A). Additionally, we observed that amino acid deprivation produced a time-dependent induction of FGF21 mRNA (Figure 2A, ARTICLE 2).

To test whether the observed induction was due to an increase in the FGF21 gene transcription, we measured the FGF21 primary transcript (hnRNA) levels. Given that introns are rapidly removed from hnRNA during splicing, this procedure is a useful measure of transcriptional activity (Lipson and Baserga, 1989). Within 2h of HisOH treatment, transcription was increased and continued to rise until reaching a peak at 4h. Then, there was a gradual decline from 4 to 10h, although even after 10h treatment the level was still elevated compared with the control (Figure 2B, ARTICLE 2).

Activating transcription factor 4 (ATF4) is known to be induced by several stress signals, including amino acid deprivation, endoplasmatic reticulum stress and oxidative stress (Harding et al., 2003). As expected, HisOH induced an increase in the translational activation of ATF4, soon as after 2h treatment (Figure 2C, ARTICLE 2). Proteosome inhibition leads to the accumulation of misfold proteins in cells, resulting in ER stress, enhancing the unfolded protein response (UPR) (Milani et al, 2009). Similarly to HisOH, MG132 and tunicamycin, an agent commonly used to induce ER stress, also increased ATF4 protein levels

(Figure R-10A). The induction of ATF4 after MG132 treatment suggests that proteosomal stabilization may be an additional mechanism of ATF4 up-regulation. Altogether, these results mean that activation of the AAR pathway resulted in increased FGF21 transcription, and that the observed induction was transient, as reported previously for other known ATF4 target genes (Chen et al., 2004; Carraro et al., 2010).

Next, we analyzed the sequence of the 5'-flanking region of the human FGF21 gene, looking for putative ATF4 binding sites. CAREs (or AAREs) are composed of half-sites for C/EBP and ATF family members. Consistent with the role of ATF4 as the primary activating factor in the AAR pathway, the ATF half-site is conserved (CATCA), whereas the C/EBP half-site is divergent (XTTX, where X refers to G, T or A nucleotides possibilities). We found two putative ATF4 response elements starting at positions -610 and -152 upstream of the transcription start site, respectively referred to as AARE1 (5'-ATTGCATCA) and AARE2 (5'-GTTACATCA), and which were found to be highly conserved among several mammalian species (Figure 3A, ARTICLE 2).

Overexpression of ATF4 induced the pGL3b-hFGF21 promoter-luciferase construct (*wt* [-768; +115]) in a concentration dependent manner (Figure 3C, ARTICLE 2). This induction was totally obliterated when AARE1 was mutated (*mut1*). Analysis of a series of 5' deletion mutants (Figure 3B, ARTICLE 2) showed that truncation of the FGF21 promoter to -608 (*delta1*), and also to -186 (*delta1/2*) (data not shown in the article), resulted in loss of most of the ATF4 response, and deletion to -134 (*delta2*) eliminated it entirely. Induction was also diminished when AARE2 was mutated (*mut2*) (Figure 3D, ARTICLE 2). Additionally, HisOH treatment increased the *wt* FGF21 reporter activity in a time-dependent manner, as did tunicamycin after 24h treatment (Figure R-11). We have also observed that ATF4 induction of FGF21 was impaired by ATF3 co-expression (Figure R-12). This same behavior have been previously described for several AARE-containing genes (Fawcett et al., 1999; Chen et al., 2004; Pan et al., 2007), referred to as the self-limiting cycle of ATF4-dependent transcription, justifying the decline observed in the FGF21 transcription rate after 4h of HisOH treatment (Figure 2B, ARTICLE 2). Collectively, these results outline the AARE1 and AARE2 sequences as ATF4-responsive elements in the FGF21 human gene.

To further analyze the functionality of the identified sequences we tested the binding of ATF4 by electrophoretic mobility shift assays (EMSA). The mammalian ATF4 has numerous dimerization partners depending on the flanking bases of the core motif (Ameri and Harris, 2008). Of interest, it has been described that C/EBPβ can heterodimerize with ATF4 at AARE sites (Siu et al., 2002; Lopez et al., 2007). In EMSA, ATF4 did not bound by itself, but it did as a C/EBPβ heterodimer, to both AARE sequence elements located between -610 and -601, and between -152 and -143 (Figure 4C, ARTICLE 2).

To determine whether ATF4 binds to the FGF21 promoter *in vivo*, chromatin immunoprecipitation (ChIP) experiments were performed. ATF4 binding to the FGF21 promoter was detected when using specific pair of primers flanking AARE1 or AARE2 regions separately, with the former having stronger binding to ATF4 than the latter, but not with primers that amplify an unrelated control region (Exon1) (Figures 4A, ARTICLE 2 and R-13B). It was still a possibility that only one of the AAREs was the responsible by the enrichment, as both sequences are too close to separate by sonication of the chromatin (Figures R-13A and R-13C). So, we have additionally revealed that the ATF4-binding enrichment is only observed when each AARE is individually amplified, and not when using primers flanking the whole region that comprises the two elements (Figures R-13B and R-13C). Thus, our results proved that ATF4 directly regulates FGF21 expression by binding to both AAREs in the promoter region.

We have also demonstrated that the induction of FGF21 produced by amino acid starvation was mediated by ATF4, because when HepG2 cells were depleted from ATF4 (ATF4-targeting siRNA) and treated with HisOH, the FGF21 mRNA levels were significantly lower compared to control siRNA-treated cells (Figure 5, ARTICLE 2). The same pattern was observed in tunicamycin-treated cells (Figure R-10B), reinforcing the role of ATF4 in the FGF21 induction.

Taking all things together, we have extensively characterized the human FGF21 gene as a target gene for ATF4, and we have identified two conserved ATF4-binding sequences in the 5' regulatory region of the human FGF21 gene. However, there was still to establish whether the molecular mechanisms involved in the regulation of gene transcription by amino acid availability were functional in the liver. To analyze the effect of amino acid

deprivation on FGF21 expression *in vivo*, we fed mice with a leucine-deficient [(-)leu hereafter] diet, or a control diet, for 7 days.

Fgf21 mRNA levels were greatly increased in liver from mice fed a leucine deprived diet compared with the control group. The dynamics of circulating FGF21 reflected that of gene expression, as serum FGF21 was also elevated in (-)leu fed mice. ATF4 protein levels were induced in liver under leucine deprivation, confirming the activation of the AAR cascade (Figure 6, ARTICLE 2).

Arrived to this point, we have also described that the fasting hormone FGF21 was induced in the fed state in the liver of mice deprived from leucine, a novel regulatory pathway of regulation of FGF21 gene expression.

4. LEUCINE DEPRIVATION SIGNALLING UNDER FASTING CONDITIONS

We have now uncovered that amino acid limitation increases FGF21 expression (ARTICLE 2). It is widely known that fasting remarkably increases hepatic FGF21 mRNA levels and its circulatory levels. Because nutrient deprivation frequently correlates with amino acid starvation, we were wondering whether the overall response to the combination of leucine deficiency and fasting would be additive, or not.

Consistent with a previous report (Guo and Cavener, 2007), in our experiment, mice fed with a (-)leu diet for 7 days, presented decreased food intake and lower body weight, compared with mice maintained on the control diet (Figure R-15). Another study have introduced a third group of mice (pair-fed mice) in their experiment, to try to discern the effects of decreased food intake from the leucine deprivation in their decreased body weight (Cheng et al., 2010) They demonstrated that body weight was less reduced in pair-fed mice, compared with control diet–fed mice. So, the effect of (-)leu feeding that we observed in the body weight reduction in our mice is probably also, at least in part, independent of the decreased caloric intake.

The fact that omnivorous animals consume substantially less of an otherwise identical experimental meal lacking a single essential amino acid is not new (Harper et al., 1970). It has been shown that without foraging possibilities or dietary choice, mice simply stop eating the deficient diet by 20 minutes. Intriguingly, the sensing of essential amino acids depletion is not accomplished by either smell or taste (Gietzen et al., 2006), but through the activation of GCN2 that selectively elevates levels of phosphorylated eIF2α in anterior pririform cortex (APC) neurons (Gietzen et al., 2004; Maurin et al., 2005; Hao et al., 2005). It seems then, that a basic mechanism of nutritional stress management functions in mammalian brain to guide food selection for survival. However, there are probably differences between this previously described short-term response in the central nervous system (CNS), and the indirect metabolic effect of leucine deficiency on appetite over a longer period, as in our experiment.

In our study we found no changes in glycemia between control or (-)leu diet groups, both in fed or fasted mice (Figure R-16A). However, others have shown that fasting blood glucose levels were lower in leucine-deprived mice compared to control or pair-fed mice (Xiao et al., 2011). We still did not find any explanation for these diverging results.

Under fasting conditions, adipose triglycerides (TG) stores are mobilized to give rise to free fatty acids (FFAs), which can then be utilized by other tissues for energy production. We have observed that leucine deprivation resulted in decreased free fatty acids in serum in fed mice (Figure R-16B), as previously described (Guo and Cavener, 2007; Cheng et al., 2010). Although they have seen that leucine deprivation accelerated triglyceride lipolysis, they have suggested that either most of the released FFAs undergo β-oxidation in WAT or are rapidly taken up from the serum and metabolized by other tissues, such as liver, BAT, or skeletal muscle. Nonetheless, our results showed that the increased levels of FFAs during fasting were not altered between control or (-)leu diet groups (Figure R-16B).

Starvation also leads to the production of ketone bodies by the liver, which are released in blood and used as an energy source for the brain. Intriguingly, we have seen that β-hydroxybutyrate levels were significantly increased in mice fed with the (-)leu diet in the *ad libitum* group. Nevertheless, the β-hydroxybutyrate high levels that we observed upon fasting, compared to *ad libitum*, remained unchanged between control or (-)leu diet groups (Figure R-16C).

Because ketone body production is regulated by HMGCS2 via multiple signals from the overall metabolic state of the organism, we have checked its hepatic mRNA levels. Surprisingly, we have found that its expression levels were not altered in (-)leu feeding mice compared to control, in fed mice (Figure R-17). However, we did not check its protein level, posttranslational modifications or enzymatic activity; it is known that succinyl-CoA regulates HMGCS2 directly by binding to and competitively inhibiting the active site (Quant et al., 1990) and that HMGCS2 may be palmitoylated, a posttranslational modification predicted to regulate enzymatic activity (Kostiuk et al., 2008). Additionally, it has been demonstrated that SIRT3 regulates the acetylation of HMGCS2, another posttranslational modification that regulates multiple metabolic pathways (Shimazu et al, 2010). Therefore, a pathway that

altered the extent of any of these modifications or its protein levels could regulate HMGCS2 activity and increase the ketogenic flux, independently of its mRNA levels.

We have also analyzed other genes related to the fatty acid oxidation and gluconeogenic pathways in liver. Such as for *Hmgcs2*, we have found that the mRNA levels of *Cpt1a*, *Pck1* and *Ppargc1α* remained unaltered between mice fed control or (-)leu diets, in the *ad libitum* group (Figure R-17). Curiously, the predicted activation of its hepatic expression in fasting, was followed by an additional increase in the (-)leu-fed mice, compared to fasted control. This effect was particularly interesting for PGC1α, which tripled its activation upon (-)leu feeding, exclusively after fasting.

It had been shown that FGF21 induces the hepatic expression of PGC1α, and causes corresponding increases in fatty acid oxidation, tricarboxylic acid cycle flux, and gluconeogenesis (Potthoff et al., 2009). We have shown that FGF21 was prominently induced upon amino acid deprivation (ARTICLE 2). However, *Ppargc1α* expression was not affected by leucine deficiency in the fed state, but exclusively after a fasting period. Based on these results, it is suggestive to speculate that in addition to the amino acid response pathway, a fasting signal is need to hyperactivate PGC1α expression, as also the other analyzed genes.

The other way around, hepatic and circulating FGF21 levels, which we have shown to be hugely increased upon leucine deprivation in fed mice, the *ad libitum* group, were somehow downregulated in fasting, if comparing merely the (-)leu groups, between fed and fasted state (Figure R-18). There was still an activation, from the increased fasting FGF21 levels from control to (-)leu diet, although this induction was faraway diminished. One of the possible explanations for this outcome, which still need further investigation to be confirmed, is that there is a feedback loop that may be regulated by PGC1α, as this key transcriptional regulator of energy homeostasis has been identified as an important negative regulator of FGF21 expression in the liver (Estall et al., 2009).

Summarizing, evidence from these last results demonstrate that the induction of FGF21 by fasting and by amino acid deprivation are not cumulative. By the contrary, it seems that a negative feedback mechanism is activated to control FGF21 expression. Besides, the levels of the analyzed metabolites (glucose, FFAs, and β-hydroxybutyrate) in mice that were

subjected to overnight fasting, remained unaltered between control and (-)leu groups, while there was a relative increase in the expression of FAO, ketogenesis and gluconeogenesis key-genes. These results suggest an underlying mechanism between amino acid and total nutrient starvation, where other unknown factors may be involved.

5. ROLE OF FGF21 IN THE AMINO ACID DEPRIVATION PHENOTYPE

SUBMITTED MANUSCRIPT: **FGF21 MEDIATES THE LIPID METABOLISM RESPONSE TO AMINO ACID STARVATION.**

We have noticed some interesting coincidences between the leucine deprivation resulting phenotype and the FGF21-dependent metabolic effects, suggested from recent studies. Reported data and ours (ARTICLE 2), made us to hypothesize a novel function for FGF21: the link between amino acid starvation and overall energy homeostasis. To investigate this hypothesis, we examined the response of FGF21-knockout (FGF21-KO hereafter) mice to amino acids (specifically leucine) deprivation.

First of all, we have checked for FGF21 gene expression in mice fed a (-)leu diet for 7 days. As expected, FGF21 is induced by leucine deprivation in serum and in liver (Figure 1, SUBMITTED MANUSCRIPT [*S.M.* hereafter]). Of interest, *Fgf21* expression levels were not affected in brown adipose tissue (BAT), but they were unexpectedly downregulated in epididymal white adipose tissue (eWAT) (Figure 1B, *S.M.*). Some reports have shown that FGF21 was induced by PPARγ agonists only at the mRNA level in WAT (Wang et al., 2008), while it was reported by others that circulating levels of FGF21 protein were also increased upon treatment with PPARγ agonists (Muise et al., 2008). It has been recently demosntrated that FGF21 serum levels are not affected at the whole-animal, but at the cellular level, as they have seen that rosiglitazone treatment (a typical PPARγ agonist) of isolated adipocytes increased FGF21 in the media (Dutchak et al., 2012). As a matter of fact, in our results, the *Fgf21* mRNA levels measured in eWAT do not positively correlate with its serum levels. Nevertheless, to my knowledge, there are no studies relying on the *Fgf21* mRNA downregulation in this tissue, although it was observed that the *Fgf21* transcript was unexplainable decreased in the WAT of FGF21-dosed DIO mice after 2 weeks of its administration (Coskun et al., 2008).

Very interesting, we have seen that FGF21 deficiency significantly attenuates weight loss under leucine deprivation, while the established reduction in food intake in (-)leu

feeding was unchanged between genotypes (Figures 2A, 2B and 2C, *S.M.*). This means that FGF21 is in part responsible for their loss of weight under amino acid deprivation, independently of the food intake. Consistent with our observation, i.e. the role of FGF21 in body weight reduction, previous studies have shown that FGF21-transgenic mice and diet-induced obese (DIO) and ob/ob mice treated with FGF21, weighted significantly less (Coskun et al., 2008; Kharitonenkov et al., 2005; Xu et al., 2009).

We performed a histological analysis of eWAT and we confirmed that as described (Cheng et al., 2010), leucine deprivation resulted in a reduction in adipocyte volume compared with mice fed a control diet. By contrast, the adipocyte volume was only slightly reduced in (-)leu FGF21-KO mice (Figure 2B, *S.M.*). This result is in agreement with others which have shown that white adipocytes from FGF21 transgenic mice are substantially smaller than those from wild type mice (Inagaki et al., 2007; Kharitonenkov et al., 2005). Here, we demonstrate that the reduction in the adipocyte volume that occurs in (-)leu feeding depends on the increased FGF21 expression and secretion under this condition.

We found that the adipocytes size remained unchanged in FGF21-KO mice on the control diet, compared to WT. Curiously, other groups reported increased (Hotta et al., 2009) or decreased (Dutchak et al., 2012) adipocytes size in FGF21-KO mice on standard diets.

It was reported that the lipolytic activity was decreased, as well as the expression of *Hsl* and *Atgl*, in the subcutaneous WAT of normal-feeding FGF21-KO mice (Hotta et al., 2009). Adipose triglyceride lipase (ATGL) and hormone sensitive lipase (HSL) are the first and second enzymes, respectively, that regulate lipolysis (Greenberg et al., 2001; Schoenborn et al., 2006), in WAT. We did not find any statistically significant changes in *Atgl* or *Hsl* mRNA levels upon leucine deprivation, although there was a small increase in the *Atgl* mRNA levels upon leucine deprivation that was somehow impaired in the eWAT of mice lacking FGF21. Moreover, their mRNA levels were unchanged in the FGF21-KO eWAT compared to WT (Figure 3A, *S.M.*), in disagreement with the previously mentioned report (Hotta et al., 2009).

Still, we have found that the levels of phosphorylated (P)-HSL were increased upon (-)leu feeding in eWAT, as it had been described (Cheng et al., 2010). So, although *Hsl* expression was unchanged, activation of the HSL protein, probably allowed increased

lipolysis. It has been demonstrated that lipolysis can occur concomitantly with decreased HSL and ATGL mRNA expression (Bézaire et al, 2009; Kralisch et al. 2005; Laurencikiene et al. 2007). Interestingly, our results show that lack of FGF21 significantly decreased P-HSL levels in the eWAT of (-)leu fed-mice, confirming the former statement about FGF21 action on lipolysis (Figure 3B, *S.M.*).

We were then starting to confirm the requirement of FGF21 for some of the amino deprivation phenotypical characteristics. In the mid 90's, it has been suggested that essential amino acids regulated fatty acid synthase (FAS) expression by altering uncharged tRNA levels (Dudek and Semenkovich, 1995). More recently, it was shown that lipid synthesis is downregulated in the liver of mice fed a (-)leu diet for several days (Guo and Cavener, 2007). Accordingly, the next step was to measure the expression of genes implicated in the lipid synthesis. In liver, we have seen that the reduction in the mRNA levels of *Srebp1c*, *Fas* and *Acc1* by (-)leu diet in WT mice, was not observed in FGF21-KO mice (Figure 4A, *S.M.*). Of interest, an inhibitory action in the lipid synthesis had been already described for FGF21, as it was demonstrated that the reduction of hepatic triglyceride levels was associated with FGF21 inhibition of SREBP1c and the expression of genes involved in fatty acid and triglyceride synthesis (Xu et al., 2009).

Within a hematoxylin and eosin (H&E) liver staining, we could observe a decreased amount of clear regions that may reflect a decrease in the lipid accumulation under leucine deprivation in WT mice that is not visible in the FGF21-KO mice (Figure 4D, *S.M.*). We suggest that the failure to repress lipogenesis is likely to be the major cause of liver increased lipid content (or steatosis) in these mice.

From analyzing liver nuclear extracts, we have seen that the synthesis of ATF4 protein was normally elevated in response to amino acid deficiency in the liver of FGF21-KO mice (Figure 4B, *S.M.*). ASNS is a ubiquitously expressed protein responsible for the biosynthesis of asparagine from aspartate and glutamine (Andrulis et al., 1987), whose transcription is known to be induced during either the AAR or the unfolded protein response (UPR) pathways, in response to ATF4 (Chen et al., 2004). We found that the *Asns* expression was also correctly induced in these mice (Figure 4C, *S.M.*). Because previous studies have indicated that *Asns* gene expression is GNC2 and ATF4 dependent (Siu et al., 2002), our

results suggest that not only FGF21 is not involved in the control of amino acid metabolism under amino acid starvation, but also that the observed metabolic effects are downstream of the ATF4 regulation. We have also seen that the transcription of ATF4 was not affected by (-)leu diet, pointing that the primary mechanism of ATF4 induction involves increased translation rate, and possibly also reduced proteosomal degradation.

Next, we have examined whether the impaired reduction in body weight observed in FGF21-KO under leucine deprivation, was not only related to lipolysis in WAT, but also to other factors that influence adipose tissue mass as lipogenesis. We have observed a significantly reduction in *Fas* mRNA levels in eWAT upon (-)leu feeding, that was totally blocked in FGF21-KO mice. *Srebp1c* and *Acc1* mRNA levels presented the same pattern, although with distinct statistical significances (Figure 4E, *S.M.*).

Recently, it has been published that FGF21 enhances adipocyte differentiation (Dutchak et al., 2012). They have observed a delayed induction of the mRNA levels of lipogenic genes (*Cebpα*, *Pparγ*, *Fas*, etc.) in preadipocytes derived from FGF21-KO mice. Although their results seem to contradict ours, it is reasonable to speculate that the observed differences in WAT gene expression are due to the FGF21 differential autocrine and endocrine effects.

It has been shown that FGF21 administration leads to increased energy expenditure (Xu et al., 2009) and elevation of *Ucp1* transcripts in BAT (Coskun et al., 2008). Coincidently, it was described that leucine deprivation increases expression of UCP1 in BAT, consistent with increased thermogenesis in these mice (Cheng et al., 2010). Thus, we have examined the levels of *Ucp1* and *Dio2*, a deiodinase that also contributes to increased thermogenesis in BAT (Bianco and Silva, 1988), and we found that their increased levels upon (-)leu feeding were impaired in FGF21-KO mice (Figure 4F, *S.M.*). Surprisingly, the levels of mRNA encoding the UCP1 upstream regulator PGC1α that were statistically increased upon (-)leu feeding, were still induced in FGF21-KO mice. However, it certainly does not mean that although *Ppargc1α* mRNA levels are unchanged by the lack of FGF21, its protein levels or posttranslational modifications are also unaffected, which would obviously modulate its activity. Importantly, FGF21 was found to regulate PGC1α activity in white adipocytes through deacetylation via SIRT1 (Chau et al, 2010). In all, these last findings point to either a

direct stimulation of UCP1 transcription by FGF21, or an indirect mechanism, through PGC1α, or other transcription factor (or coactivator) activation on the UCP1 promoter, induced upon amino acid deprivation in BAT, and regulated by FGF21.

To sum up, we have found that FGF21-deficient mice under leucine deprivation showed unrepressed lipogenesis in liver and white adipose tissue; decreased phosphorylation of HSL in white adipose tissue, probably indicating impaired lipolysis; and impaired induction of thermogenic gene expression in brown adipose tissue, demonstrating that FGF21 plays an important role in the regulation of lipid metabolism during amino acid starvation (Figure 5, *S.M.*).

CONCLUSIONS

CONCLUSIONS

- In HepG2 cells, SIRT1 plays a role on the PPARα activation of FGF21, CPT1A, HMGCS2, and PEPCK expression.
- SIRT1 activity regulates glycemia and hepatic *Pck1* expression levels in response to fasting.
- SIRT1 activity does not affect fatty acid oxidation or ketogenesis gene expression in liver, in response to different nutritional changes, as caloric restriction, the lactancy/weaning transition, and fasting.
- Through the increase in the ketone bodies production, HMGCS2 regulates the SIRT1 activation of FGF21.
- The human FGF21 gene is a target of ATF4 and presents two functional conserved amino acid response elements (AARE) in its 5' regulatory region.
- FGF21 is induced by amino acid deprivation in both mouse liver and cultured HepG2 cells.
- Leucine deprivation affects the levels of free fatty acids and ketone bodies in serum in the fed state, while it does not upon fasting.
- The fasting activation of FGF21 is impaired in mice fed with leucine deficient diet, underlying a crosstalk between the fasting and amino acid deprivation signalling.
- FGF21 mediates the regulation of lipid metabolism in liver and white adipose tissue, and thermogenesis in brown adipose tissue, during amino acid starvation.

MATERIALS AND METHODS

1. CELL CULTURE

HepG2 - human liver carcinoma cell line (ATCC No. HB-8065).

HepG2 are adherent, epithelial-like cells growing as monolayers and in small aggregates. HepG2 cell line was derived from the liver tissue of fifteen year old male with differentiated hepatocellular carcinoma.

Cells were cultured in Eagle's Minimum Essential Medium (MEM) supplemented to contain 1x nonessential amino acids, 4mM glutamine, 100µg/mL streptomycin sulfate, 100units/mL penicillin G, and 10% (v/v) fetal bovine serum (FBS). Cells were incubated at 37°C in humidified atmosphere with 5% CO_2. Culture medium was discarded and changed every 2-3 days. To passage cells, cells were briefly rinsed with PBS twice and 0.05% Trypsin-EDTA solution was added. Once cell layer was dispersed (~5 min at 37°C), trypsin was deactivated by adding complete growth medium. Cells were split in 1:4 dilution every 5 days or counted and plated according the final experiment.

1.1. REAGENTS USED IN CELL CULTURE MAINTENANCE

Minimum Essential Media (MEM) – GIBCO, 61100-087

Foetal Bovine Serum (FBS) – GIBCO, 10270-106

Pen Strep (Penicillin-Streptomycin) – GIBCO, 15140-122

L-Glutamine 200mM – GIBCO, 25030-024

Sodium bicarbonate solution 7.5% – Sigma-Aldrich, S8761

MEM Non Essential Amino Acids (NEAA) 100x – GIBCO, 11140-035

OPTI-MEM® I – GIBCO, 31985-047

Tripsin-EDTA 10x– GIBCO, 15400-054

1.2. REAGENTS USED IN CELL CULTURE SPECIFIC TREATMENTS

WY14643 (Sigma, C7081) - Selective PPARα agonist. Dissolved in DMSO to 10mM.

Acetoacetate, lithium salt (Sigma, A8509) – Ketone body. Dissolved in water to 400mM.

MG132 (Calbiochem, 474790) - Potent, reversible, and cell-permeable proteasome inhibitor. Dissolved in DMSO to 50mM.

Tunicamycin (Sigma, T7765) – endoplasmic reticulum (ER) stress inducer, inhibitor of glycosilation. Dissolved in DMSO to 5mg/µL.

L-histidinol (HisOH) (Sigma H6647) – reversible inhibitor of protein synthesis. Dissolved in water to 50mg/mL.

Following reconstitution stock solutions aliquots were stored at -20°C.

1.3. REAGENTS USED IN CELL CULTURE TRANSFECTION

Lipofectamine LTX Reagent (Invitrogen, 15338-100)

DharmaFECT® 4 Transfection Reagent (Thermo Scientific, T-2004-01)

2. PLASMID CONTRUCTS

All constructs containing 5' deletions in the human FGF21 promoter were generated by PCR from human genomic DNA (HepG2 cells), using Taq polymerase (Biotools), *KpnI*-ended sense primers, and the antisense primer DH1310. The forward primers DH1309, DH1318, DH1327 and DH1328 introduced a *KpnI* restriction site (italicized and bolded in the primer sequence; see Annex). The correspondent PCR products were cloned in the vector pGEM-T and sequenced. The plasmids were digested with *KpnI* and *SacI*, which cuts the human FGF21 sequence at position +115, to generate a 883bp, 723 bp, 301 bp and 249 bp products, which were subcloned into pGL3b vector, forming pGL3b-hFGF21 *wt*, *delta1*, *delta1/2* and *delta2*, respectively.

The mutations in the FGF21 AARE sequences were made by site-directed mutagenesis using QuickChange® Site-Directed Mutagenesis kit (Stratagene) by replacing the sequences ATTGCATCA (AARE1 core) and GTTACATCA (AARE2 core) for CAGATGGAC, in both the sense and antisense orientation, following the manufactures' instructions. The sequences and orientations of the constructions were verified by sequencing (Macrogen sequencing service).

2.1. DNA OLIGONUCLEOTIDE (PRIMERS AND PROBES)

All DNA oligos were synthesized by Sigma-Aldrich with technology ultra-high base coupling efficiency, combined with optimized cartridge purification and 100% quality control by mass spectrometry. Designed primer sequences are listed in the Annex.

3. TRANSIENT TRANSFECTION AND LUCIFERASE ASSAY

HepG2 cells (0.15 x 10^6 cells/well) were seeded on 24-well plates 18–24h before transfection with Lipofectamine LTX reagent (Invitrogen) at a ratio of 2.5µl of Lipofectamine to 1µg of DNA. For each transfection, 0.2µg of the FGF21-luciferase plasmid was used along with 0.01µg of Renilla (pRL-CMV), as an internal control, and the indicated amounts of the transcription factor expression plasmids. The total amount of transfected DNA was kept constant among experimental groups by the addition of empty pcDNA3 plasmid. 24h following transfection, cells were transferred to fresh complete MEM medium. At approximately 36h following transfection, cellular extracts were prepared for analysis of luciferase activity, by washing the cells with PBS, and harvested in 100µl of 1x Passive lysis buffer (Promega). The lysates were collected and a 10µl aliquot was used for Firefly luciferase assays using the Dual-Luciferase Reporter Assay System (Promega). Relative luciferase activity was given as the ratio of relative luciferase unit/relative Renilla unit.

4. siRNA TRANSFECTION

Specific human SIRT1 (T2004-01) and ATF4 (L-005125-00), and siControl nontargeting (D-001210-01) siRNAs were purchased from Dharmacon (Thermo Fisher). HepG2 cells were seeded in 6-well plates (MW6) at a density of 0.45 x 10^6 cells/well in MEM and grown for 24h. Transfection was performed according to the instructions of Dharmacon using 5µl of DharmaFECT-4 and a 25nM per well final siRNA concentration. At 72h following transfection, cells were rinsed with PBS, and total RNA and protein extracts were isolated and analyzed by real time PCR and immunoblotting, respectively.

5. ADENOVIRAL INFECTION

In general, HepG2 cells were seeded 24h, or 48h if siRNAs were also transfected, before infection. The cells were infected with MEM supplemented with 10% FBS at a multiplicity of infection (MOI) of 40, for 48 h. Successful overexpression was generally assessed by Western blot analysis.

AdGFP was obtained from CBATEG (#593a). AdPPARα (Homo sapiens) and AdSIRT1 (Mus musculus) were a gift from Dr. Francesc Villarroya's laboratory group (UB). Amplification of recombinant adenoviruses was performed following the instructions of Nature Protocols (Luo et al., 2007).

6. PROTEIN EXTRACTION

Whole-cell lysates from HepG2 cells were isolated using NP40 lysis buffer. Cells plated in MW6 were washed twice with ice-cold PBS, harvested with a rubber policeman, and centrifuged for 10min at 1000 x g at 4°C. The resulting pellet of cells was lysed with 50-100µL of NP40 lysis buffer with agitation for 15-20min at 4°C, and centrifuged for 5-10min at 12000 x g at 4°C. The supernatant corresponding to the proteins extract was collected, frozen, and stored at -80°C.

Nuclear extracts were prepared from HepG2 cells plated in 100-mm-diameter dishes (p100). Cells were washed twice with ice-cold PBS, harvested with a rubber policeman in 1mL PBS, and centrifuged for 5min at 800 x g at 4°C. Cell pellets were resuspended in 1mL of HB buffer, centrifuged at 800 x g for 5min. To obtain liver nuclear extracts, frozen liver was first triturated within a mortar in liquid nitrogen and immediately homogenized with a Dounce homogenizer in 1mL of HB buffer, and centrifuged at 800 x g for 5min. From here the protocol was the same for both cultured cells and tissues. The resulting pellet was resuspended in 100µL of HB buffer supplemented with 0.05% Triton X-100 (Sigma), and centrifuged for 1 min at 1000 x g. Nuclear pellets were washed with 1mL of HB buffer supplemented with 0.05% Triton X-100 and 1mL of HB buffer. Nuclei were incubated on ice for 30min in 50µL of HB buffer containing 36mM KCl and centrifuged for 5min at 10000 x g. The supernatant corresponding to the nuclear extract was collected, frozen, and stored at -80°C.

To obtain epididymal white adipose tissue (eWAT) total extracts, eWAT was homogenized in RIPA (Radio-Immunoprecipitation Assay) buffer and centrifuged at 12000 x g for 15min at 4°C. The supernatant was collected and frozen at -80°C until analysis.

NP40 lysis buffer	RIPA buffer	HB buffer
Tris-HCl 50mM pH 8	Tris HCl 10mM pH 7	Tris-HCl 15mM pH 8
NaCl 150mM	Triton X-100 1%	NaCl 15mM
NP40 1%	NaCl 150mM	KCl 60mM
	EDTA 5mM	EDTA 0.5mM

All of the buffers were supplemented with a mixture of protease inhibitors (Sigma Aldrich), 0.1mM phenylmethylsulfonyl fluoride (PMSF), and a phosphatase inhibitor cocktail (IPC3, Sigma Aldrich). Protein concentration was estimated by using the Bio-Rad protein assay with bovine serum albumin (BSA) as standard.

7. WESTERN BLOT ANALYSIS

Protein extracts were resolved by 8-10% SDS-polyacrylamide gel electrophoresis and transferred onto a PVDF membrane (Millipore) at 200mA for 2-3h or 80mA o/n at 4°C. Generally, membranes were blocked for 1h at room temperature (RT) and the blots were then incubated with primary antibody in blocking solution overnight (o/n) at 4°C. In general, antibodies were diluted according to the manufacturer's instructions. Specific blocking solutions (Tween [T] and milk/BSA different percentages) and antibody dilutions are described below.

1^{ary} Ab	**dilution**	**blocking solution**	**washes**	***observations***
SIRT1 (a)	1:1000	TBS 0.05%T 3%milk	H2O/TBS 0.05%T	*WB mouse liver*
AcLys	1:1000	TBS 0.1%T 5%BSA	TBS 0.01%T	
PPARα	1:1000	PBS 1%T 5%milk	PBS 1%T	
SIRT1 (b)	1:500	PBS 1%T 5%milk	PBS 1%T	*WB HepG2 wce*
HMGCS2	1:500	PBS 1%T 5%milk	PBS 1%T	
CPT1	1:1000	PBS 1%T 5%milk	PBS 1%T	
ATF4	1:200	TBST 0.1%T 10%milk	TBST 0.1%T 5%milk	*WB HepG2 wce*
ATF4	1:200	TN 0.1%T 5%milk	TN 0.1%T	*WB nuclear extracts*
HSL	1:1000	TBS 0.1%T 5%BSA	TBS 0.01%T	
p-HSL	1:1000	TBS 0.01%T 5%milk	TBS 0.01%T	

The blots were washed three times for 10min and incubated with horseradish peroxidase-conjugated secondary antibody in blocking buffer for 2h at RT. After three washes, the blots were developed using the EZ-ECL Chemiluminescence Detection Kit for HRP (Biological Industries). Briefly, after the final washings, membranes were incubated with substrate for peroxidase and chemiluminescence's enhancer for 1min and immediately exposed to X-ray film or imaging device. Quantitative analysis of blots was performed using Image J software (NIH, USA).

8. ANTIBODIES

8.1. PRIMARY ANTIBODIES

Rabbit anti-SIRT1/Sir2 (*a*) – 07-131 (Upstate, Millipore)

Rabbit anti-acetylated Lysine – #9441S (Cell Signalling Technology)

Rabbit anti-SIRT1 (H-300) (*b*) – sc-15404 (Santa Cruz Biotechnology, Inc.)

Rabbit anti HMGCS2 – sc-33828 (Santa Cruz Biotechnology, Inc.)

Rabbit anti-CPT1 – #139 (Dr. Diego Haro and Dr. Pedro Marrero's laboratory group, UB)

Rabbit anti-PPARα (H-98) – sc-9000 (Santa Cruz Biotechnology, Inc.)

Rabbit anti-ATF4/CREB2 (C-20) – sc-200 (Santa Cruz Biotechnology, Inc.)

Rabbit anti-HSL – #4107S (Cell Signalling Technology)

Rabbit anti -phospho HSL (Ser660) – #4126 (Cell Signaling Technology)

Mouse anti-Tubulin – CP06 (Calbiochem)

Rabbit anti-Actin – A2066 (Sigma-Aldrich)

8.2. SECONDARY ANTIBODIES

Donkey anti-rabbit IgG, whole Ab ECL antibody, horseradish peroxidase (HRP) conjugated (Amersham Biosciences, NA934V)

Goat anti-mouse IgG, whole Ab ECL antibody, horseradish peroxidase (HRP) conjugated (Amersham Biosciences, NA931V)

9. ISOLATION OF TOTAL RNA

Total RNA was extracted from HepG2 cells or frozen tissues using TRI Reagent Solution (Ambion) following the manufacter's instructions. RNA was pretreated with DNase I (Ambion) to eliminate genomic DNA contamination. Cultured cells were washed twice with cold PBS and scraped with the help of a rubber policeman. Frozen tissues were chopped in liquid nitrogen and then crushed in TRI Reagent solution with the help of a politron. RNA was dissolved in DEPC-treated water (Sigma-Aldrich) and the concentration and purity of each sample was obtained from A_{260}/A_{280} and A_{260}/A_{230} measurements in a micro-volume spectrophotometer *NanoDrop-1000* (NanoDrop Technologies, Inc. Thermo Scientific).

10. ANALYSIS OF mRNA EXPRESSION

To measure the mRNA levels of the genes of interest, cDNAs were prepared from total RNA of cells or tissues and were subjected to quantitative real time polymerase chain reaction (qPCR) with the ABI Prism 7700 Sequence Detection System (Applied Biosystems). cDNA was synthesized from one microgram of total RNA by M-MLV reverse transcriptase (Invitrogen) with random hexamers (Roche Diagnostics) and dNTPs (Attend Bio) according to the manufacturer's instructions.

mRNA levels were determined by TaqMan® qPCR assay using Gene Expression Assay (listed in the Annex) and normalized against those of 18S ribosomal RNA determined by Eukaryotic 18S rRNA endogenous control (Applied Biosystems). Each mRNA from a single sample was measured in duplicate. The PCR assays were carried out in 96-well plates and the thermal cycler protocol consisted of an initial activation step at 50°C for 2min and 95°C for 10min, and 40 cycles of denaturing at 95°C for 15s and annealing/extension at 60°C for 1min. Results were obtained by the comparative Ct method and expressed as fold of the experimental control. The relative quantification value of each target gene was analyzed using a comparative Ct method (ΔΔCt) (Pfaffl, 2001).

To measure the transcriptional activity from the human FGF21 gene, oligonucleotides derived from FGF21 intron 2 (DH1321) and exon 3 (DH1322) were used to measure the short-lived unspliced transcript (hnRNA, heterogeneous nuclear RNA). This procedure for measuring transcriptional activity is based on that described by Lipson and Baserga (1989). Real-time quantitative PCR was performed by using a SYBR-Green-I-containing PCR mix (Applied Biosystems), following manufacturer's recommendations. The reactions were incubated at 95°C for 10min to

activate the polymerase, followed by amplification at 95°C for 15s and 60°C for 1min for 40 cycles. After PCR, melting curves were acquired by stepwise increases in the temperature from 60 to 95°C to ensure that a single product was amplified in the reaction. Reactions without reverse transcriptase were performed as a negative control to rule out amplification from any residual genomic DNA.

11. CHROMATIN IMMUNOPRECIPITATION (CHIP) ANALYSIS

HepG2 cells were seeded at $2.5x10^6$/100-mm dish with complete MEM and grown for approximately 72h. Protein-DNA was cross-linked by adding formaldehyde (37%) directly to the culture medium to a final concentration of 1%, incubated at 37°C, and then stopped 10min later by the addition of glycine to a final concentration of 0.125M at RT.

Plates were washed with PBS supplemented with 0.5mM PMSF and cells were recovered by scrapping in 1mL CEI collection buffer. Cells were collected and centrifuged for 5min at 4°C (2000 x g). The supernatant was discarded and following washes were performed sequentially with cold PBS, NCPI buffer and NCPII buffer. All washing solutions were supplemented with protease inhibitors (PI). The pellet was lysed by adding 600µL Lysis buffer (supplemented with PI) and rotating it for 10min at RT, at low speed to avoid foaming. Finally, cross-linked chromatin was submitted to sonication using a Bioruptor® Next Gen (Diagenode) for ten bursts of 30s on/30s off at high power, to obtain DNA fragments of an average of 500bp. After a 10000 x g centrifugation at 4°C for 10min, the supernatant was transferred to a new tube. To evaluate the shearing efficiency before proceeding to the immunoprecipitation, an aliquot was decrosslinked, and DNA was obtained by phenol/clorophorm extraction and ethanol precipitation. After the crosslink reversal, sheared DNA was quantified and ~1µg DNA was loaded in a 1% agarose gel.

Chromatin (equivalent volume to ~25µg DNA) was first pre-cleared by adding 30µg of IgG from rabbit serum (Sigma-Aldrich) and 20µL of protein A/G PLUS-Agarose beads (Santa Cruz Biotechnology), in a final volume of 1mL supplemented IP buffer. After rotating for at least 1-2 h at slow speed at 4°C, the samples were centrifuged for 2min at 4°C (2000 x g) to eliminate the unspecific complexes. The supernatants were then incubated with 10µg of the specific antibody (anti-ATF4) or IgG from rabbit serum as the nonspecific antibody control, and rotated o/n at 4°C at slow speed. The antibody-bound complex was precipitated by protein A/G PLUS-Agarose beads preblocked with salmon sperm DNA, which was first added to the samples for an additional period (~4h) in rotation at 4°C, and then centrifuged at 4°C for 2min (2000 x g). After proceeding to sequential washings with WBI buffer, WBII buffer, WBIII buffer and TE pH8 twice, 100µL of Elution

buffer was added to the resulting pellet, and the samples were mixed at high speed in a termomixer for 2min at RT, and then centrifuged at RT for 2min (800 x g). The supernatant was transferred to a new eppendorf and the elution procedure was repeated twice, until having a final volume of 300µL. The DNA fragments in the immunoprecipitated complex were released by reversing the cross-linking overnight at 65°C and purified using a phenol/chloroform extraction and ethanol precipitation.

CEI buffer Tris-HCl 100mM pH9.4 DTT 10mM	NCPI buffer EDTA 10mM EGTA 0.5mM Hepes 10 mM pH 6.5 Triton X-100 0.25%	NCPII buffer EDTA 1mM EGTA 0.5mM Hepes 10mM pH 6.5 NaCl 200mM
Lysis buffer SDS 1% EDTA 10mM Tris-HCl 50mM pH 8 PMSF 1mM	IP buffer Tris-HCl 20mM pH 8 EDTA 2mM NaCl 150mM Triton X-100 1%	WBI buffer Tris-HCl 20mM pH 8 EDTA 2mM NaCl 150mM Triton X-100 1% SDS 0.1%
WBII buffer Tris-HCl 20mM pH 8 EDTA 2mM NaCl 500mM Triton X-100 1% SDS 0.1%	WBIII buffer Tris-HCl 10mM pH 8 LiCl 0.25M NP40 1% Deoxicholate 1% EDTA 1mM	Elution buffer SDS 1% $NaHCO_3$ 0.1M (freshly prepared)

Real-time quantitative PCR was performed by using a SYBR-Green-I-containing PCR mix (Applied Biosystems), as described previously for hnRNA quantification (see above). Specific primers were used to amplify the human FGF21 AARE1 (DH1329, DH1330), AARE2 (DH1331, DH1332), and Exon1 (DH1223, DH1224) as a negative control. Relative occupancy of the immunoprecipitated factor at a locus was calculated using the equation $2^{(Ct^{IgG} - Ct^{ATF4})}$, where Ct^{IgG} and Ct^{ATF4} are mean threshold cycles of PCR done in duplicate on DNA samples from negative control ChIP (using non-immune IgG) and target ChIP (using a specific anti-ATF4 antibody), respectively.

Semi-quantitative PCR was also performed to re-ensure that a unique amplification band was obtained with each specific pair of primers. Additionally, a PCR reaction was performed with the

forward primer of AARE1 (DH1329) and the reverse primer of AARE2 (DH1332), to amplify the whole region composed by the two response elements (~700bp amplicon).

12. ELECROPHORETIC MOBILITY-SHIFT ASSAY (EMSA)

12.1. *IN VITRO* TRANSCRIPTION AND TRANSLATION

pcDNA3 empty vector, ATF4 and C/EBPβ were transcribed and translated by using commercially available kits according to the manufacturer's instructions (Promega).

TNT REACTION

20µL TNT® T7 Quick Master Mix

1µL Methionine 1mM

1µL plasmid (500ng/µL)

3µL H2O (Vf=25 µL)

After 1h30 incubation at 30°C, aliquots were made and stored at -80°C until use.

12.2. ANNEALLING OF OLIGONUCLEOTIDES (HYBRIDIZATION REACTION)

Each oligonucleotide (0.5 mmol; see Annex for sequences) was annealed by heating at 65°C for 10min and slowly cooled down to RT (22 ± 2°C) in a buffer of Tris-HCl 10mM pH8, EDTA 1mM and NaCl 150mM.

12.3. LABELLING OF PROBE WITH DIGOXIGENIN (DIG)

The double-stranded oligonucleotide was 3'end-labeled with digoxigenin-11-ddUTP, using the reagents and following the protocol provided in the DIG Gel Shift Kit, 2nd Generation (Roche).

12.4. GEL SHIFT REACTION

An aliquot of 2µL of each factor synthesized *in vitro* was preincubated on ice for 10min in 25mM Hepes pH7.9, 60mM KCl, 5% glycerol, 0.75mM DTT, 0.1mM EDTA, 2.5mM MgCl2, 0.1µg of poly L-lysine and 1µg of poly [d(I-C)]. The total amount of protein was kept constant in each reaction by adding pcDNA3 empty vector. When indicated, anti-ATF4 antibody (1.2 µg), or a 50-fold excess of

unlabelled AARE1 or AARE2, or mutAARE1 or mutAARE2 (with the correspondent mutated sequences), was added to the reaction mixture. Next, 40fmol of DIG-labeled oligonucleotides were carefully mixed and the reaction was incubated for 15min at RT. The final volume for all the reactions was 20µL.

12.5. POLYACRYLAMIDE GEL ELECTROPHORESIS, ELECTROBLOTTING AND CROSSLINKING

Samples were electrophoresed at 4°C on a 6% polyacrylamide gel in 0.5x TBE buffer (45mM Tris-HCl pH8, 45mM boric acid, 1mM EDTA), and the DNA was transferred on to a positively charged nylon membrane (Roche), for approximately 30min at 4°C at 400mA. The membrane was baked for 20-30min at 80°C, and then the DNA was cross-linked to the membrane using a UV crosslinker (SPECTROLINKER XL-1000, Spectronics Corporation).

12.6. CHEMILUMINESCENT DETECTION

Immunological detection was performed following the manufacturer's instructions, and exposing the membrane to an imaging device. Multiple times of exposure were performed in order to achieve the desired signal strength.

13. HISTOLOGICAL EXAMINATIONS

For the histological analysis, a little piece of each fresh tissue (liver and epididymal WAT) was cut and fixed in 10% formalin (Sigma-Aldrich) at 4°C o/n and processed for embedding in paraffin. Subsequent processing was performed by the Pathology Department of the Hospital Clinic of Barcelona. Four-micrometer-thick sections were obtained and stained with hematoxylin and eosin (H&E) and examined at 20X magnification. Images of adipose tissue were analyzed to establish cell size, and of liver to determine fat accumulation. At least 10 random and independent fields were acquired from each individual mouse tissue staining, using a Leica CTR 4000 microscope with the Leica Application Suite Version 2.7.OR1 software. Quantitative data were obtained using the IMAT program developed in the Science and Technology Center of the University of Barcelona (CCIT-UB). The selection of the test objects has been performed according to color and choosing the same limits for binarization for all images.

14. ANIMALS

To perform the *in vivo* experiments mice were used. Mice were housed in cages on a 12h light:12h dark cycle at controlled temperature (25 ± 1°C). All of the experimental protocols with mice were performed with approval of the animal ethics committee of the University of Barcelona (Barcelona, Spain).

14.1. DIETARY MANIPULATIONS

Liver samples from mice subjected to caloric restriction were kindly sent by Dr. Guarente's group (Chen et al., 2008).

To the amino acid deprivation experiment, diets were obtained at Research Diets (see Annex).

14.2. SIRT1-LIVER SPECIFIC KNOCKOUT MOUSE COLONY MANAGEMENT

SIRT1 liver-specific knockout mice were generated by crossing a SIRT1 allele containing a floxed exon 4 (Cheng et al., 2003) with Cre-expressing mice driven by the liver-specific albumin promoter (Chen et al., 2008).

Dr. Guarente sent us 2 homozygous floxed-exon 4 allele expressing Cre under the liver specific albumin promoter (liver-specific knockout, SIRT1-LKO) male mice, and 4 littermates homozygous for the floxed allele, but not expressing Cre (WT) female mice. Breeding and colony management was performed in the Facultat de Farmàcia (UB) house animal facilities. At 3 weeks of age, male and female pups were moved to separate holding cages, with no more than 5 mice per cage. Pup identification was made by ear punching (see Annex). Genomic DNA was obtained from mice tail snips and genotyping was performed by PCR detection of Cre. Mice expressing Cre were SIRT1-LKO, and if they did not expressed Cre, WT.

SIRT1-LKO animals were born at the expected Mendelian frequency, gained weight appropriately with age, and were generally indistinguishable from littermate controls.

14.2.1. GENOMIC DNA EXTRACTION FROM TAILS

To extract genomic DNA (gDNA) from mice tail the following protocol was performed:

1. Obtain the last 2mm of tail and place into a 1.5mL microfuge tube (eppendorf).
2. Tails can be directly frozen at -20°C and stored until use.
3. Prepare the necessary Tail buffer supplemented with Proteinase K to a final concentration of 100µg/µL.
4. Add 700µL to each tail snip in the same eppendorf where tails were kept.
5. Close well and incubate it at 55°C with constant mixing for at least 4h. If not having an oven with rotation, samples can be incubated in a water bath with agitation at 55°C. Samples must be occasionally vortexed until tissue is degraded.
6. Once tails are dissolved, centrifuge at 14000 rpm for 10min at RT.
7. Transfer the supernatant to a new tube and add 500µL of isopropanol. Mix well, without vortexing.
8. Centrifuge at 14000 rpm for 15min at 4°C.
9. Discard supernatant and wash pellet with 500µL of cold 70% ethanol.
10. Centrifuge at 14000 rpm for 5min at 4°C.
11. Dry pellet on air and resuspend it with 100µL TE pH8.
12. Incubate for 5-10min in a 65°C water bath.
13. To check out the integrity of the DNA in the sample, an aliquot can be loaded in a 0.8-1% agarose gel, and a single band in the top of the gel should be visualized.

Tail buffer	TE pH 8
Tris-HCl 20mM pH 8 EDTA 5mM pH 8 SDS 0.5% NaCl 200mM	Tris-HCl 10mM pH 8 EDTA 1mM

14.2.2. PCR DETECTION OF CRE

To a final volume of 25µL for each reaction, a mix was prepared in excess to the amount of samples of genomic DNA from mice tails, including a negative control, where H_2O was added in spite of the DNA sample. When possible, a positive control of the PCR was used.

PCR reaction:		PCR cycling programme:	
dNTPs (10mM each)	1µL	Step 1: 95°C	5 min
Buffer (10X)	2.5µL	Step 2: 94°C	1 sec
Primer Cre-F (10µM)	2µL	Step 3: 50°C	1 min
Primer Cre-R (10µM)	2µL	Step 4: 72°C	1 min
Taq polymerase	0.2µL	Step 5: Go to step 2 for 30 times	
H_2O	12.5µL	Step 6: 72°C	7 min
Genomic DNA	2.8µL	Step 7: STOP.	

The PCR product will have around 100bp, so it should be loaded in a 2% agarose gel.

14.3. FGF21 KNOCKOUT MICE

FGF21-null mice (B6N; 129 S5-Fgf21^{tm1Lex}/Mmucd), obtained from the Mutant Mouse Regional Resource Center, were used as a collaboration with the Dr. Francesc Villarroya's laboratory group.

14.4. GLUCOSE TOLERANCE TEST (GTT) PROTOCOL

To perform the GTT the following protocol was performed:

Material

-filter-sterilized glucose solution 10mg/mL

-glucometer and strips

-razor blades

-timer

Preparation

Prepare to do the GTT in a quiet room and keep handling down to a minimum during the procedure. Mice are fasted for 15h (o/n fasting). The evening prior to the GTT mice are transferred to clean cages with new clean bottles of water but not food. Before starting the fast, each mouse must be weighted (weight determines the amount of glucose to inject) and their tails marked in the order they will be injected. For example, for each cage: 1-one red line across the tail; 2-two green line across the tail; 3-three black lines across the tail; 4-one blue long mark down tail; etc. Set up a table that you can use to record your data (see Annex). In the morning before the procedure, make the glucose solution: 10% glucose=9mL H_2O + 1g D-glucose (then add H_2O to have 10mL).

Method

The following morning the mice are prepared for the GTT. The tail is nicked with a fresh razor blade by a horizontal cut of the very end, and baseline blood glucose (0 time point) is measured using a glucometer. Each mouse is injected intraperitoneally (ip) with a filter-sterilized solution of D-glucose, with the size of the bolus determined by animal weight (1.5mg glucose/g body weight). At 20, 45, 80 and 120min blood glucose is sampled from the tail of each mouse by gently massaging a small drop of blood onto the glucometer strip. Glucose injections and blood glucose sampling is timed to take approximately the same amount of time per animal, so that the samples time are accurate for each animal. The data are plotted as blood glucose concentration (mg/dL) over time (min).

14.5. BLOOD GLUCOSE MEASUREMENT

Glycemia was assessed in mice using a Ascencia Elite XL (Bayer) to measure glucose in the blood sampled from the heart after isoflurane inhalation (anesthesia) and openning of the cardiac cavity, or from tail vein after ip injection of glucose (GTT).

14.6. SERUM EXTRACTION

After mice were fully anesthetized by isoflurane inhalation, the cardiac cavity was opened and blood was collected from heart. Serum was obtained by centrifugation of clotted blood and stored at -80°C.

14.6.1. SERUM FREE FATTY ACIDS (FFA) MEASUREMENT

Free fatty acids (non-esterified fatty acids, NEFA) were determined in mice serum by an enzymatic colorimetric assay. The Free fatty acids, Half-micro test was obtained from Roche. The measure was performed according to the manufactures' instructions.

14.6.2. KETONE BODIES MEASUREMENT

Ketones bodies in mice serum were measured as the amount of β-hydroxybutyrate present in the sample. The beta Hydroxybutyrate (beta HB) Assay Kit was obtained from Abcam. This kit utilizes beta HB Dehydrogenase to generate a product which reacts with a colorimetric probe with an

absorbance band at 450nm. The determination was performed according to the manufactures' instructions.

14.6.3. FGF21 ANALYSIS

Mouse FGF21 enzyme-linked immunosorbent assay (ELISA) kit was obtained from Millipore for the quantification of FGF21 in mice serum. The assay was conducted according to the manufacturer's protocol. Briefly, a calibration curve was constructed by plotting the difference of absorbance values at 450 and 590nm versus the FGF21 concentrations of the calibrators, and concentrations of unknown samples (performed in duplicate) were determined by using this calibration curve.

15. STATISTICAL ANALYSIS

Results are presented as mean ± SEM, from n=2 to n=6. Experimental data sets were compared by a two-sampled, two-tailed and unequal SD Student's t-test. Values of at least $p<0.05$ were considered statistically significant.

16. INFORMATION TECHNOLOGIC TOOLS

Entrez-Pubmed, National Center for Biotechnology Information (NCBI, USA) - http://www.ncbi.nlm.nih.gov/pubmed/

Basic Local Alignment Search Tool (BLAST), National Center for Biotechnology Information (NCBI, USA) - http://blast.ncbi.nlm.nih.gov/Blast.cgi

Webcutter 2.0 - http://bio.lundberg.gu.se/cutter2/

Primer3 (v. 0.4.0) - http://frodo.wi.mit.edu/primer3/

TFSEARCH: Searching Transcription Factor Binding Sites (ver 1.3) - http://www.cbrc.jp/research/db/TFSEARCH.html

17. ADDITIONAL INFORMATION

Any missing information regarding the experimental procedures, which also cannot be found in the ANNEX, means that the procedure was performed according to the detailed information given by “Molecular Cloning, a Laboratory Manual” (Sambrook, Fritsch and Maniatis) and/or “Current Protocols in Molecular Biology” (Ausubel, Bent, Kingston, Moore, Seidman, Smith and Struhl), or following the protocols provided in the instructions of the commercial kits used.

SUMMARY IN SPANISH

(RESUMEN EN CASTELLANO)

PRESENTACIÓN E OBJECTIVOS

Durante su vida un individuo se somete a diversos cambios nutricionales. La capacidad de detectar la disponibilidad de nutrientes y regular la homeostasis energética es un proceso antiguo y fundamental. Sin embargo, las células integran la información no sólo con respecto a la disponibilidad de nutrientes, sino también a factores de crecimiento y activación de los receptores hormonales, al estrés, y a la energía interna a través de un conjunto elaborado de vías de señalización. Las bases moleculares de la regulación génica por estas vías es un importante campo de investigación para estudiar la regulación de las funciones fisiológicas. Entre todos los tejidos, el hígado juega un papel indispensable, al integrar la ingesta de nutrientes y el suministro de los hidratos de carbono y los lípidos a los tejidos periféricos.

Debido a la importancia de la homeostasis de los lípidos y el trabajo previo de nuestro grupo, la regulación de la expresión génica de la oxidación de ácidos grasos y cetogénesis en el hígado tiene un papel central en este estudio. Sin embargo, debe notarse que, como resultado del curso de los hallazgos entrantes, se le dio un énfasis especial a la privación de nutrientes: el ayuno y la deficiencia de aminoácidos; y también a FGF21, una hormona que afecta al metabolismo de los carbohidratos y de los lípidos.

En concreto, los objetivos de este trabajo fueron estudiar:

- El papel de SIRT1 en la regulación de la oxidación de los ácidos grasos y la cetogénesis en respuesta a cambios nutricionales.
- El papel de SIRT1 en la regulación de FGF21 por HMGCS2.
- La regulación de FGF21 en la privación de aminoácidos.
- La señalización metabólica por deficiencia de leucina en la respuesta al ayuno.
- El papel del FGF21 en el fenotipo resultantede la privación de aminoácidos.

INTRODUCCIÓN GENERAL

1. CAMBIOS NUTRICIONALES CARACTERISTICOS DE LOS MAMIFEROS

Los mamíferos tienen la capacidad de adaptar su propia demanda metabólica para sobrevivir en un entorno variable. Hay varios estímulos externos a las que deben ser capaces de responder. Entre ellos se encuentran las fluctuaciones térmicas, los cambios rítmicos impuestos por la alternancia del día y la noche, la necesidad de adaptarse a la discontinua ingesta de alimentos, períodos de desnutrición, etc. La mayoría de las adaptaciones al medio ambiente están controlados no sólo por señales hormonales o neuronales, sino también por constituyentes de la dieta, como la glucosa, los ácidos grasos y los aminoácidos, y también el hierro, la vitamina A, etc., que pueden regular la expresión génica de una manera independiente de hormonas (Pégorier et al, 2004).

El hígado juega un papel muy importante en esta respuesta. Los hepatocitos están regularmente expuestos a las señales sistémicas y de la dieta, que coordinan la expresión génica y mantienen la homeostasis (Langhans 2003; Salto & Clarke, 1999).

1.1. LA LACTANCIA Y EL DESTETE

En la mayoría de los mamíferos, el nacimiento y el destete son dos períodos de transición nutricional. Mientras que el feto oxida principalmente glucosa, lactato y aminoácidos, el recién nacido se alimenta de la leche materna, o sea, una dieta alta en grasas y baja en carbohidratos. En el momento del destete, la leche es sustituida progresivamente por la dieta del adulto, que contiene más hidratos de carbono y menos grasa.

Durante la lactancia, el recién nacido se adapta al nuevo ambiente nutricional mediante el aumento de su capacidad para producir glucosa *de novo* (gluconeogénesis). Debido a la aparición masiva de lípidos en la sangre, procedentes de la leche, se incrementa la oxidación de los ácidos grasos en el hígado y a nivel periférico, permitiendo usar este combustible para el metabolismo energético. Se sintetizan cuerpos cetónicos a partir de los

ácidos grasos en el hígado, y disminuye la lipogénesis en el hígado y en el tejido adiposo blanco (WAT) (Girard et al., 1992).

En el destete, los genes metabólicos implicados específicamente en la gluconeogénesis y la oxidación de las grasas comienzan a disminuir. Por otra parte, la tasa de lipogénica en el hígado y WAT, así como el almacenamiento de triglicéridos, se incrementa.

1.2. AYUNO NOCTURNO E INANACIÓN

El ayuno nocturno es una situación fisiológica. Sin embargo, durante este período tienen lugar cambios importantes. Los cambios metabólicos incluyen la movilización del glucógeno y de la grasa, la gluconeogénesis, la oxidación de ácidos grasos y la cetogénesis. Hay cambios en los niveles de hormonas como la insulina, el glucagón y los glucocorticoides. Y también en los niveles de proteínas reguladoras como PGC1α, FOXO y SIRT1, entre otros.

Durante una limitación alimentaria a corto plazo (como el ayuno nocturno), el bajo nivel de glucosa en la sangre da lugar a una disminución de la secreción de insulina y un aumento de la secreción de glucagón. Inicialmente se induce la glucogenólisis y la gluconeogénesis en el hígado, y la movilización de triglicéridos del WAT (Fig. I-1).

El mantenimiento de la homeostasis energética durante la privación de alimentos se consigue a través de un aumento en la oxidación mitocondrial de los ácidos grasos en los tejidos periféricos (Gerhart-Hines et al., 2007). El ayuno prolongado conduce a la producción de cuerpos cetónicos en el hígado, que se liberan en la sangre y se utilizan como una fuente de energía para el cerebro.

Después de agotadas las reservas de glucógeno, la autofagia en el hígado y el corazón, pero no en el cerebro, también colabora con ácidos grasos y aminoácidos, que se catabolizan para producir energía (Fig. I-2).

1.3. RESTRICCIÓN CALORICA

La restricción calórica (CR) se refiere a un régimen alimenticio bajo en calorías, pero sin desnutrición. En los mamíferos, hay un conjunto de cambios fisiológicos característico de la CR a largo plazo, que pueden solaparse a las adaptaciones fisiológicas a la limitación de alimentos a corto plazo, como por ejemplo el ayuno nocturno. Uno de esos cambios es el uso de las grasas provenientes de la dieta o la grasa movilizada del WAT, para la obtención de energía. Otra es la reducción en los niveles de insulina en sangre acompañada por un aumento de sensibilidad a la insulina, es decir, la capacidad de la insulina para promover la utilización de glucosa (Weindruch & Walford, 1988). Además, la gluconeogénesis se activa en el hígado. Estos cambios en los niveles de glucosa disponible para el cerebro están estrechamente asociados con la longevidad inducida por la CR.

Hay creciente evidencia que involucra las sirtuinas de mamíferos como reguladores de las respuestas fisiológicas inducida por la CR (Schwer & Verdin, 2008). Se ha demostrado que SIRT1 media en parte los efectos fisiológicos producidos por la CR (Guarente & Picard, 2005).

A pesar de las numerosas teorías que han sido propuestas para explicar cómo funciona la CR, la teoría más apreciada es en que se activa una respuesta de defensa biológica que se desarrolló para ayudar a los organismos a sobrevivir a la adversidad (Masoro et al., 2000).

1.4. PRIVACIÓN DE AMINOÁCIDOS

En los mamíferos, las concentraciones plasmáticas de aminoácidos pueden verse afectados por la dieta o condiciones patológicas, como la desnutrición proteica, una dieta desequilibrada y diversas formas de estrés, como en el trauma o la sepsis. Los organismos multicelulares son incapaces de sintetizar todos los aminoácidos, lo que significa que hay nueve aminoácidos (valina, isoleucina, leucina, lisina, metionina, fenilalanina, treonina, histidina y triptófano) que no pueden ser sintetizados *de novo*, y tienen que ser suministrados por la dieta.

El tamaño del *pool* celular de cada aminoácido es el resultado de un equilibrio entre el aporte y la salida; la síntesis *de novo* (para aminoácidos no esenciales), la degradación de proteínas y el suministro de la dieta; y la síntesis de proteínas y la degradación de aminoácidos, respectivamente (Fig. I-3).

La respuesta a la privación de aminoácidos en los mamíferos se caracteriza tanto por la represión de la síntesis de proteínas como por la activación de la biosíntesis de aminoácidos y transportadores (Anthony et al, 2004; Averous et al, 2003; Kilberg et al, 2005). Una de las vías de transducción de señales que se activa en respuesta a la privación de proteína o aminoácidos se refiere como la vía de GCN2/eIF2α/ATF4 (Bruhat et al., 2009).

Recientemente, se ha demostrado la importancia de GCN2 para inhibir la síntesis de ácidos grasos y la movilización de los lípidos almacenados, que se producen en respuesta a la privación de leucina en ratones (Guo & Cavener, 2007). Estos resultados proporcionan nuevas evidencias que la disponibilidad de aminoácidos en la dieta puede alterar las vías metabólicas más allá de la homeostasis proteica.

2. MECANISMOS MOLECULARES QUE REGULAN LA ADAPTACIÓN DE LAS VÍAS METABÓLICAS DURANTE LOS CAMBIOS NUTRICIONALES

2.1. VIA DE SEÑALIZACIÓN DE CREB/TORC2

En condiciones de escasez de nutrientes, el suministro de glucosa a los tejidos metabólicamente activos, tales como el cerebro y los glóbulos rojos, se mantiene a través de la producción hepática de glucosa, un proceso denominado gluconeogénesis, que resulta de la activación transcripcional de los genes gluconeogénicos.

La respuesta al AMP cíclico (cAMP) depende de la fosforilación de CREB y del reclutamiento de los coactivadores CBP/p300 a los promotores de los genes de la gluconeogénesis. Sin embargo, el coactivador de CREB, TORC2, es probablemente el principal mediador de la respuesta al ayuno (Koo et al., 2005).

La actividad de TORC2 durante el ayuno está estrechamente regulada por SIK1 y modulada, además, a nivel celular por la AMPK (Koo et al., 2005). Se ha sugerido la

implicación de varios factores de transcripción y coactivators en el control nutricional y hormonal de la gluconeogénesis. Entre ellos se encuentran FOXA2, C/EBPα y HNF4α (Matsumoto & Accili, 2006).

En condiciones de alimentación, la insulina silencia la expresión hepática y la actividad transcripcional de PGC1α, a través de la fosforilación y la exportación nuclear de FOXO1 medidada por Akt, inhibiendo la vía de la gluconeogénesis (Brunet et al., 1999; Puigserver et al., 2003; Li et al., 2007). Hay también evidencia de la inactivación de CBP dependiente de Akt (Zhou et al., 2004) (Fig. I-4).

La isoforma citosólica de la phosphoneolpiruvato carboxiquinasa (PEPCK-C) y la glucosa-6-fosfatasa (G6Pase) son dos enzimas-limitantes de la velocidad de la gluconeogénesis, transcripcionalmente regulados por el glucagón y la insulina (Sutherland et al., 1996).

PGC1α es un factor importante en la regulación del metabolismo. En el hígado, PGC1α se induce durante el ayuno y en la diabetes, y estimula la expresión de los genes G6Pase y PEPCK (Yoon et al., 2001). PGC1α contribuye a la activación transcripcional de genes implicados en la termogénesis adaptativa, la biogénesis mitocondrial, la respiración, la gluconeogénesis, la oxidación de ácidos grasos y la cetogénesis (Finck et al., 2006; Lin et al., 2005).

2.2. VIA DE SEÑALIZACION DE LOS ACIDOS GRASOS

2.2.1. OXIDACIÓN DE LOS ACIDOS GRASOS

La oxidación de los ácidos grasos en el hígado es un proceso esencial, por ejemplo, durante el ayuno, de modo a garantizar un suministro adecuado de sustratos que pueden ser metabolizados por otros tejidos. Los ácidos grasos liberados del tejido adiposo en forma de triglicéridos, llegan al hígado, donde son reesterificados y secretados, o oxidados en la mitocondria (Kersten et al., 1999).

Los ácidos grasos de cadena larga (LCFA) que han sido liberados, pueden entrar en las células de forma pasiva, o por medio de proteínas transportadoras. Después de la captación

celular, los LCFA que se han acumulado en los hepatocitos, se activan a acil-CoA por la sintasa acil-CoA citosólica (ACS). La carnitina palmitoil transferasa 1 (CPT1) en la membrana externa, la carnitina acil-carnitina translocasa (CACT) y carnitina palmitoil transferasa 2 (CPT2) en la membrana mitocondrial interna, proporcionan el transporte neto de los acil-CoA (LC-CoA) de cadena larga a través de las membranas mitocondriales (McGarry & Brown, 1997). En el hígado, la CPT1A es la principal isoforma expresada, y cataliza la etapa limitante en la entrada de los LC-CoA del citosol a la mitocondria, donde la β-oxidación se lleva a cabo, que a través de una una variedad de reacciones enzimáticas, conducen a la producción de acetil-CoA (Fig. I-5).

2.2.2. CETOGÉNESIS

La cetogénesis es una vía metabólica estrechamente regulada llevada a cabo en el hígado y crucial para el suministro de energía derivada de los lípidos para el cerebro en condiciones normales, y para los tejidos periféricos durante el ayuno, ejercicio sostenido y en enfermedades como la diabetes (McGarry & Foster, 1980).

Durante un largo período de ayuno, el hígado necesita mantener el ciclo de Krebs para la producción intrahepática de ATP, y la gluconeogénesis para suministrar glucosa a los tejidos extrahepáticos. Debido a que estos dos procesos requieren los mismos intermediarios, ambos comienzan a disminuir. Como resultado, se acumula acetil-CoA en la mitocondria (Lopes-Cardozo et al., 1975). Así, a través de una serie de reacciones de condensación, los cuerpos cetónicos (acetoacetato, β-hidroxibutirato y acetona) se producen en el hígado a partir del acetil-CoA derivado de la oxidación de ácidos grasos (Laffel, 1999), y en menor medida, de amino ácidos cetogénicos. La producción de cuerpos cetónicos implica la reducción de acetoacetato a β-hidroxibutirato, con la generación concomitante de NAD^+ (Fig. I-6).

La 3-hidroxi-3-metilglutaril-CoA sintasa mitocondrial (HMG-CoA sintasa o HMGCS2) es la enzima limitante de la velocidad de esta vía, y se regula en ambos niveles transcripcional y post-transcripcional, por mecanismos que pueden aumentar tanto la cantidad como la actividad de la enzima (Hegardt, 1998; Kostiuk et al., 2010; Quant, 1994; Shimazu et al., 2010).

2.2.3. PPARα

PPARα es un factor de transcripción activado por ligando que pertenece a la superfamilia de los receptores nucleares (Mangelsdorf et al., 1995). PPARα se une a los elementos característicos de respuesta a PPAR (los PPRE), una repetición directa de dos hexanucleótidos separados por un nucleótido, como heterodímeros con el receptor de retinoide X (RXR) en los genes diana. En respuesta a los estímulos nutricionales, hormonales y ambientales, PPARα juega un papel central en el control del metabolismo de los lípidos, incluyendo el transporte de lípidos, la β-oxidación mitocondrial de los ácidos grasos y la cetogénesis (Mandard et al., 2004), siendo crucial en la respuesta adaptativa al ayuno. Se ha descrito que su activación en el hígado también promueve la gluconeogénesis (Bernal-Mizrachi et al., 2003) (Fig. I-7).

Numerosos genes involucrados en la oxidación de ácidos grasos hepáticos han sido demostrados ser inducidos por PPARα. Los resultados de nuestro grupo han sido relevantes para la identificación y caracterización de PPREs funcionales en genes reguladores clave (Barrero et al., 2003; Mascaró et al., 1998; Napal et al., 2005; Ortiz et al., 1999; Rodriguez et al., 1994).

Inicialmente se ha creído que la activación de PPARα por ligandos endógenos que se producían principalmente durante el ayuno, derivaba de la gran cantidad de ácidos grasos libres liberados de WAT (Kersten et al., 1999; Kliewer et al., 2001). Además, había clara evidencia que los ácidos grasos de la dieta también eran capaces de dar lugar a una activación potente del PPARα (Ren et al., 1997; Patsouris et al., 2006). Sin embargo, datos recientes sugieren que PPARα en el hígado no puede ser activado por los ácidos grasos libres en plasma, o sea, que estos no actúan como ligandos endógenos, mientras que puede ser activado por los ácidos grasos sintetizados *de novo* o de la dieta (Chakravarthy et al., 2005) (Fig. I-8).

Sin embargo, si los ácidos grasos libres en plasma, provenientes de la lipolisis en el WAT, no activan PPARα en el hígado durante el ayuno, es probable que PGC1α (o otros coactivadores) pueda contribuir a la inducción de los genes diana de PPARα durante el ayuno, a través del aumento de la unión de PPARα dependiente de PGC1α, a los promotores de los genes (Rhee et al., 2003; Vega et al., 2000; Yoon et al., 2001).

2.3. VÍA DE SEÑALIZACIÓN DE LA RESPUESTA A AMINOÁCIDOS (AAR)

En los primeros pasos que conducen a la iniciación de la traducción en la síntesis de proteínas, los aminoácidos se acilan a tRNA por sus enzimas amino-acil tRNA sintetasa afines. Es evidente que un suministro continuo de todos los aminoácidos deberá estar disponible para la síntesis de proteínas. El primer paso en la vía de AAR es la activación por el tRNA sin carga (deacilado) de la GCN2, que a su vez fosforila la subunidad α del factor de iniciación de la traducción (eIF2α) en la serina 51 (Kimball y Jefferson, 2004;. Wek et al, 2006). De ahí, el eIF2α fosforilado suprime la síntesis de proteínas en general, pero promueve el aumento paradójico en la traducción de un número seleccionado de mRNA, donde se incluye el que codifica para ATF4. Una vez inducido, ATF4 directa o indirectamente induce la transcripción de un subconjunto de genes específicos (Kilberg et al., 2009; Smith et al., 2003).

No obstante, ATF4 se expresa en respuesta a una variedad de condiciones de estrés a través de la traducción reforzada del mRNA preexistente (Lu et al., 2004; Vattem et al., 2004). GCN2 es sólo uno de los cuatro quinasas conocidas que fosforilan a eIF2α (Fig. I-9).

ATF4 desencadena el aumento de la transcripción mediante la unión a los elementos de respuesta C/EBP-ATF (CARE) (Fawcett et al., 1999). Como ejemplo de genes activados por ATF4 están los factores de transcripción C/EBPβ (Thiaville et al., 2008), ATF3 (Pan et al., 2007) y CHOP (Chérasse et al., 2007) (Fig. I-10).

3. MECANISMOS MOLECULARES INTEGRADOS QUE REGULAN EL METABOLISMO

3.1. SIRT1

SIRT1 es uno de los siete ortólogos de mamífero de la proteína de levadura Sir2 (sirtuinas SIRT1-7), una proteína deacetilasa dependiente de NAD^+ (Imai et al., 2000). El dominio catalítico de la actividad deacetilasa está altamente conservado en todos los miembros, y se compone de dos motivos distintos que se unen a NAD^+ y al sustrato acetil-

lisina, respectivamente, y se encuentra ubicado en los exones 3 a 8 (Brachmann et al., 1995; Voelter Mahlknecht & Mahlknecht, 2006) (Fig. I-11).

SIRT1 ejerce sus funciones a través de la desacetilación de proteínas diana, como pueden ser las histonas, factores de transcripción, y coregulators (Feige & Johan, 2008). SIRT1 cataliza una reacción que combina la desacetilación de lisina y la hidrólisis de NAD^+ (Tanny et al., 2001). Durante esta reacción, el NAD^+ se hidroliza a nicotinamida (NAM) y O-acetil-ADP ribosa (Borra et al., 2002; Tanner et al., 2000) (Fig. I-12).

SIRT1 ha surgido como un regulador clave en el metabolismo energético. De hecho, SIRT1 puede modular la expresión génica en los tejidos metabólicamente activos, tales como el músculo esquelético (Gerhart-Hines et al., 2007), hígado (Rodgers et al., 2005) y WAT (Picard et al., 2004) en respuesta a la falta de nutrientes, como la restricción calórica o el ayuno (Cohen et al., 2004). Sin embargo, también se ha demostrado que SIRT1 está involucrado en la regulación de varios procesos, como la diferenciación celular, el ciclo circadiano, la función mitocondrial, la respuesta al estrés, el silenciamiento de genes, la senescencia y la supervivencia celular (Blander & Guarente, 2004). Se ha propuesto que la activación de las sirtuinas pueden contrarrestar los mecanismos patogénicos subyacentes varios enfermedades relacionadas con el envejecimiento (Chalkiadaki & Guarente, 2012) (Fig. I-13).

La dependencia de la actividad catalítica de SIRT1 en los niveles NAD^+ constituye un vínculo fundamental entre el estado metabólico celular y la regulación de genes (Zhang et al., 2010). Curiosamente, se ha propuesto recientemente que la acetilación de las proteínas pueden regular el cómo las células pueden elegir entre el metabolismo glucolítico o oxidativo, en función de la energía disponible, y por lo tanto ayudando a determinar el almacenamiento de carbono o la utilización de la energía (Guarente, 2011). En condiciones tales como dietas bajas en energía, el acetato generado por SIRT1 al desacetilar proteínas diana, sería un sustrato para la acetil-CoA sintetasa (ACS) para generar acetil-CoA, que junto con la oxidación de ácidos grasos, haría que el ciclo de Krebs y la fosforilación oxidativa produjeran el ATP y CO^2 (Fig. I-14).

3.2. FGF21

FGF21 es un miembro de una familia atípica de de factores de crecimiento de fibroblastos (FGF), que incluyen el FGF19 (FGF15 en ratón) y FGF23, que pueden difundirse fuera de sus tejidos de origen y funcionar de manera endocrina, o sea, como hormonas (Goetz et al., 2007; Itoh et al., 2008). La señalización por FGF21 se realiza a través de receptores de superficie celular compuestos por los receptores clásicos de FGF (FGFR) y β-Klotho, los cuales se expresan abundantemente en el hígado, tejido adiposo y páncreas (Kurosu et al., 2007).

El ayuno aumenta notablemente la expresión hepática de FGF21, regulada por el receptor nuclear PPARα, el cual desempeña un importante papel en la oxidación de lípidos. En el hígado, FGF21 induce la gluconeogénesis, la oxidación de ácidos grasos y la cetogénesis, un perfil metabólico característico del estado de ayuno (Badman et al., 2007; Inagaki et al., 2007). También se ha observado que la administración FGF21 induce la expresión hepática de PGC1α (Potthoff et al., 2009). En el WAT, FGF21 estimula la absorción de glucosa y estimula la lipólisis (Coskun et al., 2008; Inagaki et al, 2007). Sin embargo, en relación a la lipólisis, todavía hay una cierta discrepancia entre los resultados de diferentes grupos (Arner et al., 2008).

Por lo tanto, parece ser que esta hormona hepática es capaz de regular de una forma potente la tolerancia a la glucosa y el metabolismo hepático de lípidos (Badman et al., 2007; Kharitonenkov et al., 2005).

Recientemente se ha descrito que FGF21 estimula a PPARγ al menos en parte mediante la prevención de su sumoilación y consecuente inactivación. Por lo tanto, es sugerente pensar que FGF21 también puede actuar en una forma autocrina o paracrina en el WAT (Fig. I-15).

A pesar del rápido progreso que se ha hecho en comprender cómo está regulado FGF21, y sus múltiples acciones, hay ciertamente mucho más por aprender sobre la fisiología de esta hormona.

RESULTADOS Y DISCUSIÓN

1. PAPEL DE SIRT1 EN LA REGULACIÓN DE OXIDACIÓN DE ÁCIDOS GRASOS Y LA CETOGÉNESIS EN RESPUESTA A LOS CAMBIOS NUTRICIONALES

El raton knockout específico de hígado de SIRT1 (ratones SIRT1-LKO en adelante) carece de una porción de su dominio catalítico (SIRT1 Δexon4) (Min et al., 2001; Milne et al., 2007) (Fig. R-1). Se ha demostrado que varios activadores de SIRT1 recapitulan muchos de los eventos moleculares en respuesta a la restricción calórica (CR) *in vivo,* tales como mejorar la biogénesis mitocondrial y las vías de señalización metabólicas (Howitz et al., 2003; Smith et al, 2009). También se ha descrito que SIRT1 es un factor importante en la activación de la gluconeogénesis (Rodgers et al., 2005).

Sin embargo, hemos detectado que los niveles de los genes clave de la oxidación de los acidos grasos y la cetogenesis, y también de la gluconeogenesis, no se vieron afectados en los ratones SIRT1-LKO en respuesta a CR, en comparación con los salvajes (WT) (Fig. R-2). Ni tampoco en el destete, una transición fisiológica donde se ha descrito que estas vias empiezan a declinar, mientras la lipogenesis aumenta (Fig. R-4).

El envejecimiento está asociado a la obesidad y a una mayor resistencia a la insulina (Ferrannini et al., 1997), y hay evidencias que indican que las sirtuinas pueden ser beneficiosas en la prevención de las enfermedades metabólicas relacionadas con la edad (Chalkiadaki y Guarente, 2012). No obstante, no hemos visto cambios en los pesos de los animales, ni en el test de tolerancia a la glucosa (GTT), comparando entre los ratones SIRT1-LKO y WT, con 7 meses de edad (Figura R-5). Puede ser que estos ratones no se puedan considerar “viejos” o envejecidos todavía, ya que varios estudios utilizan ratones de al menos 1 año como modelo. De todas formas, además de que hay varias discrepancias entre los resultados de distintos grupos si SIRT1 juega un papel protector o desencadenante de la resistencia a la insulina, recientemente se ha demostrado que en un modelo de knockout (KO) especifico de hígado de SIRT1, un 33% de los ratones KO a los 6 meses de edad, y el 100% a los 14, han desarrollado resistencia a la insulina (Wang et al., 2011).

Para comprender mejor el papel de SIRT1 en la regulación de la oxidación de ácidos grasos y la cetogénesis, hemos sobreexpresado SIRT1 a través de un adenovirus en las células HepG2. Al analizar los niveles de mRNA de las enzimas claves de estos procesos no hemos visto diferencias entre las células que sobreexpresan GFP (control) o SIRT1 (Fig. R-6).

PPARα es un factor de transcripción común y muy importante en su regulación (Hsu et al., 2001). Hemos confirmado que los genes que participan en estas vías se activan cuando se sobreexpresa PPARα (AdPPARα) en las células HepG2. Muy interesante, cuando ambas proteínas (SIRT1 y PPARα) se sobreexpresaron, los niveles de expresión de CPT1A, HMGCS2, FGF21, y también de la PEPCK, se vieron más inducidos (Fig. R-6). Este resultado sugiere que si SIRT1 regula estos genes, sin duda lo hace a través de PPARα. Para apoyar estos resultados, se utilizó la estrategia contrária. Si bien que no afecta a la expresión basal, hemos observado que la inducción por PPARα se perdió parcialmente en las células *knockdown* para SIRT1 (Fig. R-7). De acuerdo con estos resultados, parece que SIRT1 controla destas vías, aunque de forma indirecta y de manera dependiente de PPARα.

Debido a que PPARα juega un papel crucial en la respuesta adaptativa al ayuno en el hígado (Kersten et al., 1999), los ratones SIRT1-LKO fueron sometidos a ayuno durante la noche (15h). Hemos observado que los ratones SIRT1-LKO presentaban niveles aumentados de glicemia en el ayuno, comparados con los WT. Los niveles de la *Pck1* también lo estaban, sugiriendo que había un aumento en la tasa gluconeogenica en estos animales. Sin embargo, no se han observado cambios en la expresión de *G6pase* ni de *Ppargc1α* (PGC1α) (Fig. R-8).

Es interesante que hayan resultados contradictorios en relación a la regulación de la PEPCK por SIRT1. Mientras unos han visto que SIRT1 activa su transcripción a través de PGC1α (Rodgers et al., 2005; Rodgers & Puigserver, 2007), otros defienden que su activación la reprime (Banks et al., 2008; Yang et al., 2009).

Curiosamente, se ha descrito que SIRT1 inhibe la gluconeogénesis a través de la interrupción de la señalización de TORC2 (CRTC2), mientras que la activa a través de la deacetilación de FOXO1.

Parece ser que tenemos entre manos un resultado contradictorio entre los resultados de los ratones ayunados y los de las células HepG2. Pode ser que por una parte los efectos

de SIRT1 en las células sean debidos a otros que su actividad catalítica, como ya se ha observado en neuronas (Pfister et al., 2008), o que SIRT1 actúe de forma diferente dependiendo de los mecanismos moleculares que están activados, ya que se ha descrito que la PEPCK no es diana de PPARα *in vivo* en el hígado (Kersten et al., 1999), aunque presente un elemento de afinidad intermedia a los PPARs (Juge-Aubry et al., 1997).

2. PAPEL DE SIRT1 EN LA REGULACIÓN DE FGF21 POR LA HMGCS2

ARTÍCULO 1: "HUMAN HMGCS2 REGULATES FATTY ACID OXIDATION AND FGF21 EXPRESSION IN HEPG2 CELLS"

Durante el transcurso de este trabajo se ha descrito que SIRT1 desempeña un papel fundamental en la regulación de la oxidación hepática de los ácidos grasos (Rodgers y Puigserver, 2007). Además, se ha publicado que la eliminación hepática de SIRT1 afecta negativamente a la señalización por PPARα *in vivo* (Purushotham et al., 2009), lo que iba de acuerdo con nuestros resultados en la células HepG2 (Fig. R-6 y R-7).

Al mismo tiempo, trabajo proveniente de nuestro laboratorio demostró que la sobreexpresión de HMGCS2 en las células HepG2 era capaz de inducir la oxidación de ácidos grasos y la cetogénesis (Fig. 1, Art. 1). Y también que la expresión HMGCS2 era necesaria para la inducción de la oxidación de ácidos grasos mediada por PPARα (Fig. 2, Art. 1), y muy interesante, que la sobreexpresión de HMGCS2 estimula la expresión de FGF21 (Fig. 3, Art. 1).

Nuestra hipótesis era que la estimulación del FGF21 por HMGCS2 podría estar correlacionada con la actividad SIRT1, debido al aumento de los niveles intracelulares de NAD^+ proporcionados por la reducción del acetoacetato a β-hidroxibutirato.

Hemos observado que los niveles de la expresión hepática de FGF21, y también sus niveles circulantes en el suero, estaban disminuidos en los ratones SIRT1-LKO sometidos a un ayuno nocturno de 15h. Mientras que otros genes diana como la *Cpt1a* y la propia *Hmgcs2* no se vieron afectados (Figure 5, Artículo 1). A pesar de que había sido descrito que la inducción de CPT1a en el hígado de ratones ayunados era dependiente de SIRT1 (Rodgers &

Puigserver, 2007), puede ser que las diferencias encontradas sean debidas a mecanismos de adaptación que pueden compensar la ablación crónica, pero no la aguda, de SIRT1.

De manera a corroborar la hipótesis inicial, hemos visto que la inducción de FGF21 en las células HepG2 por acetoacetato (AcAc), era dependiente de SIRT1 (Fig. 6, Art. 1).

A partir de nuestros resultados, parece que a través de la generación de acetoacetato, la actividad HMGCS2 podría modular la relación [NAD^+]/[NADH] en el citosol, y por lo tanto la actividad de SIRT1. Así, el modelo que proponemos es un modelo de *feed-forward* en el que la cetogénesis activa una respuesta mediada por SIRT1, y también la oxidación de ácidos grasos de cadena larga.

3. REGULACIÓN DE FGF21 POR LA PRIVACIÓN DE AMINOACIDOS

ARTÍCULO 2: "ACTIVATING TRANSCRIPTION FACTOR 4-DEPENDENT INDUCTION OF FGF21 DURING AMINO ACID DEPRIVATION."

Siguiendo a nuestro proyecto de trabajo, estábamos muy interesados en estudiar la función de PPARα en la regulación de la homeostasis metabólica. Como era de esperar, el tratamiento con MG132 bloquea la expresión de HMGCS2 dependiente de PPARα (Blanquart et al, 2004), un prototípico gen diana de PPARα (Rodríguez et al., 1994) (Fig. 1A, Art. 2). Curiosamente la expresión de FGF21 se vio aumentada por el tratamiento con el inhibidor de proteosoma (MG132), no solo de manera independiente de la sobreexpresión de PPARα, pero también MG132 dosis-dependiente (Fig. 1A and 1B, Art. 2).

Ante esto, surgió la hipótesis de que este tratamiento podría estar disminuyendo la reserva de aminoácidos libres y activando la vía de transducción de señales en respuesta a la privación de aminoácidos, lo que nos impulsa a comprobar si FGF21 se induce durante este proceso. De hecho, hemos encontrado que FGF21 se indujo (Fig. 2A, Art. 2), mientras que los niveles de expresión de la CPT1A y HMGCS2 no se vieron afectados, por el tratamiento con HisOH, un mimetizador de la privación de aminoácidos en cultivos celulares (Fig. R-9B). En 2h de tratamiento con HisOH, la transcripción aumentó y continuó aumentando hasta alcanzar un pico a las 4h. A continuación, se produjo una disminución gradual de 4 a 10h, aunque

incluso después de 10h de tratamiento el nivel de expresión seguía todavía elevado en comparación con el control (Fig. 2B, Art. 2).

Tal como se esperaba (Harding et al., 2003), el HisOH indujo un aumento en los niveles de la proteína ATF4 después de 2h de tratamiento (Fig. 2C, Art. 2), tal como lo hicieron los tratamientos con MG132 y tunicamicina, un agente utilizado para inducir el estrés de retículo (Fig. R-10).

Hemos localizado dos secuencias de unión a ATF4 altamente conservadas (AAREs), en la región reguladora 5' del gen humano FGF21, que son responsables por la activación transcripcional dependiente de ATF4 de este gen, ya que las construcciones con delecciones o mutaciones de los respectivos elementos perdían la respuesta a ATF4 (Fig. 3, Art. 2).

También hemos observado que la inducción de FGF21 por ATF4 se veía afectada por la co-expresión de ATF3 (Fig. R-12). Este mismo comportamiento se ha descrito anteriormente para varios genes que contienen AARE (Chen et al., 2004; Fawcett et al., 1999; Pan et al., 2007), conocido como el ciclo de auto-limitación de la transcripción dependiente de ATF4, lo que también justifica la disminución observada en la tasa de transcripción de FGF21 después de las 4 h de tratamiento con HisOH (Fig. 2B, Art. 2).

A través de ensayos de retardación en gel (EMSA) hemos demostrado que ATF4 se une a cada uno de los AAREs previamente identificados, heterodimerizando con C/EBPβ (Fig. 4C, Art. 2). Y también hemos confirmado esta unión *in vivo* a través de experimentos de imunoprecipitación de la cromatina (ChIP) en las células HepG2 tratadas con HisOH (Fig. 4B, Art. 2 y Fig. R-13).

También hemos demostrado que la inducción de FGF21 producida por carencia de aminoácidos es mediada por ATF4, ya que en células HepG2 tratados con HisOH donde se interfirió la expresión de ATF4 (siRNA), los niveles de mRNA de FGF21 se encontraban significativamente más bajos en comparación con el siRNA control (Fig. 5, Art. 2). El mismo patrón se observó en las células tratadas con tunicamicina, reforzando el papel de ATF4 en la inducción de FGF21 (Fig. R-10).

Para analizar el efecto de la privación de aminoácidos en la expresión de FGF21 *in vivo*, se alimentaron ratones con una dieta deficiente en leucina [(-)leu], o una dieta control,

durante 7 días. Los niveles de mRNA de *Fgf21* se aumentaron considerablemente en el hígado de ratones alimentados con la dieta (-)leu. Hemos observado también que la dinámica de los niveles de la proteína FGF21 en suero refleja la expresión génica hepática (Fig. 6, Art. 2).

Llegados a este punto, hemos descrito que la hormona FGF21, típica de un estado de ayuno, se indujo en un estado de alimentación, en el hígado de ratones privados de leucina en la dieta, una nueva vía de la regulación de la expresión génica de FGF21.

4. SEÑALIZACIÓN POR LA PRIVACIÓN DE AMINOÁCIDOS EN UN ESTADO DE AYUNO

Hemos descubierto que la limitación de aminoácidos aumentaba la expresión de FGF21 (Art. 2). Está ampliamente conocido que el ayuno aumenta los niveles de mRNA de *Fgf21* en el hígado y sus niveles circulantes. Debido a que la falta de nutrientes se correlaciona con frecuencia con una carencia de aminoácidos, nos hemos preguntado si la respuesta global a la combinación de la deficiencia de leucina y el ayuno sería aditiva, o no.

De acuerdo con datos previamente publicados (Guo & Cavener, 2007), en nuestro experimento, los ratones alimentados con una dieta (-)leu durante 7 días, presentaron disminución de la ingesta de alimentos y un menor peso corporal, en comparación con los ratones mantenidos con la dieta control (Fig. R-15).

En nuestro estudio no se encontraron cambios en la glicemia entre los grupos control o (-)leu, tanto en los ratones alimentados como en ayunas (Fig. R-16A). Sin embargo, otros han demostrado que los niveles de glucosa en sangre eran más bajos en los ratones privados de leucina, en comparación con el control (Xiao et al., 2011).

En el ayuno, los triglicéridos (TG) del WAT se movilizan para dar lugar a ácidos grasos libres, que luego pueden ser utilizados por otros tejidos para la producción de energía. Hemos observado que la privación de leucina ha resultado en una disminución de los ácidos grasos libres en suero en los ratones alimentados, como se describió previamente (Cheng et al., 2010; Guo & Cavener, 2007). Sin embargo, nuestros resultados mostraron que el

aumento de los niveles de los ácidos grasos libres en el ayuno no se modificó, comparando entre los grupos de dieta control o (-)leu (Fig. R-16B).

Curiosamente, hemos visto que los niveles de β-hidroxibutirato se incrementaron significativamente en los ratones alimentados con la dieta (-)leu en el grupo *ad libitum*. Sin embargo, los altos niveles de β-hidroxibutirato que hemos observado en el ayuno, en comparación con el *ad libitum*, se mantuvieron sin cambios entre los grupos control o (-)leu (Fig. R-16C).

Dado que la producción de cuerpos cetónicos se regula por la HMGCS2 y a través de múltiples señales del estado metabólico general del organismo, hemos comprobado sus niveles de mRNA en el higado. Sorprendentemente, hemos encontrado que sus niveles de expresión no se alteraron en los ratones del grupo (-)leu en comparación con el control, en los ratones alimentados. De todas formas, una vía que altere el grado de cualquiera sus modificaciones (acetilación, succinilación, etc.) o sus niveles de proteína, podría estar regulando la actividad HMGCS y aumentando el flujo cetogénico, independientemente de sus niveles de mRNA.

También hemos analizado otros genes relacionados con la oxidación de los ácidos grasos y la gluconeogénesis en el hígado. Tal como para *Hmgcs2*, hemos encontrado que los niveles de mRNA de *Cpt1a*, *Pck1* (PEPCK) y *Ppargc1α* (PGC1α) permanecieron inalterados entre los ratones alimentados con las dietas control o (-)leu, en el grupo *ad libitum*. Curiosamente, la activación de su expresión hepática esperada en el ayuno, se vió seguida por un aumento adicional en el grupo de ratones (-)leu, en comparación con el control, ambos en el estado de ayuno. Este efecto fue particularmente interesante para PGC1α, que triplicó su activación en la alimentación (-)leu, exclusivamente después del ayuno.

Se ha demostrado que FGF21 induce la expresión hepática de PGC1α (Potthoff et al., 2009). Resulta sugerente pensar que además de la ruta de la respuesta a la privación de aminoácidos, se necesita una señal de ayuno para hiperactivar la expresión de PGC1α. Al contrário, los niveles de FGF21 hepáticos y circulantes, que nosotros hemos mostrado previamente que se aumentan enormemente en respuesta a la privación de leucina en un grupo de ratones *ad libitum*, fueron de alguna manera regulados a la baja en el ayuno, si comparamos sólo los grupos (-)leu, entre alimentados y en ayunas. Una de las posibles

explicaciones para este resultado, que aún requiere investigación para ser confirmado, es que haya un circuito de retroalimentación regulado por PGC1α, ya que este regulador clave de la homeostasis energética ha sido identificado como un importante regulador negativo de la expresión de FGF21 en el hígado (Estall et al., 2009).

5. PAPEL DE FGF21 EN EL FENOTIPO RESULTANTE DE LA PRIVACIÓN DE AMINOÁCIDOS

Hemos observado algunas coincidencias interesantes entre el fenotipo resultante de la privación de leucina y los efectos metabólicos que dependen de FGF21, sugeridos a partir de estudios recientes. Los datos reportados y los nuestros, nos hizo plantear la hipótesis de una nueva función para FGF21: el vínculo entre la carencia de aminoácidos y el balance energético global. Para investigar esta hipótesis, se analizó la respuesta de ratones FGF21-*knockout* (FGF21-KO) a la privación del aminoácido esencial leucina.

Para empezar, hemos confirmado que los niveles de *Fgf21* estaban aumentados en el hígado, y también en el suero, de los ratones alimentados con la dieta (-)leu; no se vieron cambios en tejido adiposo marrón (BAT), y inexplicablemente estaban disminuidos en el tejido adiposo blanco (WAT) (Fig. 1, manuscrito enviado; *m.e.* adelante).

Muy interesante, hemos visto que la deficiencia de FGF21 atenuaba significativamente la pérdida de peso causada por la privación de leucina, mientras que la reducción en la ingesta de alimentos en los grupo (-)leu se mantuvo sin cambios entre los genotipos (Fig. 2A, 2B y 2C, *m.e.*). A través de un análisis histológico del WAT hemos confirmado que tal como se había descrito (Cheng et al., 2010), la privación de leucina resulta en una reducción del volumen de los adipocitos en comparación con los ratones alimentados con una dieta control. Al contrario, el volumen de los adipocitos apenas se había reducido en los ratones FGF21-KO del grupo (-)leu, confirmando que la reducción del tamaño de los adipocitos depende de la inducción de FGF21 (Fig. 2D, *m.e.*).

Hemos visto que los niveles de la HSL fosforilada [(P)-HSL] se incrementaron en la alimentación (-)leu en WAT, tal como había sido descrito (Cheng et al, 2010.). Aunque los niveles de mRNA de *Hsl* y *Atgl* se mantuvieron sin cambios, la activación de la proteína HSL,

probablemente permitió que la lipólisis aumentara. Nuestros resultados demuestran que el aumento en los niveles de fosforilación de HSL en respuesta a la dieta (-)leu estaba bloqueado en los ratones FGF21-KO (Fig. 3, *m.e.*).

El siguiente paso fue medir la expresión de genes implicados en la síntesis de lípidos. En el hígado, hemos visto que la reducción esperada en los niveles de mRNA de *Srebp1c*, *Fas* y *Acc1* por la dieta (-)leu, no se observó en los ratones FGF21-KO (Fig. 4A, *m.e.*). Es interesante señalar que una acción inhibitoria en la síntesis de lípidos ya había sido descrita para FGF21 (Xu et al., 2009). En una tinción de hígado con hematoxilina y eosina (H&E), se observó una disminución en la cantidad de regiones claras, que pueden reflejar una disminución en la acumulación de lípidos, en la privación de leucina en ratones WT, que no ocurrió en los ratones FGF21-KO (Fig. 4D, *m.e.*). Esto sugiere que la no-represión de la lipogénesis sea probablemente la causa principal de la esteatosis hepática en estos ratones.

Por otra parte, hemos confirmado que la respuesta típica a la privación de aminoácidos no estaba afectada en los ratones FGF21-KO, ya que tal como se esperaba, los niveles de proteína ATF4 y el mRNA de *Asns* estaban aumentados en estos animales (Fig. 4B y 4C, *m.e.*). Nuestros resultados indican no sólo que FGF21 no está implicado en el control del metabolismo de aminoácidos en la privación de aminoácidos, sino también que sus efectos son *downstream* a la regulación por ATF4.

A continuación, hemos analizado si el bloqueo en la reducción del peso corporal observado en los FGF21-KO privados de leucina, no sólo se relacionaba con la lipólisis en el WAT, sino también a otros factores que influencian la masa del tejido adiposo, como la lipogénesis. Hemos observado una significativa reducción en los niveles de mRNA de *Fas* en el WAT bajo la alimentación (-)leu, que se vio bloqueado por completo en los ratones FGF21-KO. Los niveles de mRNA de *Srebp1c* y *Acc1* presentaron el mismo patrón, aunque con distintas significancias estadísticas (Fig. 4E, *m.e.*).

Hemos examinado los niveles de la expresión de *Ucp1* y *Dio2*, genes que codifican proteínas implicadas en el aumento de la termogénesis en el BAT (Bianco & Silva, 1988), y hemos encontrado que su elevada activación en el grupo de la alimentación (-)leu se bloqueaba en los ratones FGF21-KO. Sorprendentemente, los niveles de mRNA que codifican para el regulador de UCP1 (i.e. PGC1α), que se aumentaron estadísticamente en el grupo (-

)leu, no se vieron afectados en los ratones FGF21-KO (Fig. 4F, *m.e.*). Estos últimos hallazgos parecen apuntar a una estimulación directa de la transcripción de la UCP1 por FGF21, o a un mecanismo indirecto, a través de un factor de transcripción (o coactivador), probablemente inducido por la privación de aminoácidos en el BAT, y regulado por FGF21.

En resumen, hemos encontrado que los ratones FGF21-KO con una dieta privada de leucina, presentan un bloqueo en la represión de la lipogénesis en el hígado y el WAT; una disminución de la fosforilación de la HSL en el WAT, lo que probablemente indica que la lipólisis no está inducida; y la inducción de la expresión termogénica alterada en el BAT, demostrando que FGF21 juega un papel importante en la regulación del metabolismo de los lípidos durante la privación de aminoácidos (Fig. 5, *m.e.*).

CONCLUSIONES

- En las células HepG2, SIRT1 desempeña un papel en la activación por PPARα de la expresión de FGF21, CPT1A, HMGCS2, y PEPCK.
- La actividad de SIRT1 regula los niveles de glicemia y la expresión de PCK1 en hígado, en la respuesta al ayuno.
- La actividad de SIRT1 no afecta a la expresión de los genes de la oxidación de los ácidos grasos o la cetogénesis en el hígado, en respuesta a diferentes cambios nutricionales, como la restricción calórica, la transición de la lactancia/destete, y el ayuno.
- A través del aumento de la producción de cuerpos cetónicos, la HMGCS2 regula la activación de FGF21 por SIRT1, en respuesta al ayuno.
- El gen humano FGF21 es diana de ATF4 y presenta dos elementos funcionales de respuesta a amino ácidos (AARE) conservados en su región reguladora 5'.
- FGF21 se induce por la privación de aminoácidos en el hígado de ratón y en las células de cultivo HepG2.
- La privación de leucina afecta a los niveles de ácidos grasos libres y cuerpos cetónicos en suero en el estado de alimentación, mientras que no lo hace en el ayuno.
- La activación de FGF21 en el ayuno se ve afectada en los ratones alimentados con una dieta deficiente en leucina, subyacente a un *crosstalk* entre la señalización del ayuno y la privación de aminoácidos.
- FGF21 media la regulación del metabolismo de los lípidos en el hígado y el tejido adiposo blanco, y la termogénesis en el tejido adiposo marrón, durante la privación de aminoácidos.

REFERENCES

A

Adams AC, Astapova I, Fisher FM, Badman MK, Kurgansky KE, Flier JS, Hollenberg AN, Maratos-Flier E (2010) Thyroid hormone regulates hepatic expression of fibroblast growth factor 21 in a PPARalpha-dependent manner. J Biol Chem 285(19):14078-82.

Ameri K, Harris AL (2008) Activating transcription factor 4. Int J Biochem Cell Biol 40(1):14-21.

Andrulis IL, Chen J, Ray PN (1987) Isolation of human cDNAs for asparagine synthetase and expression in Jensen rat sarcoma cells. Mol Cell Biol 7(7):2435-43.

Anthony TG, McDaniel BJ, Byerley RL, McGrath BC, Cavener DR, McNurlan MA, Wek RC (2004) Preservation of liver protein synthesis during dietary leucine deprivation occurs at the expense of skeletal muscle mass in mice deleted for eIF2 kinase GCN2. J Biol Chem 279(35):36553-61.

Arner P, Pettersson A, Mitchell PJ, Dunbar JD, Kharitonenkov A, Ryden M (2008) FGF21 attenuates lipolysis in human adipocytes: a possible link to improved insulin sensitivity. FEBS Lett 582:1725-30.

B

Badman MK, Pissios P, Kennedy AR, Koukos G, Flier JS, Maratos-Flier E (2007) Hepatic fibroblast growth factor 21 is regulated by PPARalpha and is a key mediator of hepatic lipid metabolism in ketotic states. Cell Metab 5(6):426-37.

Badman MK, Koester A, Flier JS, Kharitonenkov A, Maratos-Flier E (2009) Fibroblast growth factor 21-deficient mice demonstrate impaired adaptation to ketosis. Endocrinology 150(11):4931-40.

Banks AS, Kon N, Knight C, Matsumoto M, Gutiérrez-Juárez R, Rossetti L, Gu W, Accili D (2008) SirT1 gain of function increases energy efficiency and prevents diabetes in mice. Cell Metab 8(4):333-41.

Barbosa-Tessmann IP, Chen C, Zhong C, Siu F, Schuster SM, Nick HS, Kilberg MS (2000) Activation of the human asparagine synthetase gene by the amino acid response and the endoplasmic reticulum stress response pathways occurs by common genomic elements. J Biol Chem 275(35):26976-85.

Barrero MJ, Camarero N, Marrero PF, Haro D (2003) Control of human carnitine palmitoyltransferase II gene transcription by peroxisome proliferator-activated receptor through a partially conserved peroxisome proliferator-responsive element. Biochem J 369(Pt 3):721-9.

Berger F, Ramírez-Hernández MH, Ziegler M (2004) The new life of a centenarian: signalling functions of NAD(P). Trends Biochem Sci 29(3):111-8.

Berlanga JJ, Santoyo J, De Haro C (1999) Characterization of a mammalian homolog of the GCN2 eukaryotic initiation factor 2alpha kinase. Eur J Biochem 265(2):754-62.

Bernal-Mizrachi C, Weng S, Feng C, Finck BN, Knutsen RH, Leone TC, Coleman T, Mecham RP, Kelly DP, Semenkovich CF (2003) Dexamethasone induction of hypertension and diabetes is PPAR-alpha dependent in LDL receptor-null mice. Nat Med 9(8):1069-75.

Bézaire V, Mairal A, Anesia R, Lefort C, Langin D (2009) Chronic TNFalpha and cAMP pre-treatment of human adipocytes alter HSL, ATGL and perilipin to regulate basal and stimulated lipolysis. FEBS Lett 583(18):3045-9.

Bianco AC, Silva JE (1988) Cold exposure rapidly induces virtual saturation of brown adipose tissue nuclear T3 receptors. Am J Physiol 255(4 Pt 1):E496-503.

Blander G, Guarente L (2004) The Sir2 family of protein deacetylases. Annu Rev Biochem 73:417-35

Blanquart C, Barbier O, Fruchart JC, Staels B, Glineur C (2002) Peroxisome proliferator-activated receptor alpha (PPARalpha) turnover by the ubiquitin-proteasome system controls the ligand-induced expression level of its target genes. J Biol Chem 277(40):37254-9.

Blanquart C, Mansouri R, Fruchart JC, Staels B, Glineur C (2004) Different ways to regulate the PPARalpha stability. Biochem Biophys Res Commun 319(2):663-70.

Bordone L, Guarente L (2005) Caloric Restriction, Sirt1 and metabolism: Understanding longevity. Mol Cell Bio (Nature Reviews) 6:299-305

Bordone L, Motta MC, Picard F, Robinson A, Jhala US, Apfeld J, McDonagh T, Lemieux M, McBurney M, Szilvasi A, Easlon EJ, Lin SJ, Guarente L (2006) Sirt1 regulates insulin secretion by repressing UCP2 in pancreatic beta cells. PLoS Biol 4(2):e31.

Borra MT, O'Neill FJ, Jackson MD, Marshall B, Verdin E, Foltz KR, Denu JM (2002) Conserved enzymatic production and biological effect of O-acetyl-ADP-ribose by silent information regulator 2-like NAD +-dependent deacetylases. J Biol Chem 277:12632-41.

Brachmann CB, Sherman JM, Devine SE, Cameron EE, Pillus L, Boeke JD (1995) The SIR2 gene family, conserved from bacteria to humans, functions in silencing, cell cycle progression, and chromosome stability. Genes Dev 9(23):2888-902.

Bruhat A, Jousse C, Wang XZ, Ron D, Ferrara M, Fafournoux P (1997) Amino acid limitation induces expression of CHOP, a CCAAT/enhancer binding protein-related gene, at both transcriptional and post-transcriptional levels. J Biol Chem 272(28):17588-93.

Brunet A, Bonni A, Zigmond MJ, Lin MZ, Juo P, Hu LS, Anderson MJ, Arden KC, Blenis J, Greenberg ME (1999) Akt promotes cell survival byphosphorylating and inhibiting a Forkhead transcription factor. Cell 96:857-68.

Brunet A, Sweeney LB, Sturgill JF, Chua KF, Greer PL, Lin Y, Tran H, Ross SE, Mostoslavsky R, Cohen HY, Hu LS, Cheng HL, Jedrychowski MP, Gygi SP, Sinclair DA, Alt FW, Greenberg ME. (2004) Stress-dependent regulation of FOXO transcription factors by the SIRT1 deacetylase. Science 303(5666):2011-5.

C

Cantó C, Jiang LQ, Deshmukh AS, Mataki C, Coste A, Lagouge M, Zierath JR, Auwerx J (2010) Interdependence of AMPK and SIRT1 for metabolic adaptation to fasting and exercise in skeletal muscle. Cell Metab 11(3):213-9.

Carmona MC, Hondares E, Rodríguez de la Concepción ML, Rodríguez-Sureda V, Peinado-Onsurbe J, Poli V, Iglesias R, Villarroya F, Giralt M (2005) Defective thermoregulation, impaired lipid metabolism, but preserved adrenergic induction of gene expression in brown fat of mice lacking C/EBPbeta. Biochem J 389(Pt 1):47-56.

Carraro V, Maurin AC, Lambert-Langlais S, Averous J, Chaveroux C, Parry L, Jousse C, Ord D, Ord T, Fafournoux P, Bruhat A (2010) Amino acid availability controls TRB3 transcription in liver through the GCN2/eIF2α/ATF4 pathway. PLoS One 5(12):e15716.

Chakravarthy MV, Lodhi IJ, Yin L, Malapaka RR, Xu HE, Turk J, Semenkovich CF (2009) Identification of a physiologically relevant endogenous ligand for PPARalpha in liver. Cell 138(3):476-88.

Chakravarthy MV, Pan Z, Zhu Y, Tordjman K, Schneider JG, Coleman T, Turk J, Semenkovich CF (2005) "New" hepatic fat activates PPARalpha to maintain glucose, lipid, and cholesterol homeostasis. Cell Metab 1(5):309-22.

Chakravarty K, Cassuto H, Reshef L, Hanson RW (2005) Factors that control the tissue-specific transcription of the gene for phosphoenolpyruvate carboxykinase-C. Crit Rev Biochem Mol Biol 40:129-154.

Chalkiadaki A, Guarente L (2012) Sirtuins mediate mammalian metabolic responses to nutrient availability. Nat Rev Endocrinol 8(5):287-96.

Chau MD, Gao J, Yang Q, Wu Z, Gromada J (2010) Fibroblast growth factor 21 regulates energy metabolism by activating the AMPK-SIRT1-PGC-1alpha pathway. Proc Natl Acad Sci U S A 107(28):12553-8.

Chaveroux C, Lambert-Langlais S, Cherasse Y, Averous J, Parry L, Carraro V, Jousse C, Maurin AC, Bruhat A, Fafournoux P (2010) Molecular mechanisms involved in the adaptation to amino acid limitation in mammals. Biochimie 92(7):736-45.

Chavez AO, Molina-Carrion M, Abdul-Ghani MA, Folli F, Defronzo RA, Tripathy D (2009) Circulating fibroblast growth factor-21 (FGF-21) is elevated in impaired glucose tolerance and type 2 diabetes and correlates with muscle and hepatic insulin resistance. Diabetes Care 32:1542-6.

Chen D, Bruno J, Easlon E, Lin SJ, Cheng HL, Alt FW, Guarente L (2008) Tissue-specific regulation of SIRT1 by calorie restriction. Genes Dev 22:1753-7.

Chen H, Pan YX, Dudenhausen EE, Kilberg MS (2004) Amino acid deprivation induces the transcription rate of the human asparagine synthetase gene through a timed program of expression and promoter binding of nutrient-responsive basic region/leucine zipper transcription factors as well as localized histone acetylation. J Biol Chem 279(49):50829-39.

Cheng HL, Mostoslavsky R, Saito S, Manis JP, Gu Y, Patel P, Bronson R, Appella E, Alt FW, Chua KF (2003) Developmental defects and p53 hyperacetylation in Sir2 homolog (SIRT1)-deficient mice. Proc Natl Acad Sci U S A 100(19):10794-9.

Cheng Y, Meng Q, Wang C, Li H, Huang Z, Chen S, Xiao F, Guo F (2010) Leucine deprivation decreases fat mass by stimulatiom of lipolysis in white adipose tissue and upregulation of uncoupling protein 1 (UCP1) in brown adipose tissue. Diabetes 59(1):17-25.

Cohen HY, Miller C, Bitterman KJ, Wall NR, Hekking B, Kessler B, Howitz KT, Gorospe M, de Cabo R, Sinclair DA (2004) Calorie restriction promotes mammalian cell survival by inducing the SIRT1 deacetylase. Science 305(5682):390-2.

Coskun T, Bina HA, Schneider MA, Dunbar JD, Hu CC, Chen Y, Moller DE, Kharitonenkov A (2008) Fibroblast growth factor 21 corrects obesity in mice. Endocrinology 149(12):6018-27.

D

Deng J, Harding HP, Raught B, Gingras AC, Berlanga JJ, Scheuner D, Kaufman RJ, Ron D, Sonenberg N (2002) Activation of GCN2 in UV-irradiated cells inhibits translation. Curr Biol 12(15):1279-86.

Dever TE (2002) Gene-specific regulation by general translation factors. Cell 108(4):545-56.

Dudek SM, Semenkovich CF (1995) Essential amino acids regulate fatty acid synthase expression through an uncharged transfer RNA-dependent mechanism. J Biol Chem 270(49):29323-9.

Dutchak PA, Katafuchi T, Bookout AL, Choi JH, Yu RT, Mangelsdorf DJ, Kliewer SA (2012) Fibroblast growth factor-21 regulates PPARγ activity and the antidiabetic actions of thiazolidinediones. Cell 148(3):556-67.

E

Erion DM, Yonemitsu S, Nie Y, Nagai Y, Gillum MP, Hsiao JJ, Iwasaki T, Stark R, Weismann D, Yu XX, Murray SF, Bhanot S, Monia BP, Horvath TL, Gao Q, Samuel VT, Shulman GI (2009) SirT1 knockdown in liver decreases basal hepatic glucose production and increases hepatic insulin responsiveness in diabetic rats. Proc Natl Acad Sci U S A 106(27):11288-93.

F

Fabrizio P, Gattazzo C, Battistella L, Wei M, Cheng C, McGrew K, Longo VD (2005) Sir2 blocks extreme life-span extension. Cell 123(4):655-67.

Fawcett TW, Martindale JL, Guyton KZ, Hai T, Holbrook NJ (1999) Complexes containing activating transcription factor (ATF)/cAMP-responsive-element-binding protein (CREB) interact with the CCAAT/enhancer-binding protein (C/EBP)-ATF composite site to regulate Gadd153 expression during the stress response. Biochem J 339 (Pt 1):135-41.

Feige JN, Johan A (2008) Transcriptional targets of sirtuins in the coordination of mammalian physiology. Curr Opin Cell Biol 20:303-9.

Ferrannini E, Natali A, Capaldo B, Lehtovirta M, Jacob S, Yki-Järvinen H (1997) Insulin resistance, hyperinsulinemia, and blood pressure: role of age and obesity. European Group for the Study of Insulin Resistance (EGIR). Hypertension 30(5):1144-9.

Ferré P, Decaux JF, Issad T, Girard J (1986) Changes in energy metabolism during the suckling and weaning period in the newborn. Reprod Nutr Dev. 26(2B):619-31.

Finck BN, Kelly DP (2006) PGC-1 coactivators: inducible regulators of energy metabolism in health and disease. J Clin Invest 116:615–622.

Finn PF, Dice JF (2006) Proteolytic and lipolytic responses to starvation. Nutrition 22(7-8):830-44.

Fisher FM, Chui PC, Antonellis PJ, Bina HA, Kharitonenkov A, Flier JS, Maratos-Flier E (2010) Obesity is a fibroblast growth factor 21 (FGF21)-resistant state. Diabetes 59(11):2781-9.

Fisher FM, Kleiner S, Douris N, Fox EC, Mepani RJ, Verdeguer F, Wu J, Kharitonenkov A, Flier JS, Maratos-Flier E, Spiegelman BM (2012) FGF21 regulates PGC-1α and browning of white adipose tissues in adaptive thermogenesis. Genes Dev 26(3):271-81.

Foster DW (2004) The role of the carnitine system in human metabolism. Ann N Y Acad Sci 1033:1-16.

Franckhauser S, Munoz S, Pujol A, Casellas A, Riu E, Otaegui P, Su B, Bosch F (2002) Increased fatty acid re-esterification by PEPCK overexpression in adipose tissue leads to obesity without insulin resistance. Diabetes 51:624-630.

Fulco M, Sartorelli V (2008) Comparing and contrasting the roles of AMPK and SIRT1 in metabolic tissues. Cell Cycle 7(23):3669-79.

Fulco M, Schiltz RL, Iezzi S, King MT, Zhao P, Kashiwaya Y, Hoffman E, Veech RL, Satorelli V (2005) Sir2 regulates skeletal muscle differentiation as a potential sensor of the redox state. Mol. Cell 12:51-62.

G

Gerhart-Hines Z, Rodgers JT, Bare O, Lerin C, Kim S-H, Mostoslavsky R, Alt FW, Wu Z, Puigserver P (2007) Metabolic control of muscle mitochondrial function and fatty acid oxidation through SIRT1/PGC-1alpha. EMBO J 26:1913-23.

Ghosh HS (2008) The anti-aging, metabolism potential of SIRT1. Curr Opin Investig Drugs 9: 1095-102.

Gibbons G (2005) Old fat, make way for new fat. Nat Med 11(7):722-3.

Gietzen DW, Rogers QR (2006) Nutritional homeostasis and indispensable amino acid sensing: a new solution to an old puzzle. Trends Neurosci 29(2):91-9.

Gietzen DW, Ross CM, Hao S, Sharp JW (2004) Phosphorylation of eIF2alpha is involved in the signaling of indispensable amino acid deficiency in the anterior piriform cortex of the brain in rats. J Nutr 134(4):717-23.

Girard J, Duéee PH, Ferré P, Pégorier JP, Escriva F, Decaux JF (1985) Reprod Nutr Dev 25(1B):303-19.

Girard J, Ferré P, Pégorier JP, Duee PH (1992) Adaptations of glucose and fatty acid metabolism during perinatal period and suckling-weaning transition. Physiol Rev 72:507-62.

Goetz R, Beenken A, Ibrahimi OA, Kalinina J, Olsen SK, Eliseenkova AV, Xu C, Neubert TA, Zhang F, Linhardt RJ, Yu X, White KE, Inagaki T, Kliewer SA, Yamamoto M, Kurosu H, Ogawa Y, Kuro-o M, Lanske B, Razzaque MS, Mohammadi M (2007) Molecular insights into the klotho-dependent, endocrine mode of action of fibroblast growth factor 19 subfamily members. Mol Cell Biol 27:3417-28.

Greenberg AS, Shen WJ, Muliro K, Patel S, Souza SC, Roth RA, Kraemer FB (2001) Stimulation of lipolysis and hormone-sensitive lipase via the extracellular signal-regulated kinase pathway. J Biol Chem 276(48):45456-61.

Guarente L (2011) The logic linking protein acetylation and metabolism. Cell Metab 14(2):151-3.

Guarente L, Picard F (2005) Calorie restriction - the SIR2 connection. Cell 120(4):473-82.

Guo F, Cavener DR (2007) The GCN2 eIF2a Kinase Regulates Fatty-Acid Homeostasis in the Liver during Deprivation of an Essential Amino Acid. Cell Metab 5(2):103-14.

H

Hansen BS, Vaughan MH, Wang L (1972) Reversible inhibition by histidinol of protein synthesis in human cells at the activation of histidine. J Biol Chem 247:3854-7.

Hao S, Sharp JW, Ross-Inta CM, McDaniel BJ, Anthony TG, Wek RC, Cavener DR, McGrath BC, Rudell JB, Koehnle TJ, Gietzen DW (2005) Uncharged tRNA and sensing of amino acid deficiency in mammalian piriform cortex. Science 307(5716):1776-8.

Harding HP, Calfon M, Urano F, Novoa I, Ron D (2002) Transcriptional and translational control in the Mammalian unfolded protein response. Annu Rev Cell Dev Biol 18:575-99.

Harding HP, Zhang Y, Zeng H, Novoa I, Lu PD, Calfon M, Sadri N, Yun C, Popko B, Paules R, Stojdl DF, Bell JC, Hettmann T, Leiden JM, Ron D (2003) An integrated stress response regulates amino acid metabolism and resistance to oxidative stress. Mol Cell 11(3):619-33.

Harper AE, Benevenga NJ, Wohlhueter RM (1970) Effects of ingestion of disproportionate amounts of amino acids. Physiol Rev 50(3):428-558.

Hegardt FG (1998) Transcriptional regulation of mitochondrial HMG-CoA synthase in the control of ketogenesis. Biochimie 80(10):803-6.

Hegardt FG (1999) Mitochondrial 3-hydroxy-3-methylglutaryl-CoA synthase: a control enzyme in ketogenesis. Biochem J 338 (Pt 3):569-82.

Herzig S, Long F, Jhala US, Hedrick S, Quinn R, Bauer A, Rudolph D, Schutz G, Yoon C, Puigserver P, Spiegelman B, Montminy M (2001) CREB regulates hepatic gluconeogenesis through the coactivator PGC-1. Nature 413:179-83.

Hirschey MD, Shimazu T, Capra JA, Pollard KS, Verdin E (2011) SIRT1 and SIRT3 deacetylate homologous substrates: AceCS1,2 and HMGCS1,2. Aging (Albany NY) 3(6):635-42.

Hotta Y, Nakamura H, Konishi M, Murata Y, Takagi H, Matsumura S, Inoue K, Fushiki T, Itoh N (2009) Fibroblast growth factor 21 regulates lipolysis in white adipose tissue but is not required for ketogenesis and triglyceride clearance in liver. Endocrinology 150(10):4625-33.

Howitz KT, Bitterman KJ, Cohen HY, Lamming DW, Lavu S, Wood JG, Zipkin RE, Chung P, Kisielewski A, Zhang LL, Scherer B, Sinclair DA (2003) Small molecule activators of sirtuins extend Saccharomyces cerevisiae lifespan. Nature 425(6954):191-6.

Hsu MH, Savas U, Griffin KJ, Johnson EF (2001) Identification of peroxisome proliferator-responsive human genes by elevated expression of the peroxisome proliferator-activated receptor alpha in HepG2 cells. J Biol Chem 276(30):27950-8.

Hutson RG, Kilberg MS (1994) Cloning of rat asparagine synthetase and specificity of the amino acid-dependent control of its mRNA content. Biochem J 304 (Pt 3):745-50.

Iizuka K, Takeda J, Horikawa Y (2009) Glucose induces FGF21 mRNA expression through ChREBP activation in rat hepatocytes. FEBS Lett. 583(17):2882-6.

Imai S, Armstrong CM, Kaeberlein M, Guarente L (2000) Transcriptional silencing and longevity protein Sir2 is an NAD-dependent histone deacetylase. Nature 403:795-800.

Inagaki T, Dutchak P, Zhao G, Ding X, Gautron L, Parameswara V, Li Y, Goetz R, Mohammadi M, Esser V, Elmquist JK, Gerard RD, Burgess SC, Hammer RE, Mangelsdorf DJ, Kliewer SA (2007) Endocrine regulation of the fasting response by PPARalpha-mediated induction of fibroblast growth factor 21. Cell Metab 5(6):415-25.

Inagaki T, Lin VY, Goetz R, Mohammadi M, Mangelsdorf DJ, Kliewer SA (2008) Inhibition of growth hormone signaling by the fasting-induced hormone FGF21. Cell Metab 8:77-83.

Itoh N, Ornitz DM (2008) Functional evolutionary history of the mouse Fgf gene family. Dev Dyn 237:18-27.

J

Jiang H-Y, Wek RC (2005) Phosphorylation of the α-subunit of the eukaryotic initiation factor-2 (eIF2α) reduces protein synthesis and enhances apoptosis in response to proteosome inhibition. J Biol Chem 280(14):14189-202.

Juge-Aubry C, Pernin A, Favez T, Burger AG, Wahli W, Meier CA, Desvergne B (1997) DNA binding properties of peroxisome proliferator-activated receptor subtypes on various natural peroxisome proliferator response elements. Importance of the 5'-flanking region. J Biol Chem 272(40):25252-9.

K

Kaeberlein M, McVey M, Guarente L (1999) The SIR2/3/4 complex and SIR2 alone promote longevity in Saccharomyces cerevisiae by two different mechanisms. Genes Dev 13(19):2570-80.

Kaufman RJ (1999) Stress signaling from the lumen of the endoplasmic reticulum: coordination of gene transcriptional and translational controls. Genes Dev 13(10):1211-33.

Kersten S, Seydoux J, Peters JM, Gonzalez FJ, Desvergne B, Wahli W (1999) Peroxisome proliferator-activated receptor alpha mediates the adaptive response to fasting. J Clin Invest 103(11):1489-98.

Kersten S, Seydoux J, Peters JM, Gonzalez FJ, Desvergne B, Wahli W (1999) Peroxisome proliferator–activated receptor α mediates the adaptive response to fasting. J. Clin. Invest. 103:1489-98

Kharitonenkov A, Shiyanova TL, Koester A, Ford AM, Micanovic R, Galbreath EJ, Sandusky GE, Hammond LJ, Moyers JS, Owens RA, Gromada J, Brozinick JT, Hawkins ED, Wroblewski VJ, Li DS, Mehrbod F, Jaskunas SR, Shanafelt AB (2005) FGF-21 as a novel metabolic regulator. J Clin Invest 115(6):1627-35.

Kharitonenkov A, Wroblewski VJ, Koester A, Chen YF, Clutinger CK, Tigno XT, Hansen BC, Shanafelt AB, Etgen GJ (2007) The metabolic state of diabetic monkeys is regulated by fibroblast growth factor-21. Endocrinology 148(2):774-81.

Kilberg MS, Shan J, Su N (2009) ATF4-dependent transcription mediates signaling of amino acid limitation. Trends Endocrinol Metabol 20(9):436-43.

Kim J, Guan KL (2011) Amino acid signaling in TOR activation. Annu Rev Biochem 80:1001-32.

Kliewer SA, Forman BM, Blumberg B, Ong ES, Borgmeyer U, Mangelsdorf DJ, Umesono K, Evans RM (1994) Differential expression and activation of a family of murine peroxisome proliferator-activated receptors. Proc Natl Acad Sci U S A 91(15):7355-9.

Kliewer S, Xu H, Lambert M, Willson, T (2001) Peroxisome proliferator-activated receptors: from genes to physiology. Recent Prog Horm Res 56:239-63.

Koehnle TJ, Russell MC, Morin AS, Erecius LF, Gietzen DW (2004) Diets deficient in indispensable amino acids rapidly decrease the concentration of the limiting amino acid in the anterior piriform cortex of rats. J Nutr 134(9):2365-71.

Koo SH, Flechner L, Qi L, Zhang X, Screaton RA, Jeffries S, Hedrick S, Xu W, Boussouar F, Brindle P, Takemori H, Montminy M (2005) The CREB coactivator TORC2 is a key regulator of fasting glucose metabolism. Nature 437:1109-11.

Kostiuk MA, Keller BO, Berthiaume LG (2010) Palmitoylation of ketogenic enzyme HMGCS2 enhances its interaction with PPARalpha and transcription at the Hmgcs2 PPRE. FASEB J 24(6):1914-24.

Kralisch S, Klein J, Loosner U, Bluher M, Paschke R, Stumvoll M, Fasshauer M (2005) Isoproterenol, TNFalpha, and insulin downregulate adipose triglyceride lipase in 3T3-L1 adipocytes. Mol Cell Endocrinol 240(1-2):43-9.

Kren BT, Steer CJ (1996) Posttranscriptional regulation of gene expression in liver regeneration: role of mRNA stability. FASEB J 10(5):559-73.

Kroemer G, Mariño G, Levine B (2010) Autophagy and the integrated stress response. Mol Cell 40(2):280-93.

Kuma A, Hatano M, Matsui M, Yamamoto A, Nakaya H, Yoshimori T, Ohsumi Y, Tokuhisa T, Mizushima N (2004) The role of autophagy during the early neonatal starvation period. Nature 432(7020):1032-6.

Kurosu H, Choi M, Ogawa Y, Dickson AS, Goetz R, Eliseenkova AV, Mohammadi M, Rosenblatt KP, Kliewer SA, Kuro-o M (2007) Tissue specific expression of beta-Klotho and fibroblast growth factor (FGF) receptor isoforms determines metabolic activity of FGF19 and FGF21. J Biol Chem 282:26687-95.

L

Lagouge M, Argmann C, Gerhart-Hines Z, Meziane H, Lerin C, Daussin F, Messadeq N, Milne J, Lambert P, Elliot P Geny B, Laakso M, Puigserver P, Auwerx J (2006) Resveratrol improves mitochondrial function and protects against metabolic disease by activating SIRT1 and PGC-1alpha. Cell 127:1109-22.

Landry J, Sutton A, Tafrov ST, Heller RC, Stebbins J, Pillus L, Sternglanz R (2000) The silencing protein SIR2 and its homologs are NAD-dependent protein deacetylases. Proc Natl Acad Sci U S A 97(11):5807-11.

Laurencikiene J, van Harmelen V, Arvidsson Nordström E, Dicker A, Blomqvist L, Näslund E, Langin D, Arner P, Rydén M (2007) NF-KB is important for TNF-α-induced lipolysis in human hepatocytes. J Lipid Res 48:1069-77.

Lavu S, Boss O, Elliott PJ, Lambert PD (2008) Sirtuins - novel therapeutic targets to treat age-associated diseases. Nat Rev Drug Discov 7(10):841-53.

Lee IH, Cao L, Mostoslavsky R, Lombard DB, Liu J, Bruns NE, Tsokos M, Alt FW, Finkel T (2008) A role for the NAD-dependent deacetylase Sirt1 in the regulation of autophagy. Proc Natl Acad Sci U S A Mar 4;105(9):3374-9.

Li X, Monks B, Ge Q, Birnbaum MJ (2007) Akt/PKB regulates hepatic metabolism by directly inhibiting PGC1-alpha transcription coactivator. Nature 447:1012-6.

Lin J, Handschin C, Spiegelman BM (2005) Metabolic control through the PGC-1 family of transcription coactivators. Cell Metab 1:361-70.

Lin SJ, Kaeberlein M, Andalis AA, Sturtz LA, Defossez PA, Culotta VC, Fink GR, Guarente L (2002) Calorie restriction extends Saccharomyces cerevisiae life-span by increasing respiration. Nature 418:344-8.

Lipson KE, Baserga R (1989) Transcriptional activity of the human thymidine kinase gene determined by a method using the polymerase chain reaction and an intron-specific probe. Proc Natl Acad Sci U S A 86(24):9774-7.

Liu Y, Dentin R, Chen D, Hedrick S, Ravnskjaer K, Schenk S, Milne J, Meyers DJ, Cole P, Yates J 3rd, Olefsky J, Guarente L, Montminy M (2008) A fasting inducible switch modulates gluconeogenesis via activator/coactivator exchange. Nature 456(7219):269-73.

Long YC, Zierath JR (2006) AMP-activated protein kinase signaling in metabolic regulation. J Clin Invest 116(7):1776-83.

Longo VD, Finch CE (2003) Evolutionary medicine: from dwarf model systems to healthy centenarians? Science 299(5611):1342-6.

Longo VD, Kennedy BK (2006) Sirtuins in aging and age-related disease. Cell 126(2):257-68.

Lopes-Cardozo M, Mulder I, van Vugt F, Hermans PG, van den Bergh SG, Klazinga W, de Vries-Akkerman E (1975) Aspects of ketogenesis: control and mechanism of ketone-body formation in isolated rat-liver mitochondria. Mol Cell Biochem 9(3):155-73.

Lundåsen T, Hunt MC, Nilsson LM, Sanyal S, Angelin B, Alexon SE, Rudling M (2007) PPARalpha is a key regulator of hepatic FGF21. Biochem Biophys Res Commun 360(2):437-40.

Luo J, Deng ZL, Luo X, Tang N, Song WX, Chen J, Sharff KA, Luu HH, Haydon RC, Kinzler KW, Vogelstein B, He TC (2007) A protocol for rapid generation of recombinant adenoviruses using the AdEasy system. Nat Protoc 2(5):1236-47.

Luo J, Nikolaev AY, Imai S, Chen D, Su F, Shiloh A, Guarente L, Gu W (2001) Negative control of p53 by Sir2alpha promotes cell survival under stress. Cell 107:137-48.

Lynch CJ, Shah ZH, Allison SJ, Ahmed SU, Ford J, Warnock LJ, Li H, Serrano M, Milner J (2010) SIRT1 undergoes alternative splicing in a novel auto-regulatory loop with p53. PLoS One 5(10):e13502.

M

Mandard S, Muller M, Kersten S (2004) Peroxisome proliferator-activated receptor alpha target genes. Cell. Mol. Life Sci. 61:393-416.

Mangelsdorf DJ, Thummel C, Beato M, Herrlich P, Schutz G, Umesono K, Blumberg B, Kastner P, Mark M, Chambon P, Evans RM (1995) The nuclear receptor superfamily: the second decade. Cell 83:835-9.

Mascaró C, Acosta E, Ortiz JA, Marrero PF, Hegardt FG, Haro D (1998) Control of human muscle-type carnitine palmitoyltransferase I gene transcription by peroxisome proliferator-activated receptor. J Biol Chem 273(15):8560-3.

Masoro EJ. (2000) Caloric restriction and aging: an update. Exp Gerontol. 35(3):299-305.

Matsumoto M, Accili D (2006) The tangled path to glucose production. Nat Med 12(1):33-4.

Maurin AC, Jousse C, Averous J, Parry L, Bruhat A, Cherasse Y, Zeng H, Zhang Y, Harding HP, Ron D, Fafournoux P (2005) The GCN2 kinase biases feeding behavior to maintain amino acid homeostasis in omnivores. Cell Metab 1(4):273-7.

McBurney MW, Yang X, Jardine K, Hixon M, Boekelheide K, Webb JR, Lansdorp PM, Lemieux M (2003) The mammalian SIR2alpha protein has a role in embryogenesis and gametogenesis. Mol Cell Biol 23:38-54.

McGarry JD, Brown NF (1997) The mitochondrial carnitine palmitoyltransferase system. From concept to molecular analysis. Eur J Biochem 244:1-14.

McGarry JD, Foster DW (1980) Regulation of hepatic fatty acid oxidation and ketone body production. Annu Rev Biochem 49:395-420.

Milani M, Rzymski T, Mellor HR, Pike L, Bottini A, Generali D, Harris AL (2009) The role of ATF4 stabilization and autophagy in resistance of breast cancer cells treated with Bortezomib. Cancer Res 69(10):4415-23.

Milne JC, Lambert PD, Schenk S, Carney DP, Smith JJ, Gagne DJ, Jin L, Boss O, Perni RB, Vu CB, Bemis JE, Xie R, Disch JS, Ng PY, Nunes JJ, Lynch AV, Yang H, Galonek H, Israelian K, Choy W, Iffland A, Lavu

S, Medvedik O, Sinclair DA, Olefsky JM, Jirousek MR, Elliott PJ, Westphal CH (2007) Small molecule activators of SIRT1 as therapeutics for the treatment of type 2 diabetes. Nature 450(7170):712-6.

Min J, Landry J, Sternglanz R, Xu RM (2001) Crystal structure of a SIR2 homolog-NAD complex. Cell 105:269-79.

Mizushima N, Yamamoto A, Matsui M, Yoshimori T, Ohsumi Y (2004) In vivo analysis of autophagy in response to nutrient starvation using transgenic mice expressing a fluorescent autophagosome marker. Mol Biol Cell 15(3):1101-11.

Motta MC, Divecha N, Lemieux M, Kamel C, Chen D, Gu W, Bultsma Y, McBurney M, Guarente L (2004) Mammalian SIRT1 represses forkhead transcription factors. Cell 116(4):551-63.

Muise ES, Azzolina B, Kuo DW, El-Sherbeini M, Tan Y, Yuan X, Mu J, Thompson JR, Berger JP, Wong KK (2008) Adipose fibroblast growth factor 21 is up-regulated by peroxisome proliferator-activated receptor gamma and altered metabolic states. Mol Pharmacol 74(2):403-12.

N

Nadal A, Marrero PF, Haro D (2002) Down-regulation of the mitochondrial 3-hydroxy-3-methylglutaryl-CoA synthase gene by insulin: the role of the forkhead transcription factor FKHRL1. Biochem J 366(Pt 1):289-97.

Napal L, Marrero PF, Haro D (2005) An intronic peroxisome proliferator-activated receptor-binding sequence mediates fatty acid induction of the human carnitine palmitoyltransferase 1A. J Mol Biol 354(4):751-9.

O

Ortega-Molina A, Efeyan A, Lopez-Guadamillas E, Muñoz-Martin M, Gómez-López G, Cañamero M, Mulero F, Pastor J, Martinez S, Romanos E, Mar Gonzalez-Barroso M, Rial E, Valverde AM, Bischoff JR, Serrano M (2012) Pten positively regulates brown adipose function, energy expenditure, and longevity. Cell Metab 15(3):382-94.

Ortiz JA, Mallolas J, Nicot C, Bofarull J, Rodríguez JC, Hegardt FG, Haro D, Marrero PF (1999) Isolation of pig mitochondrial 3-hydroxy-3-methylglutaryl-CoA synthase gene promoter: characterization of a peroxisome proliferator-responsive element. Biochem J 337 (Pt 2):329-35.

Ozcan L, Wong CC, Li G, Xu T, Pajvani U, Park SK, Wronska A, Chen BX, Marks AR, Fukamizu A, Backs J, Singer HA, Yates JR 3rd, Accili D, Tabas I (2012) Calcium Signaling through CaMKII Regulates Hepatic Glucose Production in Fasting and Obesity. Cell Metab 15(5):739-51.

P

Pan YX, Chen H, Thiaville MM, Kilberg MS (2007) Activation of the ATF3 gene through a coordinated amino acid-sensing response programme that controls transcriptional regulation of responsive genes following amino acid limitation. Biochem J 401:299-307.

Park SJ, Ahmad F, Philp A, Baar K, Williams T, Luo H, Ke H, Rehmann H, Taussig R, Brown AL, Kim MK, Beaven MA, Burgin AB, Manganiello V, Chung JH (2012) Resveratrol ameliorates aging-related metabolic phenotypes by inhibiting cAMP phosphodiesterases. Cell 148(3):421-33.

Patsouris D, Reddy JK, Müller M, Kersten S (2006) Peroxisome proliferator-activated receptor alpha mediates the effects of high-fat diet on hepatic gene expression. Endocrinology 147(3):1508-16.

Pégorier JP, Le May C, Girard J (2004) Controlo f Gene Expressin by Fatty Acids. J. Nutr. 134:2444S-9S

Pfaffl MW (2001) A new mathematical model for relative quantification in real-time RT-PCR. Nucleic Acids Res 29(9):e45.

Pfister JA, Ma C, Morrison BE, D'Mello SR (2008) Opposing effects of sirtuins on neuronal survival: SIRT1-mediated neuroprotection is independent of its deacetylase activity. PLoS One 3(12):e4090.

Pfluger PT, Herranz D, Velasco-Miguel S, Serrano M, Tschop MH (2008) Sirt1 protects against high-fat diet-induced metabolic damage. Proc Natl Acad Sci U S A 105(28):9793-8.

Picard F, Kurtev M, Chung N, Topark-Ngarm A, Senawong T, Machado De Oliveira R, Leid M, McBurney MW, Guarente L (2004) Sirt1 promotes fat mobilization in white adipocytes by repressing PPAR-gamma. Nature 429:771-6.

Pilkis SJ, el-Maghrabi MR, Claus TH (1988) Hormonal regulation of hepatic gluconeogenesis and glycolysis. Annu Rev Biochem 57:755-83.

Pollak N, Dölle C, Ziegler M (2007) The power to reduce: pyridine nucleotides--small molecules with a multitude of functions. Biochem J 402(2):205-18.

Potthoff MJ, Inagaki T, Satapati S, Ding X, He T, Goetz R, Mohammadi M, Finck BN, Mangelsdorf DJ, Kliewer SA, Burgess SC (2009) FGF21 induces PGC-1alpha and regulates carbohydrate and fatty acid metabolism during the adaptive starvation response. Proc Natl Acad Sci U S A. 106(26):10853-8.

Puigserver P, Rhee J, Donovan J, Walkey CJ, Yoon JC, Oriente F, Kitamura Y, Altomonte J, Dong H, Accili D, Spiegelman BM (2003) Insulin-regulated hepatic gluconeogenesis through FOXO1-PGC-1alpha interaction. Nature 423(6939):550-5.

Purushotham A, Schug TT, Xu Q, Surapureddi S, Guo X, Li X (2009) Hepatocyte-specific deletion of SIRT1 alters fatty acid metabolism and results in hepatic steatosis and inflammation. Cell Metab 9(4):327-38.

Q

Quant PA (1994) The role of mitochondrial HMG-CoA synthase in regulation of ketogenesis. Essays Biochem 28:13-25.

R

Rabinowitz JD, White E (2010) Autophagy and metabolism. Science 330(6009):1344-8.

Randle PJ, Garland PB, Hales CN, Newsholme EA (1963) The glucose-fatty acid cycle: its role in insulin sensitivity and the metabolic disturbances of diabetes mellitus. Lancet i:785-9

Ren B, Thelen AP, Peters JM, Gonzalez FJ, Jump DB (1997) Polyunsaturated fatty acid suppression of hepatic fatty acid synthase and S14 gene expression does not require peroxisome proliferator-activated receptor alpha. J Biol Chem 272(43):26827-32.

Rhee J, Inoue Y, Yoon JC, Puigserver P, Fan M, Gonzalez FJ, Spiegelman BM (2003) Regulation of hepatic fasting response by PPARgamma coactivator-1alpha (PGC-1): requirement for hepatocyte nuclear factor 4alpha in gluconeogenesis. Proc Natl Acad Sci U S A 100(7):4012-7.

Rial E, González-Barroso MM (2001) Physiological regulation of the transport activity in the uncoupling proteins UCP1 and UCP2. Biochim Biophys Acta 1504(1):70-81.

Rodgers JT and Puigserver P (2007) Fasting-dependent glucose and lipid metabolic response through hepatic sirtuin 1. Proc Natl Acad Sci U S A. 104(31):12861-6.

Rodgers JT, Lerin C, Haas W, Gygi SP, Spiegelman BM, Puigserver P (2005) Nutrient control of glucose homeostasis through a complex of PGC-1alpha and SIRT1. Nature 434(7029):113-8.

Rodríguez JC, Gil-Gómez G, Hegardt FG, Haro D (1994) Peroxisome proliferator-activated receptor mediates induction of the mitochondrial 3-hydroxy-3-methylglutaryl-CoA synthase gene by fatty acids. J Biol Chem 269(29):18767-72.

Rzymski T, Milani M, Singleton DC, Harris AL (2009) Role of ATF4 in regulation of autophagy and resistance to drugs and hypoxia. Cell Cycle 8(23):3838-47.

S

Sahlin K, Sallstedt EK, Bishop D, Tonkonogi M (2008) Turning down lipid oxidation during heavy exercise - what is the mechanism? J Physiol Pharmacol 59 Suppl 7:19-30.

Saltiel AR (2001) New perspectives into the molecular pathogenesis and treatment of type 2 diabetes. Cell 104(4):517-29.

Sasaki K, Cripe TP, Koch SR, Andreone TL, Petersen DD, Beale EG, Granner DK (1984) Multihormonal regulation of phosphoenolpyruvate carboxykinase gene transcription. The dominant role of insulin. J Biol Chem 259(24):15242-51.

Schoenborn V, Heid IM, Vollmert C, Lingenhel A, Adams TD, Hopkins PN, Illig T, Zimmermann R, Zechner R, Hunt SC, Kronenberg F (2006) The ATGL gene is associated with free fatty acids, triglycerides, and type 2 diabetes. Diabetes 55(5):1270-5.

Schwer B, Verdin E (2008) Conserved metabolic functions of sirtuins. Cell Metab 7:104-12.

Shan J, Lopez MC, Baker HV, Kilberg MS (2010) Expression profile after activation of amino acid deprivation response in HepG2 human hepatoma cells. Physiol Genomics 41:315-27.

Shimazu T, Hirschey MD, Hua L, Dittenhafer-Reed KE, Schwer B, Lombard DB, Li Y, Bunkenborg J, Alt FW, Denu JM, Jacobson MP, Verdin E (2010) SIRT3 deacetylates mitochondrial 3-hydroxy-3-methylglutaryl CoA synthase 2 and regulates ketone body production. Cell Metab 12(6):654-61.

Siu F, Bain PJ, LeBlanc-Chaffin R, Chen H, Kilberg MS (2002) ATF4 is a mediator of the nutrient-sensing response pathway that activates the human asparagine synthetase gene. J Biol Chem 277:24120-7.

Smith JJ, Kenney RD, Gagne DJ, Frushour BP, Ladd W, Galonek HL, Israelian K, Song J, Razvadauskaite G, Lynch AV, Carney DP, Johnson RJ, Lavu S, Iffland A, Elliott PJ, Lambert PD, Elliston KO, Jirousek MR, Milne JC, Boss O (2009) Small molecule activators of SIRT1 replicate signaling pathways triggered by calorie restriction in vivo. BMC Syst Biol 3:31.

Sood R, Porter AC, Olsen DA, Cavener DR, Wek RC (2000) A mammalian homologue of GCN2 protein kinase important for translational control by phosphorylation of eukaryotic initiation factor-2alpha. Genetics 154(2):787-801.

Storlien L, Oakes ND, Kelley DE (2004) Metabolic flexibility. Proc Nutr Soc 63:363-8.

Sutherland C, O'Brien RM, Granner DK (1996) New connections in the regulation of PEPCK gene expression by insulin. Philos. Trans. R. Soc. Lond. B Biol. Sci. 351:191-9.

T

Tanner KG, Landry J, Sternglanz R, Denu JM (2000) Silent information regulator 2 family of NADdependent histone/protein deacetylases generates a unique product, 1-O-acetyl-ADP-ribose. Proc Natl Acad Sci U S A 97:14178-82.

Tanny JC, Moazed D (2001) Coupling of histone deacetylation to NAD breakdown by the yeast silencing protein Sir2: Evidence for acetyl transfer from substrate to an NAD breakdown product. Proc Natl Acad Sci U S A 98:415-20.

U

Uebanso T, Taketani Y, Yamamoto H, Amo K, Ominami H, Arai H, Takei Y, Masuda M, Tanimura A, Harada N, Yamanaka-Okumura H, Takeda E (2011) Paradoxical regulation of human FGF21 by both fasting and feeding signals: is FGF21 a nutritional adaptation factor? PLoS One.6(8):e22976.

Um JH, Park SJ, Kang H, Yang S, Foretz M, McBurney MW, Kim MK, Viollet B, Chung JH (2010) AMP-activated protein kinase-deficient mice are resistant to the metabolic effects of resveratrol. Diabetes 59(3):554-63.

V

Van Schaftingen E, Gerin I (2002) The glucose-6-phosphatase system. Biochem J 362:513-532.

Vattem KM, Wek RC (2004) Reinitiation involving upstream ORFs regulates ATF4 mRNA translation in mammalian cells. Proc Natl Acad Sci U S A 101(31):11269-74.

Vega RB, Huss JM, Kelly DP (2000) The coactivator PGC-1 cooperates with peroxisome proliferator-activated receptor alpha in transcriptional control of nuclear genes encoding mitochondrial fatty acid oxidation enzymes. Mol Cell Biol 20(5):1868-76.

Voelter-Mahlknecht S, Mahlknecht U (2006) Cloning, chromosomal characterization and mapping of the NAD-dependent histone deacetylases gene sirtuin 1. Int J Mol Med 17(1):59-67.

W

Wang H, Qiang L, Farmer SR (2008) Identification of a domain within peroxisome proliferator-activated receptor gamma regulating expression of a group of genes containing fibroblast growth factor 21 that are selectively repressed by SIRT1 in adipocytes. Mol Cell Biol 28(1):188-200.

Wang Q, Mora-Jensen H, Weniger MA, Perez-Galan P, Wolford C, Hai T, Ron D, Chen W, Trenkle W, Wiestner A, Ye Y (2009) ERAD inhibitors integrate ER stress with an epigenetic mechanism to activate BH3-only protein NOXA in cancer cells. Proc Natl Acad Sci U S A 106(7):2200-5.

Wang RH, Sengupta K, Li C, Kim HS, Cao L, Xiao C, Kim S, Xu X, Zheng Y, Chilton B, Jia R, Zheng ZM, Appella E, Wang XW, Ried T, Deng CX (2008) Impaired DNA damage response, genome instability, and tumorigenesis in SIRT1 mutant mice. Cancer Cell 14:312-23.

Wang RH, Kim HS, Xiao C, Xu X, Gavrilova O, Deng CX (2011) Hepatic Sirt1 deficiency in mice impairs mTorc2/Akt signaling and results in hyperglycemia, oxidative damage, and insulin resistance. J Clin Invest 121(11):4477-90.

Wang Y, Solt LA, Burris TP (2010) Regulation of FGF21 expression and secretion by retinoic acid receptor-related orphan receptor alpha. J Biol Chem 285(21):15668-73.

Waterlow JC, Jackson AA (1981) Nutrition and protein turnover in man. Br Med Bull 37(1):5-10.

Wei W, Dutchak PA, Wang X, Ding X, Wang X, Bookout AL, Goetz R, Mohammadi M, Gerard RD, Dechow PC, Mangelsdorf DJ, Kliewer SA, Wan Y (2012) Fibroblast growth factor 21 promotes bone loss by potentiating the effects of peroxisome proliferator-activated receptor γ. Proc Natl Acad Sci U S A 109(8):3143-8.

Weindruch R, Walford RL (1988) The retardation of aging and disease by dietary restriction. Charles C Thomas, Springfield (Illinois).

Wood JG, Rogina B, Lavu S, Howitz K, Helfand SL, Tatar M, Sinclair D. (2004) Sirtuin activators mimic caloric restriction and delay ageing in metazoans. Nature 430: 686-9.

X

Xiao F, Huang Z, Li H, Yu J, Wang C, Chen S, Meng Q, Cheng Y, Gao X, Li J, Liu Y, Guo F (2011) Leucine deprivation increases hepatic insulin sensitivity via GCN2/mTOR/S6K1 and AMPK pathways. Diabetes 60(3):746-56.

Xu J, Lloyd DJ, Hale C, Stanislaus S, Chen M, Sivits G, Vonderfecht S, Hecht R, Li YS, Lindberg RA, Chen JL, Jung DY, Zhang Z, Ko HJ, Kim JK, Véniant MM (2009) Fibroblast growth factor 21 reverses hepatic steatosis, increases energy expenditure, and improves insulin sensitivity in diet-induced obese mice. Diabetes 58(1):250-9.

Y

Yang J, Kong X, Martins-Santos ME, Aleman G, Chaco E, Liu GE, Wu SY, Samols D, Hakimi P, Chiang CM, Hanson RW (2009) Activation of SIRT1 by resveratrol represses transcription of the gene for the cytosolic form of phosphoenolpyruvate carboxykinase (GTP) by deacetylating hepatic nuclear factor 4alpha. J Biol Chem 284(40):27042-53.

Yeung F, Hoberg JE, Ramsey CS, Keller MD, Jones DR, Frye RA, Mayo MW (2004) Modulation of NF-κB-dependent transcription and cell survival by the SIRT1 deacetylase. EMBO 23:2369-80.

Yoon JC, Puigserver P, Chen G, Donovan J, Wu Z, Rhee J, Adelmant G, Stafford J, Kahn CR, Granner DK, Newgard CB, Spiegelman BM (2001) Control of hepatic gluconeogenesis through the transcriptional coactivator PGC-1. Nature 413(6852):131-8.

Yu J, Zhao L, Wang A, Eleswarapu S, Ge X, Chen D, Jiang H (2012) Growth hormone stimulates transcription of the fibroblast growth factor 21 gene in the liver through the signal transducer and activator of transcription 5. Endocrinology 153(2):750-8.

Z

Zechner R, Strauss JG, Haemmerle G, Lass A, Zimmermann R (2005) Lipolysis: pathway under construction. Curr Opin Lipidol 16(3):333-40.

Zhang T, Kraus WL (2010) SIRT1-dependent regulation of chromatin and transcription: linking NAD(+) metabolism and signaling to the control of cellular functions. Biochim Biophys Acta 1804(8):1666-75.

Zhang Y, Lei T, Huang JF, Wang SB, Zhou LL, Yang ZQ, Chen XD (2011) The link between fibroblast growth factor 21 and sterol regulatory element binding protein 1c during lipogenesis in hepatocytes. Mol Cell Endocrinol 342(1-2):41-7.

Zhong C, Chen C, Kilberg MS (2003) Characterization of the nutrient-sensing response unit in the human asparagine synthetase promoter. Biochem J 372(Pt 2):603-9.

Zhou G, Myers R, Li Y, Chen Y, Shen X, Fenyk-Melody J, Wu M, Ventre J, Doebber T, Fujii N, Musi N, Hirshman MF, Goodyear LJ, Moller DE (2001) Role of AMP-activated protein kinase in mechanism of metformin action. J Clin Invest 108:1167-74.

Zhou XY, Shibusawa N, Naik K, Porras D, Temple K, Ou H, Kaihara K, Roe MW, Brady MJ, Wondisford FE (2004) Insulin regulation of hepatic gluconeogenesis through phosphorylation of CREB-binding protein. Nat Med 10(6):633-7.

ANNEX

1. ABBREVIATIONS

Ab	Antibody
AcAc	Acetoacetate
Ac-Lys	Acetyl lysine
ACS	Acetyl-CoA synthethase
AMP	Adenosine monophosphate
APS	Ammonium persulfate
ATCC	American Type Culture Collection
ATP	Adenosine triphosphate
BAT	Brown adipose tissue
BLAST	Basic Local Alignment Search Tool
β-OHB	β-hydroxybutyrate or 3- hydroxybutyrate
BSA	Bovine serum albumin
°C	Degree Celsius
cAMP	Cyclic AMP
CBP	CREB binding protein
cDNA	Complementary DNA
C/EBP	CCAAT/enhancer-binding protein
ChIP	Chromatin immunoprecipitation
ChREBP	Carbohydrate responsive element-binding protein
CMV	Cytomegalovirus
CoA	Coenzyme A
CPT	Carnitine palmitoyltransferase
CR	Caloric restriction
CREB	cAMP response element binding protein
CRTC2	CREB regulator transcriptional coactivator 2, TORC2
Ctl	Control
D	Day
DEPC	Diethylpyrocarbonate
DMSO	Dimetylsulfoxid
DNA	Deoxyribonucleic acid
DTT	Dithiothreitol

E. coli	*Escherichia coli*
EDTA	Ethylenediamine tetraacetic acid
EGTA	Ethylene glycol tetraacetic acid
ER	Endoplasmatic reticulum
ERK	Extracellular signal-regulated kinase
FAS	Fatty acid synthase
FBS	Fetal bovine serum
FFA	Free fatty acids
FOXA2	Forkhead box protein A2
FOXO1	Forkhead box protein O1
G6Pase	Glucose 6 phosphatase
GFP	Green fluorescent protein
H&E	Hematoxylin and eosin
HAT	Histone acetyltransferase
HDAC	Histone deacetylase
HEPES	4-(2-hydroxyethyl)-1-piperazineethanesulfonic acid
HisOH	Histidinol
HMG-CoA	3-hydroxy-3-methylglutaryl-coenzyme A
HMGCS1	HMG-CoA synthase 1 (cytosolic)
HMGCS2	HMG-CoA synthase 2 (mitochondrial)
HNF4	Hepatocyte nuclear factor
HSL	Hormone sensitive lipase
Ig	Immunoglobulin
IPTG	Isopropyl-beta-D-thiogalactopyranoside
Kb	Kilobase
kDa	Kilodalton
LAP	Liver-enriched transcriptional activatory protein
(-)leu	Leucine deficient or deficiency
LKO	Liver specific knockout
Luc	Luciferase gene, from *Photinus pyralis*
MAPK	Mitogen-Activated Protein Kinase
MEM	Minimum Essential Medium
min	Minute(s)
mL	Milliliter(s)

MOI	Multiplicity of infection
mut	Mutated
µ	Micro (10^{-6})
NAD	Nicotinamide adenine dinucleotide, oxidizing agent
NADH	Nicotinamide adenine dinucleotide, reducing agent
NAM	Nicotinamide
NcoR	Nuclear receptor co-repressor
NEFA	Non esterified fatty acid
ng	Nanogram(s)
NP40	Nonidet P 40
o/n	Overnight
ORF	Ppen reading frame
PBS	Phosphate-buffered saline
PCR	Polymerase chain reaction
PEPCK	Phosphoenolpyruvate carboxylase kinase
PGC1	PPAR gamma coactivator factor 1
PMSF	Phenylmethanesulfonyl fluoride
PPAR	Peroxisome proliferator activated receptor
PPRE	PPAR response element
PVDF	Polyvinylidene difluoride
RNA	Ribonucleic acid
RT	Room temperature
RXR	Retinoid X receptor
SIK	Salt-inducible kinase
SIRT1	Sirtuin 1
SREBP	Sterol response element binding protein
TBS	Tris-buffered saline
TCA	Tricarboxilic acid cycle, Krebs cycle
TE	Tris-EDTA
TEMED	Tetramethylethylenediamine
TORC2	Transducer of regulated CREB protein 2, CRTC2
Tris	Tris(hydroxymethyl)aminomethane
UCP	Uncoupling protein
WAT	White adipose tissue

WB	Western blot
WT	Wild type

2. MOLECULAR SIZE MARKERS

100 bp Ladder DNA Marker (Biotools, 31.006)

1 Kb Ladder DNA Marker (Biotools, 31.005)

Prestained Protein Molecular Weight Marker (Fermentas, SM0441)

Novex® Sharp Pre-stained Protein Standards (Invtrogen, 57318)

3. REAGENTS, COMMERCIAL KITS AND OTHER PRODUCTS

30% Acrylamide/Bis Solution, 29:1 – Bio.Rad, 161-0156

40% Acrylamide/Bis Solution, 29:1 – Bio.Rad, 161-0146

Agarose – Sigma-Aldrich, A5093

Albumin from bovine serum (BSA) – Sigma-Aldrich, A7906

Ampicilin – Roche, 10 835 242 001

beta Hydroxybutyrate (beta HB) Assay Kit – abcam, ab83390

Bio-Rad Protein Assay – Bio-Rad, 500-0006

BioThermTM Taq Polymerase – Attend Bio, GC-002-0500

Blood glucose test strips (Elite) – Bayer, 3921C

Bovine Serum Albumin, Fraction V, fatty acid free – Roche, 775827

DEPC-treated water – Sigma-Aldrich

DIG Gel Shift Kit, 2nd Generation –Roche, 03 353 591 910

DNA Polymerase 5U/µL – Biotools, 10.068

DNase I – Ambion, AM1906

dNTPs 100mM EACH – Attend Bio, GC-013-001

Dual-Luciferase Reporter Assay System – Promega, E1960

Ethidium bromide – Sigma-Aldrich, E4134

EZ-ECL Chemiluminescence Detection Kit for HRP – Biological Industries, 20-500-120

Formaldehyde solution min. 37% – Merck, 104003

Formalin solution, neutral buffered, 10% – Sigma-Aldrich HT501128

Free fatty acids, Half-micro test – Roche, 11 383 175 001

GlycoBlue – Ambion, AM9516

Glucose – Sigma-Aldrich, G7528

IgG from rabbit serum – Sigma-Aldrich, I8140-50MG

IPTG – Applichem, A10080025

M-MLV reverse transcriptase – Invitrogen, 28025-021

NP 40 alternative – Calbiochem, 492016

Nylon Membranes, positively charged – Roche, 11 417 240 001

Passive lysis buffer 5X – Promega, E194A

Phenylmethanesulfonyl fluoride (PMSF) – Sigma-Aldrich, P7626

Phosphatase Inhibitor Cocktail 1 – Sigma-Aldrich, P2850

Phosphatase Inhibitor Cocktail 3 – Sigma-Aldrich, P0044

Platinum® qPCR SuperMix-UDG with ROX – Invitrogen, 11743-500

Power SYBR® Green PCR Master Mix (2X) – Applied Biosystems, 4367659

Protease Inhibitor Cocktail (4-(2-aminoethyl)benzenesulfonyl fluoride (AEBSF), pepstatinA, E-64, bestatin, leupeptin, and aprotinin) – Sigma-Aldrich, P8340

Protein A/G PLUS-Agarose beads – Santa Cruz Biotechnology, sc-2003

Proteinase K – Fermentas, E00491

PVDF membrane (Immobilon®-P, 0.45µm) – Millipore, IPVH00010

QuickChange® Site-Directed Mutagenesis kit – Stratagene, 200518-5

Random hexamers p(dN)6 – Roche, 1103473001

Rat/Mouse FGF-21 ELISA Kit – Millipore, EZRMFGF21-26K

Reverse transcriptase M-MLV – Invitrogen, 28025-013

T4 DNA Ligase – Promega, M180A

TEMED – Bio-Rad, 161-0801

TNT® T7 Quick Coupled Transcription/Translation System – Promega, L1170

TRI Reagent® Solution – Ambion, AM9738

Triton-X – Sigma-Aldrich, T8787

Tween®20 Reagent – Calbiochem, 655205

UV-cuvette, micro, centerlenght 15mm – Fisher, 759220

4. VECTORS

4.1. CLONING VECTORS

pGEM®-T (Promega Cat. A3600)**:** The pGEM®-T Vector Systems are convenient systems for the cloning of PCR products. The pGEM®-T Vector is prepared by cutting the pGEM®-5Zf(+) Vector with EcoRV and adding a 3´ terminal thymidine to both ends. These single 3´-T overhangs at the insertion site greatly improve the efficiency of ligation of a PCR product into the plasmid by preventing recircularization of the vector and providing a compatible overhang for ligation of PCR products generated by thermostable polymerases that add a single deoxyadenosine to the 3´-ends of amplified fragments. T7 and SP6 RNA polymerase promoters flank a multiple cloning region within the α-peptide coding region for β-galactosidase. Insertional inactivation of the α-peptide allows recombinant clones to be directly identified by color screening on indicator plates (AIX plates: 100mg/L ampicilin, 8mg/L IPTG, and 40mg/L X-Gal). Positive white colonies are incapable to hydrolyze the substrate X-Gal because the insert causes the lost of the β-galactosidase activity, while colonies that have incorporated the empty vector (negative colonies) are blue due to the presence of the X-Gal hydrolysis products.

4.2. REPORTER VECTORS

Reporter vectors provide a basis for the quantitative analysis of factors that potentially regulate mammalian gene expression. These vectors contain a modified coding region for firefly (*Photinus pyralis*) luciferase that has been optimized for monitoring transcriptional activity in transfected eukaryotic cells.

The **pGL3-Basic Vector** (Promega, Ref. E1751) lacks eukaryotic promoter and enhancer sequences, allowing maximum flexibility in cloning putative regulatory sequences. Expression of luciferase activity in cells transfected with this plasmid depends on insertion and proper orientation of a functional promoter upstream from *luc*+. After transfection in eucariotic cells, binding of transcription factors at this promoter results in the expression of firefly luciferase, an enzyme capable of catalyzing a powerful bioluminescent reaction. Light emitted from the chemical reaction detected in the cell lysate is directly proportional to the amount of expressed enzyme and thus the binding activity of the targeted transcription factor.

The pRL Vectors are a family of wild type *Renilla* luciferase (*Rluc*) control reporter vectors. The pRL Vectors, which provide constitutive expression of *Renilla* luciferase, can be used in combination with a firefly luciferase vector to cotransfect mammalian cells. Expression of *Renilla* luciferase provides an internal control value to which expression of the experimental firefly luciferase reporter gene may be normalized. The pRL Vectors contain the cDNA encoding *Renilla* luciferase (*Rluc*) cloned from the anthozoan coelenterate *Renilla reniformis*. There are different promoter configurations. The CMV immediate early enhancer/promoter region (**pRL-CMV**, Promega, Ref. E2261) was used.

4.3. OTHER VECTORS

pcDNA3 – eukaryotic expression empty vector, was a kind gift from Dr. Ronald Evans (Umesono et al., 1991).

pRK-ATF4 – human ATF4 expression vector, obtained from Addgene – plasmid 26114 (Wang et al., 2009).

pRK-ATF3 – human ATF3 expression vector, obtained from Addgene – plasmid 26115 (Wang et al., 2009).

pSCT-LAP – mammalian expression vector for the active C/EBPβ isoform, starting at the second ATG, under control of the CMV promoter, was a kind gift from Dr. Marta Giralt (Carmona et al., 2005).

5. TAQMAN PROBES (APPLIED BIOSYSTEMS)

For HepG2 cell line experiments, human probes were used:

CPT1A Hs00157079_m1

Egr1 Hs00152928_m1

FGF21 Hs00173927_m1

HMGCS2 Hs00985427_m1

PEPCK-C Hs00159918_m1

For mice experiments, mouse probes were used:

Acc1 (Acaca) Mm01342777_m1

Asns Mm00803785_m1

Atf4 Mm00515324_m1

Atgl (Pnpla2) Mm00503040_m1

Cpt1a Mm00550438_m1

Cpt2 Mm00487202_m1

Dio2 Mm00515664_m1

Fas (Fasn) Mm00662319_m1

Fgf21 Mm00840165_g1

G6pase (G6pc3) Mm00616234_m1

Hmgcs2 Mm00550050_m1

Hsl Mm00495359_m1

Pck1 Mm01247058_m1

Pgc1α Mm00447181_m1

Srebp1c (Srebf1) Mm00550338_m1

Ucp1 Mm00494069_m1

As an endogenous control, for both HepG2 cells and mice experiments, the 18S rRNA Probe dye VIC-MGB (4319413E – 1006049) was used.

6. PRIMERS

6.1. GENOTYPING

Cre-F (DH1186) – 5'-GCGGTCTGGCAGTAAAAACTATC

Cre-R (DH1187) – 5'-GTGAAACAGCATTGCTGTCACTT

6.2. CLONING

Human FGF21 promoter constructs

wt (-768;+115) – 883 bp

Foward DH1309 5'-***GGTACC***AGCCAACCTGTCTTCCCTCT (-768;-750)

Reverse DH1310 5'-CTCTGGCCCACACTCACTTT (+383;+402)

Delta1 (-608;+115) – 723 bp

Forward DH1318 5'-***GGTACC***GGAGGAGGAGGCTGGGA (-608;-592)

Reverse DH1310 5'-CTCTGGCCCACACTCACTTT (+383;+402)

Delta1/2 (-186;+115) – 301 bp

Forward DH1328 5'-***GGTACC***CTGGCCCTCCATTGAAAG (-186;-169)

Reverse DH1310 5'-CTCTGGCCCACACTCACTTT (+383;+402)

Delta2 (-134;+115) – 249 bp

Forward DH1327 5'-***GGTACC***TGCCACGATGGAATTCTGTA (-134;-115)

Reverse DH1310 5'-CTCTGGCCCACACTCACTTT (+383;+402)

6.3. SITE-DIRECTED MUTAGENESIS

Human FGF21 promoter constructs

AARE1 (mut)

Foward DH1319 5'-TGAAAGAAACACCAGGcagatggacGGGAGGAGGAGGCTG

Reverse DH1320 5'-CAGCCTCCTCCTCCCgtccatctgCCTGGTGTTTCTTTCA

AARE2 (mut)

Foward DH1339 5'- ATTGAAAGGACCCCAGcagatggacTCCATTCAGGCTGC

Reverse DH1340 5'- GCAGCCTGAATGGAgtccatctgCTGGGGTCCTTTCAAT

6.4. TRANSCRIPTION RATE MEASUREMENT

Heterologous RNA (Intron2 - Exon3) human FGF21 – 190bp

Foward DH1321 5'-CCTGGATCCTGGGTCTTACA

Reverse DH1322 5'-CGGTGTGGGGACTTGTTC

6.5. CHROMATIN IMMUNOPRECIPITATION (CHIP)

Human FGF21 promoter and exon1

AARE1 (-768;-574) – 195 bp

Foward DH1329 5’-AGCCAACCTGTCTTCCCTCT

Reverse DH1330 5’-ATGCTCAGACCCTGGACATC

AARE2 (-300;-101) – 200 bp

Foward DH1331 5’-GCTTGAGACCCCAGATCCTT

Reverse DH1332 5’-CATTTGGCAGGAGCTACAGA

Exon1 (+184;+338) – 155 bp

Foward DH1223 5’-GGACTGTGGGTTTCTGTGCT

Reverse DH1224 5’-ATCTCCAGGTGGGCTTCTGT

6.6. ELECTROPHORETIC MOBILITY-SHIFT ASSAY (EMSA)

Human FGF21 promoter

AARE1 (wt) – protuberant 5’ hanging

Foward DH1386 5’-**GTACT**AAGAAACACCAGGATTGCATCAGGGAGGAGGAGG

Reverse DH1387 5’-**GTACT**CCTCCTCCTCCCTGATGCAATCCTGGTGTTTCTT

AARE1 (wt)

Foward DH1316 5’-TGAAAGAAACACCAGGATTGCATCAGGGAGGAGGAGGCTG

Reverse DH1318 5’-CAGCCTCCTCCTCCCTGATGCAATCCTGGTGTTTCTTTCA

AARE1 (mut)

Foward DH1319 5’-TGAAAGAAACACCAGGcagatggacGGGAGGAGGAGGCTG

Reverse DH1320 5’-CAGCCTCCTCCTCCCgtccatctgCCTGGTGTTTCTTTCA

AARE2 (wt) – protuberant 5’ hanging

Foward DH1388 5’-**GTACT**GAAAGGACCCCAGGTTACATCATCCATTCAGGCT

Reverse DH1389 5’-**GTACT**AGCCTGAATGGATGATGTAACCTGGGGTCCTTTC

AARE2 (wt)

Foward DH1337 5’-ATTGAAAGGACCCCAGGTTACATCATCCATTCAGGCTGC

Reverse DH1338 5’-GCAGCCTGAATGGATGATGTAACCTGGGGTCCTTTCAAT

AARE2 (mut)

Foward DH1339 5’- ATTGAAAGGACCCCAGcagatggacTCCATTCAGGCTGC

Reverse DH1340 5’- GCAGCCTGAATGGAgtccatctgCTGGGGTCCTTTCAAT

7. GLUCOSE TOLERANCE TEST (GTT) SAMPLE DATA TABLE

									Glycemia				
						tail	body	start	baseline	after Glucose injection			
#	birth	cage	**mouse ID**	genotype	sex	mark	weight	time	time 0	15min	30min	60min	120min
1													
2													
3													
4													
5													
6													
7													
8													
9													
10													

8. GENOTYPING TABLE

#	**ear punching mark**	birth date	progenitors	**mouse ID**	sex	PCR	**genotype**
1	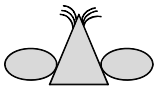						
2	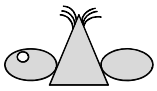						
3	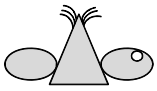						
4	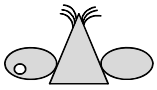						
5	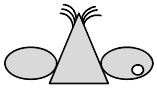						
6	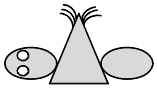						
7	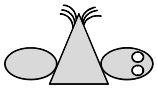						
8	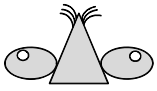						
9	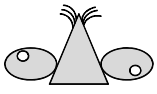						
10	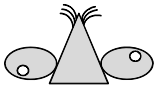						
11	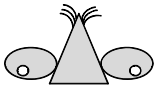						
12	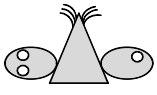						
13	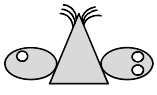						

9. MICE DIET INFORMATION

A10021B and A05080202

L-Amino Acid Rodent Diet and Same Without Added Leucine

Product #	A10021B		A05080202	
	gm%	kcal%	gm%	kcal%
Protein	17	18	16	16
Carbohydrate	69	71	70	72
Fat	5	12	5	12
kcal/gm		3.9		3.9
Ingredient (gm)				
L-Arginine	10	40	10	40
L-Histidine-HCl-H2O	6	24	6	24
L-Isoleucine	8	32	8	32
L-Leucine	12	48	0	0
L-Lysine-HCl	14	56	14	56
L-Methionine	6	24	6	24
L-Phenylalanine	8	32	8	32
L-Threonine	8	32	8	32
L-Tryptophan	2	8	2	8
L-Valine	8	32	8	32
L-Alanine	10	40	10	40
L-Asparagine-H2O	5	20	5	20
L-Aspartate	10	40	10	40
L-Cystine	4	16	4	16
L-Glutamic Acid	30	120	30	120
L-Glutamine	5	20	5	20
Glycine	10	40	10	40
L-Proline	5	20	5	20
L-Serine	5	20	5	20
L-Tyrosine	4	16	4	16
Total L-Amino Acids	*170*	0	*158*	0
Corn Starch	550.5	2202	562.5	2250
Maltodextrin 10	125	500	125	500
Cellulose	50	0	50	0
Corn Oil	50	450	50	450
Mineral Mix S10001	35	0	35	0
Sodium Bicarbonate	7.5	0	7.5	0
Vitamin Mix V10001	10	40	10	40
Choline Bitrartrate	2	0	2	0
Red Dye, FD&C #40	0	0	0.025	0
Blue Dye, FD&C #1	0.05	0	0	0
Yellow Dye, FD&C #5	0	0	0.025	0
Total	**1000.05**	**3872**	**1000.05**	**3872**

Formulated by Research Diets, Inc.

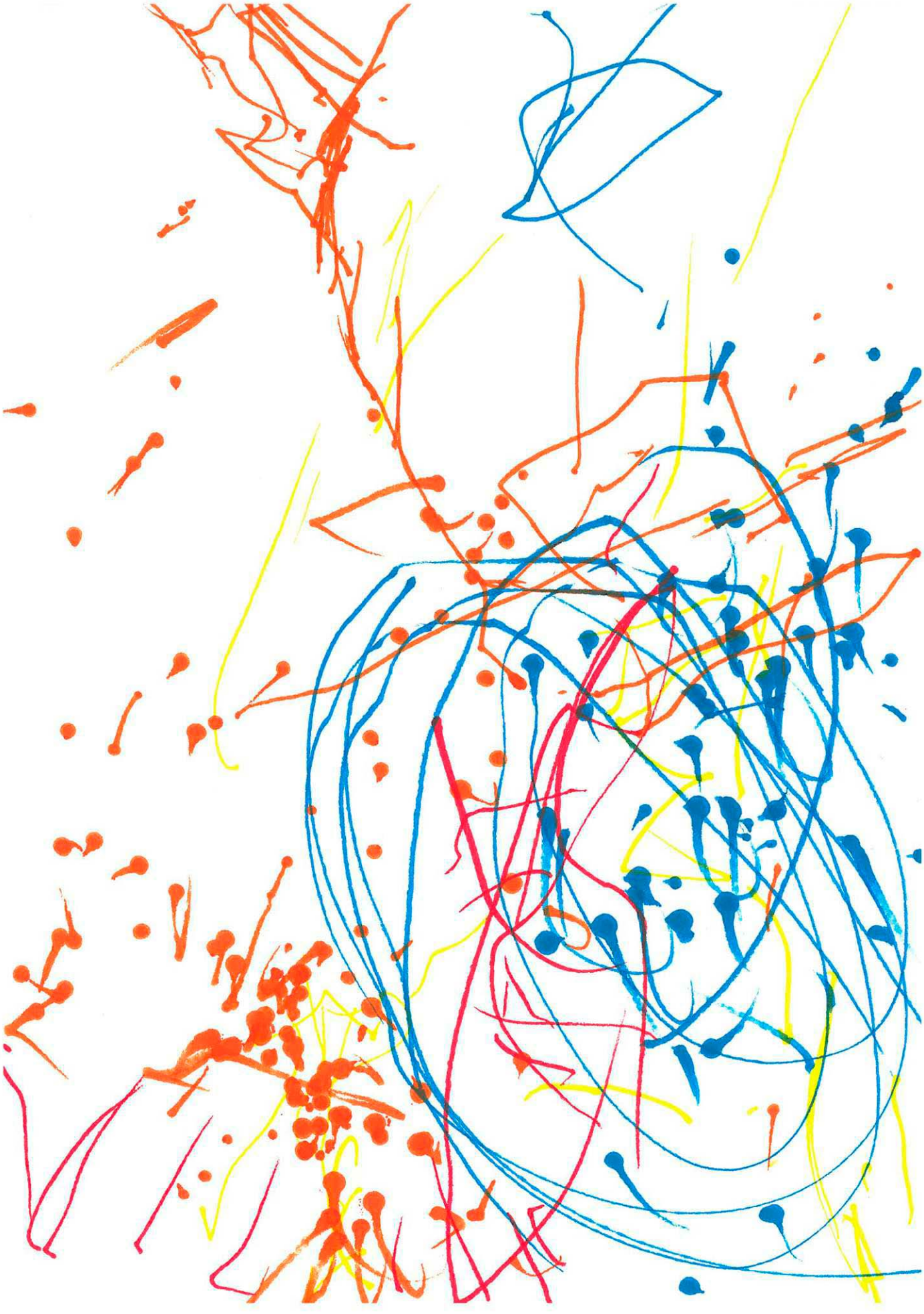

THE END